The Synthesis and Characterization of Styrene-Grafted Epoxidized Natural Rubber (ENR50-PS) by Gradient HPLC Analysis

BY

A.J.P. van Zyl

Thesis presented in partial fulfilment of the requirements for the degree of

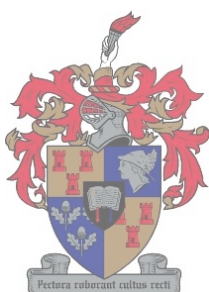**Master of Science (Polymer Science)**

at the

University of Stellenbosch

Study Leader:

Prof. R.D. Sanderson

Co-study Leader:

Prof. H. Pasch

Stellenbosch

December 1999

Declaration

I, the undersigned, hereby declare that the work contained in this thesis is my own original work and that I have not previously in its entirety or in part submitted it at any university for a degree.

24 – 11 – 1999

Date

Abstract

In order to enhance the properties of polymers, it is first necessary to have a clear understanding of their chemical microstructure. Materials resulting from a grafting reaction have a very complex chemical microstructure due to the fact that grafting is random and emulsion polymerization is a heterogeneous process. In a grafting reaction between two polymers it is possible that grafted (either crosslinked or non-crosslinked) and non-grafted material will be formed. These products can be determined by gradient HPLC techniques which are based on the differences in the solubility/adsorption of the polymers present after the grafting reaction has taken place. Gradient HPLC allows separation by means of chemical composition distribution (CCD) as well as molar mass. Separation is determined by chromatographic conditions e.g. solvent/non-solvent pairs, columns, gradients etc.

Styrene was grafted onto epoxidized natural rubber (ENR50) in an emulsion reaction. The initiator and monomer concentrations were chosen to represent five distinct reaction conditions, to be able to compare the gradient HPLC analyses of the different products. Solubility tests were performed on the ENR50 and solubility parameters evaluated for the rubber as well as for solvents. Cloudpoint determinations were performed both titrimetrically and chromatographically to determine which solvent/non-solvent pair was best suited for the separation process, as well as to investigate certain theoretical aspects of gradient HPLC. Other preliminary experiments performed on the styrene-grafted ENR50 included GPC, FTIR and LC-transform analyses. The results of these experiments were to be used to ease the explanation of gradient HPLC analysis results and to investigate the influence of the reaction conditions on the epoxidized natural rubber. The study was concluded with the optimization of the gradient HPLC method and consequent analysis of the grafted samples by gradient HPLC analysis. Results of these analyses confirmed that separation of the graft copolymerization mixture into the desired graft copolymer, non-grafted precursors and monomer was indeed possible.

The presence of the graft peaks in the gradient chromatograms not only proved that grafting had taken place, but the very low intensity of the peaks also confirmed the low transfer coefficient of styrene. Unfortunately much of the grafted product crosslinked (polystyrene radicals terminate by coupling) and was therefore not soluble.

Keywords: gradient HPLC, styrene-grafted epoxidized natural rubber, cloudpoints, GPC, LC-transform, FTIR, solubility parameters, chemical composition distribution (CCD).

Opsomming

Om die eienskappe van polimere te bevorder, is dit noodsaaklik om 'n duidelike begrip van die chemiese struktuur van 'n polimeriese materiaal te hê. Materiale wat voortvloei uit entkopolimerisasie reaksies het 'n baie komplekse chemiese mikrostruktuur as gevolg van die feit dat enting willekeurig is en emulsie polimerisasie 'n heterogene proses is. As gevolg van die entingsreaksie tussen twee polimere is dit dus moontlik dat geënte sowel as ongeënte materiaal aan die einde van die reaksie teenwoordig kan wees. Die moontlikheid bestaan ook dat sommige van die geënte materiaal 'n gekruisbinde netwerk tydens die emulsie reaksie kan vorm. Deur gebruik te maak van gradiënt hoë-druk vloeistofchromatografie, wat gebaseer is op die oplosbaarheid/adsorpsie van die polimere wat teenwoordig is na afloop van die entingsreaksie, is dit dus moontlik om bostaande verskynsel te ondersoek en te analiseer. Gradiënt hoë-druk vloeistofchromatografie laat skeiding op die basis van chemiese komposisie distribusie sowel as molekulêre massa toe en die skeiding is afhanklik van verskeie chromatografiese veranderlikes, byvoorbeeld oplosmiddel/presipiteermiddel pare, kolomme, gradiënte ensovoorts.

Vir hierdie studie is ge-epoksideerde natuurlike rubber (ENR50) met stireen geënt deur middel van 'n emulsie reaksie. Die inisieerder- en monomeer-konsentrasies is spesifiek gekies om vyf duidelike reaksie kondisies voor te stel om sodoende die vergelyking van die resultate van die gradiëntchromatografie analise te vergemaklik. Oplosbaarheidstoetse van ENR50 is uitgevoer en oplosbaarheids-parameters geëvalueer vir die rubber asook vir die oplosmiddels. Presipitasiepuntevaluerings is gedoen deur middel van titrasies en chromatografiese analises en resultate gevolglik aangewend om die oplosmiddel/presipiteermiddel te kies wat die beste skeiding sou verteenwoordig. Hierdie evaluasies is egter ook gebruik om sekere teoretiese aspekte te ontleed en te verklaar.

Sekere preliminêre eksperimente is ook uitgevoer met die oog op vereenvoudiging van die verduideliking van die gradiënteksperimente, sowel as om die invloed van die reaksie kondisies op die ge-epoksideerde natuurlike rubber te bestudeer. Eksperimente het permeasiechromatografie, infrarooi spektroskopie en permeasiechromatografie gekoppel aan infrarooi spektroskopie ingesluit.

Die studie is gevolglik afgesluit deur die optimisering en gevolglike analise van die geënte monsters deur gradiënt hoë-druk vloeistofchromatografie. Hierdie analises het bevestig dat skeiding moontlik is tussen die verlangde entkopolimeer en homopolimere. Die teenwoordigheid van die entpieke het bewys dat enting wel plaasgevind het, maar die lae intensiteit van die pieke het ook die lae oordragkoëffisiënt van stireen, wat enting moes bewerkstellig, bevestig, asook die feit dat baie van die geënte polimeer 'n gekruisbinde netwerk gevorm het (polistireenradikale termineer deur middel van koppeling) en dus nie oplosbaar was nie.

Sleutelwoorde: gradiënt hoë-druk vloeistofchromatografie, stireen geënte ge-epoksieerde natuurlike rubber, presipitasiepunte, permeasiechromatografie, permeasiechromatografie gekoppel aan infrarooi spektroskopie, infrarooi spektroskopie, oplosbaarheids-parameters, chemiese komposisie distribusie.

The Synthesis and Characterization of Styrene-Grafted Epoxidized Natural Rubber (ENR50-PS) by Gradient HPLC Analysis

BY

A.J.P. van Zyl

Accepted: ---

Prof. R.D. Sanderson (Study Leader)

Director, Institute of Polymer Science

University of Stellenbosch

Approved: ---

Prof. H. Pasch (Co-study Leader)

Deutsches Kunststoff-Institute

Approved: ---

Prof. B. Klumperman (External Examiner)

Eindhoven University of Technology

Approved: ---

Dr. A.J. van Reenen (Internal Examiner)

Institute of Polymer Science

University of Stellenbosch

Acknowledgements

On a more personal note, I would like to thank my parents for giving me the opportunity to further my studies and helping me to achieve my goals. I would also like to thank all my friends at the Institute (Charl Morkel, Jerry Vermeulen, Sven Graef, Malan Calitz, Ewan Sprong, Mozzy, Monja, Cor Beyers, Albert, Willie, Jaco, Elna, James and all the others) for all their support and the enjoyable Friday afternoon pub lunches. Then I have to thank Gerrit and Niël for helping me to clear my mind by taking me to the golf course and on some nice bike rides. I also have to thank Leon van Niekerk for all the encouragement and interest and for making my classes a lot less boring. Last, but not least, I have to thank Susan for her endless support and love. Thanks for supporting me and tolerating all my moods - which sometimes seemed to have a close relation with the progress of the project. Thank you very much everybody!

List of Contents

Chapter 4: Synthesis of Styrene-Grafted Epoxidized Natural Rubber (ENR50-PS)

Chapter 7: Gradient HPLC of Styrene-Grafted Epoxidized Natural Rubber (ENR50): Development of the Method, Results and Discussions

List of Symbols and Abbreviations

	Description	Units
ACN	acetonitrile	
AU	absorbance units	
Avg	average	
b	gradient steepness parameter	%.min^{-1}
Berol 291	nonyl phenol non-ionic surfactant	
C_{18}	octadecyl sorbent	
$CaCl_2$	calcium chloride	
CCD	chemical composition distribution	
CCl_4	carbon tetrachloride	
CN	cyanopropyl sorbent	
CP	cloudpoint	% non-solvent
CRYSTAF	crystallization analysis fractionation	
CSC	critical solvent composition	% non-solvent
D	polydispersity, $D = M_w / M_n$	
DBSASS	dodecylbenzene sulfonic acid sodium salt	
DCM	dichloromethane	
DDI	distilled de-ionized	
DKI	Deutsches Kunststoff-Institut	
DRC	dry rubber content	%
DRC_{ENR50}	dry rubber content of ENR50	%
dV	change in volume	ml
ΔE_{coh}	change in cohesive energy density	J.mol^{-1}
ΔE_1, ΔE_2	change in evaporation energy	J.mol^{-1}
E_{coh}	cohesive energy density	J.mol^{-1}
E_d	dispersive term of the cohesive energy density	J.mol^{-1}
E_h	hydrogen bonding term of the cohesive energy density	J.mol^{-1}
E_{hi}	group molar contribution of structural unit i for the 3-value solubility parameter concept	J.mol^{-1}
E_i	group molar contribution of structural unit i	J.mol^{-1}
E_p	polarity term of the cohesive energy density	J.mol^{-1}
E_1, E_2	energies of evaporation of compounds 1 and 2	J.mol^{-1}
ELSD	evaporative light scattering detector	
ENR25	25% epoxidized natural rubber	

ENR50	50% epoxidized natural rubber	
ENR75	75% epoxidized natural rubber	
ENRPS1-10	styrene-grafted epoxidized natural rubber (samples 1-10)	
EPDM	ethylene propylene diene terpolymer	
EtOH	ethanol	

F	group molar contribution of structural unit	$J^{1/2}.mol^{-1}.cm^{-3/2}$
F_{di}	group molar contribution of structural unit i for the 3-value solubility parameter concept	$J^{1/2}.mol^{-1}.cm^{-3/2}$
F_i	group molar contribution of structural unit i	$J^{1/2}.mol^{-1}.cm^{-3/2}$
F_{pi}	group molar contribution of structural unit i for the 3-value solubility parameter concept	$J^{1/2}.mol^{-1}.cm^{-3/2}$
F_{rate}	flow rate	$m^3.s^{-1}$
FTD	functionality type distribution	
FTIR	Fourier transform infrared spectroscopy	

ΔG_M	free energy of mixing	$J.mol^{-1}$
G	band compression factor	
g	fractional migration	
GC/MS	gas chromatography coupled to mass spectrometry	
GC-IR	gas chromatography coupled to infrared spectroscopy	
GPC	gel permeation chromatography	
GPC-FTIR	gel permeation chromatography coupled to FTIR spectroscopy	
GPEC	gradient polymer elution chromatography	

ΔH_M	enthalpy of mixing	$J.mol^{-1}$
ΔH_{vap}	molar heat of evaporation	$J.mol^{-1}$
HPLC	high-performance liquid chromatography	

k	capacity factor
k'	capacity factor
k_a	instantaneous value of the capacity factor
k_f	final value of the capacity factor when the solute band reaches the end of the column i.e. at the time of elution
k_i	value of the capacity factor for a given solute injected at the column inlet at any time t after the gradient separation begins
k_t	value of the capacity factor when a solute band leaves the column in gradient elution; equal to k_a at $t = t_g$

k_z	value of the capacity factor for compound z	
k_0	value of the capacity factor at the start of the gradient	
k_{01}, k_{02}	values of k_0 for 2 adjacent solutes	
KBr	potassium bromide	
KOH	potassium hydroxide	
kPa	kiloPascal	
KPS	potassium persulfate	
L	length of column	m
LAC	liquid adsorption chromatography	
LCCC	liquid chromatography at critical conditions	
LNR	liquid natural rubber	
LSS	linear solvent strength	
M	molar	g.mol^{-1}
M_n	number average molar mass	g.mol^{-1}
M_p	molar mass at the maximum of the molar mass distribution	g.mol^{-1}
M_w	weight average molar mass	g.mol^{-1}
MeOH	methanol	
MM	molar mass	
MMA	methyl methacrylate	
MMD	molar mass distribution	
mV	millivolt	mV
%NS	percentage non-solvent	%
N	column plate number	
n	constant in normal phase liquid chromatography	
NMR	nuclear magnetic resonance	
NP	normal phase	
NR	natural rubber	
NS	non-solvent	
ODS	octadecyl-modified silica gel	
p	value contributing to the band compression factor	%.min^{-1}
PB	polybutadiene	
PiP	polyisoprene	
PiP1	polyisoprene (M_p=1350)	
PiP10	polyisoprene (M_p=3300000)	
PiP2	polyisoprene (M_p=3190)	
PiP3	polyisoprene (M_p=8000)	
PiP4	polyisoprene (M_p=27000)	

PiP5	polyisoprene (M_p=62800)	
PiP6	polyisoprene (M_p=115000)	
PiP7	polyisoprene (M_p=295000)	
PiP8	polyisoprene (M_p=550000)	
PiP9	polyisoprene (M_p=1200000)	
PL	Polymer Laboratories	
polENR50	polymerized ENR50	
PS	polystyrene	
PS1	polystyrene (M_p=500)	
PS10	polystyrene (M_p=20000000)	
PS2	polystyrene (M_p=2450)	
PS3	polystyrene (M_p=5050)	
PS4	polystyrene (M_p=9200)	
PS5	polystyrene (M_p=66000)	
PS6	polystyrene (M_p=156000)	
PS7	polystyrene (M_p=570000)	
PS8	polystyrene (M_p=1075000)	
PS9	polystyrene (M_p=7000000)	
PTFE	polytetrafluoroethylene	
R	molar gas constant	8.3144 J.mol^{-1}.K^{-1}
r	fractional distance migrated by solute in the column	
R_S	resolution	
RI	refractive index	
RP	reversed-phase	
rpm	revolutions per minute	min^{-1}
RT	retention time	
ΔS_M	entropy of mixing	J.mol^{-1}.K^{-1}
$\%S_g$	percentage of solvent at the start of the gradient	%
%S	percentage solvent	%
S	constant for GPEC	
S	solvent	
SEC	size exclusion chromatography	
SEC-FTIR	size exclusion chromatography coupled to FTIR spectroscopy	
SF	solvent front	
SLS	sodium lauryl sulfate	
T	absolute temperature	K
t	time	min

t_D	gradient delay time	min
t_G	gradient time	min
t_H	gradient hold time	min
t_R	solute retention time	min
t_{sg}	time needed for the gradient to reach the detector	min
t_0	column dead time	min
t_{1-x}	time needed to migrate a fractional distance $1-x$ within the column	min
t_1, t_2	retention times for adjacent solutes	min
T_g	glass transition temperature	K
THF	tetrahydrofuran	
TSC	total solids content	%
TUE	Eindhoven University of Technology	
ΔU_{vap}	internal energy of evaporation	J.mol^{-1}
U_E	linear velocity of the eluent	m.s^{-1}
U_p	linear velocity of the polymer	m.s^{-1}
UV	ultraviolet	
ΔV	change in volume	ml
V	group molar volume	cm^3.mol^{-1}
V_D	dwell or hold-up volume	ml
V_I	interstitial volume	m^3
V_i	group molar volume of structural unit i	cm^3.mol^{-1}
V_m	column dead volume	ml
V_{mob}	volume accessible by the eluent	m^3
V_P	pore volume	m^3
V_R	retention volume of the solute	ml
V_R'	solute retention volume corrected for V_m	ml
V_t	volume of mobile phase eluted from the column during time t	ml
V^{NS}	volume of the non-solvent	ml
V^S	volume of the solvent	ml
V_1, V_2	molar volumes of compounds 1 and 2	cm^3.mol^{-1}
V	volt	V
W	solute baseline width	min
W_1, W_2	baseline bandwidths of solutes 1 and 2	min
WISP	Waters Intelligent Sample Processor	
wt	weight	g

x	fraction solute migration during pre-elution as a result of the equipment hold-up volume V_D	
X_B	mole fraction of solvent B in the mobile phase for normal phase liquid chromatography	
α_g	separation factor in gradient elution	
α_i	isocratic separation factor for 2 adjacent solute bands, equal to the ratio of their k-values (retention factors)	
δ	solubility parameter	$\text{MPa}^{1/2}$
δ_d	solubility parameter dispersive term	$\text{MPa}^{1/2}$
δ_{ENR50}	solubility parameter of ENR50	$\text{MPa}^{1/2}$
δ_h	solubility parameter hydrogen-bonding term	$\text{MPa}^{1/2}$
δ_{mix}	solubility parameter of a mixture of solvents	$\text{MPa}^{1/2}$
δ_p	solubility parameter polarity term	$\text{MPa}^{1/2}$
δ_t	total solubility parameter	$\text{MPa}^{1/2}$
δ_{THF}	solubility parameter of THF	$\text{MPa}^{1/2}$
δ_v	$\sqrt{\left(\delta_d^2 + \delta_p^2\right)}$	$\text{MPa}^{1/2}$
δ_1, δ_2	solubility parameters of compounds 1 and 2	$\text{MPa}^{1/2}$
$\Delta\phi$	change in the volume fraction during the gradient	
$\Delta\phi_S$	steepness of the gradient curve	$\%.\text{min}^{-1}$
ϕ	volume fraction of solvent	
ϕ'	gradient steepness	$\%.\text{min}^{-1}$
ϕ''	gradient steepness equal to $\phi't_0$	$\%$
ϕ_0	value of ϕ at the start of the gradient	$\%$
ϕ_1, ϕ_2	volume fractions of components 1 and 2	
ω	bandwidth	min

List of Figures

Chapter 6: Preliminary Experimental Analyses (FTIR, GPC, GPC-FTIR) Performed on Styrene-Grafted Epoxidized Natural Rubber

Chapter 7: Gradient HPLC of Styrene-Grafted Epoxidized Natural Rubber (ENR50): Method Development, Results and Discussions

Chapter 8: Summary and Conclusions

List of Tables and Schemes

Chapter 6: Preliminary Experimental Analyses (FTIR, GPC, GPC-FTIR) Performed on Styrene-Grafted Epoxidized Natural Rubber

Chapter 7: Gradient HPLC of Styrene-Grafted Epoxidized Natural Rubber (ENR50): Method Development, Results and Discussions

List of Appendices

Chapter 1

General Introduction and Objectives

1.1 Introduction

In an ever-growing technological and industrial world, product properties play an enormous role. Not only does the increasing consumer market demand better products, but with the rising number of environmentally friendly groups, the question of biodegradability has also escalated. Today, polymer products are inevitable with applications ranging from agriculture to cosmetics. Needless to say, this is from one extreme to the other! This has created the absolute necessity to tailor-make products to fit their need, and in doing so, it has also created a new and challenging task for analytical chemists.

Up to now, the most commonly used techniques for product characterization included gel permeation chromatography (GPC), Fourier transform infrared spectroscopy (FTIR) and NMR. But with the advent of copolymers, polymer blends, polymer alloys, additives, laminates, paints and glues, these techniques have become less favorable and in some cases obsolete. The problem with GPC is that polymer mixtures have overlapping hydrodynamic volumes causing co-elution of the macromolecules. Some of the copolymers also have broad molecular mass distributions which can lead to peak overlapping; hence poor or no separation. Furthermore, GPC is very insensitive to the analysis of chemical composition distribution which makes this technique not favorable for the analysis of exotic polymers.

With FTIR and NMR the inclusion of the precursors can be confirmed, but the way in which it was included cannot be identified.

An analytical technique was therefore needed to separate polymers on the basis of their chemical composition, thereby allowing good qualitative analysis of the polymer in question.

In 1952 Tiselius and co-workers [1] introduced the technique of gradient elution analysis. This was followed by Snyder [2] who theoretically described the gradient process with his Linear Solvent Strength (LSS) model. The foundation was therefore laid and a new analytical technique born.

Gradient elution uses a mixed-solvent mobile phase whose components change with time, thereby creating a solvent gradient. Due to the fact that the building blocks of polymer blends, copolymers etc. are made up of different polymers (e.g. ungrafted precursors and grafted polymeric material), separation is possible on the basis of the difference in solubility of these building blocks. Even separation according to molecular mass is possible due to the difference in solubility.

With the use of gradient HPLC it is therefore possible to deduce whether or not grafting did take place. Polymers can also be separated from their additives if deemed necessary in certain preparative or analytical applications. Gradient elution can also be used for on-line analysis of reactions, thereby following the reaction from start to finish. Reactions can therefore be stopped when a certain stage is reached and in doing so a method is created to monitor and control polymer reactions. Gradient HPLC can therefore be used to analyze and evaluate polymers which were previously not characterizable. By doing this, the gap between analysis and product properties is dramatically shrinked; hence giving a better understanding of processes and products which allows the improvement in quality required to be globally competitive.

Although gradient HPLC has made a dramatic impact on polymer analysis, certain aspects of this technique must still be exploited in order to make it more applicable to more complex macromolecules now needed in the market. This is what fuelled the idea of this thesis along with the quest for knowledge and a better understanding of the gradient HPLC technique.

It is therefore the hope of the author to create a better understanding and to emphasize the importance of this technique to all readers throughout the remainder of this thesis.

1.2 Objectives

The main objective of this thesis was to evaluate styrene-grafted epoxidized natural rubber (ENR50) samples by using gradient HPLC in order to deduce whether or not grafting was achieved.

Towards this goal there were certain secondary objectives. These included:

1. Creating a stable latex system in which grafting can take place.
2. Evaluation of solubility parameters of the polymer precursors and solvents to determine the best solvents for the precursors as well as the grafted products.
3. Evaluation of the solubilities of the polymer precursors in order to determine the best way to solubilize them.
4. Evaluation of different solvent/non-solvent systems to determine the miscibility of such solvent pairs and to evaluate the cloudpoints of the polymer precursors.
5. Evaluation of the relevant gradient HPLC theory.
6. Preliminary experiments including GPC, FTIR and LC-transform to be able to acquire a better understanding of the grafted samples which will aid in the explanation of the gradient HPLC results.
7. Development of a gradient HPLC method.
8. Optimization of gradient HPLC to be able to obtain adequate separation between the precursors and the grafted material, hence allowing us to verify whether or not grafting had taken place.

By accomplishing the secondary objectives, sufficient knowledge and information will be gathered to analyze the grafted samples and to provide sufficient analytical results.

1.3 References

1   R.S. Alm, R.J.P. Williams, A Tiselius; *Gradient Elution Analysis I. A General Treatment*; Acta Chemica Scandinavica; **6**, 1952, 826-836

2   L.R. Snyder, H.D. Warren; *Linear Adsorption Chromatography VIII. Gradient Elution Practice. The Effect of Alkyl Substituents on Retention Volume*; Journal of Chromatography; **15**, 1964, 344-360

Chapter 2

Historical Overview: Synopsis of Gradient HPLC Analyses over the Last 50 Years

2.1 Introduction

Over the last century chromatography has developed into one of the most important, most used and most described analytical tools that is currently available. Although most forms of chromatography are based on differential solubility or adsorption, quite a few different forms were either developed or modified to allow for improved analysis or to do analysis which was previously not possible. This was all made possible through the introduction of new stationary phases, columns and detectors. Although this historical overview will be focussed on the development of gradient HPLC analysis, a quick overview of the most important dates in chromatography history will serve as a short introduction. This will therefore act as a sufficient "stationary phase" to separate chromatography into its vast amount of building blocks allowing thereafter the thorough investigation and evaluation of gradient elution chromatography.

A summary of the most important chromatography dates can be seen in Table 2.1. Due to the fact that both reversed-phase and normal phase gradient HPLC were used for experimental analysis during the course of this thesis, both types will be included in the historical discussion. Discussions will follow a chronological order.

Date	Researcher/s	Major achievements
1903	M.S. Tswett	Reported the process of column adsorption chromatography (coined the term chromatography from the Latin for "color writing"). Separated plant pigments through differential adsorption by passing plant tissue through a chalk column.
1915	R.M. Willstätter	Analyzed chlorophyll and other plant pigments.
1922	L.S. Palmer	Used Tswett's technique on various natural products.
1930	A. Tiselius	Electrochromatography
1931	R. Kuhn	Used chromatography to separate isomers of polyene pigments.
1938	N.A. Izmailov M.S. Shraiber	Developed thin-layer chromatography.
1941	A.J.P. Martin R.L.M. Synge	Created liquid-liquid partition chromatography.
1944	A.J.P. Martin R. Consden A.H. Gordon	Created paper chromatography.
1945	F. Prior	Developed the first analytical gas-solid (adsorption) chromatograph. In the mid 1950s, combined techniques e.g. GC/MS and GC-IR followed.
1950	A. Tiselius	Gradient elution
1966	C. Horvàth	High pressure liquid chromatography (HPLC)

Table 2.1: A summary of the most important dates in the development of chromatography as an analytical technique [1].

2.2 Gradient HPLC: The last 50 years

In 1952 Alm *et al.* [2] introduced the technique of gradient elution analysis for the evaluation of compound mixtures. This technique was merely a solution to all the problems that plagued them due to zone spreading resulting from a stepwise gradient. Because of all these problems, they saw the importance of investigating the effect of continuously increasing the solvent power and how this would influence the way in which a substance would move through a column. In gradient elution, zone spreading will not occur, but rather zone development. Alm explained it as follows: at low concentrations of the eluting solvent, movement of the tail will be nominal because of strong adsorption. At higher concentrations the zone will start to move but the tail will move more slowly and this will cause spreading. At still higher concentrations, the tail and front will move at equal rates and spreading stops. The zone is therefore developed and no spreading occurs. Alm also found that by pretreatment of the adsorbent the shape of the zones improved and the recovery value increased to nearly 100%. They therefore noticed that this technique could even be used for very strongly adsorbed compounds as well as for small quantities of material.

A lot of pioneering work on the theory of gradient elution was done by Snyder [3-9] during the 1960s. During the following years numerous gradient elution articles were published by him, leading to the Linear Solvent Strength model of gradient elution which he published in 1980 [10] and again in 1998 [11]. These two articles covered the theory of gradient elution extensively, starting with isocratic elution and showing the transition to gradient elution. Other important factors in these articles included the optimization of the gradient separation, computer simulation of gradient elution and normal phase elution in comparison to reversed-phase elution. Information contained in these articles formed the basis of theoretical discussions in this thesis.

During the early years of gradient elution HPLC, problems with reproducibility played a big role due to the fact that equipment producing the solvent gradient was not always that effective. Another problem was the lack of a simple method for the quantitative detection of materials without a suitable chromophore.

Only homopolymers and copolymers containing UV-absorbing groups were detectable in column gradient separations. With the advent of new technological breakthroughs this problem was overcome. In 1986 Mourey [12] reported on the analysis of poly(alkyl acrylate) and poly(alkyl methacrylate) homopolymers and copolymers with an evaporative light-scattering detector (ELSD). This detector made it possible to detect polymers which were otherwise difficult to detect by spectrophotometry and also allowed the use of good solvents or those having UV chromophores. With the incorporation of ELSD detectors, gradient elution became more suitable for the analysis of a wider range of polymers. This led to an increased number of applications associated with this technique.

In 1988 and 1989 Mori [13,14] investigated the separation of styrene-acrylate and styrene-methacrylate copolymers through liquid adsorption chromatography. Ethanol and chloroform were used as the mobile phase and both these solvents were good solvents for the polymers to be investigated. This trend of using two good solvents as a solvent gradient was introduced by Danielewicz and Kubin [15] in 1981 and is referred to as normal phase chromatography. A whole new way of separating copolymers was therefore started. In addition to the normal phase elution system that Mori used, the effect of column temperature, ethanol content in the mobile phase, the relationship between the composition of the copolymer and retention volume and molecular mass dependence on retention volume were also investigated. Through experiments it was concluded that an increase in column temperature lead to peak broadness and a retardation of copolymer elution. By obtaining a calibration curve for copolymer composition versus retention time and by doing size exclusion analysis of the copolymer, a 3-dimensional contour map (molecular mass, chemical composition distribution and copolymer weight fraction) were also demonstrated.

Although reversed-phase chromatography is the most popular mode used in liquid chromatography, the introduction of new synthetic polymers has accentuated the necessity of normal phase gradient chromatography. Through the use of normal phase chromatography, polymers can be separated on the basis of polarity of their functional groups thereby creating the opportunity to separate copolymers that were usually inseparable or which had a very low resolution.

Even though this mode of chromatography is not as frequently documented as reversed-phase chromatography, its applications are limitless and in some instances of great importance. In 1990 Schultz and Engelhardt [16] analyzed styrene and acrylonitrile copolymers by applying a normal phase gradient, from n-heptane to dichloromethane (DCM). By addition of methanol (MeOH) to DCM, the eluent composition of the copolymers was found to be independent of the nature of the stationary phase, indicating that solubility was the governing separation mechanism. In doing so, it was possible for them to evaluate both adsorption and precipitation systems and the consequent influence of different stationary phases on the selected system. The conclusion was that a non-porous stationary phase is advantageous in the case of precipitation chromatography due to the fact that porous stationary phases can lead to the formation of colloidal solutions due to the different velocities of the excluded polymers and the solvent front penetrating the pores. In the case of adsorption chromatography, porous stationary phases were preferred due to the higher interaction of the polymer with the stationary phase. They concluded that both techniques, for the styrene acrylonitrile copolymers, showed similar retention relationships.

Another important factor which was bound to be investigated, sooner or later, was the effect of sample remaining on the column after fractionation of the copolymer in question. In 1991 Teramachi and co-workers [17] studied the amount of sample retained on an ODS (octadecyl-modified silica gel) and a phenyl column under reversed-phase gradient conditions from acetonitrile (ACN) to tetrahydrofuran (THF). For the ODS column it was found that small peaks appeared with blank injections after the actual sample injection. After several blank injections, a perfect baseline was once again obtained. To ensure that no samples where injected accidentally, the sample injector and injector needle were thoroughly washed before each blank THF injection. It was therefore clear that peaks obtained on the ODS column for blank injections were caused by sample components remaining on the column. This phenomenon was not observed for the phenyl column. Unfortunately no clear explanation to the sample remaining on the column was given.

Another interesting aspect that was also studied in 1991 by Shalliker *et al.* [18], was the behavior of high molecular mass polystyrenes on a C_{18} reverse-phase column in a methanol-dichloromethane solvent system.

They were especially interested in looking at the influence of column pore size, sample load and flow-rate. Studies were done on 120 Å, 300 Å and 4000 Å columns to determine the influence of pore size on molecular mass. From these studies it was evident that elution occurred after the solvent solubility composition (solvent composition at which the polymer dissolves) if the polymer had access to the pores. This indicated a normal adsorption process. On the other hand, polymers which were excluded from the pores showed elution at or before the solvent solubility composition. By using columns of small pore size, the above effect was predominant. After evaluating different theories [19], Shalliker presented an explanation for what he termed "pre-elution". According to him, the high molecular mass polymers dissolve at the solvent solubility composition with the addition of good solvent via gradient elution and the polymer begins to elute. While the polymer is in solution and moving down the column, the solvent molecules have access to the pores but the polymers are excluded. This causes the velocity of the polymer along the column to be equal to that of the eluent but greater than that of the better solvent used in the solvent gradient and the polymer can again enter the poorer solvent gradient thus precipitation can again occur. This can be recurrent. However, as the molecular mass increases, an increasing time is required for the good solvent to diffuse out of the larger soluble polymer and thus allows delayed precipitation to occur. Through other experimental verifications, Shalliker also showed that the extent of pre-elution increased as the flow rate increased and that the effect of mass load dependence showed that there was a limited quantity of polymer which could be solvated at any time. Through his evaluations he concluded that a greater degree of selectivity could be obtained by using a column with large pores, but that band broadening still occurred.

In 1992 Teramachi and co-workers [20] again did work on the separation of poly(methyl methacrylate)-graft-polystyrene by adsorption high-performance liquid chromatography on an ODS column. They evaluated the chemical composition distribution of the copolymers by first studying and converting three samples of different compositions to chemical composition distribution. These samples were therefore used as standards. By following their own results of a previously discussed article, blank injections were done prior to sample injections to ensure a straight baseline.

Although the chemical composition distributions that they obtained for the grafted samples were very broad, this was in good accordance with theoretical predictions.

The ever-increasing numbers of polymers that are synthesized in the polymer industry demand that the chromatography equipment also keeps up with the changing times. This creates the opportunity to study and evaluate new columns, solvent systems, detectors etc. 1993 saw the introduction of a new column by Kirkland and co-workers [21]. The Zorbax Rx-SIL was prepared internally by them and contained highly purified, low-acidity unmodified porous silica microspheres. To evaluate this column, the Zorbax Rx-SIL was compared with the Zorbax SIL which consists of type A silicas and is generally more acidic and less purified. Comparisons were made on the influence of water level modifier in the organic mobile phase on solute retention, column efficiency, peak asymmetry and sample loadability. Results obtained from these comparison experiments showed that the Zorbax Rx-SIL could be used with a wider range of water modifier concentrations with little effect on separation resolution and that it has much better surface homogeneity than the Zorbax SIL. Zorbax SIL only showed better sample loadability, but that was due to the large surface area of the silica (330 m^2/g compared to 180 m^2/g for the Zorbax Rx-SIL). To conclude their evaluations, the Zorbax Rx-SIL was compared with eight commercial unmodified silica columns in terms of retention, selectivity, column efficiency and peak shape. Results confirmed that highly purified, less acidic type silicas e.g. Zorbax Rx-SIL generally give superior results and better reproducibility in normal phase HPLC.

From 1993 to 1994 Glöckner and co-workers [22-26] wrote a series of articles on sudden-transition gradients in normal phase as well as reversed-phase chromatography. In ordinary gradient elution chromatography, the two dominant modes of chromatography are normal phase (NP) and reversed-phase (RP). NP is usually used to separate polymers with a difference in polarity on a polar column by applying a gradient with increasing polarity. For RP chromatography a non-polar column is used and the gradient is of decreasing polarity. For RP, retention and solution are due to adsorption and solubility and in the case of NP, where separation is performed in the solubility range, the mechanism is governed by adsorption.

It is therefore clear that in order to acquire appropriate dissolution power and polarity, both adsorption and solubility must be increased simultaneously. With the use of sudden-transition gradients, Glöckner showed that it was possible to independently control both adsorption and solubility effects. By using sudden-transition gradients, fine tuning of solubility and adsorption effects are possible, optimization of a separation with respect to selectivity and time can be achieved and the occurrence of column breakthrough can also be overcome. To demonstrate sudden-transition gradients in the NP mode, Glöckner separated copolymers from styrene and acrylonitrile on a cyanopropyl column. The sample was injected into a non-polar starting eluent (n-heptane) and after rapid addition of a good solvent of moderate polarity (THF), elution was allowed by a strong polar eluent (MeOH). By applying the sudden-transition gradient, Glöckner was therefore able to separately control the solubility (by addition of the THF) and the polarity (MeOH) and in doing so proper retention could be achieved. Glöckner also showed the possibility of performing the sudden-transition gradient on a RP column when he separated styrene/ethyl methacrylate copolymers on a RP C_{18} bonded phase column. Here the sample was injected into a column filled with a polar non-solvent (ACN) which ensured proper retention of the samples on the non-polar column. With the sudden addition of THF, the dissolution power of the starting eluent was increased but not to the extent necessary for elution. By addition of a non-solvent of low polarity (n-heptane), elution was possible. Here eluting power was the consequence of its modifying effect on the polarity of the eluent mixture. This is better understood on the basis of the additivity of solubility parameters (δ) of solvents and non-solvents for a polymer

based on $\delta_{mix} = \dfrac{V_a x_a \delta_a + V_b x_b \delta_b}{V_a x_a + V_b x_b}$, where x is the molar fraction of solvents a and b

and V is the molar volume. Glöckner also showed the possibility of separating styrene/methyl methacrylate copolymers in NP as well as RP modes when using sudden-transition gradients. Glöckner concluded this series of articles with an appendix on how to perform sudden-transition gradients. This showed a comparison between normal gradients and sudden-transition gradients as well as a quick reference to preparing sudden-transition gradients.

Several articles on gradient HPLC were published in 1994 apart from those already mentioned above from Glöckner.

Schunk [27] reported on the CCD separation of methyl methacrylate-methacrylic acid copolymers by normal phase gradient elution HPLC. Separations were performed on a 10 μm LiChrospher Si100 100 Å pore silica column and a toluene/MeOH gradient was applied. Analyses showed excessive peak broadening with increasing methyl methacrylate content of the samples due to strong interactions with the column. By addition of glacial acetic acid, which is a good displacer for the strongly adsorbed copolymers, narrow peaks and reduced elution volumes were obtained. Schunk also evaluated the influence of molar mass on retention and confirmed similar findings of Shalliker [18] which was discussed earlier in this chapter. To evaluate the retention mechanism, Schunk compared HPLC elution data with turbidimetric titration results. From this he found that a strong solvent concentration was required to elute the copolymers thereby pointing to an adsorption mechanism. To conclude his work, he evaluated an orthogonal separation. In this instance fractions were obtained by gradient HPLC and then characterized by size exclusion chromatography (SEC) for molecular mass distribution. Through these analyses, a 3-dimensional plot was obtained.

Gradient HPLC does not only have to be used for chemical composition distributions as has been shown by Cools *et al.* [28]. They used the gradient HPLC technique (or GPEC, gradient polymer elution chromatography, as they have coined it) to evaluate the critical solvent conditions (CSC) for homopolymers. Existing methods to evaluate the CSC were described by Gorshkov [29,30,31] but these methods were time consuming and labor intensive. Cools evaluated homopolymers with different molar masses at constant temperature by starting with 100% solvent and increasing the non-solvent composition, thereby obtaining the retention time for each molar mass of the homopolymer at a specific non-solvent composition isocraticaly. By plotting the retention volumes vs. non-solvent composition for all the molecular masses, an intersection of the curves can be found. This intersection is indicative of the non-solvent composition at which the homopolymers with the same chemical structure but with different molar mass will elute simultaneously. Cools also determined the influence of chemical composition on the CSC by evaluating polybutadiene (PB) standards in the same way as described above. The CSC value obtained for PB showed a difference to the CSC of the PS standards previously evaluated.

Cools concluded that the CSC is dependent on the temperature, type of polymer and solvent/non-solvent combination. Through his work he also showed the improvement and greater accuracy of this technique in comparison with the existing method.

Staal *et al.* [32], who is part of the above-mentioned group of Cools [28], reported (in the same year) on the use of GPEC to evaluate the presence of polymer and oligomers in stored monomer. Staal pointed out that other techniques e.g. SEC and cloudpoint titrations can be used to obtain similar results but that oligomers of PS are soluble up to n=5. For SEC, evaluation of the monomer must be undiluted and this leads to column overload. The use of GPEC can overcome all these problems with the added advantage that the molecular masses of the oligomers and polymers can be calculated if well defined polymer standards were also evaluated under exactly the same conditions. Staal showed the advantages of GPEC by comparing the technique with turbidimetric titration measurements where it was not always possible to detect the cloudpoints visually due to the small amounts of polymer used.

In 1994 Heinisch and co-workers [33] designed a computer program to optimize gradient elution conditions with ternary solvent mobile phases in reversed-phase liquid chromatography (RPLC). In order to do this, preliminary experiments in gradient elution mode were necessary to predict the retention surface for each solute over the whole triangular solvent composition space. Values obtained through these experiments were then subjected to a computer algorithm which determined values for the gradient retention time, column dead time, resolution and mobile phase composition in which the more retained solute is eluted. The next step in the algorithm was then applied to calculate the capacity factors and, in turn, values for the gradient slope and initial solvent composition were calculated. These latter two values were further optimized through the algorithm until solvent composition values were reached which provide maximum resolution and best analysis times. To illustrate the accuracy of this computerized optimization, 12 phenyl urea herbicides were separated. From these experiments he showed that the predictions were in good agreement with the actual results.

In 1996 Zhu [34,35] went a step further by also allowing for changes in temperature in computer prediction of separation.

To perform the optimization step, four initial experiments, which included two different gradient times and two different temperatures, had to be conducted. Gradient retention as a function of temperature was predicted with reasonable accuracy.

Similar to the above two authors, Jandera [36-38] showed in 1997 and 1998 the prediction and optimization of retention in isocratic and gradient-elution normal phase high-performance liquid chromatography with binary and ternary solvents. Jandera also used retention data, which was acquired in initial runs under different conditions, to determine the parameters for the retention equations.

The retention equations described the dependence of the retention factor on the composition of the mobile phase.

The discussion of gradient HPLC literature of 1994 will be concluded with a review article by Cretier and Rocca [39]. In this article they reported on computer optimization of preparative reversed-phase liquid chromatography in order to obtain the largest amount of a specified component with an optimum purity level. To do the optimizations, BIOPREP was used. This is a commercially available computer program which uses the theory of the Linear Solvent Strength model to perform its optimizations. In order to do so, three preliminary experiments are required. The first two require the solute to be carried out chromatographically with two different gradient times to calculate the solute retention. The last experiment is used to calculate a constant value which is associated with a high injection volume. Apart from the optimization, they also studied the effect of sample overloading in gradient elution.

In 1995 Treiber [40] reported on the separation of a wide range of polar samples by using a relay gradient on a diol-column under normal phase conditions. Due to the fact that certain compounds are more polar than others, gradients must be applied accordingly to facilitate sufficient separation. To cover the widest possible polarity range, Treiber used a relay gradient which consisted of a series of consecutive gradients. The gradient that he used started from hexane (0.0) to ethyl acetate (4.4), from ethyl acetate (4.4) to acetic acid (6.2) and from acetic acid (6.2) to water (9.0). The polarity index numbers are given in brackets.

Every gradient started from 100% of the less polar solvent to 100% of the more polar solvent, with conditioning of the column between every consecutive gradient. Conditioning is very important and was performed by first washing the column, going from the most polar solvent to the least polar solvent of the new gradient. Treiber found that washing times were critical and had to be optimized to ensure reproducibility. Shorter wash cycles could result in insufficient displacement of the more polar solvent from the column, leading to less active polar sites and therefore reduced retention times. By applying the relay gradient, Treiber could therefore succeed in separating mixtures with a wide polarity range. By using polarity markers, these mixtures could also be classed according to polarity.

In the same year Schoonbrood and co-workers [41] used gradient polymer elution chromatography (GPEC) to analyze the microstructure of bulk and emulsion copolymers of styrene and 2-hydroxyethyl methacrylate. By determining the chemical composition distribution of the copolymers they showed, convincingly, that copolymerization did in fact take place. Due to the fact that there was a difference in retention times of the copolymer peaks, they concluded that the composition of the copolymers depended on molecular mass.

In 1996 Klumperman *et al.* [42] reported on the influence of molar mass on retention in gradient elution. They stressed the necessity of minimizing the effect of molar mass on separation when determining chemical composition distributions. By using a ACN/THF gradient (i.e. from a weak non-solvent to a good solvent) on a C_{18} modified silica column, they clearly showed that for the lower molar mass polystyrene standards, separation was possible. However, for molar masses above 100 000, the gradient was not suitable to separate the standards sufficiently. By applying a H_2O/THF gradient (i.e. from a strong non-solvent to a good solvent), better separation was obtained for standards from 500 to 2 700 000. Klumperman pointed out that the reason for the above was that gradient polymer elution chromatography is governed by a precipitation/redissolution mechanism. In other words, if all molar masses dissolved near the CSC, then separation and hence resolution would be limited. It is therefore necessary for the higher molar masses to dissolve at solvent fractions higher than the CSC and to obtain this, a strong non-solvent and good solvent must be used as eluent.

Apart from the above article, a whole range of articles by the same Dutch research group was published in 1996. Cools *et al.* [43] reported on the evaluation of the chemical composition distribution of styrene and butadiene copolymers by gradient elution HPLC. Cools pointed out that systematic method development is necessary to obtain good resolution of chromatograms; hence good results. The whole process of choosing the right solvent pairs and preliminary experiments were discussed, making this a very good and informative article for aspirant gradient HPLC chromatographers. Cools started out by first choosing different solvent and non-solvent pairs which he used to calculate the cloudpoint compositions (CPCs) of the relevant homopolymer standards (polystyrene and polybutadiene). By using a wide range of molar masses of the homopolymer standards, he also evaluated the influence of molar mass on the cloudpoints and on the GPEC separation and concluded that the dependence of molar mass on GPEC separations was negligible. By visual presentations of the cloudpoint graphs, Cools showed that an adequate difference between the cloudpoint composition of the polystyrene and polybutadiene homopolymers were obtainable in a THF/ACN solvent/non-solvent system. This was therefore the solvent system which was used with a C_{18} column for further chromatographic evaluations. By performing actual GPEC evaluations on the homopolymer standards with the specified solvent system, a sufficient difference between the retention times of the homopolymers was obtained which confirmed the cloudpoint evaluations. Well-defined homogeneous polystyrene-butadiene copolymers were also evaluated to obtain a relation between the chemical composition distribution and the retention time. This was done to obtain a calibration curve which was used to evaluate the emulsion polymerized copolymers. The calibration curve enabled them to calculate the chemical composition distribution of the copolymers. The article enabled Cools to show the importance of systematically planning a GPEC experiment and by obtaining good and representative results, the importance of the technique was once again confirmed.

Philipsen *et al.* [44,45,46] reported on the analysis of polyesters by means of gradient polymer elution chromatography. The regions of his investigations included the practical parameters and application of the analysis of polyester resins under reversed-phase conditions, the solubility effects of polyester resins and the behavior of crystalline polyesters under reversed-phase conditions.

Philipsen began the study by first evaluating the influence of some practical parameters which included loadability, injection volume, gradient shape and temperature. He found that by using a steeper gradient the number of oligomers that can be separated decreased. On the other hand, for a slower gradient the analysis time increased considerably and a trade off was reached between analysis time and gradient speed. A slight convex shaped gradient also provided a small improvement in resolution. An increase in temperature caused an increase in resolution of the chromatogram. Philipsen ascribed this to the increase in diffusion coefficients which leads to a faster mass transfer and therefore a decrease in peak broadening. Sample load was studied by injecting constant volumes of polyester samples of different concentrations. No effect was observed. An increase in injection volume caused peak broadening when increased to a certain volume. It was therefore concluded that injection volume should be kept as low as possible to minimize peak broadening. Valuable information resulting from the GPEC analyses included confirmation that the polyesters were mainly separated according to molar mass, but that the lower molar mass part of the samples showed a further separation based on chemical composition distribution. The study of the solubility of the polyester samples (second part of the study) was done under chromatographic conditions due to the dependence of cloudpoints on molar mass and concentration. Before any evaluations were performed, a suitable inert media had to be found, hence pure silica, non-porous glass, a stainless steel pre-column filter and a C_{18} column were compared. Non-porous glass was used as inert media and results obtained showed that concentrations of the eluting fractions were considerably lower than the maximum solubility. Philipsen explained that this phenomenon was due to kinetic effects which influenced re-dissolution.

In the third part of the study of polyesters Philipsen looked at the behavior of crystalline polyesters, as opposed to amorphous polyesters (as in the first two articles), under reversed-phase conditions. The study showed that crystalline polyesters produced non-reproducible results but that reproducible results could be obtained if the temperature is raised above the melting point of the polyester, where elution behavior is governed by sorption due to the prevention of crystal formation. The difference in elution behavior of crystalline and amorphous polymers made it possible to separate blends of both types of resins through eluent and temperature programming.

Philipsen also studied the effect of injection volume, flow rate and precipitation medium and found that all these effects changed the morphology of the precipitate, therefore giving rise to different redissolution behaviors. The reason for the difference in behavior between crystalline and amorphous polymer resins was that crystalline polyesters crystallized on the column after precipitation, whereas the amorphous polymers formed a swollen polymer-rich phase, rather than a solid-phase. Elution and separation of crystalline polyesters was therefore governed by thermodynamics and not by redissolution kinetics, as was the case for the amorphous polyesters.

In 1997 Meyer [47] investigated the equilibration time of a LiChrosorb type A (refer to [21]) silica column in the normal phase mode. Although silica columns are known for their long equilibration times, Meyer showed that for the reproducible separation of ten compounds of low to medium polarity, short equilibration times could be obtained if solvents of low to medium polarity were used as the mobile phase.

In the same year, a review article on the analysis of complex polymers by interaction chromatography was presented by Pasch [48]. Different aspects of HPLC were discussed and the separation of a graft copolymer of methyl methacrylate onto ethylene propylene diene terpolymer (EPDM) on a cyanopropyl-modified silica column described.

In 1998, Pasch and Trathnigg [49] also published a book on the HPLC of polymers. This book included an in-depth study of size-exclusion chromatography (SEC), liquid adsorption chromatography (LAC), liquid chromatography at the critical point of adsorption or liquid chromatography at critical conditions (LCCC), two-dimensional chromatography as well as the equipment and materials (e.g. detectors, solvent and columns) used for various HPLC applications. Every application is discussed through an introduction, theoretical overview, equipment specifications and overview as well as a few experimental examples. This provides the reader with a wealth of information and is an absolute necessity for any scientist starting out with or performing HPLC analyses.

2.3 Future trends in gradient HPLC

Due to the ever-increasing polymer market, new polymers have to be analyzed every day. This demands that new stationary and mobile phases have to be developed and increasing research has to be done to keep up with scientific innovations. Not only does this require ongoing research, but the advent of new techniques tickles the curiosity of actively linking different analytical techniques for better understanding of the structural features of tailored polymers. The coupling of CRYSTAF (crystallization analysis fractionation) and gradient HPLC has already been proposed by Graef [50] to analyze polyolefins.

It is therefore evident that gradient HPLC is indispensable in the analytical laboratory and that continuous research is necessary in the future to understand polymer structure/property relationships in order to be able to produce better polymer products.

2.4 References

1   M.S. Lesney; *Creating a Central Science. A Brief History of "Color Writing"*; Today's Chemist at Work; 7(8), 1998, 67-68, 71-72

2   R.S. Alm, R.J.P. Williams, A. Tiselius; *Gradient Elution Analysis I. A General Treatment*; Acta Chemica Scandinavica; 6, 1952, 826-836

3   L.R. Snyder; *Linear Elution Adsorption Chromatography I. Conditions for Existence*; Journal of Chromatography; 5, 1961, 430-441

4   L.R. Snyder; *Linear Elution Adsorption Chromatography II. Compound Separability with Alumina as Adsorbent*; Journal of Chromatography; 6, 1961, 22-52

5   L.R. Snyder; *Linear Elution Adsorption Chromatography III. Further Delineation of the Eluent Role in Separations over Alumina*; Journal of Chromatography; 8, 1962, 178-200

6   L.R. Snyder; *Linear Elution Adsorption Chromatography IV. Group Localization in the Adsorbate. Extension of the Role of Solute Structure in Separations over Alumina*; Journal of Chromatography; 8, 1962, 319-324

7   L.R. Snyder; *Linear Elution Adsorption Chromatography V. Silica as Adsorbent. Adsorbent Standardization*; Journal of Chromatography; 11, 1963, 195-227

8   L.R. Snyder; *Linear Elution Adsorption Chromatography VI. Deactivated Florisil as Adsorbent*; Journal of Chromatography; 12, 1963, 488-509

9   L.R. Snyder; *Linear Elution Adsorption Chromatography VII. Gradient Elution Theory*; Journal of Chromatography; 13, 1964, 415-434

10   L.R. Snyder; *Gradient Elution; High-Performance Liquid Chromatography. Advances and Perspectives*; C. Horvàth, Ed.; **1**, 1980, 207-316

11   L.R. Snyder, J.W. Dolan; *The Linear-Solvent-Strength Model of Gradient Elution*; Advances in Chromatography; **38**, 1998, 115-188

12   T.H. Mourey; *Polymer Adsorption Chromatography with Evaporative Light-Scattering Detection*; Journal of Chromatography; **357**, 1986, 101-106

13   S. Mori; *Determination of Chemical Composition and Molecular Weight Distribution of High-Conversion Styrene-Methyl Methacrylate Copolymers by Liquid Adsorption and Size Exclusion Chromatography*; Analytical Chemistry; **60**, 1988, 1125-1128

14   S. Mori, M. Mouri; *Separation of Styrene-Acrylate and Styrene-Methacrylate Copolymers According to Composition by Liquid Adsorption Chromatography*; Analytical Chemistry; **61**, 1989, 2171-2175

15   M. Danielewicz, M. Kubin; *High-Performance Column Adsorption Chromatography of Random Copolymers Styrene-Acrylics*; Journal of Applied Polymer Science; **26**, 1981, 951-956

16   R. Schultz, H. Engelhardt; *HPLC of Synthetic Polymers II. Chromatographic Characterization of Copolymers from Styrene and Acrylonitrile*; Chromatographia; **29**(7/8), 1990, 325-332

17   S. Teramachi, A. Hasegawa, T. Matsumoto; *Sample Remaining in an ODS Column after Compositional Fractionation of Copolymers by High-Performance Liquid Chromatography*; Journal of Chromatography; **547**, 1991, 429-433

18   R.A. Shalliker, P.E. Kavanagh, I.M. Russell; *Reversed-Phase Gradient Elution Behavior of Polystyrenes in a Dichloromethane-Methanol Solvent System*; Journal of Chromatography; **543**, 1991, 157-169

19   G. Glöckner; Gradient HPLC of Copolymers and Chromatographic Cross-Fractionation; Springer-Verlag, Heidelberg Berlin; 1991

20   S. Teramachi, A Hasegawa, T. Matsumoto, K, Kitahara, Y. Tsukahara, Y. Yamashita; *Determination of Chemical Composition Distribution of Poly(Methyl Methacrylate)-Graft-Polystyrene by Adsorption High-Performance Liquid Chromatography*; Macromolecules; **25**, 1992, 4025-4031

21   J.J. Kirkland, C.H. Dilks, J.J. DeStefano; *Normal-Phase High-Performance Liquid Chromatography with Highly Purified Porous Silica Microspheres*; Journal of Chromatography; **635**, 1993, 19-30

22   G. Glöckner; *Control of Adsorption and Solubility in Gradient High Performance Liquid Chromatography 1. Principles of Sudden Transition Gradients and Elution Characteristics of Copolymers from Styrene and Methacrylates*; Chromatographia; **37**(1/2), 1993, 7-12

23   G. Glöckner, D. Wolf, H. Engelhardt; *Control of Adsorption and Solubility in Gradient High-Performance Liquid Chromatography. Part 2: Sudden-Transition Gradient Elution of Styrene/Ethyl Methacrylate Copolymers*; Chromatographia; **38**(9/10), 1994, 559-565

24   G. Glöckner, D. Wolf, H. Engelhardt; *Control of Adsorption and Solubility in Gradient High-Performance Liquid Chromatography. Part 3. Sudden-Transition Gradient Elution of Styrene/Acrylonitrile Copolymers*; Chromatographia; **38**(11/12), 1994, 749-755

25   G. Glöckner, D. Wolf, H. Engelhardt; *Control of Adsorption and Solubility in Gradient High Performance Liquid Chromatography. Part 4. Sudden-Transition Gradient Elution of Styrene/Ethyl Methacrylate copolymers in Reversed-Phase Mode*; Chromatographia; **39**(3/4), 1994, 170-174

26   G. Glöckner, D. Wolf, H. Engelhardt;. *Control of Adsorption and Solubility in Gradient High Performance Liquid Chromatography. Part 5. Separation of Styrene/Methyl Methacrylate Copolymers by Sudden-Transition Gradients in Normal-Phase and Reversed Phase Mode*; Chromatographia; **39**(9/10), 1994, 557-563

27   T.C. Schunk; *Composition Distribution Separation of Methyl Methacrylate-Methacrylic Acid Copolymers by Normal-Phase Gradient Elution High-Performance Liquid Chromatography*; Journal of Chromatography A; **661**, 1994, 215-226

28   P.J.C.H. Cools, A.M. van Herk, A.L. German, W. Staal; *Critical Retention Behavior of Homopolymers*; Journal of Liquid Chromatography; **17**(14/15), 1994, 3133-3143

29   A.V. Gorshkov, S.S. Verenich, V.V. Evreinov, S.G. Entelis; Chromatographia, **26**, 1988, 338-342

30   A.V. Gorshkov, V.V. Evreinov, B. Lausecker, H. Pasch, H. Becker, G. Wagner; *Liquid Chromatography of Macromolecules under Critical Conditions. Fractionation of Poly(oxypropylene polyols) according to Functionality*; Acta Polymerica; **37**, 1986, 740-741

31   A.V. Gorshkov, H. Much, H. Becker, H. Pasch, V.V. Evreinov, S.G. Entelis; *Chromatographic Investigations of Macromolecules in the "Critical Range" of Liquid Chromatography I. Functionality Type and Composition Distribution in Polyethylene Oxide and Polypropylene Oxide Copolymers*; Journal of Chromatography; **523**, 1990, 91-102

32   W.J. Staal, P. Cools, A.M. van Herk, A.L. German; *Monitoring of Originated Polymer in Pure Monomer with Gradient Polymer Elution Chromatography (GPEC)*®; Journal of Liquid Chromatography; **17**(14/15), 1994, 3191-3199

33   S. Heinisch, P. Riviere, J.L. Rocca; *Computerized Optimization of Gradient Elution Conditions with Ternary Solvent Mobile Phases in RPLC*; Chromatographia; **39**(3/4), 1994, 216-223

34   P.L. Zhu, L.R. Snyder, J.W. Dolan, N.M. Djordjevic, D.W. Hill, L.C. Sander, T.J. Waeghe; *Combined use of Temperature and Solvent Strength in Reverses-Phase Gradient Elution I. Predicting Separation as a Function of Temperature and Gradient Conditions*; Journal of Chromatography A; **756**, 1996, 21-39

35   P.L. Zhu, J.W. Dolan, L.R. Snyder, N.M. Djordjevic, D.W. Hill, J.-T. Lin, L.C. Sander, L. van Heukelem; *Combined use of Temperature and Solvent Strength in Reversed-Phase Gradient Elution IV. Selectivity for Neutral (Non-Ionized) Samples as a Function of Sample Type and Other Separation Conditions*; Journal of Chromatography A; **756**, 1996, 63-72

36   P. Jandera, L. Petránek, M. Kucerová; *Characterization and Prediction of Retention in Isocratic and Gradient Elution Normal-Phase High-Performance Liquid Chromatography on Polar Bonded Stationary Phases with Binary and Ternary Solvent Systems*; Journal of Chromatography A; **791**, 1997, 1-19

37   P. Jandera, M. Kucerová; *Prediction of Retention in Gradient-Elution Normal-Phase High-Performance Liquid Chromatography with Binary Solvent Gradients*; Journal of Chromatography A; **759**, 1997, 13-25

38   P. Jandera; *Optimization of Gradient Elution in Normal-Phase High-Performance Liquid Chromatography*; Journal of Chromatography A; **797**, 1998, 11-22

39   G. Cretier, J.L. Rocca; *Gradient Elution in Preparative Reversed-Phase Liquid Chromatography*; Journal of Chromatography A; **658**, 1994, 195-205

40   L.R. Treiber; *Normal-Phase High-Performance Liquid Chromatography with Relay Gradient Elution I.   Description of Method*; Journal of Chromatography A; **696**, 1995, 193-199

41   H.A.S. Schoonbrood, A.M. Aerdts, A.L. German, G.P.M. van der Velden; *Determination of the Intra- and Intermolecular Microstructure of Bulk and Emulsion Copolymers of Styrene and 2-Hydroxyethyl Methacrylate by Means of Proton NMR and Gradient Polymer Elution Chromatography*; Macromolecules; **28**, 1995, 5518-5525

42   B. Klumperman, P. Cools, H. Philipsen, W. Staal; *A Qualitative Study to the Influence of Molar Mass on Retention in Gradient Polymer Elution Chromatography (GPEC)*; Macromolecular Symposia; **110**, 1996, 1-13

43   P.J.C.H. Cools, F. Maesen, B. Klumperman, A.M. van Herk, A.L. German; *Determination of the Chemical Composition Distribution of Copolymers of Styrene and Butadiene by Gradient Polymer Elution Chromatography*; Journal of Chromatography A; **736**, 1996, 125-130

44   H.J.A. Philipsen, B. Klumperman, A.L. German; *Characterization of Low-Molar-Mass Polymers by Gradient Polymer Elution Chromatography I Practical Parameters and Applications of the Analysis of Polyester Resins under Reversed-Phase Conditions*; Journal of Chromatography A; **746**, 1996, 211-224

45   H.J.A. Philipsen, M.R. de Cooker, H.A. Claessens, B. Klumperman, A.L. German; *Characterization of Low-Molar-Mass Polymers by Gradient Polymer Elution Chromatography II Solubility Effects in the Analysis of Polyester Resins under Reversed-Phase Conditions*; Journal of Chromatography A; **761**, 1997, 147-162

46   H.J.A. Philipsen, M. Oestreich, B. Klumperman, A.L. German; *Characterization of Low-Molar-Mass Polymers by Gradient Polymer Elution Chromatography III   Behavior of Crystalline Polyesters under Reversed-Phase Conditions*; Journal of Chromatography A; **775**, 1997, 157-177

47   V.R. Meyer; *Example of Gradient Elution in Normal-Phase Liquid Chromatography*; Journal of Chromatography A; **768**, 1997, 315-319

48   H. Pasch; *Analysis of Complex Polymers by Interaction Chromatography*; Advances in Polymer Science; Springer-Verlag; **128**, 1997

49   H. Pasch, B. Trathnigg; HPLC of Polymers; Springer-Verlag, Heidelberg Berlin; 1998

50   S.M. Graef; Ph.D. Proposal; Institute for Polymer Science, University of Stellenbosch; 1999

Chapter **3**

The Theory of Gradient Elution High-Performance Liquid Chromatography

3.1 Introduction

Although chromatography has been an active component in the scientific community for almost a century [1], the technique of gradient elution chromatography was only introduced in the 1950's by Alm and co-workers [2]. Since then, the use of gradient HPLC has grown in strength and is today a very important analytical method. In the 1960's Snyder [3] began to investigate the theory behind gradient HPLC and is still publishing relevant topics on gradient elution today [4-10].

In the following sections, an in depth study on the theory of gradient elution, based on Snyder's work [3,11,12], will be presented.

3.2 Theory of gradient elution

3.2.1 General theoretical aspects of gradient elution

To facilitate an explanation of the gradient elution technique, it will be compared to the well-known isocratic elution technique. As the name implies, isocratic HPLC means separation of compounds into different fractions through application of a solvent with a fixed composition, i.e. the solvent composition stays the same throughout the whole separation process and separation is based on the interaction of the different fractions with the column.

In gradient elution the solvent composition changes continuously with time, hence the name gradient, and separation is based on the difference in solubility of the composing fractions. The advantages of gradient elution can best be explained if the disadvantages of isocratic elution are first pointed out.

Isocratic elution is ineffective for samples that contain a wide range of retention values i.e. a wide range of k' (capacity factor) values, where the capacity factor is an indication of the retention of a certain compound in a particular solvent system due to column interactions. This can cause early eluting bands to have retention times, t_R, very near to the column dead time, t_0, causing poor resolution. Later eluting bands, on the other hand, will produce long retention times resulting in band broadening, tailing and also in poor resolution.

Gradient elution will give much better resolution of early eluting bands and it will also cause later eluting bands (in isocratic mode) to elute earlier, therefore eliminating band broadening and tailing. Also, if large concentrations of early eluting bands are present in isocratic elution, it can overload the column and result in overlapping and tailing of late eluting bands. This can be overcome by the application of a gradient. In isocratic elution, later eluting bands can interfere with the next sample injected and can also be irreversibly adsorbed by the column. Gradient elution will not pose such problems due to an ever-increasing solvent strength which will desorb the more strongly adsorbed compounds from the column before the next injection.

To define the term gradient elution it is necessary to look into the composing factors which gradient HPLC is based on. These factors include the solvent gradient, the separation process, the effect of solvents A and B on separation, the effect of gradient steepness on separation, the effect of gradient shape on separation, retention in isocratic vs. gradient mode and column capacity in gradient elution.

3.2.1.1 The solvent gradient

The solvent gradient forms the backbone of gradient elution. Due to the fact that the solvent composition is changing continuously, with time, it is clear that the solvents used are not the only driving forces, but also how the gradient changes with time.

By varying the steepness and also the shape of the gradient, different variations of solvent strength as a function of time are possible and this will clearly have an effect on separation. These three factors (nature of solvents, gradient steepness and gradient shape) can therefore have a huge impact on the outcome of separation and will be explained in more detail.

3.2.1.1.1 Solvents used

Solvents used should adhere to two basic requirements, namely, they should be miscible throughout the entire gradient and one solvent should be chromatographically stronger than the other one. The use of only two solvents (binary gradient) is not compulsory as three solvents (ternary gradient) may be used in conjunction with one another.

In the case of a ternary gradient, the gradient can start off as a mixture of two solvents and then either go to a stronger solvent straight away, or it can first go to an intermediate solvent and then to the strongest solvent. In the binary gradient case, the gradient can go from one weaker solvent to a strong solvent. A schematic presentation of the different solvent systems can be seen below in Scheme 3.1.

100%A	→	100%C			A = weak solvent
50%A/50%C	→	100%C			B = intermediate solvent
50%A/50%B	→	100%B	→	100%C	C = strong solvent

Scheme 3.1: Schematic presentation of different solvent systems.

The % fraction of A, B and C in the gradient is relevant to the separation process and was chosen arbitrarily here just to clarify a statement.

3.2.1.1.2 Gradient steepness

The gradient steepness can be defined as the rate at which the gradient is applied, i.e. the change in % of solvent A as a function of time.

Gradient steepness is represented by ϕ' where

$$\phi' = (change\ in\ volume\ fraction\ A)/time \qquad\qquad (3.1)$$

Thus for 0 – 100% A,

$$\phi' = 1/t_G \ (min^{-1}) \qquad\qquad (3.2)$$

where t_G = time from beginning to the end of the gradient.
Another way to represent gradient steepness is

$$\phi'' = (change\ in\ volume\ fraction)/(t/t_0) \qquad\qquad (3.3)$$

$$= \phi't_0 \qquad\qquad (3.4)$$

$$= t_0/t_G \qquad\qquad (3.5)$$

where t_0 is the column dead time.

3.2.1.1.3 Gradient shape

The gradient shape does not have to be linear, but can accept different shapes to achieve best separation results. Through the different shapes it is possible to incorporate important factors into the gradient, for example, gradient hold, gradient delay and gradient reversal. Gradient hold is used to keep the gradient at a certain end condition, in other words, the gradient is kept at pure solvent C (referring to Figure 3.1(a)) for a certain amount of time t_H. Gradient delay, on the other hand, is if the elution is started with pure solvent A (Figure 3.1(b)) and kept there for a certain amount of time (isocratic) before starting the actual gradient. Reverse gradient is when the solvent goes back to pure A from pure C in order to restore the original column conditions (Figure 3.1(d)). This is also called column regeneration and is usually performed before subsequent sample injections. A few gradient shapes can be seen in Figure 3.1.
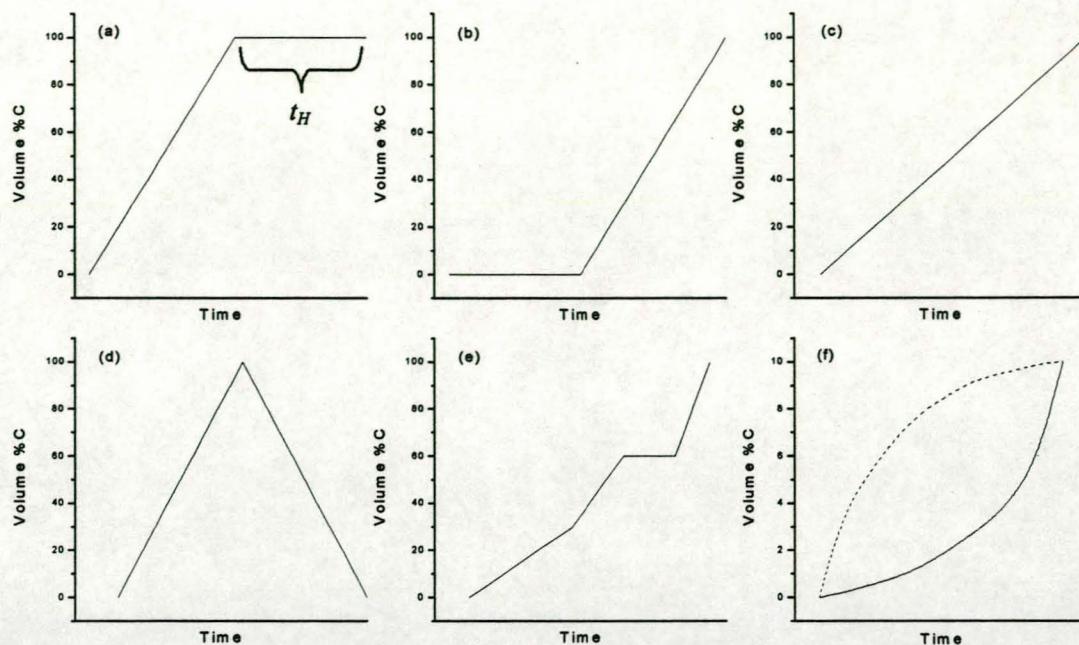
Figure 3.1: Presentation of a few possible gradient shapes [11].

3.2.1.2 The separation process

Isocratic elution can result in problems related to band broadening of later eluting bands and also a reduction in sensitivity. This is not the case in gradient elution, as can be explained with a simple example.

Figure 3.2 represents a compound (X) with capacity factor $k' \geq 10$, in other words, X represents a late eluting band. The capacity factor is represented by the dashed line and decreases with time, while r (fractional distance between the column inlet and outlet) increases with time (solid line). The retention time is denoted with t and t_X is the time at which the compound will leave the column.

For early eluting bands, $k' \leq 1$, and therefore elution will be complete before any significant change in mobile phase composition occurs. A similar elution pattern between isocratic and gradient elution can therefore be expected. For later eluting bands it can be seen from Figure 3.2 that the capacity factor falls in the range $1 < k' < 10$.
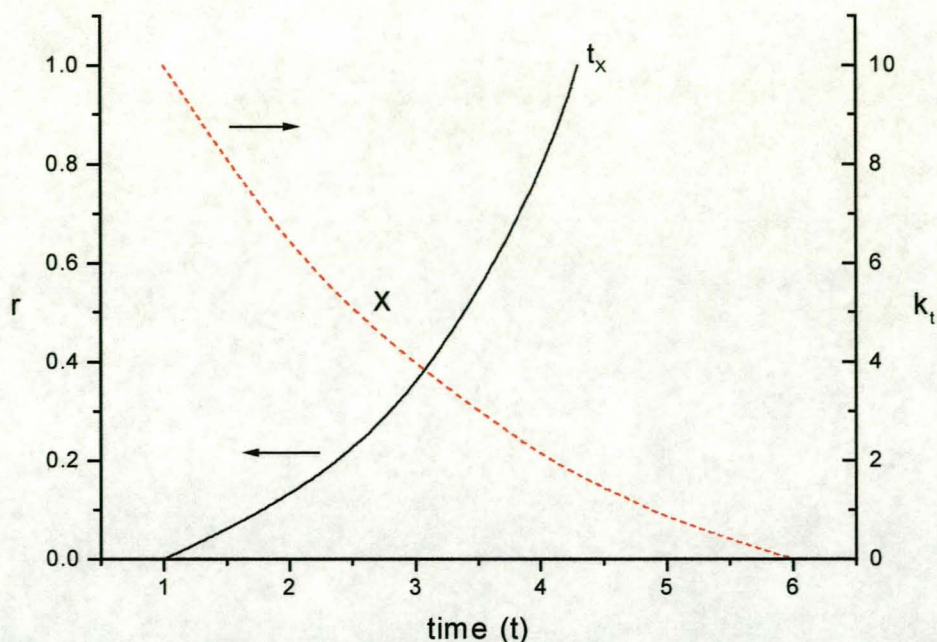
Figure 3.2: Illustration of the fractional migration (r) of a band along the column and the value of band k' (k_t at time t) as a function of the time [11].

In isocratic separation, the resolution is given as

$$R_s = \left(\tfrac{1}{4}\right)(\alpha_i - 1)N^{1/2}\left[k'(1+k')\right] \tag{3.6}$$

and bandwidth w as

$$w = \left(4/N^{1/2}\right)t_0(1+k') \tag{3.7}$$

where α_i is the isocratic separation factor for two adjacent solute bands equal to the ratio of their retention factors and N is the column plate number. A value of $k' \geq 2$ favors maximum resolution. For gradient elution k' decreases with time, but for isocratic elution k' increases. From Equations 3.6 and 3.7 it is clear that small k' values will produce narrow bands and increased sensitivity and it can therefore be concluded that gradient elution will produce better separation than its isocratic counterpart. Equations 3.6 and 3.7 are not entirely correct for gradient elution due to the absence of a band compression factor G which will be explained later (Section 3.3.1.2). This, however, will not have an effect on the above explanation.

3.2.1.3 Effect of specific solvents A and B on the separation

The choice of solvents in a gradient elution system is very important due to the effect it has on resolution and bandwidth. If solvent A is too strong and solvent B too weak (A being the non-solvent and B the solvent), the quality of the separation will be reduced due to the fact that all the bands will elute near the end of the gradient. Also, if A is too weak and B too strong, all the bands will elute near the beginning of the gradient and separation time will be wasted. To clarify the above statements, the terms strong and weak solvents and strong and weak non-solvents will be defined. A strong solvent for a particular compound is a solvent that is capable of solubilizing the compound to a high degree. More non-solvent is necessary to precipitate a compound solubilized with a strong solvent. A weak solvent, for the same compound as above, is a solvent that is capable of solubilizing the compound but not to the same high degree as a strong solvent. Less non-solvent is needed to precipitate the compound solubilized with a weak solvent. A strong non-solvent will be able to keep a compound out of solution to a much better extent and consequently more solvent has to be added to solubilize the compound. A weak non-solvent, on the other hand, will not be able to keep the same compound (as above) out of solution so effectively and will need less solvent to solubilize the compound.

When choosing solvents, care must be taken to avoid solvents whose strengths are too dissimilar because this can cause solvent demixing, leading to deterioration of the separation in the center of the chromatogram, accompanied by a sudden reduction in bandwidth at that point in the separation.

3.2.1.4 Effect of gradient steepness on the separation

Gradient steepness is the speed at which a gradient is applied, in other words, the increase in gradient strength in %/min. E.g. a gradient of 5%/min will require 20 minutes to go from 0% to 100% solvent strength and will therefore be very steep. A gradient of 2%/min, on the other hand, will require 50 minutes to complete and the steepness of the gradient will decrease dramatically.

A decrease in steepness will lead to broader bands, decreased detection sensitivity and longer separation times. Separation can therefore be improved by adjusting the gradient steepness until an optimal value is obtained. Note that adjustment of the steepness will produce a compromise between sensitivity and resolution, as can be seen in the graph of resolution (R_s) and sensitivity (peak height) versus $1/b$ (time) where b is the gradient steepness applied (Figure 3.3). The best selection is located around the intersection of the two curves.
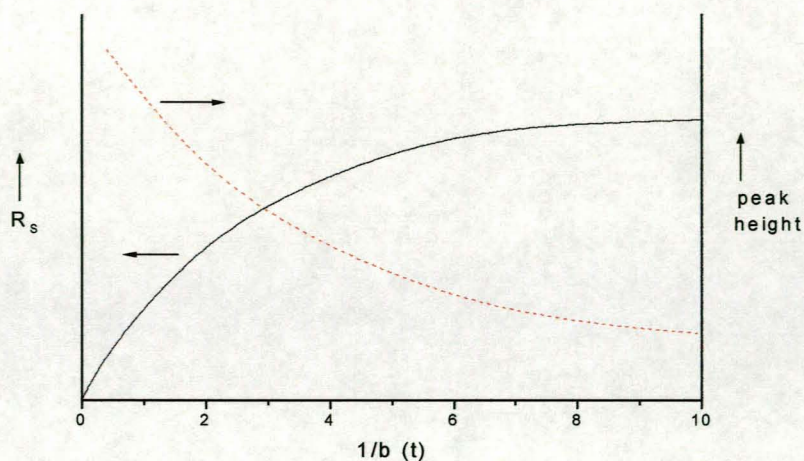
Figure 3.3: Illustration of the compromise between resolution (R_s) and sensitivity (peak height) for gradient elution [11].

3.2.1.5 Effect of gradient shape on separation

Gradient shape plays a big role in the separation of compounds. Different shapes include all those in Figure 3.1, but discussions here will be limited to the shapes in 3.1(c) and 3.1(f). In 3.1(f) two different shapes are visible, namely a concave shape (solid line) and a convex shape (dashed line). The concave shape will start off with a fast gradient and gradually decrease as a function of time. The slower gradient at the end will therefore produce band broadening and early eluting bands will be closer together. The convex shape will produce the opposite effect (band broadening of early eluting bands and bunching of later eluting bands) due to a slow gradient in the beginning which increases more rapidly as the gradient nears completion. The shape in 3.1(c) is linear, and is used most frequently in the separation of compounds. Convex or concave gradient shapes are generally used to increase resolution in a specific part of the gradient.

3.2.1.6 Column capacity in gradient elution

Column overloading increases with the k' value of the band in isocratic elution, hence the capacity of the column is usually less for later eluting bands. This problem does not affect gradient elution due to the average capacity factor that is maintained throughout all the bands. This results in greater column capacity when compared to isocratic elution and therefore better separation efficiency.

3.2.2 Other factors affecting gradient and separation performance

3.2.2.1 Solvent degassing

Solvent degassing is very important because in a low pressure solvent delivery system air bubbles can form causing interference with the pumps during each pump stroke and leading to incorrect gradient delivery. Three methods of degassing are available namely (1) degassing by vacuum, (2) on-line degassing and (3) helium sparging. By applying helium sparging, the dissolved air in the solvent is replaced by helium and, due to the low solubility of helium in all solvents, it can easily be removed through on-line degassing.

3.2.2.2 Baseline

Baseline drift and noise can be caused by solvent impurities and also dissolved oxygen in the solvent resulting in absorbance at wavelengths below 260 nm. Solvent impurity problems can be eliminated by the use of HPLC-grade solvents or, in the case of a water gradient, the use of de-ionized distilled water. Baseline drift due to oxygen can be rectified by degassing and helium sparging.

3.2.2.3 Column regeneration

Column regeneration must be done after each sample injection to take the column back to its original conditions before the next injection occurs. This can be done by applying a reverse gradient from the end solvent e.g. B to the beginning solvent e.g. A, and keeping the system at A for a few minutes before injecting the next sample.

The reverse gradient can be done at higher flow rates and gradient steepness than gradients applied during the separation step, thus decreasing the time involved. The time necessary to keep the column at condition A before the next injection is usually calculated as the time necessary for the pumps to deliver two to three column-volumes of solvent.

3.3 Theory through mathematical modeling

3.3.1 The Linear Solvent Strength (LSS) Model [11,12]

The fundamental equation of gradient elution is based on a stepwise gradient due to its easy mathematical manipulation. However, if an infinite number of steps are to be taken, then a continuous gradient can be modeled using this equation. The equation for gradient elution is:

$$\int_{0}^{V_R'} \frac{1}{V_m} \frac{dV}{k_a} = 1 \qquad (3.8)$$

The equation is based on the integration of solute retention volumes from 0 to V_R' where V_R' is the solute retention volume corrected for V_m (column dead volume). V_R' can be expressed as the cumulative volume of mobile phase that has passed through the column and k_a is the instantaneous value of k for the solute band at any time during the gradient. Due to each volume element dV of the mobile phase passing through the band center, the band will undergo band migration $dx = dV/V_m k_a$. The sum of all the band migrations must be equal to 1 ($\sum dx = 1$) if the total volume of mobile phase passing through the band center equals the corrected retention volume.

Therefore, if k is known as a function of V_t or t where $t = V_t / F_{rate}$ (F_{rate} = flow rate), then Equation 3.8 can be solved for the solute retention volume or solute retention time $t_R = V_R / F_{rate}$.

Before going further, it is important to note that a linear gradient for a gradient elution system can be represented by

$$\phi = \phi_0 + \left(\frac{\Delta\phi}{t_G} \right) t \qquad\qquad (3.9)$$

where ϕ_0 is the value of ϕ at $t = 0$, $\Delta\phi$ is the change in ϕ during the gradient run and t_G is the duration of the gradient.

The capacity factor k_i for different compounds can be expressed as

$$log\, k_i = log\, k_0 - S\phi \qquad\qquad (3.10)$$

where k_i is the capacity factor at a given time after a gradient separation begins, k_0 is the capacity factor at the beginning of the gradient, ϕ is the volume fraction of solvent and S is a constant for a gradient elution system. The above equation holds for reverse-phase (RP) gradient elution systems.

For normal phase (NP) gradient elution systems, Equation 3.10 will have the form

$$log\, k = c - n\, log\, X_B \qquad\qquad (3.11)$$

where c and n are constants and only the mole fraction X_B of strong solvent (e.g. solvent B) varies. Note that the capacity factor can change linearly with time due to the linear increase of solvent strength. By utilizing all of the above equations it is therefore possible to do a mathematical presentation of gradient elution through the LSS model.

This model makes it possible to derive equations for retention, bandwidth and resolution of a gradient elution system. Although equations will be derived for a RP system, a NP system LSS model can also be derived by using Equation 3.11 instead of Equation 3.10.

3.3.1.1 Retention

For a RP gradient system Equation 3.10 can be re-written by combination with Equation 3.9 to give

$$log\ k = log\ k_0 - \left(\frac{S\Delta\phi}{t_G}\right)t \tag{3.12}$$

$$= log\ k_0 - b\left(\frac{t}{t_0}\right) \tag{3.13}$$

In Equation 3.13, b can be defined as

$$b = \frac{t_0\Delta\phi S}{t_G} = \frac{V_m\Delta\phi S}{t_G F_{rate}} \tag{3.14}$$

and is a function of the gradient steepness.

To express the retention time in equation form, it is first necessary to re-write Equation 3.8 as a function of retention time and not retention volume and to take $k_a = k$. After substitution with Equation 3.13 and integration, the retention time can be defined as follows:

$$t_R = \frac{t_0}{b} log\ (2.3k_0 b + 1) + t_0 \tag{3.15}$$

This equation will simplify to

$$t_R = \frac{t_0}{b} log\ (2.3k_0 b) + t_0 \tag{3.16}$$

for solutes that are strongly retained i.e. k_0 very large. Both equations must be corrected for the dwell or hold-up volume (the delay of the arrival of the gradient at the column inlet) so that Equation 3.16 now becomes

$$t_R = \frac{t_0}{b} log\,(2.3k_0 b) + t_0 + t_D \qquad (3.17)$$

where $t_D = V_D / F_{rate}$.

In situations where k_0 is not very large and the dwell time is long, pre-elution can occur where the solute can travel a long distance along the column before the gradient reaches it. In this case Equation 3.17 will not hold and must therefore be corrected by subtracting the extra time of solute travel. The extra distance that the solute will travel before the gradient reaches it, is

$$x = \frac{t_D}{t_0 k_0} \qquad (3.18)$$

and the correction term (t_{1-x}) is then the time required to migrate through the remaining part of the column. The correction term is given by

$$t_{1-x} = \frac{t_0}{b} log\,[2.3k_0 b(1-x)+1] + (1-x)t_0 \qquad (3.19)$$

The retention time can then be calculated by substituting Equation 3.19 into

$$t_R = t_0 + t_{1-x} \qquad (3.20)$$

If the solute does not elute during the applied gradient, Equation 3.17 again does not hold. In this instance the retention time is given as

$$t_R = t_G + t_0 + t_D + (1-r)k_z t_0 \qquad (3.21)$$

where the fractional migration (r) is given by $r = \dfrac{10^g}{2.3k_0 b}$ and k_z is the value of k_a at the end of the gradient. In the fractional migration, $g = bt_G / t_0$.

3.3.1.2 Bandwidth

To determine the bandwidth of a given solute, it is necessary to have the final k value (k_f) as the band elutes from the column. To do so, it is necessary to use the equation which assigns a value to k_a after a certain fractional migration distance has been reached. This equation can be written as

$$k_a = \frac{1}{2.3br + 1/k_0} \qquad (3.22)$$

The k_f value will be obtained as the band leaves the column which implies that $r = 1$. Equation 3.22 can then be re-written as

$$k_f = \frac{1}{2.3b + 1/k_0} \qquad (3.23)$$

for $r = 1$ and taking $k_a = k_f$.

For k_0 very large, Equation 3.23 becomes

$$k_f = \frac{1}{2.3b} \qquad (3.24)$$

This value for k_f can now be substituted into the bandwidth equation used for isocratic elution, giving

$$W = 4N^{-1/2}t_0\left(1 + k_f\right) \quad \text{(no band compression)} \qquad (3.25)$$

To allow for band compression during migration, an extra band compression factor must be included in the equation, thus giving

$$W = 4GN^{-1/2}t_0\left(1 + k_f\right) \quad \text{(band compression)} \qquad (3.26)$$

In the above equations N is the plate number and is given by

$$N = 16\left\{\frac{(2.3b + 1)Gt_0}{2.3bW}\right\}^2 \qquad (3.27)$$

and the band compression factor is given by

$$G^2 = \frac{1 + p + \frac{p^2}{3}}{(1 + p)^2} \qquad (3.28)$$

with $p = \frac{2.3k_0b}{k_0 + 1} \approx 2.3b$ (for large k_0).

3.3.1.3 Resolution

The resolution of gradient elution can also be put into equation form by substituting W_1, W_2, t_1 and t_2 into

$$R_S = \frac{2(t_2 - t_1)}{W_1 + W_2} \qquad (3.29)$$

The above equation is for isocratic elution, but becomes valid for gradient elution after substituting the gradient values for W_1, W_2, t_1 and t_2. The values for gradient elution can be written as follows

$$t_1 = \frac{t_0}{b}\log(2.3k_{01}b) + t_0 + t_D \qquad (3.30)$$

and

$$t_2 = \frac{t_0}{b}\log(2.3k_{02}b) + t_0 + t_D \qquad (3.31)$$

Similar equations with k_{01} and k_{02} will follow for W_1 and W_2 and after substitution into Equation 3.29, the resolution for a gradient system can be written as

$$R_S = \frac{2.3}{4} log\left(\frac{k_{01}}{k_{02}}\right) N^{1/2} \left[(2.3b + 1)G\right]^{-1} \qquad (3.32)$$

and further simplified to

$$R_S = \frac{1}{4}(\alpha_g - 1) N^{1/2} \left[(2.3b + 1)G\right]^{-1} \qquad (33)$$

for small values of x where $2.3 log\ x \approx x - 1$. α_g is the separation factor in gradient elution.

3.4 Conclusions

Through mathematical modeling via already existing isocratic equations, it is possible to derive equations for gradient elution HPLC. This LSS model makes it possible for the chromatographer to do some preliminary calculations to predict (and optimize) gradient separation before any experiments are done, thus eliminating time spent on manually trying to obtain the perfect separation. The LSS model also allows us to model gradient separation on a computer (e.g. DryLab, LC Resources) [12] leading to a better understanding of the separation phenomena and enabling us to enhance this chromatography technique.

3.5 References

1   L.R. Snyder; *Modern Practice of Liquid Chromatography: Before and After 1971*; Journal of Chemical Education; **74**(1), 1997, 37-44

2   R.S. Alm, R.J.P. Williams, A. Tiselius; *Gradient Elution Analysis: I. A General Treatment*; Acta Chemica Scandinavica; **6**,1952, 826-836

3   L.R. Snyder; *Linear Elution Adsorption Chromatography VII Gradient Elution Theory*; Journal of Chromatography; **13**, 1964, 415-434

4   L.R. Snyder, J.J. Kirkland, J.L. Glajch; Practical HPLC Method Development, Second Edition; Wiley, New York; 1997

5   L.R. Snyder, K. Valko, J.L. Glajch; *Retention in Reversed-Phase Liquid Chromatography as a Function of Mobile-Phase Composition*; Journal of Chromatography; **656**(1-2), 1993, 501-519

6   L.R. Snyder, J.J. DeStefano, J.A. Lewis; *Reverse-Phase High Performance Liquid Chromatography Method Development Based on Column Selectivity*; LC-GC; **10**(2), 1992, 130, 133-134, 136, 138-139

7   L.R. Snyder, A. Drouen, J.W. Dolan, A. Poile, P.J. Schoenmakers; *Software for Chromatographic Method Development*; LC-GC; **9**(10), 1991, 714-716,718, 720-722, 724

8   L.R. Snyder, D.D. Lisi, J.D. Stuart; *Computer Simulation of Gradient Elution Separation. Accuracy of Predictions for Non-linear Gradients*; Journal of Chromatography; **555**(1-2), 1991, 1-19

9   L.R. Snyder, M.A. Stadalius, J.S. Berus; *Reversed-phase HPLC of Basic Samples*; LC-GC; **6**(6), 1988, 494-496, 498-500

45

10   L.R. Snyder; *Mobile-phase Effects in Liquid-solid Chromatography*; High-Performance Liquid Chromatography; **3**, 1983, 157-223

11   L.R. Snyder; *Gradient Elution*; High-performance Liquid Chromatography. Advances and Perspectives; **1**, 1980, 207-316

12   L.R. Snyder, J.W. Dolan; *The Linear Solvent Strength Model of Gradient Elution*; Advances in Chromatography; **38**, 1998, 115-188

Chapter 4

Synthesis of Styrene-Grafted Epoxidized Natural Rubber (ENR50-PS)

4.1 Introduction

Styrene-grafted epoxidized natural rubber was selected as a model system for analysis by gradient high-performance liquid chromatography. It was chosen because of the functionality of the epoxide groups and also because of the presence of the chromophore (the benzene ring) in the styrene which would make the copolymer "visible" in a UV-detector.

In order to synthesize the copolymer it was necessary to either prepare or purchase the styrene monomer and the polymer. Epoxidized natural rubber (ENR50) was used as the polymer in a latex form. Due to the fact that the rubber was already in a latex form, a further emulsion polymerization process was thought to be an efficient way to prepare the copolymer.

4.2 Historical overview of epoxidized natural rubber (ENR) and the grafting of styrene onto natural rubber (NR)

4.2.1 Epoxidized natural rubber (ENR)

Natural rubber (NR) was first epoxidized in 1922 by Pummerer as reported by Gelling [1]. During the following years, extensive experiments on the epoxidation of NR were carried out to enhance the already valuable properties of ENR.

This was done by looking at various reaction conditions and also secondary ring-opening reactions that could occur under certain conditions.

In 1981, Ng and Gan [2] epoxidized natural rubber in latex form by reacting it with *in situ* generated performic acid. Due to the insolubility of the samples, analysis of the ENR was done with infrared spectroscopy. It was seen that the reacted NR had three new adsorption bands i.e. a broad hydroxyl absorption in the region $3600 - 3200$ cm^{-1}, a carboxyl absorption at 1720 cm^{-1} and absorption from the THF ring at 1065 cm^{-1}. By changing the hydrogen peroxide concentration, which was used with the performic acid in the epoxidation reaction, the extent of the reaction could be changed. At low hydrogen peroxide concentration, ENR was isolated as the sole product. The epoxide formation decreased with an increase in hydrogen peroxide concentration, with an accompanying increase in the formation of tetrahydrofuran ring structures. Through their experiments they found that the formation of epoxide groups had a limiting value which coincides with the coagulation of the rubber. The reaction scheme of the THF ring formation can be seen in Figure 4.1.
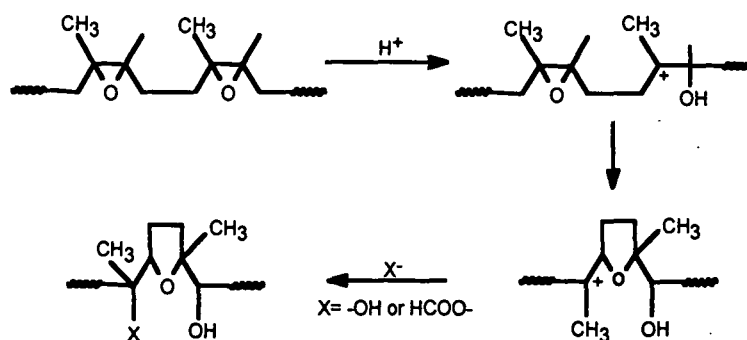
Figure 4.1: THF ring formation during epoxidation of NR [2].

Crosslinking of polymeric chains with epoxide groups through the formation of ether linkages can be seen in Figure 4.2.

In 1984 Gelling [1,3] modified natural rubber with peracetic acid to form ENR. By varying the different reaction conditions, he obtained different degrees of epoxidation and also different end products, depending on the temperature and acidity.
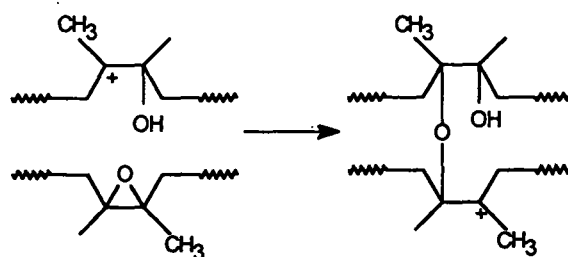
Figure 4.2: Crosslinking through the formation of an ether linkage [2].

He showed experimentally that the glass transition temperature (T_g) of ENR increased with an increasing level of epoxidation and that the T_g was well defined. Epoxide ring-opened structures, however, showed a broadening of T_g. He also showed that molecular mass decreased with increasing levels of epoxidation, but that this was complicated by the fact that the solubility decreased with increasing levels of epoxidation due to higher gel contents. Further experiments involved the investigation of the effect of epoxidation on scorch delay, strain crystallization, resistance to hydrocarbon oils and gas permeability.

In the same year (1984) Burfield *et al.* [4] investigated three different epoxidation routes. These routes included the use of bromohydrin intermediates, hydrogen-peroxide-catalyzed systems and peracetic acid which allowed a high degree of epoxidation of NR with no detectable side reactions. For the bromohydrin route they found that a high pH will prevent coagulation and ensure a high degree of epoxidation and therefore eliminate the chance of any side reaction (Figure 4.3).
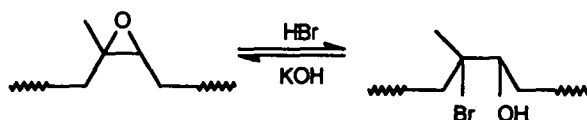
Figure 4.3: Epoxidation via the bromohydrin route [4].

Hydrogen peroxide, on the other hand, could be used alone or catalyzed as an efficient epoxidation agent for low molecular mass alkenes. The last route that they followed was the addition of preformed peracetic acid to the latex. At low temperatures, this route proved to be an excellent way to epoxidize NR, with no evidence of ring-opened epoxide groups.

In 1985, Bradbury and Perera [5] showed, by using carbon NMR spectroscopy, that epoxidation of NR occurs by a random process in a homogeneous solution as well as in the rubber latex. This showed that the performic acid is able to penetrate the latex droplet. This was a great breakthrough because it is cheaper to epoxidize NR in latex form than in organic solvent.

In 1991, Nguyen Viet Bac *et al.* [6] looked at stabilizing the NR latex by a nonionic surfactant to synthesize products with a large range of epoxide contents and no side-ring opening groups. They also studied the influence of the degree of epoxidation on the stability and gel content of ENR and showed that the gel content increased and solubility decreased with increasing epoxidation due to the presence of new polar groups in the polymer backbone. Lastly, they studied the effect of epoxidation by gel permeation chromatography (GPC) and concluded that for the soluble fraction, epoxidation was accompanied by a decrease in molecular mass and a change in molecular mass distribution.

In 1993 Nguyen Viet Bac *et al.* [7] used a reducing agent to degrade NR into short chain segments, thus obtaining a liquid natural rubber (LNR). From here on they studied the epoxidation of LNR and also its influence on the gel content. Results showed that the gel content decreased dramatically in the presence of the reducing agent. Chain scission could also be applied after epoxidation of the NR.

In 1997 Gan and Hamid [8] did work on the partial conversion of epoxide groups to diols in ENR. This was done to enhance the chemical and physical properties of ENR.

Epoxidation of natural rubber is quoted as a random process and several degrees of epoxidation can be obtained i.e. 25 % epoxidized (ENR25), 50 % epoxidized (ENR50) and 75 % epoxidized (ENR75).

4.2.2 Grafting of styrene onto natural rubber

Grafting of monomers onto NR has been carried out from as early as 1938 [9].

In 1955 Bloomfield [10] reported on the grafting of styrene onto NR and the effect of grafting on the physical properties of the rubber.

Unfortunately there is no literature available on the grafting of styrene onto ENR, but reaction conditions similar to those used in the styrene/NR grafting system were used in these experiments.

4.3 Experimental

4.3.1 Purification of the styrene monomer

Before use, the styrene monomer was purified from any inhibitors and/or other impurities by distillation. The monomer was first washed with a 0.3 M potassium hydroxide (KOH) solution to remove the hydroquinone inhibitor. To do this, 400 ml of styrene monomer and 100 ml of the KOH solution was brought into a 500 ml separation funnel and carefully shaken to ensure that most of the inhibitor is washed out into the aqueous KOH phase. This was done three times with venting in-between to prevent pressure build-up in the funnel. The separation funnel was then left to stand for a few minutes for the phases to separate after which the bottom KOH layer was carefully removed. The monomer was then transferred to a 1 liter roundbottom flask and boiling stones added. The flask was then connected to a distillation setup as shown in Figure 4.4.

Distillation was done under vacuum and with low heat applied to the flask. Care had to be taken that the temperature of the vapor did not exceed 55 °C as spontaneous polymerization could then occur.

The first 40 ml fraction collected was discarded to ensure that the distilled monomer was free from any impurities and also water. The second fraction collected was therefore considered pure and was stored at −8 °C to retard polymerization. $CaCl_2$ was also added to ensure a completely water-free product. The distilled styrene monomer used in all further reactions was never more than 5 days old.

Stellenbosch University https://scholar.sun.ac.za

51
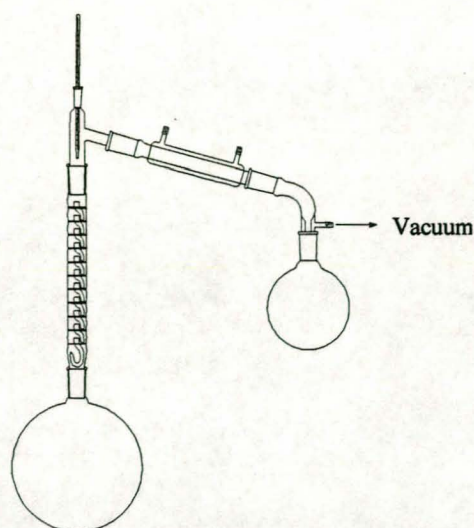
Figure 4.4: Monomer distillation setup.

4.3.2 Grafting of styrene onto epoxidized natural rubber

The epoxidized natural rubber used in the experiments was 50 % epoxidized (ENR50). Two types of ENR50 were used. In experiments 1 to 5, an old batch of epoxidized rubber was used (2 years old). In experiments 6 to 10 a fresh batch (reference number: UF 50/01/5) of epoxidized rubber was used (one week old). All epoxidized rubber was obtained from the Malaysian Rubber Board in Kuala Lumpur and was in latex form. The old batch has a dry rubber content (DRC) of 40 % and the new batch a DRC of 59,41 %. The total solids content (TSC) of the new batch was 61,85 %.

To maintain consistency in the experimental work, the rubber used from the new batch was diluted to 40 % DRC by adding distilled de-ionized (DDI) water to a pre-measured quantity of latex. Calculation of dilution was done as follows:

In 50.00g latex there is 29.705g rubber and 20.295g H_2O (59,41 % DRC). To dilute the latex to 40 % DRC, x gram of DDI water must be added to the latex. In a 40 % DRC there will therefore be 29.705g rubber and $(20.295 + x)$ gram DDI water. The ratio between the rubber mass and the total mass must be 40 % or 0.40.

Therefore

$$\frac{29.705}{50+x} = 0.40$$

$$\Rightarrow \qquad x = 24.263 \text{ g DDI}$$

Therefore for every 50 g of latex used, 24.263 g of DDI water must be added to ensure that the correct DRC is used.

Different types of surfactant i.e. Berol 291 (nonylphenol ethoxylate non-ionic surfactant), sodium lauryl sulfate (SLS) and dodecylbenzene sulfonic acid sodium salt (DBSASS) were also evaluated during the experiments to see which surfactant would be most suitable for stabilizing the emulsion reaction. The outcome of the results for the above evaluations will be discussed later. Potassium persulfate (KPS) was used as initiator. Apart from the surfactant, the experimental procedure was also adapted to prevent coagulation of the rubber particles and to ensure a stable latex system. This will also be explained later, in Section 4.3.4.

4.3.3 Formulations for the grafting of styrene onto ENR50

Formulations for the individual grafting reactions are tabulated in Tables 4.1 and 4.2. Note that in experiments 4, 5, 9 and 10 the volume of the reactor water was reduced and this difference in volume added to the initiator solution to ensure solubility of the initiator (due to the large amount of initiator used). This did not pose a problem as the total amount of reactor water and initiator water remained constant. The initiator and monomer concentrations were chosen to represent 5 distinct reaction conditions. This was done to obtain five different grafting conditions to be able to compare the results of analyses of the different products. The different initiator and monomer concentrations can be plotted as five points on a graph and are represented in Figure 4.5.

4.3.4 Basic polymerization setup and procedure

The experimental setup used for the graft reaction is shown in Figure 4.6.

During the first few experiments, the experimental procedure was adapted to optimize the polymerization reaction. This was done by changing the surfactants and formulations.
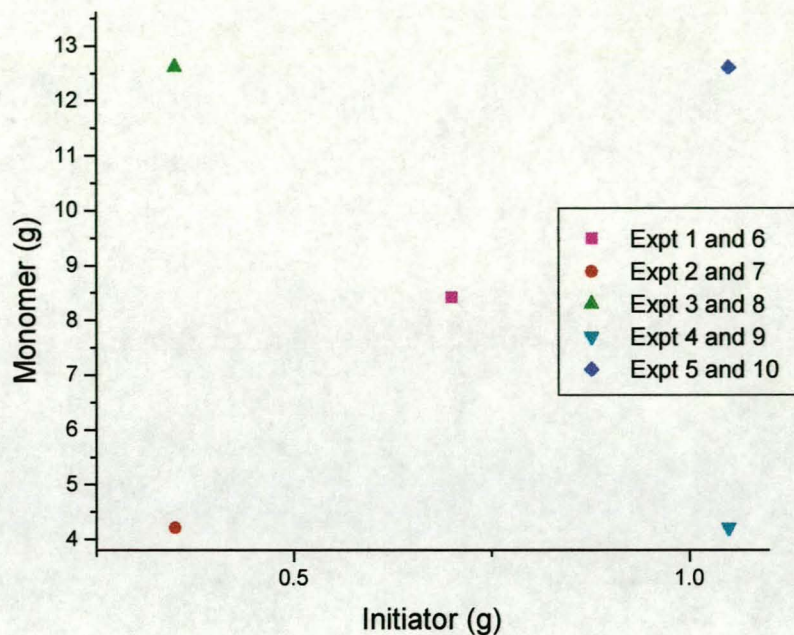
Figure 4.5: Graphic representation of the monomer concentration versus the initiator concentration used for the ten different graft reactions.
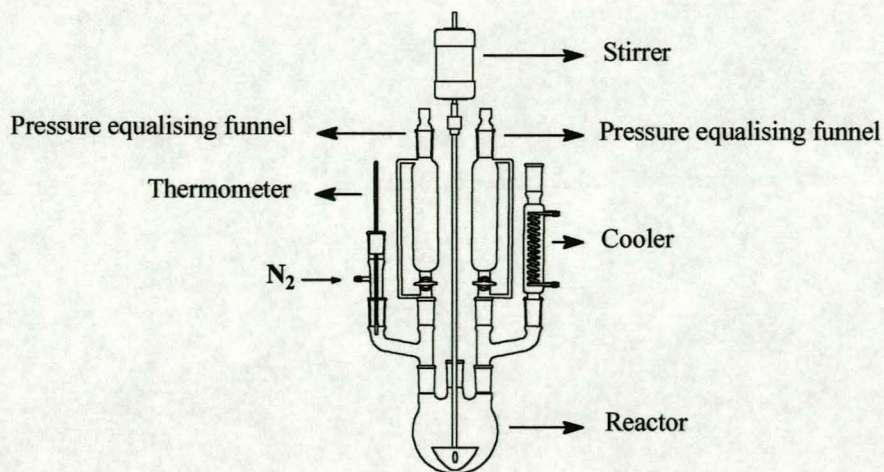
Figure 4.6: Experimental setup used for the emulsion polymerization reaction.

The basic reaction procedure will first be discussed, followed by a detailed description of how the procedure was changed through the experimental trials.

The monomer, emulsifier, rubber and water were weighed off and added to a roundbottom flask to which was connected a stirrer (Figure 4.7). Stirring continued for 15 to 20 minutes to ensure good mixing i.e. to make sure that the monomer swelled the rubber latex. Emulsifier was used to stabilize the monomer/rubber mixture.
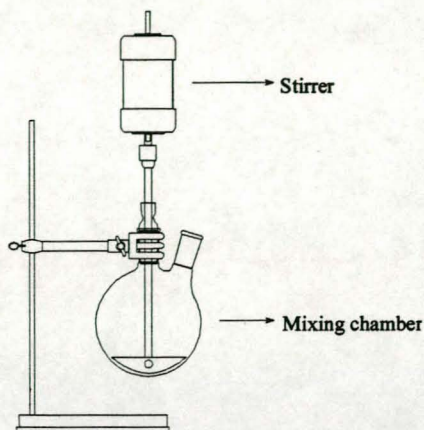
Figure 4.7: Pre-mixing of emulsifier, rubber and monomer.

The solution was then transferred to a pressure equalizing dropping funnel (see Figure 4.6) and initiator was added to a second pressure equalizing dropping funnel, also connected to the main reactor. The main reactor was then charged with water and heated to 82 °C under nitrogen flow. To start the reaction, 2% of the monomer/rubber solution and 25 % of the initiator solution were added to the reactor, and kept at 82 °C for 15 minutes. The reactor was stirred for the duration of the experiment by an overhead stirrer (250 rpm). The remainder of the monomer/rubber solution was added over a 4-hour period. After addition, the reactor was heated to 85 °C for 30 minutes to ensure completion of the grafting reaction.

Due to the fact that different monomer and initiator concentrations were used during the experiments (Figure 4.5), the emulsion system acted differently under these conditions throughout the various experiments. The surfactant used also caused a problem and a suitable surfactant had to be found for the styrene/ENR50 system. The surfactants used included Berol 291, sodium lauryl sulfate (SLS) and dodecylbenzenesulfonic acid sodium salt (DBSASS).

		Ingredient mass (g)	Solid weight content (g)	Weight measured (g)	Weight measured (g)	Weight measured (g)	Weight measured (g)	Weight measured (g)
Date				26/03/98	29/03/98	29/03/98	08/04/98	09/04/98
Exp. No.				1A	1B	1C	2	3A
Reactor								
Water	DDI	10		10.0912	10.0235	10.0379	10.0213	10.0694
Monomer Emulsion								
Water	DDI	23.125		23.1630	23.1358	23.2092	23.1775	23.1524
Rubber	ENR50	47.73	19.09	47.7541	47.7521	47.8205	47.7574	47.7457
Emulsifier	Berol 291	2.8	2.8	2.8575				
Emulsifier	DBSASS	2.8	2.8		1.4060	2.8180		
Emulsifier	SLS*	2.8	2.8				2.8026	2.8104
Monomer	Styrene	8.4	8.4	8.4086	8.4070	8.4060		
Monomer	Styrene	4.2	4.2				4.2300	
Monomer	Styrene	12.6	12.6					12.6120
Initiator Solution								
Water	DDI	14		14.2047	14.0042	14.0800	14.0241	14.0717
Initiator	KPS	0.7	0.7	0.7289	0.7204	0.7149		
Initiator	KPS	0.35	0.35				0.3530	0.3628

*Anionic detergent used to solubilize proteins [11]

Table 4.1: Formulations of the grafting reactions between styrene and ENR50 for experiments 1 to 3A.

Date				12/04/98	10/04/98	14/04/98	04/05/98	05/05/98	06/05/98	07/05/98	08/05/98
Exp. No.				3B	4	5	6	7	8	9	10
Reactor		Ingredient mass (g)	Solid wt content (g)	Weight (g)	Weight (g)	Weight (g)	Weight (g)	Weight (g)	Weight (g)	Weight (g)	Weight (g)
Water	DDI	10		10.0752			10.0636	10.0030	10.0171		
Water	DDI	6			6.0258	5.7947				6.0876	6.0144
Rubber Emulsion											
Water	DDI	23.125		23.1324	23.1272	23.1478	23.1274	23.1262	23.1364	23.1298	23.1369
Rubber	ENR50	47.73	19.09	47.7437	47.7328	47.7313	47.7413	47.7398	47.7470	47.7405	47.7477
Emulsifier	SLS*	2.8	2.8	2.8153	2.8045	2.8018	2.8024	2.8017	2.8024	2.8008	2.8016
Monomer											
Monomer	Styrene	8.4	8.4				8.4014				
Monomer	Styrene	4.2	4.2		4.2116			4.2091		4.2019	
Monomer	Styrene	12.6	12.6	12.6059		12.6086			12.6065		12.6009
Initiator solution											
Water	DDI	14		14.0306			14.0134	14.0271	14.0031		
Water	DDI	18			18.0564	18.2733				18.0091	18.0220
Initiator	KPS	0.7	0.7				0.7024				
Initiator	KPS	0.35	0.35	0.3518				0.3509	0.3545		
Initiator	KPS	1.05	1.05		1.0521	1.0500				1.0501	1.0505

*Anionic detergent used to solubilize proteins [11]

Table 4.2: Formulations of the grafting reactions between styrene and ENR50 for experiments 3B to 10.

Experiment 1A

Experiment 1A was done with Berol 291 as emulsifier (2.8g). The reaction procedure was as explained above. Unfortunately the latex was not stable at the end of the grafting reaction and this led to coagulation of the latex. The surfactant was therefore not suitable to stabilize the latex system.

Experiment 1B

To avoid coagulation, a different surfactant was chosen in 1B. Dodecylbenzenesulfonic acid sodium salt (DBSASS)(1.4g) was used as surfactant. The latex system coagulated after two hours due to the small amount of surfactant used.

Experiment 1C

In Experiment 1C, DBSASS was again used as surfactant, but double the quantity was used (2.8g). At the end of the grafting reaction the latex was much more stable than in 1A and 1B, but larger particles were present in the latex.

Although a stable latex was possible in 1C, the reaction procedure was further adapted to try and obtain an even more stable latex system. Due to the larger particles present in 1C, the use of yet another surfactant was deemed necessary in Experiment 2.

Experiment 2

Sodium lauryl sulfate (SLS) was used as surfactant in Experiment 2 (2.8g). This caused the styrene monomer to enter the rubber phase and swell it quite extensively during the pre-mixing process. This was observed visually. Good stabilization of the grafted product was obtained.

Experiment 3A

Again SLS was used as surfactant. In Experiment 3A a problem occurred due to the large amount of styrene used (12.6g). When the monomer was added to the rubber and surfactant in the pre-mixing stage, the large amount of monomer relative to the surfactant caused the rubber particles to coagulate and stabilization was therefore insufficient.

Experiment 3B

To avoid coagulation, the rubber and surfactant were pre-mixed and then added to the reactor where stirring continued. The styrene was added to the one pressure equalizing dropping funnel and initiator to the other funnel. To start off the reaction, 25% of the initiator solution and 2% of the monomer solution were added to the reactor and the temperature kept at 82 °C for 15 minutes. After 15 minutes the remainder of the monomer and initiator were dripped into the reactor, over a 4-hour period, after which the reactor was heated to 85 °C and the temperature kept constant for 30 minutes to ensure complete reaction.

By dripping the monomer into the reactor over a 4-hour period, problems with the surfactant due to the large amount of monomer was avoided, as was coagulation. The grafted product obtained was very stable.

Experiment 4

Sodium lauryl sulfate was used as surfactant and the monomer emulsion consisting of the rubber, surfactant, monomer and water was dripped into the reactor. A stable latex product was obtained after 4 hours.

Experiment 5

Due to the large quantity of monomer used, the same reaction procedure as in Experiment 3B was followed, leading to a very stable end product.

Experiments 6-10

In Experiments 6 to 10 the new batch of ENR50 was used after dilution to 40% DRC. In all these experiments the same reaction procedure as in experiment 3B was followed, leading to very stable latex systems.

4.3.5 Precipitation and drying of the grafted rubber

The grafted rubber was removed from the latex by the addition of excess methanol. The precipitated rubber was placed in a vacuum oven and dried for two days at ambient temperature. The color of the dried product ranged from white to yellow-brown and most of the samples were brittle.

4.4 Overview

Throughout the experiments it was found that sodium lauryl sulfate was the best surfactant to use in the grafting of styrene onto epoxidized natural rubber. By dripping the monomer, and not the monomer/rubber solution into the reactor, flooding the system with monomer, which can lead to coagulation, can be avoided, thus creating a much more stable latex end product.

4.5 References

1   I.R. Gelling; *Modification of Natural Rubber Latex with Peracetic Acid*; Rubber Chemistry and Technology; **58**, 1984, 86-96

2   S.-C. Ng, L.-H. Gan; *Reaction of Natural Rubber Latex with Performic Acid*; European Polymer Journal; **17**, 1981, 1073-1077

3   C.S.L. Baker, I.R. Gelling, R. Newell; *Epoxidized Natural Rubber*; Rubber Chemistry and Technology; **58**, 1984, 67-85

4   D.R. Burfield, Kooi-Ling Lim, Kai-Sang Law; *Epoxidation of Natural Rubber Latices: Methods of Preparation and Properties of Modified Rubbers*; Journal of Applied Polymer Science; **29**, 1984, 1661-1673

5   J.H. Bradbury, M.C.S. Perera; *Epoxidation of Natural Rubber Studied by NMR Spectroscopy*; Journal of Applied Polymer Science; **30**, 1985, 3347-3364

6   Nguyen Viet Bac, L. Terlemezyan, M. Mihailov; *On the Stability and In Situ Epoxidation of Natural Rubber in Latex by Performic Acid*; Journal of Applied Polymer Science; **42**, 1991, 2965-2973

7   Nguyen Viet Bac, L. Terlemezyan, M. Mihailov; *Epoxidation of Natural Rubber in Latex in the Presence of a Reducing Agent*; Journal of Applied Polymer Science; **50**, 1993, 845-849

8   Seng-Neon Gan, Ziana Abdul Hamid; *Partial Conversion of Epoxide Groups to Diols in Epoxidized Natural Rubber*; Polymer; **38**(5), 1997, 1953-1956

9   R.G.R. Bacon, E.H. Farmer, P. Schidrowitz; Proceedings of the Rubber Technology Conferences; W. Heffner & Sons Ltd., Cambridge, England; **525**, 1938

10   G.F. Bloomfield, F.M. Merrett, F.J. Popham, P. McL. Swift; *Graft Polymers Derived from Natural Rubber*; Rubber World; 1954, 358-360,418

Chapter 5

Solubility Parameters of Solvents, Non-solvents and Polymers

5.1 Introduction

The solubility parameters of polymers and polymer solubility play important roles in gradient HPLC because separation is based on the solubility and precipitation of the polymer in question [1,2]. For separation to take place it is necessary for the polymer to be soluble, or to at least have a representative soluble fraction. By determining the solubility parameters of solvents, non-solvents and polymers, a range of solvent/non-solvent pairs can be selected, thereby eliminating time which would otherwise be wasted in manually selecting the correct pairs. By doing actual gradient runs, the best solvent pairs can then be selected, with which optimum separation is possible.

A solubility parameter can be used for correlating and understanding polymer solvent interactions, and is defined as the square root of the cohesive energy density, which is the cohesive energy per unit of volume [3].

Hildebrand stated in 1916 [3] that the order of solubility of a given solute in a series of solvents is determined by the internal pressures of the solvents. This concept was modified in 1931 by Scatchard, and again in 1936 by Hildebrand [3]. In 1949 Hildebrand coined the term solubility parameter and the symbol δ [3].

In the following sections, the principle of solubility parameters and how it was applied to obtain actual solubility parameter values will be explained. Furthermore, the solubility of polymers and cloudpoint measurements will also be discussed.

5.2 Principles and theory of polymer and solvent solubility parameters

Polymer solubility is largely determined by its chemical structure, but the physical state of the polymer is also very important to solubility properties. Examples of the above statements are the relative insolubility of crystalline polymers and also the fact that solubility decreases with an increase in molecular mass [4,5].

The solubility dependence on molecular mass is also the principle of reverse-phase gradient HPLC, thereby emphasizing the importance of solubility parameters. Of interest is also whether or not a given polymer is soluble in a particular solvent, where the commonly used rule of thumb is "like dissolves like". In other words, a polar polymer will dissolve in a polar solvent and *vice versa* [6]. This argument can also be explained or clarified by the solubility parameter concept e.g. polystyrene with solubility parameter δ = 18.7 will dissolve in benzene (δ = 18.7), but not in methanol (δ = 29.6). Another way to explain the above is to say that if benzene lies on or inside the solubility sphere of polystyrene, solubility will be possible. Note that the above will not hold for crosslinked polymers. The whole concept of solubility spheres will be explained later, but first the solubility parameter will be defined mathematically.

The solubility of a substance is based on the free energy of mixing ΔG_M, where two substances are mutually soluble if ΔG_M is negative. The free energy of mixing can be defined as

$$\Delta G_M = \Delta H_M + T\Delta S_M \tag{5.1}$$

where ΔH_M is the enthalpy of mixing, ΔS_M is the entropy of mixing and T is the absolute temperature. Due to the fact that ΔS_M has a positive value arising from increased conformational mobility of the polymer chains in solution, it is clear that the magnitude of ΔH_M determines the sign of ΔG_M.

In 1949 Hildebrand [7] proposed that the heat of mixing, ΔH_M, for a binary system is related to concentration and energy parameters by the expression

$$\Delta H_M = V_M \left[\left(\frac{\Delta E_1}{V_1} \right)^{1/2} - \left(\frac{\Delta E_2}{V_2} \right)^{1/2} \right]^2 \phi_1 \phi_2 \qquad (5.2)$$

where V_M is the total volume of the mixture, V_1 and V_2 are molar volumes (molecular mass/density) of the two components, ϕ_1 and ϕ_2 are their volume fractions and E_1 and E_2 are the energies of evaporation (cohesive energies). The terms $\Delta E_1/V_1$ and $\Delta E_2/V_2$ are called the cohesive energy densities. The cohesive energy, E_{coh}, is closely related to the molar heat of evaporation (ΔH_{vap}) through the equation

$$E_{coh} = \Delta U_{vap} = \Delta H_{vap} - p\Delta V \approx \Delta H_{vap} - RT \qquad (5.3)$$

where ΔU_{vap} is the internal energy of evaporation. The solubility parameter is written as the square root of the cohesive energy density

$$\delta = \left(\frac{\Delta E_{coh}}{V} \right)^{1/2} \qquad (5.4)$$

and by substitution into Equation 5.2, it can therefore be written as

$$\Delta H_M = V_M \left(\delta_1 - \delta_2 \right)^2 \phi_1 \phi_2 \qquad (5.5)$$

From the above equation it is clear that in order for a polymer to dissolve, $\left(\delta_1 - \delta_2 \right)^2$ must be small, in other words, δ_1 and δ_2 must be of about equal magnitude. This makes it possible to predict whether or not a polymer will be soluble in a specific solvent or not, as solvents and polymers with similar δ values will yield a value for $\Delta H_M \approx 0$.

5.3 Determination of Solubility Parameters for Solvents and Polymers

Solubility parameters for solvents can easily be determined by using the latent heat of vaporization ΔH_{vap} and the equation

$$\Delta E = \Delta H_{vap} - RT \qquad (5.6)$$

This can unfortunately not be done for polymers as degradation will occur rather than vaporization at high temperatures [8] and therefore δ has to be calculated by using group molar attraction constants as proposed by Small, Van Krevelen, Hoy and Fedors [3,9]. Table 5.2 shows the values for the group molar attraction constants as well as values for the group molar volumes. Solubility parameters can thus be calculated by using

$$E_{coh} = \frac{\left(\sum_i F_i\right)^2}{\sum_i V_i} \qquad (5.7)$$

and substitution into Equation 5.4 (Small, Van Krevelen and Hoy) or by direct substitution of $\sum_i E_i$ into Equation 5.4 (Fedors) [3].

By using the values of Fedors in Table 5.2, the solubility parameters of THF and epoxidized natural rubber (ENR50) (Figure 5.1) were calculated. The solubility parameter values are given in Table 5.1.
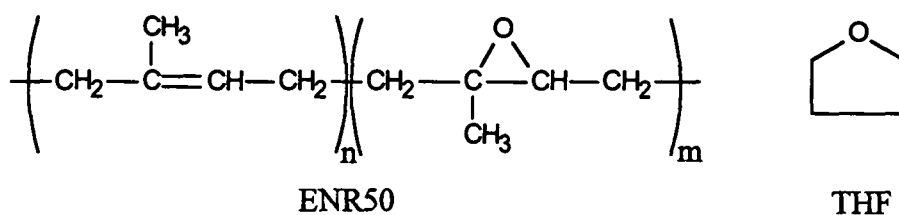
Figure 5.1: Chemical structures of ENR50 and THF.
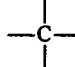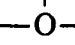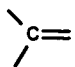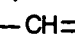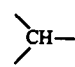
	ENR50		THF	
	E_{coh} (J/mol)	V (cm^3/mol)	E_{coh} (J/mol)	V (cm^3/mol)
2(-CH$_3$)	9420	67		
4(-CH$_2$-)	19760	64.4	19760	64.4
—C—	1470	-19.2		
—O—	3350	3.8	3350	3.8
C=	4310	-5.5		
—CH=	4310	13.5		
CH—	3430	-1.0		
	46050	123	23110	68.2

Table 5.1: Group molar attraction constants for ENR50 and THF.

$$\delta_{ENR50} = \left(\frac{E_{coh}}{V}\right)^{1/2} = \left(\frac{46050}{123}\right)^{1/2} = 19.35\,(J^{1/2}.cm^{-3/2})$$

$$\delta_{THF} = \left(\frac{E_{coh}}{V}\right)^{1/2} = \left(\frac{23110}{68.2}\right)^{1/2} = 18.40\,(J^{1/2}.cm^{-3/2})$$

5.4 Refinement of δ through the incorporation of the 3-value solubility parameter concept

Hildebrand only used dispersion forces between structural units in calculating δ. Due to the fact that in many polymers the cohesive energy is also dependant on interaction between the polar groups and the hydrogen bonds [3], Hildebrand's definition for δ was refined to incorporate these interactions yielding

$$E_{coh} = E_d + E_p + E_h \tag{5.8}$$

where E_d is the dispersive term, E_p the polar term and E_h the hydrogen bonding term.
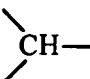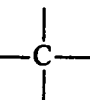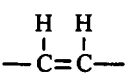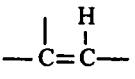
Structural Group	F ($J^{1/2}.mol^{-1}.cm^{-3/2}$)			E_{coh} (J/mol) Fedors (1974)	V ($cm^3.mol^{-1}$) Fedors & Van Krevelen	V ($cm^3.mol^{-1}$) Hoy
	Small (1953)	VKrevelen (1965)	Hoy (1970)			
—CH_3	438	420	303.4	4710	33.5	21.548
—CH_2—	272	280	269.0	4940	16.1	15.553
$\backslash$CH—	57	140	176.0	3430	-1.0	9.557
—C—	-190	0	2.5	1470	-19.2	3.562
—CH(CH_3)—	495	560	(479.4)	(8140)	32.5	31.105
—C(CH_3)$_2$—	686	840	(672.3)	(10890)	47.8	46.658
—C=C— (H H)	454	444	497.4	8620	36.5	26.834
—C=C— (H)	266	304	421.5	(8620)	8.0	--
— C(CH_3)= CH —	(704)	724	(724.9)	(13330)	61.3	--
cyclopentyl	--	1384	1295.1	(24240)	--	--
cyclohexyl	--	1664	1473.3	29180	--	--
phenyl	1504	1517	1398.4	31940	71.4	--
p-phenylene	1346	1377	1442.3	31940	52.4	--
—F	(250)	164	84.5	4190	18.0	11.200
—Cl	552	471	419.6	11550	24.0	19.504
—Br	696	614	527.7	15490	30.0	25.305
—I	870	--	--	16740	31.5	--
—CN	839	982	725.5	25530	24.0	23.066
—CH_2CN—	(896)	1122	(901.5)	28960	--	--
—OH	--	754	462.0	29800	24.0	10.647
—O—	143	256	235.3	3350	3.8	6.462
—CO—	563	685	538.1	17370	10.8	17.265

Table 5.2: Group molar attraction constants and group molar volumes according to Van Krevelen, Small, Hoy and Fedors [3,9].

Structural Group	F ($J^{1/2}.mol^{-1}.cm^{-3/2}$)			E_{coh} (J/mol) Fedors (1974)	V ($cm^3.mol^{-1}$) Fedors & Van Krevelen	V ($cm^3.mol^{-1}$) Hoy
	Small (1953)	VKrevelen (1965)	Hoy (1970)			
—COOH	--	652	(1000.1)	27630	28.5	26.102
—COO—	634	512	668.2	18000	18.0	23.728
—O–C(=O)–O—	--	767	(903.5)	17580	22.0	30.190
—C(=O)–O–C(=O)—	--	767	1160.7	30560	30.0	40.993
—C(=O)–N(H)—	--	1228	(906.4)	33490	9.5	28.302
—O–C(=O)–N(H)—	--	1483	(1036.5)	26370	18.5	34.784
—S—	460	460	428.4	14150	12	18.044
—CH=	--	--	--	4310	13.5	--
>C=	--	--	--	4310	-5.5	--

Table 5.2: Continued.

The solubility parameter can therefore be written as

$$\delta_t = \left(\delta_d^2 + \delta_p^2 + \delta_h^2\right)^{1/2} \tag{5.9}$$

Values for δ_d, δ_p and δ_h can be calculated from group molar contributions according to Hoftyzer and Van Krevelen (1976) [3]. They used the following equations:

$$\delta_d = \frac{\sum F_{di}}{V} \tag{5.10}$$

$$\delta_p = \frac{\sqrt{\sum F_{pi}^2}}{V} \tag{5.11}$$

$$\delta_h = \sqrt{\frac{\sum E_{hi}}{V}}$$ (5.12)

The values for the three components can be seen in Table 5.4. The solubility parameter for ENR50 was also calculated according to the above method as can be seen in Table 5.3.
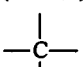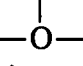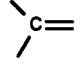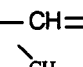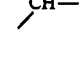
Structural Groups	F_{di} $(J^{1/2}.cm^{3/2}.mol^{-1})$	F_{pi} $(J^{1/2}.cm^{3/2}.mol^{-1})$	E_{hi} (J/mol)
2(-CH₃)	840	0	0
4(-CH₂-)	1080	0	0
—C—	-70	0	0
—O—	100	400	3000
＼c= /	70	0	0
—CH=	200	0	0
＼CH— /	80	0	0
	2300	400	3000

Table 5.3: Group molar attraction constants for ENR50 according to the 3-value solubility parameter concept.

Substitution of the values (from Table 5.3) into Equations 5.10, 5.11 and 5.12 yields $\delta_d = 18.69$, $\delta_p = 3.25$ and $\delta_h = 4.9$ which, after substitution into Equation 5.9, gives the 3-value solubility parameter for ENR50.

$$\delta_{ENR50} = \left\{ (18.69)^2 + (3.25)^2 + (4.9)^2 \right\}^{1/2} = 19.59$$

By plotting a graph of δ_v vs. δ_h, where

$$\delta_v = \sqrt{(\delta_d^2 + \delta_p^2)}$$ (5.13)

for a certain polymer and different solvents, the good solvents for the particular polymer can be found. The good solvents will lie in a certain area around the polymer (this area can be denoted by a circle and the radius of the circle will be inherent of the polymer) as can be seen in Figure 5.2.
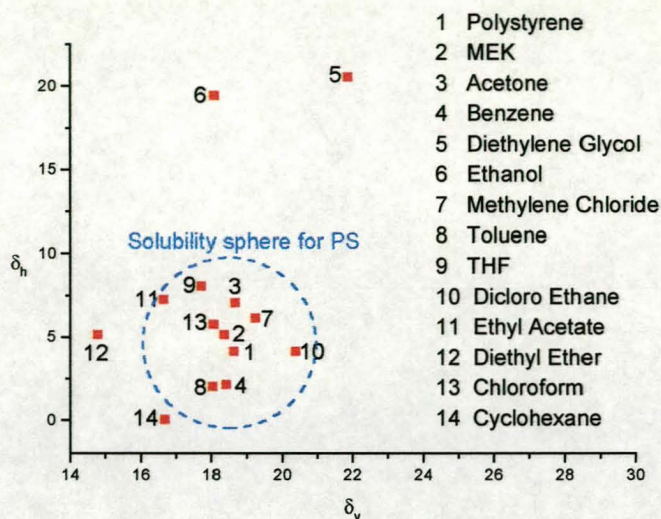
Figure 5.2: Solubility sphere for polystyrene.

The solvents inside the circle represent good solvents, the two solvents that are situated at the top of the graph are weak solvents and the two solvents just outside the circle are intermediate solvents. Solubility parameter values for the solvents and polystyrene are shown in Table 5.5.

Similarly, a 3-dimensional graph of δ_d, δ_p and δ_h can be plotted for different solvents and polystyrene. Here the good solvents will be inside a 3-dimensional solubility sphere for polystyrene (Figure 5.3).

5.5 Solubility of ENR50

Through the calculation of solubility parameters it was possible to select appropriate solvents for ENR50 and polystyrene. However, due to the fact that the rubber was crosslinked, methods were investigated to enhance the solubility of the rubber in the appropriate solvents.
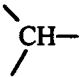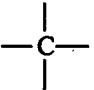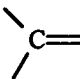
Structural Groups	F_{di} ($J^{1/2}.cm^{3/2}.mol^{-1}$)	F_{pi} ($J^{1/2}.cm^{3/2}.mol^{-1}$)	E_{hi} (J/mol)
-CH$_3$	420	0	0
-CH$_2$-	270	0	0
$\diagdown$CH— $\diagup$	80	0	0
—$\overset{\vert}{\underset{\vert}{C}}$—	-70	0	0
=CH$_2$	400	0	0
=CH-	200	0	0
$\diagdown$C== $\diagup$	70	0	0
-F	(220)	--	--
-Cl	450	550	400
-Br	(550)	--	--
-CN	430	1100	2500
-OH	210	500	20000
-O-	100	400	3000
-COH	470	800	4500
-CO-	290	770	2000
-COOH	530	420	10000
-COO-	390	490	7000
-NH$_2$	280	--	8400
-NH-	160	210	3100
-S-	440	--	--
-NO$_2$	500	1070	1500
=PO$_4$-	740	1890	13000
HCOO-	530	--	--

Table 5.4: Group molar attraction constants for the 3-value solubility parameter concept.

	Solubility Parameters ($J^{1/2}.cm^{-3/2}$)				
	δ_d	δ_p	δ_h	δ_v	δ_t
Polymers					
Polystyrene	17.6	6.1	4.1	18.6	19.1
ENR50	18.7	3.3	4.9	19.0	19.6
Solvents					
Methyl Ethyl Ketone	15.9	9.2	5.1	18.4	19.1
Acetone	15.5	10.4	7.0	18.7	19.9
Benzene	18.4	1.0	2.1	18.4	18.5
Diethylene Glycol	16.2	14.7	20.5	21.9	30.0
Ethanol	15.8	8.8	19.4	18.1	26.5
Toluene	18.0	1.4	2.0	18.1	18.2
Tetrahydrofuran	16.8	5.7	8.0	17.7	19.5
Dichloroethane	19.0	7.4	4.1	20.4	20.8
Ethyl Acetate	15.8	5.3	7.2	16.7	18.2
Diethyl Ether	14.5	2.9	5.1	14.8	15.6
Chloroform	17.8	3.1	5.7	18.1	18.9
Cyclohexane	16.7	0.0	0.0	16.7	16.7
Dichloromethane	18.2	6.3	6.1	19.3	20.2
Acetonitrile	15.3	18.0	6.1	23.6	24.4
Methanol	15.1	12.3	22.3	19.5	29.6
Water	15.6	16.0	42.4	22.3	47.9

Table 5.5: Solubility parameters for polystyrene and solvents.
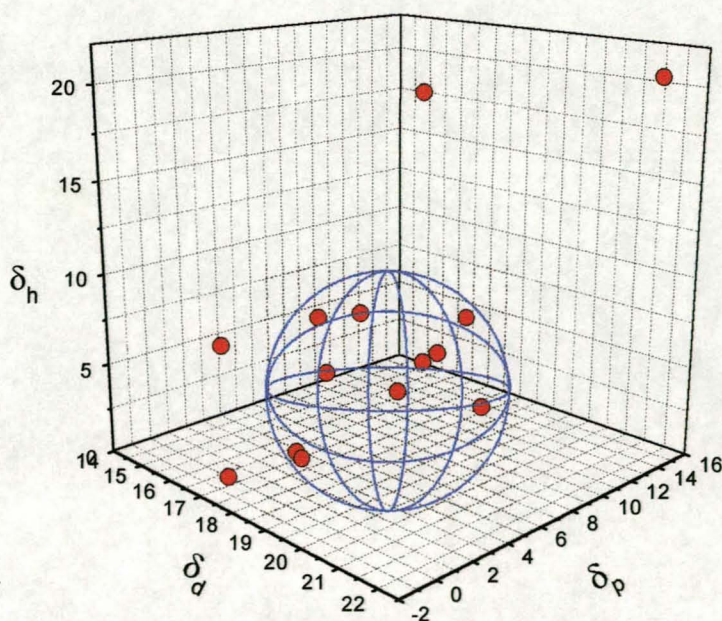
Figure 5.3: 3-Dimensional solubility sphere for polystyrene.

These methods included drying and milling of the rubber on a twin-mill roll, shearing of the rubber latex with a Silverson L4R and addition of an enzyme (trypsin) to the latex to destabilize it. Apart from the above procedures, solubility of the rubber as is (unmilled, just precipitated) was also investigated to compare with the solubility of the rubber that has been subjected to the destructive methods.

5.5.1 Sample preparation

ENR50 was precipitated with methanol (or ethanol, depending on the experiment) and the precipitated rubber dried in a vacuum oven until completely dry. The dried rubber was then milled on a twin-mill roll [10] for 5, 10, 15 minutes respectively (nip set at 1 mm, speed of rollers at 11 revolutions/minute and temperature at room temperature). To ensure uniformity, ±0.01g of rubber was weighed off and added to 10 ml solvent (a 1% solution was used because this is the typical concentration used in gradient HPLC). The rubber was added to the solvent immediately after milling to avoid recombination of radicals which formed during the destructive milling process. In non-milling experiments, ±0.01g dried rubber was added to the solvents.

In solubility experiments where the rubber latex was used, it was necessary to compensate for the other ingredients (water, surfactant, etc.) present in the latex. Therefore ±0.0167g latex (DRC_{ENR50} = 40%) was weighed off and added to the solvents.

Shearing of the rubber was done on a Silverson L4R. Shearing was done for 10, 60 and 180 minutes, at room temperature. The latex sheared for 10 minutes had to be precipitated by addition of MeOH. However, due to the destabilization effect of shearing, the latex sheared for 60 and 180 minutes coagulated and ±0.01g of this rubber coagulum was used in the solubility experiments.

In yet another solubility experiment, a similar method to that used by Bac and co-workers [11] was followed. Here the rubber was precipitated by either MeOH or EtOH, washed with distilled water and then dried at 100°C for 15 and 60 minutes in the case of MeOH and for 15 minutes in the case of EtOH.

In all of the above experiments, the weighed rubber/latex was added to the specific solvents and stirred for a 24 hour period prior to examination and cloudpoint determinations.

5.5.2 Results

Results of the solubility experiments can be seen in Table 5.6. From the results it is clear that a completely soluble ENR50 is possible when milled on a twin-mill roll. All further cloudpoint experiments were therefore done on milled samples to ensure maximum solubility of the samples. Although milling of the samples involved physical breakage of chemical bonds (crosslinks etc.), it was proven through gradient HPLC analysis that milled samples were representative of the complete sample. Results of this proof can be seen in Chapter 7, Section 7.3.2.

5.6 Cloudpoint determinations

Cloudpoint determinations are used as a preliminary experimental tool to help predict the position and separation of polymers in a chromatogram. This can be achieved due to the fact that cloudpoint measurements are based on the same principles as the actual gradient run in gradient HPLC. In other words, in cloudpoint measurements the polymer is dissolved in a solvent (S) and titrated with a non-solvent (NS). This simulates the gradient, although, in gradient HPLC this would actually be the other way around, i.e. where the polymer is precipitated and then redissolved. To correlate the two techniques, the percentage solvent (%S) used to redissolve or the percentage non-solvent (%NS) to precipitate the polymer must be calculated and this is possible through the following equation [12]

$$Cloudpoint\ Composition\ (CP) = \%NS = \frac{V^{NS}}{V^{S} + V^{NS}} \cdot 100 \qquad (5.14)$$

where V^{NS} = volume of the non-solvent added when the cloudy suspension appears

V^{S} = volume of solvent used to solubilize the polymer (10 ml of solvent used to solubilize 10 mg of polymer in all experiments)

	Latex (ENR50) (used as is)	Preptd with MeOH	Preptd with MeOH (Dried overnight under vacuum)	Preptd with MeOH (dried and milled)	Preptd with MeOH (washed with distilled H$_2$O and dried under vacuum)	Preptd with MeOH (washed with distilled H$_2$O and dried at 100 °C for 15 min)	Preptd with MeOH (washed with distilled H$_2$O and dried at 100 °C for 60 min)
Comments:	± 0.0167 g latex used in 10 ml solvent	± 0.02 g rubber used in 10 ml solvent	±.01 g rubber used in 10 ml solvent	rubber milled for 5 minutes ±.01 g rubber used	±.01 g rubber used in 10 ml solvent	±.01 g rubber used in 10 ml solvent	±.01 g rubber used in 10 ml solvent
Toluene	Very swollen (difficult to see the swollen network). Gel particles form during titration. Cloudpoint at 9.92 cm^3.	Very swollen (difficult to see the swollen network). Gel particles form during titration. Cloudpoint at 9.89 cm^3.	Very swollen (difficult to see the swollen network). Gel particles form during titration. Cloudpoint at 10.08 cm^3.	Clear solution. Solution stays clear during titration. Cloudpoint at 10.55 cm^3.	Very swollen polymer network (difficult to see). Gel network forms during titration. Cloudpoint at 10.51 cm^3.	Very swollen rubber network. Almost impossible to see network. Gel particles that form during titration break up into smaller pieces. Cloudpoint at 10.45 cm^3.	Very swollen polymer network. Gel forms but break up into smaller pieces during titration. Cloudpoint at 9.85 cm^3.
Trichlorobenzene	Solution is clear but there are gel particles on the inside of the beaker at the solvent/air interface. Solution stays clear during titration. Cloudpoint at 4.70 cm^3.	Very swollen (difficult to see the swollen network). Gel particles form during titration. Cloudpoint at 5.60 cm^3.	Very swollen (difficult to see the swollen network). Gel particles form during titration. Cloudpoint at 6.23 cm^3.	Clear solution. No visible swollen network present in the solution. Solution stays clear during titration. Cloudpoint at 6.35 cm^3.	Very swollen network. Gel particles form during titration. Cloudpoint at 6.46 cm^3.	Very swollen rubber network. Gel particles form during titration. Cloudpoint at 6.45 cm^3.	Very swollen polymer network. Gel particles form during titration. Cloudpoint at 6.33 cm^3.
THF	Very swollen particles. There are pieces of swollen rubber floating around and sticking to the bottom of the beaker. Particles whiten on titration. Cloudpoint at 9.26 cm^3.	Partly swollen cloudy particles present in otherwise clear solution. Gel particles form during titration. Cloudpoint at 8.90 cm^3.	Very swollen. Gel particles form during titration. Cloudpoint at 9.39 cm^3.	Clear solution. Solution stays clear during titration. Cloudpoint at 9.79 cm^3	Partly swollen polymer network. Gel particles form during titration. Cloudpoint at 9.08 cm^3.	Swollen cloudy rubber particles present in solution. Gel particles form during titration. Cloudpoint at 9.35 cm^3.	Partly swollen. Gel particles form during titration. Cloudpoint at 9.23 cm^3.
Benzene	Very swollen (difficult to see the swollen network). Fine gel particles form during titration. Cloudpoint at 9.09 cm^3.	Very swollen. Almost completely see through. Forms a gel during titration. Cloudpoint at 9.22 cm^3.	Very swollen (difficult to see the swollen network). Gel particles form during titration. Cloudpoint at 9.72 cm^3.	Clear solution but very small particles present at the bottom of the beaker. Solution stays clear during titration. Cloudpoint at 10.18 cm^3.	Very swollen (difficult to see the swollen network). Gel particles form during titration. Cloudpoint at 9.38 cm^3.	Very swollen rubber network present. Macro and micro gel particles form during titration. Cloudpoint at 9.11 cm^3.	Very swollen. Almost impossible to see swollen network. Small gel particles form during titration. Cloudpoint at 9.51 cm^3.
Dichloro ethane	Very swollen latex particles floating in solution. Particles are broken up into finer particles during titration. Cloudpoint at 14.22 cm^3.	Partly swollen cloudy rubber particles. Forms a gel during titration. Cloudpoint at 14.31 cm^3.	Swollen rubber network. Cloudy particles in otherwise clear solution. Gel particles form during titration. Cloudpoint at 14.62 cm^3.	Clear solution. Solution stays clear during titration. Cloudpoint at 15.62 cm^3	Partly swollen rubber network. Gel particles form during titration. Cloudpoint at 14.06 cm^3.	Partly swollen cloudy network present. Small white particles form during titration but no big particles/networks are present. Cloudpoint at 14.39 cm^3.	Very swollen polymer network. Gel flakes form during titration. Cloudpoint at 14.14 cm^3.
Butanone	Latex sticks to the bottom of the beaker. It is partly swollen and looks the same during titration. Cloudpoint is at 6.48 cm^3.	Partly swollen rubber particles present in the solution. White rubbery particles form during titration. Cloudpoint at 6.72 cm^3.	Partly swollen rubber network. Network whitens during titration. Cloudpoint at 6.88 cm^3.	Clear solution. Solution stays clear during titration. Cloudpoint at 7.10 cm^3	Partly swollen cloudy network. Cloudy gel networks form during titration. Cloudpoint at 6.01 cm^3.	Partly swollen cloudy network present. Network whitens during titration. Cloudpoint at 6.79 cm^3.	Partly swollen cloudy network present in solution. Gel particles form during titration. Cloudpoint at 6.38 cm^3.
Ethyl Acetate	Latex sticks to the bottom of the beaker. Partly swollen. The swollen network stays the same during titration. Cloudpoint is at 6.05 cm^3.	Partly swollen rubber network present in solution. Cloudpoint at 4.18 cm^3.	Partly swollen cloudy particles. Gel particles form during titration. Cloudpoint at 6.37 cm^3.	Clear solution. Solution stays clear during titration. Cloudpoint at 6.33 cm^3	Partly swollen cloudy network. Gel structures form during titration. Cloudpoint at 6.01 cm^3.	Partly swollen cloudy network present. Network whitens during titration. Cloudpoint at 6.43 cm^3.	Partly swollen cloudy network present in solution. Gel particles form during titration. Cloudpoint at 6.48 cm^3.

Table 5.6: Solvent and sample preparation evaluation.

	Preptd with MeOH (dried and milled for 10 min) nip set at 1 mm speed set at 11 rev/min	Preptd with MeOH (dried and milled for 15 min) nip set at 1 mm speed set at 11 rev/min	Preptd with EtOH (washed with distilled H_2O and dried at 100 °C for15 min)	Latex sheared with Silverson L4R for 10 min	Latex sheared with Silverson L4R for 60 min	Latex sheared with Silverson L4R for 180 min	ENR50 and enzyme (trypsin) conc. Trypsin = 1g/10 ml DDI H_2O
Comments:	±0 .01 g rubber used in 10 ml solvent	±0 .01 g rubber used in 10 ml solvent	±0 .01 g rubber used in 10 ml solvent	±0 .01 g rubber used in 10 ml solvent	±0 .01 g rubber used in 10 ml solvent	±0 .01 g rubber used in 10 ml solvent	±0 .0168 g latex used in 10 ml solvent
Toluene	Clear solution. Solution stays clear during titration. Cloudpoint at 11.5 cm^3.	Clear solution. Solution stays clear during titration. Cloudpoint at 11.7 cm^3.	Very swollen. Difficult to see swollen network. Gel particles form during titration. Cloudpoint at 10.14 cm^3.	Partly swollen cloudy polymer network. Solution clouds prematurely due to microgel formation. Cloudpoint obscured.	Swollen polymer network. Impossible to see cloudpoint due to formation of gel flakes during titration.	Invisible particles present in solution. Microgels start to form during titration which makes it impossible to see cloudpoint.	Partly swollen cloudy polymer network. Gel particles form during titration. Cloudpoint at 10.30 cm^3.
Trichlorobenzene	Clear solution. Solution stays clear during titration. Cloudpoint at 5.62 cm^3.	Clear solution. Solution stays clear during titration. Cloudpoint at 5.55 cm^3.	Very swollen rubber network. Almost impossible to see network. Gel particles form during titration. Cloudpoint at 6.37 cm^3.	Solution is already cloudy before titration due to microgel formation. Cloudpoint obscured.	Swollen polymer network. Impossible to see cloudpoint due to formation of gel flakes during titration.	Invisible particles present in solution. Microgels start to form during titration which makes it impossible to see cloudpoint.	Partly swollen cloudy polymer network. Lots of small particles present. Gel particles form during titration. Cloudpoint at 6.55 cm^3.
THF	Clear solution. Solution stays clear during titration. Cloudpoint at 11.43 cm^3.	Clear solution. Solution stays clear during titration. Cloudpoint at 11.50 cm^3.	Very swollen rubber network. Gel particles form during titration. Cloudpoint at 9.81 cm^3.	Partly swollen, white polymer network. Big and small gel pieces form during titration. Cloudpoint at 10.16 cm^3.	Impossible to see cloudpoint due to formation of small gel flakes during titration.	Small white particles present in cloudy solution. Solution becomes even more cloudier during titration which makes it impossible to see cloudpoint.	Polymer network is partly swollen and broken into small pieces. Solution is cloudy before titration. Cloudpoint at 9.20 cm^3.
Benzene	Clear solution. Solution stays clear during titration. Cloudpoint at 11.60 cm^3.	Clear solution. Solution stays clear during titration. Cloudpoint at 10.41 cm^3.	Very swollen rubber network present. Macro and micro gel structures form during titration. Cloudpoint at 11.00 cm^3.	Partly swollen cloudy polymer network. Solution clouds prematurely due to microgel formation. Cloudpoint obscured.	Impossible to see cloudpoint due to formation of small gel flakes during titration.	Rubber looks dissolved but microgel formation starts before the addition of 4 cm^3 non-solvent. This makes the evaluation of the cloudpoint impossible.	Partly swollen cloudy network. Particles whiten on titration. Cloudpoint at 9.27 cm^3.
Dichloro ethane	Clear solution. Solution stays clear during titration. Cloudpoint at 16.00 cm^3.	Clear solution. Solution stays clear during titration. Cloudpoint at 16.44 cm^3.	Partly swollen network in otherwise clear solution. Gel particles form during titration. Cloudpoint at 15.10 cm^3.	Partly swollen cloudy network present. Small gel particles floating around. Solution clouds prematurely due to microgel formation. Cloudpoint obscured.	Impossible to see cloudpoint due to formation of small gel flakes during titration.	Rubber looks dissolved but microgel formation during titration makes cloudpoint evaluation impossible.	Not much swollen network present in solution. Network stays the same during titration. Cloudpoint at 13.87 cm^3.
Butanone	Clear solution. Solution stays clear during titration. Cloudpoint at 6.91 cm^3.	Clear solution. Solution stays clear during titration. Cloudpoint at 6.94 cm^3.	Partly swollen cloudy network present in solution. Network whitens during titration. Cloudpoint at 6.42 cm^3.	Partly swollen, white polymer network in clear, yellow solution. Yellow color obstructs cloudpoint.	Partly swollen, white rubber network present in a clear yellow solution. The solution stays the same during titration. Get cloudpoint at 14.9 cm^3.	White rubber particles present in cloudy solution. Solution becomes even cloudier during titration which makes it impossible to see cloudpoint.	Not much swollen network present in solution. Solution is cloudy before titration which makes it impossible to see cloudpoint.
Ethyl Acetate	Clear solution. Solution stays clear during titration. Cloudpoint at 6.40 cm^3.	Clear solution. Solution stays clear during titration. Cloudpoint at 6.08 cm^3.	Partly swollen cloudy network present in solution. Network whitens during titration. Cloudpoint at 6.19 cm^3.	Partly swollen cloudy network. Small gel particles form during titration. Solution clouds prematurely due to microgel formation. Cloudpoint obscured.	Clear solution with white swollen polymer network. Polymer network starts to break up during titration. Cloudpoint at 12.7 cm^3.	White rubber particles present in cloudy solution. Solution becomes even cloudier during titration which makes it impossible to see cloudpoint.	Not much swollen polymer network. Solution is already cloudy before titration which makes cloudpoint observation very difficult. Cloudpoint at 6.21 cm^3.

Table 5.6: Continued.

By doing cloudpoint determinations on the polymers in question in specific solvent/non-solvent systems, it is therefore possible to predict if sufficient separation is possible by looking at "where" (%NS) the polymers precipitate. If the differences between the CP values of the two polymers are large enough to allow good separation, the particular S/NS system can then be applied in the gradient HPLC analysis. The difference between the CP values is critical, as this must be large enough to allow for the copolymer which will elute between its two homopolymers (this will be explained in more detail in Chapter 7, Section 7.1). Failure to comply will lead to peak overlapping and a decrease in resolution.

Table 5.7 represents cloudpoint measurements performed on ENR50. ENR50 was milled, solubilized and then filtered through a 0.45 μm PTFE filter. Cloudpoints were determined by titration with five different non-solvents under continuous stirring.

Cloudpoint values for polystyrene can be seen in Table 5.8, as obtained from experimental work done by Staal [12].

If cloudpoints from ENR50 and polystyrene are compared, it is clear that using THF as a solvent and methanol as a non-solvent will not give good separation as the cloudpoints, or regions of precipitation of ENR50 and polystyrene, are too close together. Using toluene as solvent and methanol as non-solvent will, however, result in sufficient separation between the two polymers, leading to better analytical results.

5.6.1 Comparison of cloudpoints obtained from titration and HPLC methods

To conclude the chapter, cloudpoints obtained from titration and HPLC methods will be compared. The results will be used to explain certain theoretical principals of gradient HPLC and will also be used to show how S/NS selections are made prior to actual analysis runs.

Non-solvents / Solvents	Methanol			2,2,4-Trimethylpentane			N-Heptane		
	Vol NS titrated (cm3)	Avg vol NS titrated (cm3)	Cloudpoint (%) NS	Vol NS titrated (cm3)	Avg vol NS titrated (cm3)	Cloudpoint (%) NS	Vol NS titrated (cm3)	Avg vol NS titrated (cm3)	Cloudpoint (%) NS
Toluene	12.20 12.20 12.18	12.19	54.94	15.80 15.80 15.81	15.80	61.25	15.91 16.10 15.65	15.89	61.37
Dichlorobenzene	11.70 11.63 11.63	11.65	53.82	23.55 23.53 23.20	23.43	70.08	24.90 24.82 24.80	24.84	71.30
Trichlorobenzene	6.35 6.34 6.38	6.36	38.86	23.95 24.00 24.03	23.99	70.58	25.20 25.20 25.22	25.21	71.60
THF	9.33 9.28 9.29	9.30	48.19	23.95 23.90 24.10	23.98	70.57	25.60 25.64 25.60	25.61	71.92
Ethyl Acetate	6.60 6.60 6.60	6.60	39.76	22.00 21.97 22.00	21.99	68.74	24.00 24.02 24.00	24.01	70.59
Benzene	12.68 12.67 12.68	12.68	55.90	17.55 17.20 17.10	17.28	63.35	17.26 17.30 17.30	17.29	63.35
Dicloroethane	16.06 16.07 16.08	16.07	61.64	24.00 24.00 24.00	24.00	70.59	23.40 23.40 23.40	23.40	70.06
Diethyl Ether	5.50 5.50 5.60	5.53	35.62	0.46 0.44 0.48	0.46	4.40	0.82 0.86 0.86	0.85	7.81
CCl$_4$	11.57 11.57 11.63	11.59	53.68	13.58 13.46 13.54	13.53	57.50	13.38 13.44 13.42	13.41	57.29
Chloroform	15.55 15.50 15.50	15.52	60.81	42.80 42.89 42.88	42.86	81.08	51.60 51.56 51.46	51.54	83.75
Butanone	6.17 6.10 6.11	6.13	37.99	24.00 24.00 23.96	23.99	70.58	24.68 24.76 24.80	24.75	71.22
Acetone	1.55 1.58 1.60	1.58	13.62	23.10 23.10 23.14	23.11	69.80	24.44 24.58 24.42	24.48	71.00
Cyclohexane	Not miscible with MeOH	—	—	0.27 0.26 0.28	0.27	2.63	2.40 2.50 2.40	2.43	19.57

Table 5.7: Cloudpoint values for ENR50.

Non-solvents / Solvents	Ethanol			Water		
	Vol NS titrated (cm3)	Avg vol NS titrated (cm3)	Cloudpoint (%) NS	Vol NS titrated (cm3)	Avg vol NS titrated (cm3)	Cloudpoint (%) NS
Toluene	24.06 24.02 24.06	24.05	70.63	Not miscible with water	—	—
Dichlorobenzene	24.30 24.26 24.32	24.29	70.84	Not miscible with water	—	—
Trichlorobenzene	14.90 14.98 14.96	14.95	59.91	Not miscible with water	—	—
THF	24.50 24.40 24.40	24.43	70.96	1.56 1.56 1.58	1.57	13.54
Ethyl Acetate	15.76 15.70 15.60	15.69	61.07	Not miscible with water	—	—
Benzene	24.84 24.80 24.74	24.79	71.26	Not miscible with water	—	—
Dicloroethane	32.50 32.50 32.48	32.49	76.47	Not miscible with water	—	—
Diethyl Ether	7.80 7.86 7.70	7.79	43.78	Not miscible with water	—	—
CCl₄	25.20 25.22 25.16	25.19	71.59	Not miscible with water	—	—
Chloroform	36.20 36.18 36.14	36.17	78.34	Not miscible with water	—	—
Butanone	17.38 17.32 17.44	17.38	63.48	Not miscible with water	—	—
Acetone	7.22 7.06 7.18	7.15	41.70	0.20 0.20 0.20	0.20	1.96
Cyclohexane	22.58 22.46 22.54	22.53	69.26	Not miscible with water	—	—

Table 5.7: Continued.

Non-solvents / Solvents	2,2,4-Trimethylpentane (%NS)	Methanol (%NS)	Water (%NS)
THF	55	40	10
Toluene	49	23	Immiscible
Ethyl Acetate	37	8	Immiscible
Chloroform	65	27	Immiscible
Butanone	39	12	Immiscible
Cyclohexane	12	Immiscible	Immiscible

Table 5.8: Cloudpoint values for polystyrene [12].

5.6.2 Samples used and sample preparation

Polystyrene (PS) and cis-polyisoprene (PiP) standards were used in cloudpoint determinations. Standards were obtained from Polymer Laboratories as well as TSK Standards (Tosoh Corporation). Approximately 10 mg of each sample was weighed and dissolved in 10 ml THF (1% solution) (see Appendices 2-12). Samples were left to stand overnight to ensure complete solubility and shaken prior to experiments, to ensure homogeneity of the solution. 2 ml of each sample was used for cloudpoint evaluations.

5.6.3 Cloudpoint determinations through titration

Cloudpoint determinations through titration were done on a Dosimat 665. The rate of titration was computer controlled and was set at 1ml/min to ensure very accurate titration values. Stirring was continuous throughout titrations and the value of the %NS used was taken at the first sight of cloudiness. Cloudpoints were determined according to Equation 5.14. In all experiments THF was used as solvent, while the non-solvents were H_2O, ACN, H_2O/ACN and heptane. Cloudpoint values obtained for the PS and PiP samples can be seen in Appendices 2-8. Graphs of log MM vs. the %S used can be seen in Figure 5.4. The cloudpoint measurement of PiP dissolved in THF, with heptane as NS, could not be done due to the fact that heptane could not be used as a NS. Therefore, on titration with heptane, no precipitation was possible.

5.6.4 Cloudpoint determinations through gradient HPLC analysis

Cloudpoint measurements were performed on the Waters Alliance 2690 Separations Module. The Waters 486 Tunable Detector was set at 254 nm and the Polymer Laboratories PL-EMD 960 evaporative light scattering detector (ELSD) was used as a second detector. The solvent flow was set at 0.500 ml/min and 5.0 μl of sample was injected. The column-oven temperature was set at 35 °C and the air temperature of the ELSD at 70 °C. Flow-rate of N_2 in the ELSD was 4.9 l/min.
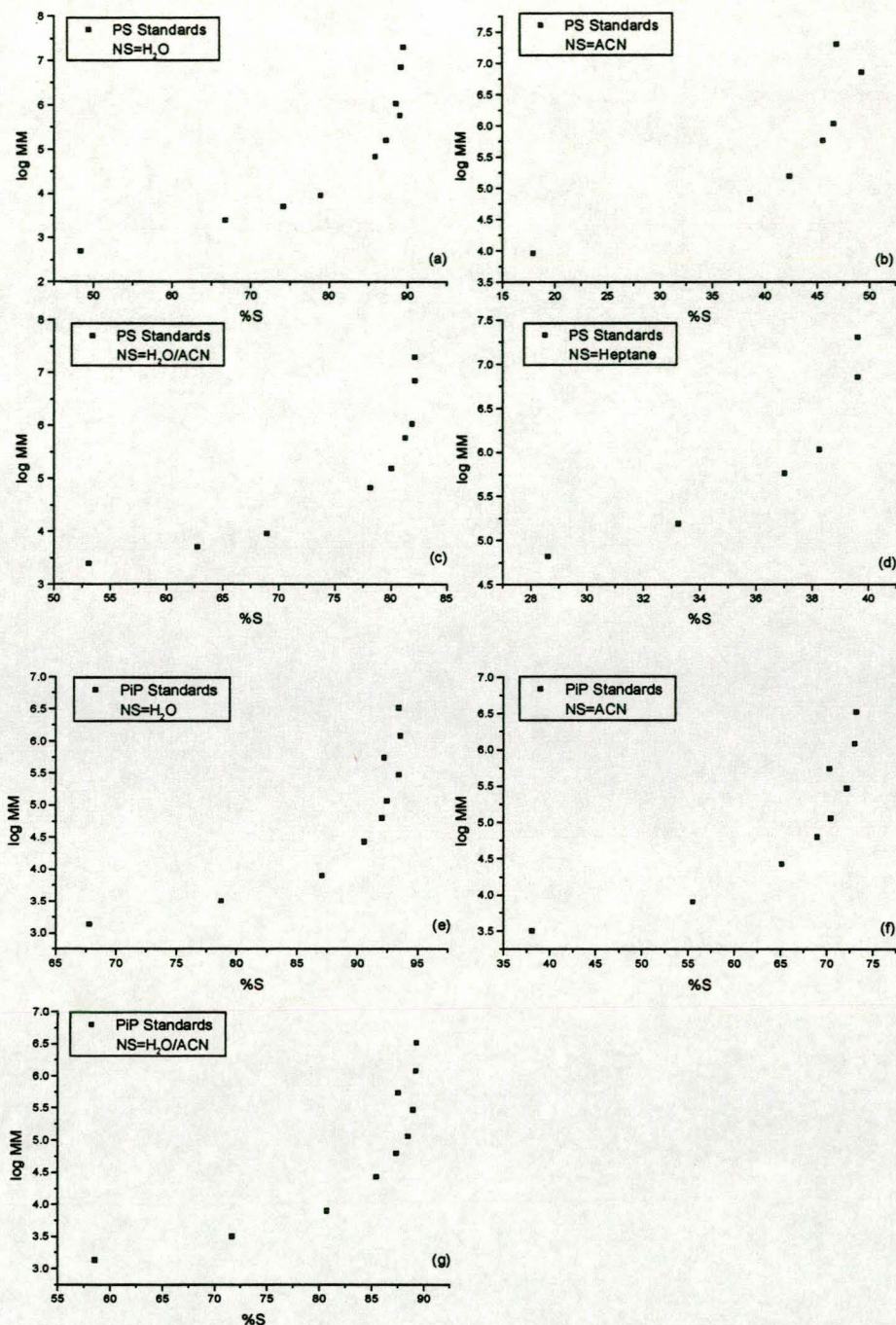
Figure 5.4: Cloudpoint measurements for PS (a-d) and PiP (e-g).

For both PS and PiP the cloudpoints were evaluated chromatographically, with THF as solvent and ACN and H_2O/ACN as non-solvents. The retention times of the different MM polymers were used to calculate the S/NS concentration at the time of redissolution and hence the cloudpoints were obtained.

Due to the fact that all chromatographic equipment is associated with a dead time, the following equation was used to calculate the %S needed for redissolution at corrected retention time values.

$$%S = (RT - t_0)\Delta\phi_s + %S_g \qquad (5.15)$$

$$%S = (RT - t_{sg} - t_g)\Delta\phi_s + %S_g \qquad (5.16)$$

where RT is the polymer's retention time, t_0 is the dead time, t_{sg} is the time needed for the gradient to reach the detector, t_g is the gradient time, $\Delta\phi_s$ is the gradient speed (%S/min) and %S_g is the percentage solvent at the beginning of the gradient. Results of cloudpoint measurements can be seen in Figure 5.5 and values in Appendices 9-12.
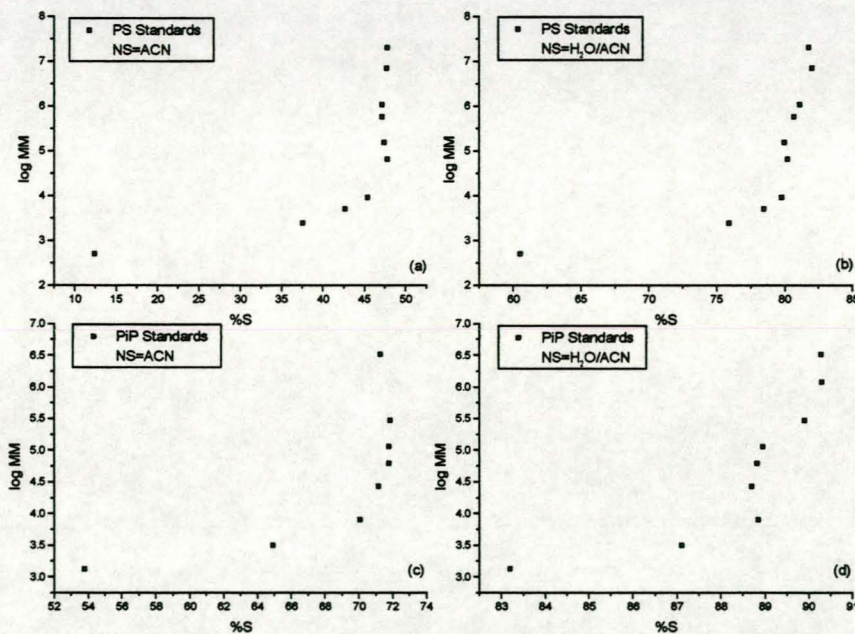
Figure 5.5: Cloudpoints for PS and PiP obtained chromatographically.

The cloudpoint values obtained chromatographically and through titration can now be compared. The results are displayed in Figure 5.6. The two methods yield comparable values.
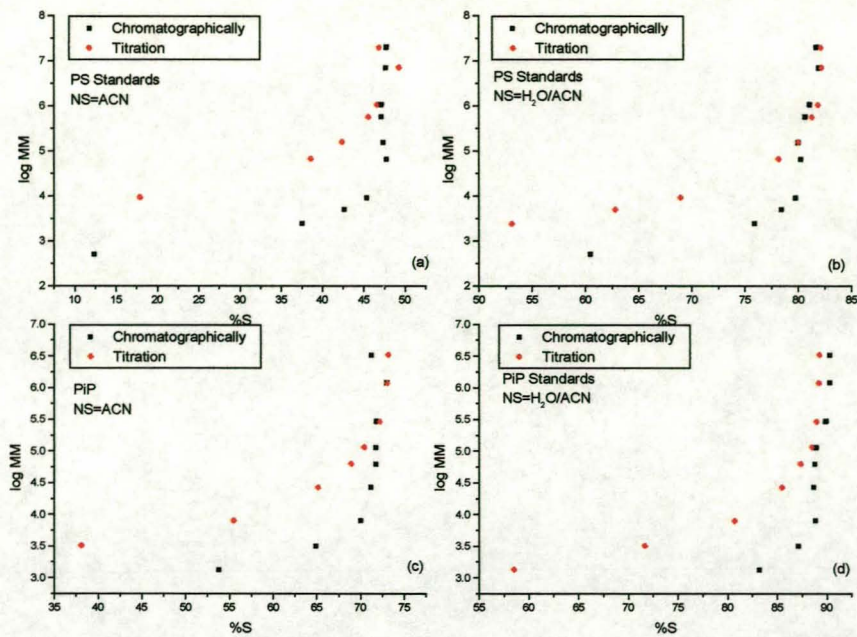
Figure 5.6: Comparison of cloudpoint values obtained chromatographically and through titration.

Finally, it is possible to deduce which S/NS combination will produce the best separation. This can be done by plotting the cloudpoint values obtained chromatographically on one chart and looking at the distance between the %S-values for PS and PiP (Figure 5.7).
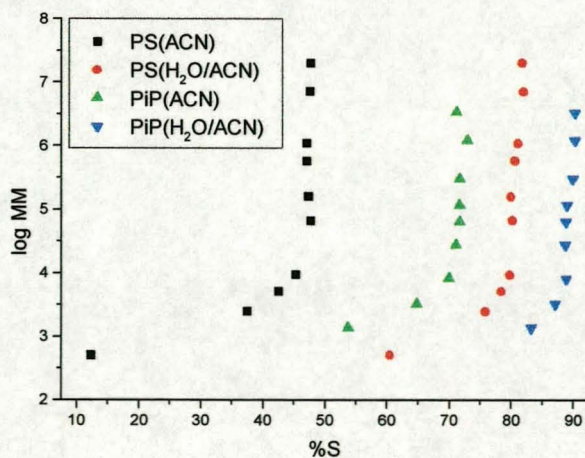
Figure 5.7: Comparison of cloudpoint values for PS and PiP for different non-solvents.

From the graph it is clear that the best separation between PS and PiP is possible if ACN is used as non-solvent.

5.7 Conclusions

The use of solubility parameters and cloudpoint determinations play a very important role in gradient HPLC. Through solubility parameters it is possible to decide which solvents to use in gradient HPLC experiments and other elementary questions e.g. miscibility can also easily be answered. Time wasted on solvent testing is therefore eliminated. Cloudpoint evaluations, on the other hand, provide a way to see whether or not a sufficient separation will be possible. By using different non-solvents in the evaluations and plotting the results on one graph, quick and easy decisions can be made regarding the type of gradient to use.

5.8 References

1   P.J.C.H. Cools, F. Maesen, B. Klumperman, A.M. van Herk, A.L. German;
         *Determinations of the Chemical Composition Distribution of Copolymers of
         Styrene and Butadiene by Gradient Polymer Elution Chromatography*;
         Journal of Chromatography A; **736**, 1996, 125-130

2   P.J.C.H. Cools, A.M. van Herk, A.L. German, W. Staal; *Critical Retention
         Behavior of Homopolymers*; Journal of Liquid Chromatography; **17**(14+15),
         1994, 3133-3141

3   D.W. van Krevelen; Properties of Polymers.   Their Correlation with
         Chemical Structure; their Numerical Estimation and Prediction from
         Additive Group Contributions; Elsevier Science Publishers B.V., 1990

4   R.A. Shalliker, P.E. Kavanagh, I.M. Russel; *Reversed-phase Gradient
         Elution Behavior of Polystyrenes in a Dichloromethane-methanol Solvent
         System*; Journal of Chromatography; **543**, 1991, 157-169

5   G. Glöckner; Gradient HPLC of Copolymers and Chromatographic Cross-
         Fractionation; Springer-Verlag, Heidelberg Berlin; 1991

6   J.A. Brydson; Rubber Chemistry; Applied Science Publishers LTD London

7   F.W. Billmeyer; Textbook of Polymer Science, Second Edition; Wiley-
         Interscience, a Division of John Wiley and Sons, Inc., 1962

8   J. Brandrup, E.H. Immergut; Polymer Handbook, Second Edition; Wiley-
         Interscience Publication, 1975

9   A.F.M Barton; CRC Handbook of Solubility Parameters and Other
         Cohesion Parameters, Second Edition; CRC Press, 1991

10   S.N. Gan; Z.A. Hamad; *Partial Conversion of Epoxide Groups to Diols in Epoxidized Natural Rubber*; Polymer; **38**(8), 1997, 1953-1956

11   N.V. Bac, L Terlemezyan, M. Mihailov; *Epoxidation of Natural Rubber in Latex in the Presence of a Reducing Agent*; Journal of Applied Polymer Science; **50**, 1993, 845-849

12   W.J. Staal; Gradient Polymer Elution Chromatography; Ph.D. Thesis; Eindhoven University of Technology, Eindhoven, The Netherlands; 1996

Chapter **6**

Preliminary Experimental Analyses (FTIR, GPC, GPC-FTIR) Performed on Styrene-Grafted Epoxidized Natural Rubber

6.1 Introduction

The importance of gel permeation chromatography (GPC), or size exclusion chromatography (SEC), has been widely discussed by Pasch [1] and Glöckner [2]. Both these authors emphasized the importance of SEC as an analytical tool for copolymers. Not only does SEC gives valuable information about the molecular mass distribution (MMD) of a given sample, but it can also supply information about the chemical composition along the MMD peak if dual detectors are used. The incorporation of a refractive index (RI) detector and ultraviolet (UV) detector will be able to produce such results, as UV-detectors measure the UV absorbing groups in a polymer and RI-detectors measure the concentration of the molecules in a polymer sample. UV absorbing groups can be situated in the end groups of the polymer or in the repeating unit. By using the dual detector method it is therefore possible to see changes in retention time (hydrodynamic volume) and MMD as a function of the monomer/initiator concentrations as used in grafting reactions between styrene and ENR50.

Fourier-transform infrared (FTIR) spectroscopy can be used to determine whether certain chemical compositions are present in a polymer or not.

Although FTIR analysis can be done on copolymers, the results will not give any indication of the degree of copolymerization or if any copolymerization took place at all. It will however show peaks resulting from the individual homopolymers or the copolymer and, by evaluating the peak area ratios, make it possible to calculate the relative amount of a specific precursor present in the sample. This can then be correlated with the starting conditions (monomer/initiator concentrations). Apart from the above, it is also possible to detect chemical changes i.e. disappearance or appearance of functional groups in the homopolymers. These changes could be due to the reaction conditions or reactions between the homopolymers.

Another analytical tool that can be used in preliminary experiments is SEC coupled to FTIR (SEC-FTIR) or LC-transform [3,4]. SEC-FTIR was introduced in 1991 and has since then grown as a very important laboratory technique. By using this technique it is possible to determine the compositional variations, i.e. the distribution, of the two homopolymers in a copolymer. By combining chromatography and spectroscopy, samples can quickly and easily be deformulated.

The above 3 techniques have been used to perform preliminary analytical experiments on the grafted samples (see Chapter 4, Section 4.3.3 for formulations) in order to obtain results which will be used to get a better understanding of the composition of the grafted samples, hence allowing better explanation of the gradient HPLC analyses results. The following sections will include an in-depth discussion on the sample preparation, analysis and results obtained by using these techniques.

6.2 Equipment

6.2.1 Equipment for FTIR analysis

Due to the different natures of the samples to be analyzed by FTIR (gel part, soluble part and dried sample), different FTIR spectroscopy techniques were applied in the analysis of the various parts. The dried samples and soluble part of the samples were analyzed on a Shimadzu FTIR-8101M Fourier Transform Infrared Spectrometer. Shimadzu Hyper IR software was used for computer manipulation of the data.

The gel part of the sample was analyzed on a Perkin Elmer Photo Acoustic FTIR spectrometer (Paragon 1000 PC). Data analysis was done by using GRAMS Analyst 1000.

6.2.2 Equipment for GPC analysis

The GPC system consisted of a Waters 510 HPLC pump, Waters 486 tunable absorbance detector at 260nm, Waters 410 differential refractometer and a TSP (Thermo Separations Products) Spectra Series AS100 autosampler. Five columns and a pre-column filter were used (Table 6.1) and the column oven was set at 30°C. PSS WinGPC Scientific V4.02 was used for data analysis. Tetrahydrofuran (THF) was used as solvent and the flow rate was 1.06ml/min. The volume of the samples injected was 180μl.

Column	Column serial number	Effective molecular mass range
Styragel® HR1	WAT 044234	100-5000
Styragel® HR3	WAT 044222	500-30000
Styragel® HR4	WAT 044225	5000-600000
Styragel® HR5	WAT 044260	$50000-4 \times 10^6$
Styragel® HR6	WAT 044268	$200000-1 \times 10^7$

Table 6.1: Columns used in GPC analysis.

6.2.3 Equipment for GPC-FTIR analysis

GPC-FTIR equipment used consisted of a Waters 510 pump, Nicolet 460 FTIR and a Lab Connections LC-transform with a Germanium disk. THF was used as solvent and the solvent flow was set at 1ml/min. Columns used (in series) can be seen in Table 6.2 and the columns were used at room temperature. Omnic 3.1 was used for data analysis.

Column	Particle size	Pore size	Effective molecular mass range
PLgel	10 μ	10^5 Å	10^5-10^6
PLgel	5 μ (mixed D)	---	200-4×10^5
PLgel	3 μ (mixed E)	---	100-3×10^4
PLgel	5 μ	50 Å	100-1000

Table 6.2: Columns used in GPC-FTIR analysis.

6.3 Sample preparation

6.3.1 General sample preparation

Ten styrene-grafted epoxidized natural rubber latex samples (±10g of each) was weighed off and added to 10g H_2O in a 500ml beaker. The diluted latex was continuously stirred with a magnetic stirrer while 200ml MeOH was slowly added (one drop/second) through a dropping funnel. After addition of the MeOH, the precipitated rubber was left until most of the rubber had settled at the bottom of the beaker. The excess MeOH was then carefully decanted, after which a further 100ml MeOH was added to the precipitated particles to rinse out as much water as possible. Again the surplus MeOH was carefully decanted and the precipitated rubber decanted into a flat-glass evaporating dish. The precipitated rubber was then dried under vacuum at room temperature until completely dry. The dried rubber was white in color and most of the samples were brittle, except for samples 3 and 7 that were not rubbery but a bit tougher than the other samples.

6.3.2 Sample preparation for FTIR

Due to the insolubility of the grafted samples, the presence of styrene in the soluble as well as the insoluble part of the sample had to be evaluated. This was done by FTIR analyses of the complete sample, the soluble part of the sample and the gel part of the sample. FTIR analysis of the completely dried sample was done by incorporation of the dried sample in a KBr matrix and then pressing of FTIR discs with the matrix.

Discs were made by weighing off ±0.02g of the dried sample and adding completely dry and water-free KBr until the total sample weight was ±4.2g. The mixture was then ground with a pestle and mortar to ensure complete incorporation of the sample in the KBr matrix. Sample/KBr-discs could then be prepared by casting this mixture into a copper ring and applying vacuum and pressure (150 kPa) to it for 5 minutes.

FTIR analysis on the soluble part was performed by making KBr discs and placing them on a heated table. The soluble part was then dropped onto the heated discs and the solvent vaporized, leaving the deposited sample on the KBr disc.

For the above two methods, clear KBr windows were made for background scans prior to every sample scan.

Gel fractions had to be completely dry before analyses. The gels were therefore extensively dried in a vacuum oven at room temperature before any analysis could commence.

6.3.3 Sample preparation for GPC analysis

For GPC analysis, 10mg of the dried samples were dissolved in 3ml THF. The samples were left overnight in solution and then filtered first through a Gelman Glass Acrodisc® and then a Gelman GHP Acrodisc GF 0.45μm.

6.3.4 Sample preparation for GPC-FTIR analysis

±300mg dried sample was weighed and added to 25ml of THF (HPLC grade). The solution was left in an oven at 50 °C for 24 hours to obtain maximum solubility. After 24 hours the soluble part was drawn off from the solution with a syringe and then filtered through two filters (Gelman Glass Acrodisc® and Gelman GHP Acrodisc GF 0.45μm) into a clean, weighed roundbottom flask. The flask was then connected to a rotary evaporator and all the solvent evaporated off, until only the solvent-free sample remained in the flask. The flask was then weighed again and the amount of sample left in the flask calculated. This was done to ensure that a certain amount (±20mg) of polymer was left in the flask after vaporizing of the solvent in order to obtain a high enough concentration (±20mg/ml) of polymer for GPC-FTIR analysis.

6.4 Results and discussions

6.4.1 FTIR Analysis

As already mentioned, analysis was performed on the complete sample, the soluble part of the sample as well as the gel part of the sample. This was mainly done to compare the styrene content in the different samples and to try and correlate this with the initiator/monomer concentrations that were used in the polymerization reactions of the individual samples. The styrene contents in the complete, gel and soluble part of the sample were also used to explain trends in the gradient HPLC analysis. Furthermore, an ENR50 sample that was subjected to reaction conditions similar to the respective samples was evaluated. The only difference here was that no monomer was added during the reaction. This created the opportunity to see if any chemical changes of the structure of the rubber resulted during the polymerization reaction. This sample will be referred to as polymerized ENR50 or polENR50.

6.4.1.1 Analysis of the completely dried sample

Results of FTIR analysis done on the KBr-pressings of the ENR50 grafted samples can be seen in Figure 6.1. From the analysis it could clearly be seen that the grafted samples contained styrene and that the intensity of the styrene peak varied from sample to sample. The two peaks that were monitored were the peaks at 1452 cm^{-1} and 698 cm^{-1}. The peak at 1452 cm^{-1} was ascribed to the CH-bands present in both the rubber and styrene and the peak at 698 cm^{-1} was ascribed to the aromatic structure of the styrene. Therefore, by evaluating the peak areas of these two peaks, and calculating the ratio between them, the relative amount of styrene in the total sample could be evaluated. It must be noted that this was not an analysis to see whether styrene had grafted, but rather to see whether the initial amount of styrene used in the polymerization reaction correlated with the amount of styrene in the grafted sample. Results of the calculated peak areas can be seen in Table 6.3.

Unfortunately it was not possible to prepare a KBr pressing of sample 3 due to the rubbery nature of the sample.

	Area (Styrene) 698 cm^{-1}	Area (Styrene+ENR50) 1452 cm^{-1}	Area $\left(\dfrac{Styrene}{Styrene + ENR50}\right)$
ENRPS1	7.0177	11.016	0.6370
ENRPS2	2.1139	11.235	0.1881
ENRPS3	---	---	---
ENRPS4	4.7089	11.635	0.4047
ENRPS5	12.915	11.651	1.1085
ENRPS6	6.8788	9.3499	0.7357
ENRPS7	2.1009	3.3218	0.6324
ENRPS8	10.530	10.745	1.0000
ENRPS9	5.4013	12.118	0.4457
ENRPS10	13.815	11.335	1.2188

Table 6.3: Calculation of the relative amounts of styrene present in the total styrene-grafted ENR50 samples.

Of samples 1-5, sample 5 had the highest amount of styrene present, followed by sample 1 and then samples 4 and 2, in descending order of styrene content. This is in good correlation with the graph of the amount of monomer vs. amount of initiator used (Figure 6.2). Of samples 6-10, sample 10 had the highest amount of styrene present, followed by sample 8 and then sample 6, in descending order. Following them were sample 7 and sample 9. Sample 2 and sample 7 were supposed to correlate because the same monomer and initiator concentrations were used in the preparation of both samples, but they did not. The same effect was also seen for MMA grafted ENR50 and is due to the type of latex used (older latex vs. the newer latex – refer to Chapter 4) [5].
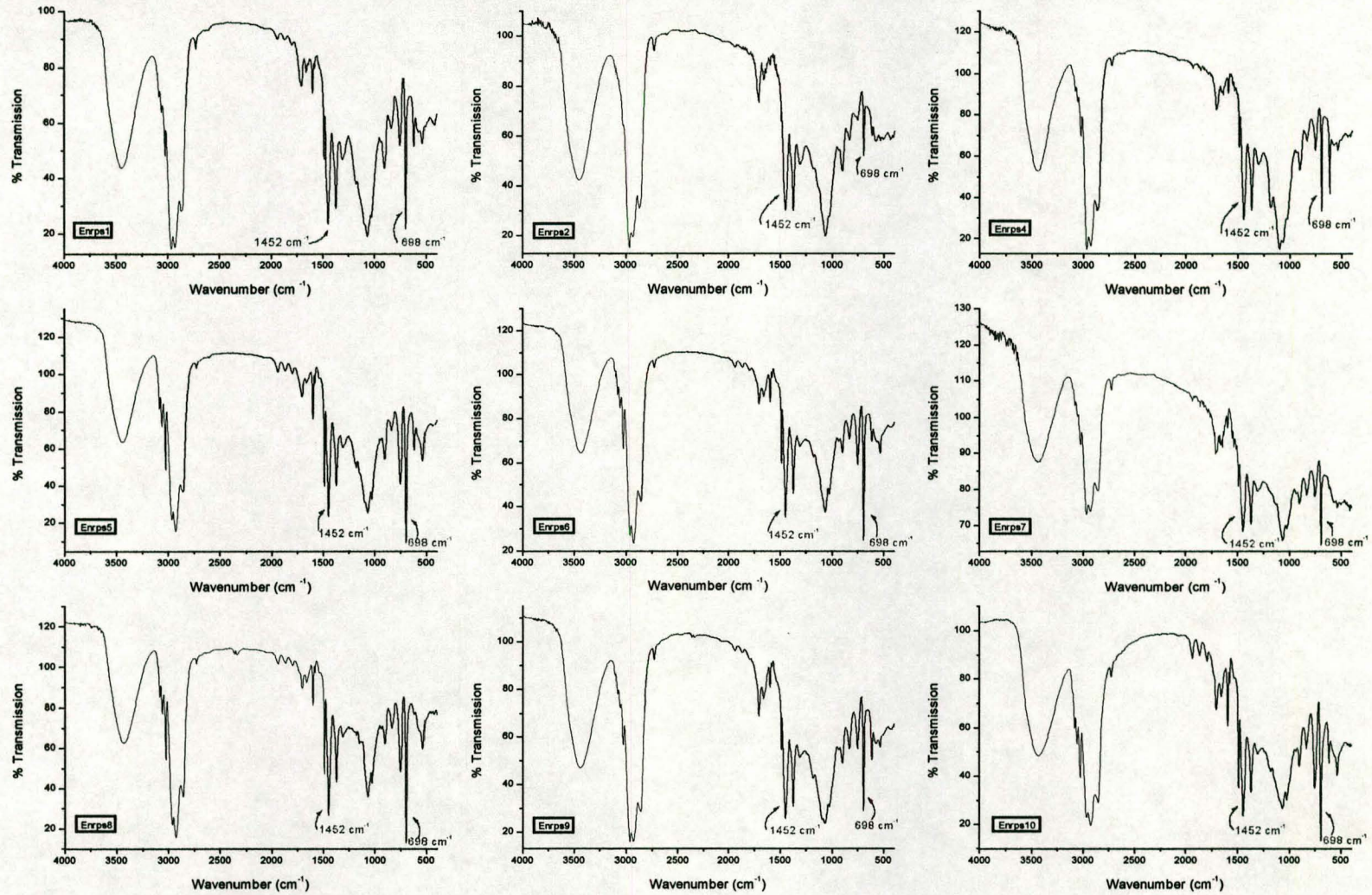
Figure 6.1: FTIR spectra of the dried styrene-grafted ENR50 samples. Peaks at 1452 cm^{-1} and 698 cm^{-1} were monitored.
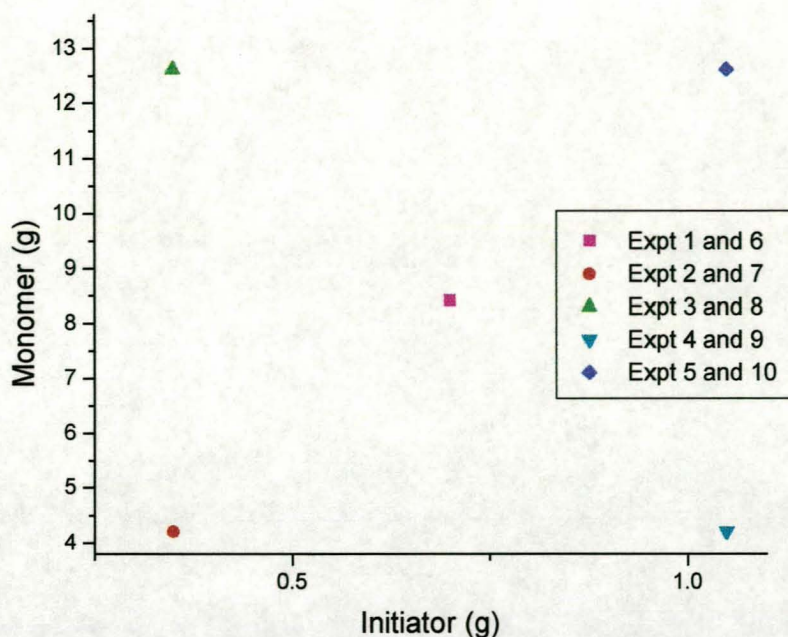
Figure 6.2: Experimental conditions used for the preparation of styrene-grafted ENR50.

6.4.1.2 Analysis of the soluble part of the sample

Analyses of the soluble part of the styrene-grafted ENR50 can be seen in Figure 6.3. Values for the relative amount of styrene present in the samples can be seen in Table 6.4. These values can however not be correlated with the starting monomer/initiator concentrations as the total styrene content is not represented in the soluble part of the samples if grafting is assumed. This is due to the fact that not all the grafted material is soluble.

The styrene content of the different samples can however be compared with the styrene content of the total sample. By doing this, it is clear that the styrene content compared to the rubber content, for the soluble part, is much higher. This is due to the fact that the ENR50 has a limited solubility. The higher styrene content can be correlated with gradient HPLC results (Chapter 7, Section 7.4.2) where big ungrafted polystyrene peaks are visible for the soluble part of the sample. If grafting took place, the soluble part of the grafted sample will also contribute to the styrene FTIR peak.
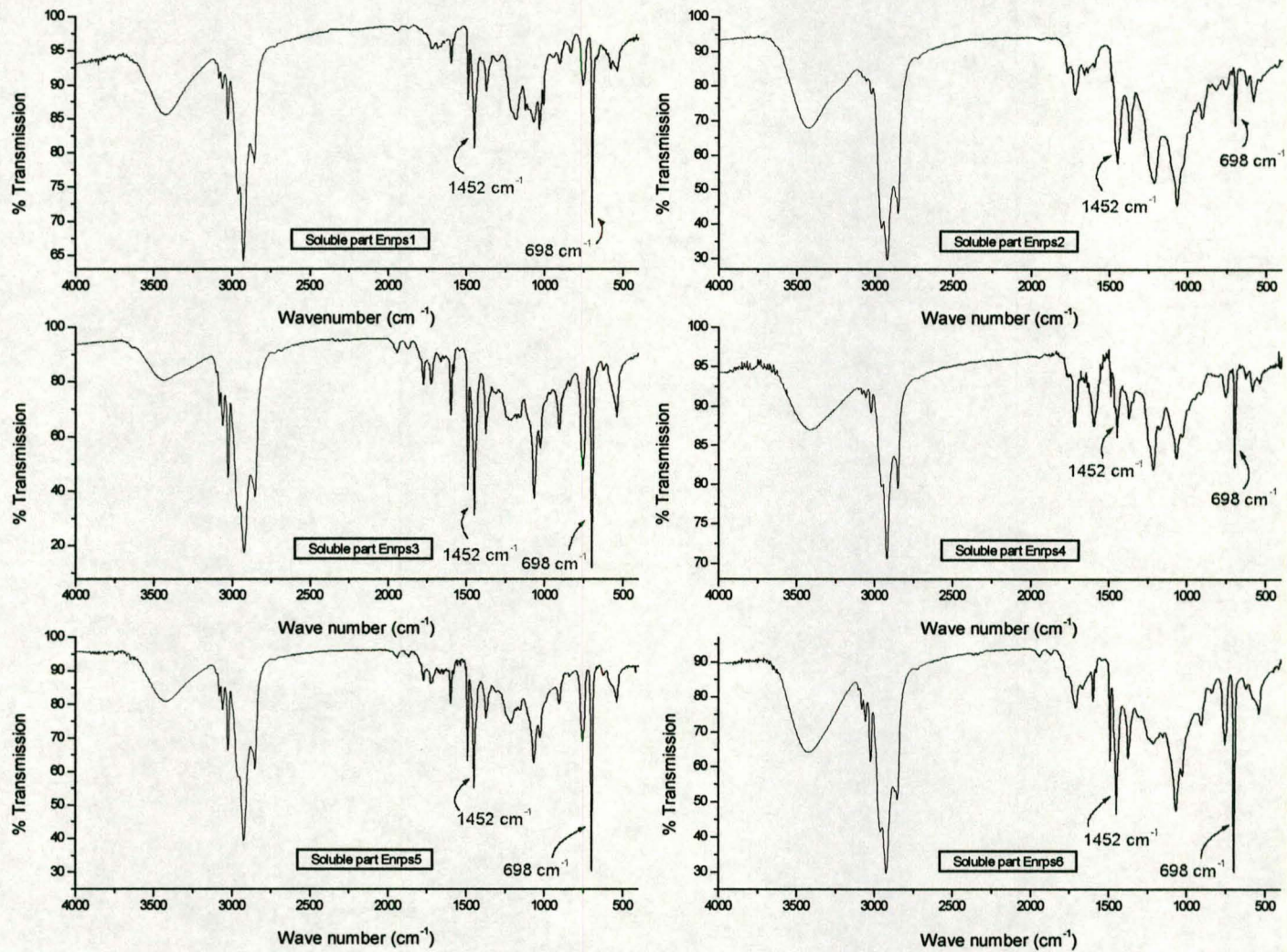
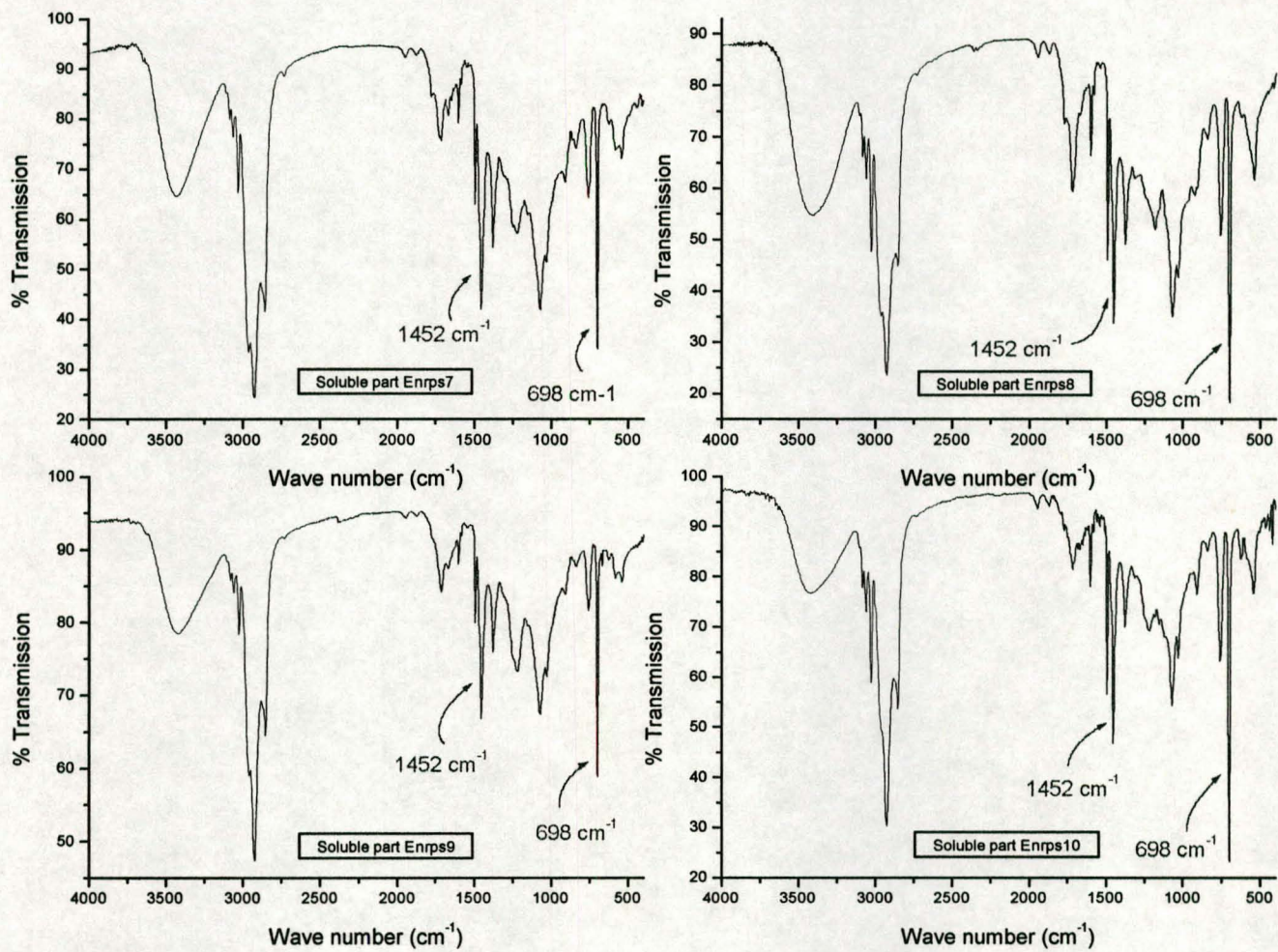Figure 6.3: FTIR analysis of the soluble part of the styrene-grafted ENR50. Peaks at 1452 cm^{-1} and 698 cm^{-1} were monitored.

Figure 6.3: Continued.

	Area (Styrene) 698 cm^{-1}	Area (Styrene+ENR50) 1452 cm^{-1}	Area $\left(\dfrac{Styrene}{Styrene + ENR50}\right)$
ENRPS1	1.8323	1.4241	1.2866
ENRPS2	0.9691	4.9692	0.1950
ENRPS3	10.319	7.5255	1.3712
ENRPS4	0.6860	0.7910	0.8673
ENRPS5	5.2887	3.5057	1.5086
ENRPS6	5.6332	4.7560	1.0583
ENRPS7	4.3141	6.3458	0.6798
ENRPS8	7.5640	6.3160	1.11976
ENRPS9	1.9501	2.8216	0.6911
ENRPS10	6.5954	4.7362	1.3926

Table 6.4: Calculation of the relative amounts of styrene present in the soluble part of the styrene-grafted ENR50 samples.

6.4.1.3 Analysis of the gel part of the sample

FTIR spectra of the gel parts of the samples are shown in Figure 6.4. Values for the relative styrene contents of the samples are displayed in Table 6.5. Analysis of the gel part revealed very interesting trends. As can be seen in Tables 6.4 and 6.5, the values of the styrene contents in the gel are lower than for the styrene content in the soluble part, except for samples 2, 8 and 9. This can be due to the fact that insufficient grafting took place, if it did take place, or it could be that a high percentage of the grafted sample was solubilized. There is also a possibility of ungrafted polystyrene being partially trapped in the gel network. If it can be assumed that the grafted material is incorporated in the gel and that some of the grafted material is also present in the soluble phase, then correlation with results of gradient HPLC analysis is very good. Sample 9 shows a higher styrene content in the gel phase than in the soluble phase, in other words more grafting has taken place.
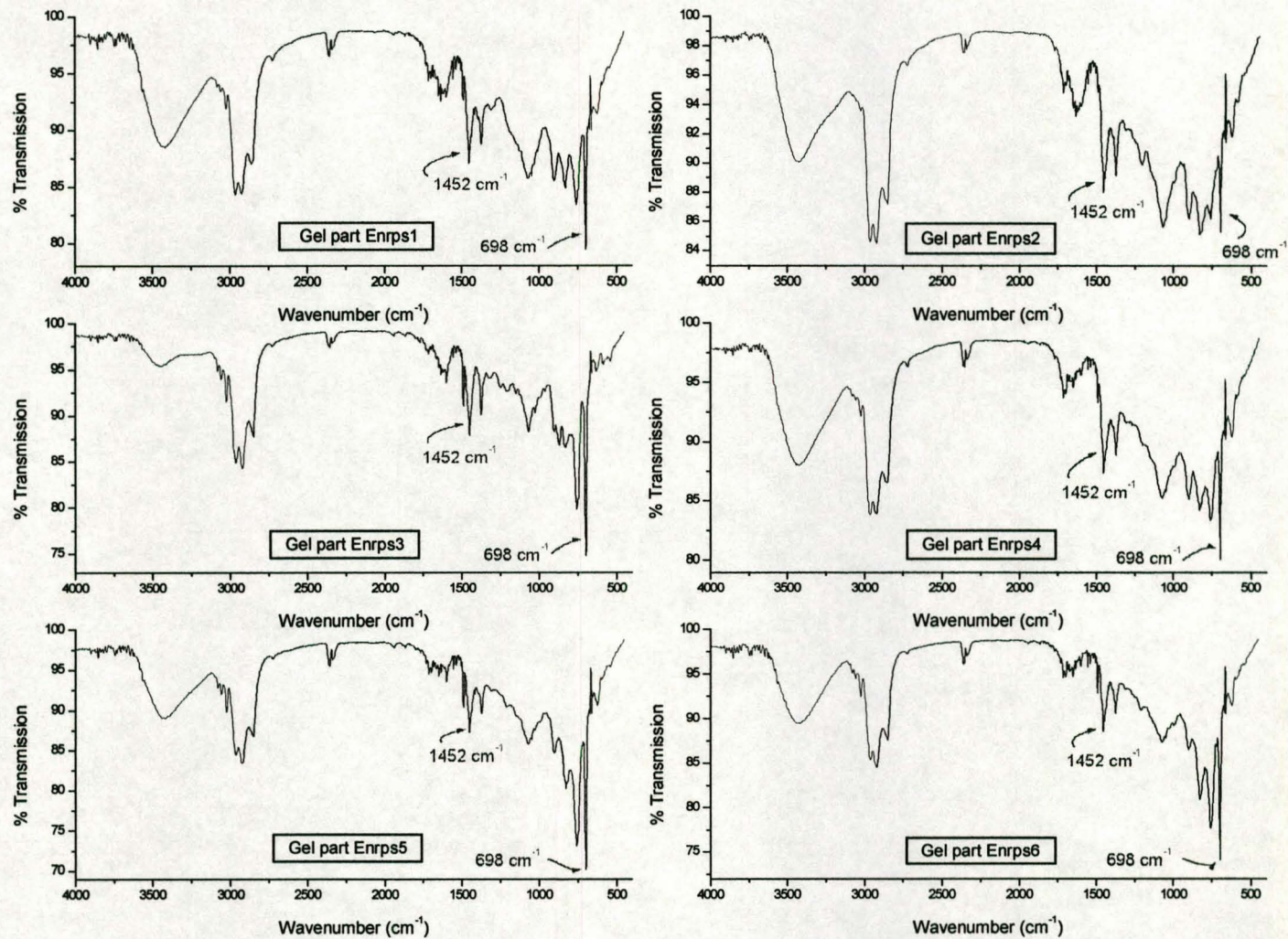
Figure 6.4: FTIR analysis of the gel part of the styrene-grafted ENR50. Peaks at 1452 cm^{-1} and 698 cm^{-1} were monitored.
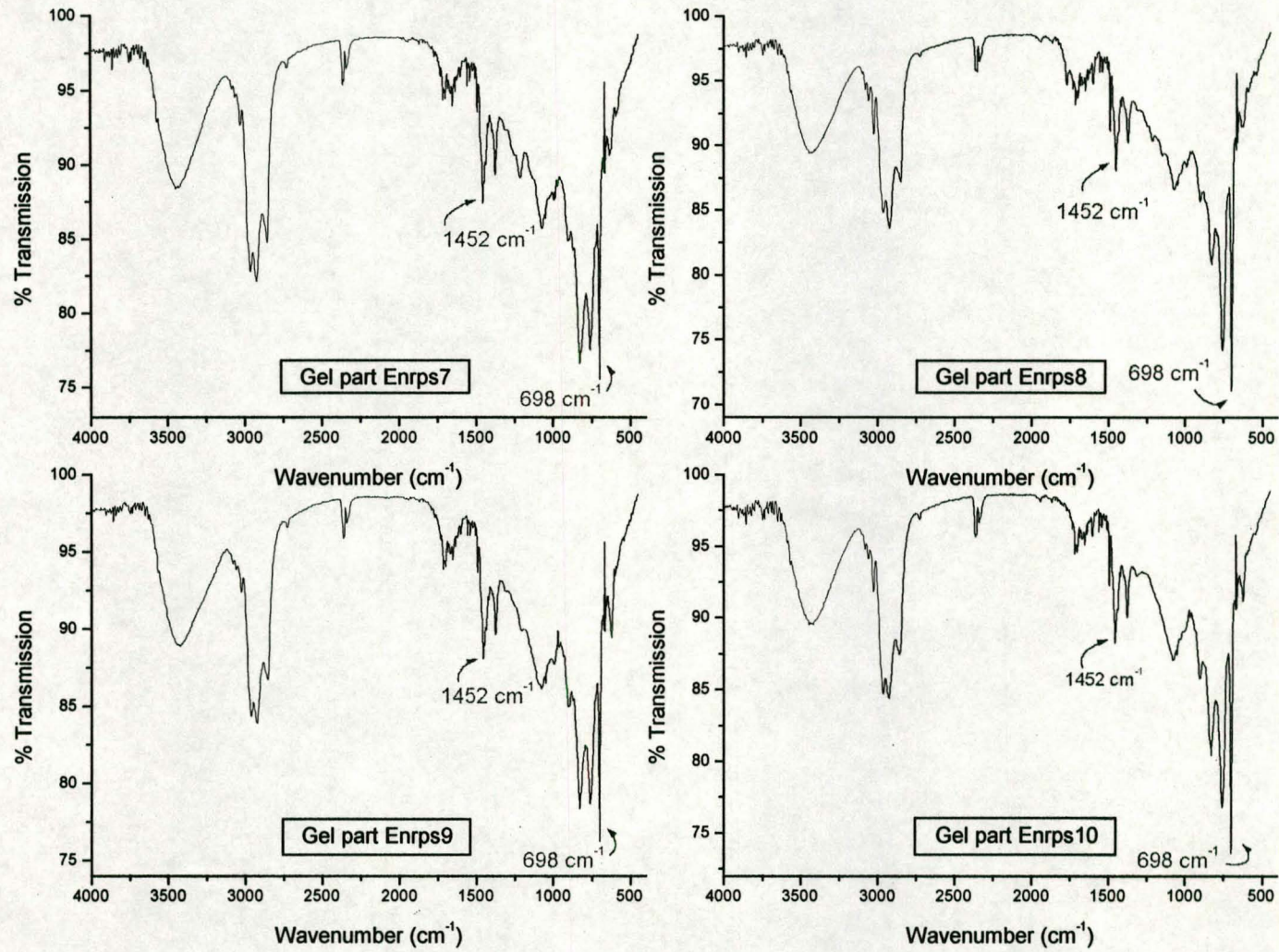
Figure 6.4: Continued.

	Area (Styrene) 698 cm^{-1}	Area (Styrene+ENR50) 1452 cm^{-1}	Area $\left(\dfrac{Styrene}{Styrene + ENR50} \right)$
ENRPS1	127.738	180.603	0.707
ENRPS2	67.584	180.133	0.375
ENRPS3	276.919	229.267	1.207
ENRPS4	115.870	211.067	0.548
ENRPS5	243.629	172.818	1.409
ENRPS6	199.176	177.905	0.965
ENRPS7	142.611	233.691	0.610
ENRPS8	240.554	191.078	1.258
ENRPS9	150.662	211.240	0.713
ENRPS10	211.739	207.751	1.019

Table 6.5: Calculation of the relative amounts of styrene present in the gel part of the styrene-grafted ENR50 samples.

By looking at gradient analysis of the grafted samples (Chapter 7, Figure 7.33), the copolymer peak will reveal that the highest concentration of styrene in the copolymer peaks can be found in sample 9. The chromatogram also shows a very low free (ungrafted) PS content. From this it follows that the soluble part of the sample is made up of free PS and grafted PS. The last question that has to be answered is why is sample 9 more soluble? The answer can also be found in GPC results where it is shown that sample 9 has a very low molecular mass due to the fact that a high initiator concentration and low monomer concentration were used, leading to the formation of short chains. Sample 9 can therefore be better solubilized and will give the biggest copolymer peak in gradient HPLC analysis.

Sample 2 also shows a higher styrene content, but in this case less initiator was used, leading to longer chains and less solubility. This also correlates with results of gradient analysis. All gradient analysis chromatograms will be shown in Chapter 7, where the trends of the copolymer peaks will be discussed, with the inclusion of FTIR data for better understanding.

6.4.1.4 Evaluation of ENR50 and polymerized ENR50 (subjected to reaction conditions) by FTIR analysis

The rubber (ENR50) was subjected to polymerization conditions to see if a change in the structure occurred. All conditions as used for the polymerization reactions were used, except that no styrene monomer was added during the reaction. For reaction conditions see Table 6.6.

Reactor	
ENR50	47.69 g
SLS (Emulsifier)	2.83 g
Water (DDI)	33.12 g
Initiator Solution	
Initiator (KPS)	0.36 g
Water (DDI)	13.99 g

Table 6.6: Reaction conditions for polymerized ENR50.

The reactor was charged with rubber, emulsifier and water and heated to 82 °C, while stirring under argon. Initiator was dripped into the reactor over a 4-hour period. Both ENR50 and polymerized ENR50 were subjected to FTIR analysis. Results can be seen in Figure 6.5.

FTIR data obtained for ENR50 and polymerized ENR50 was compared to results of work done by Viet Bac and co-workers [6,7]. They showed that prolonged storing of the ENR or when it was reacted at temperatures above 50 °C for a long period of time could lead to ring-opened products. They also assigned peak values for natural rubber and its derivatives thereby creating the opportunity to evaluate the polymerized ENR50.

The peak at 3284 cm^{-1} (Figure 6.5) is due to the formation of ring-opening products (stretching bands of OH groups).
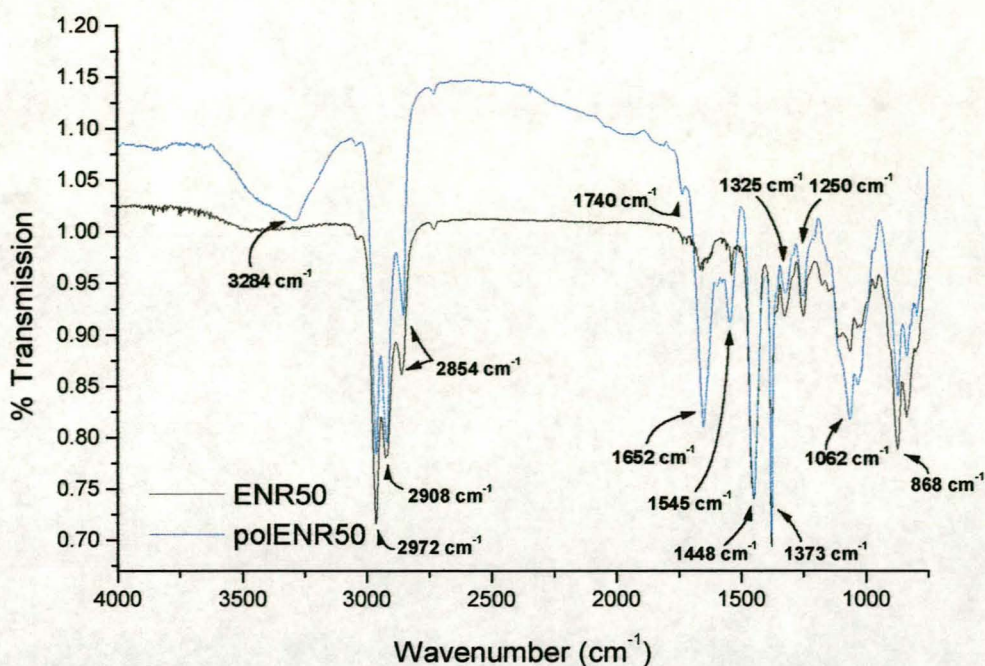
Figure 6.5: FTIR spectra of ENR50 and polymerized ENR50.

The band at 1062 cm^{-1} is assigned to a tetrahydrofuran (THF) ring, also formed during the ring-opening side reaction. The epoxide groups show characteristic bands at 868 cm^{-1} (asymmetrical ring stretching) and 1250 cm^{-1} (symmetrical ring stretching). The band at 2854 cm^{-1} is due to CH_2 (symmetrical) groups and that at 2972 cm^{-1} is due to CH_3 bands. The band at 2908 cm^{-1} is caused by the CH_2 (asymmetrical) groups. The peaks at 1448 cm^{-1} and 1373 cm^{-1} are comparable and they are caused by methylene methyl (CH_2CH_3) and methyl (CH_3) groups respectively. The band appearing at 1740 cm^{-1} is also caused by ring-opened products (ester carbonyl groups). The very strong peak appearing in the polENR50 spectrum (1652 cm^{-1}) is caused by the cis-alkene functional groups (Me-C=CH-) and is also a product of ring opening. The ring-opening reaction and consequent formation of the THF ring can be seen in Figure 6.6.

Through FTIR analysis of the polymerized ENR50, it is therefore possible to say that a slight change in chemical structure of the ENR50 occurred during the grafting reaction. Further proof of structural change as a result of reaction conditions will also be evident in the SEC analysis of the samples, which can be seen in the next section.
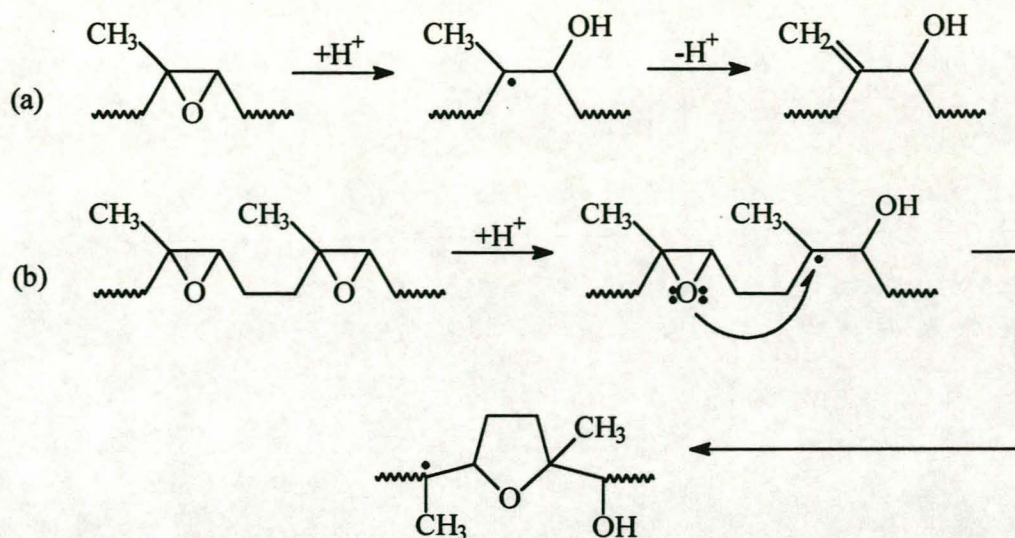
Figure 6.6: Schematic representation of (a) the ring-opening reaction and (b) the THF ring formation.

6.4.2 Size exclusion chromatography (SEC) analysis

Size exclusion chromatography (SEC) was performed on all the styrene-grafted epoxidized natural rubber samples to evaluate the molecular masses of the samples and to correlate the results with the initiator/monomer concentrations as used in the polymerization reactions of the individual samples. By comparing results obtained from the different detectors used, it was also possible to make assumptions on the incorporation of the styrene in the sample, i.e. to see whether more styrene was incorporated in the lower or higher MM part of the sample.

Furthermore, SEC chromatograms of ENR50 and polymerized ENR50 were compared to see if the changes in chemical structure had any influence on MM and, if so, to what extent. The reproducibility between the soluble part of the dried sample and the soluble part of the latex was also compared.

6.4.2.1 Comparison between SEC results for the dried sample and SEC results for the latex sample for reproducibility purposes

The reproducibility of the dried samples and the latex samples was evaluated by comparing SEC results. Here, evaluation of reproducibility refers to the determination of whether or not the soluble part of the dried sample can be used for analysis purposes instead of the soluble part of the latex. UV and refractive index (RI) signals, obtained for both samples (dried and latex), can be seen in Figure 6.7 and Figure 6.8 respectively.
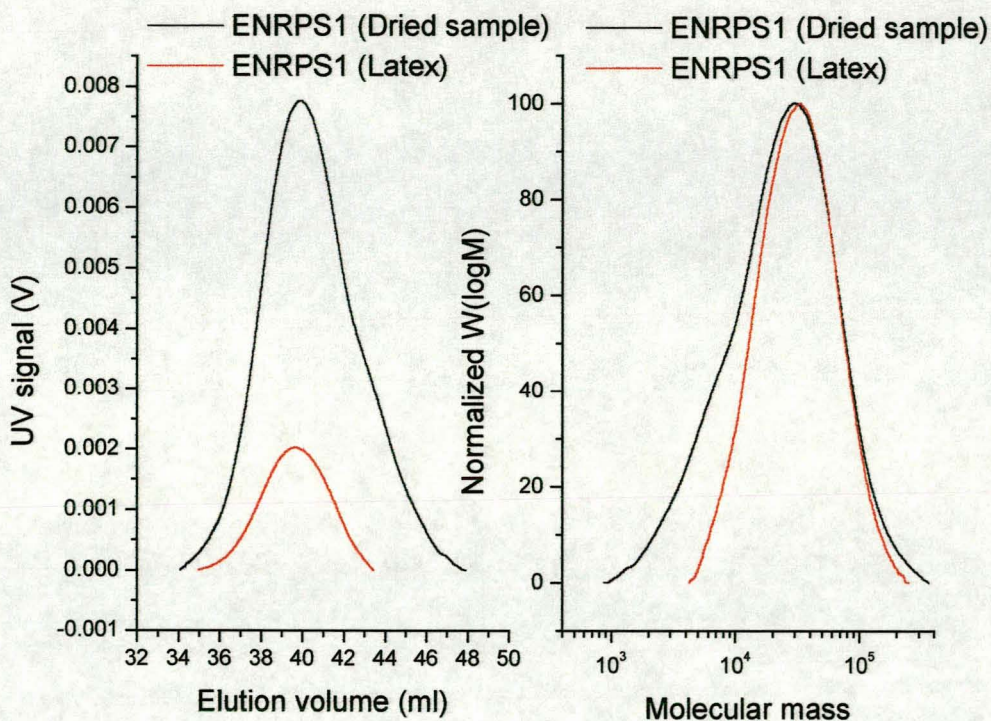
Figure 6.7: (a) Comparison of the UV signal of the dried sample and the latex sample and (b) comparison of the normalized UV signal for the dried and latex sample.

The elution volumes and peak distributions can be seen in Table 6.7. A similar analysis was also done for ENRPS2 and results are shown in Table 6.7, where it is clear that the same elution volumes and peak distributions can be obtained for both soluble parts and that results of the experiments are reproducible. It was therefore possible to carry out further experiments using only the soluble part of the dried rubber.
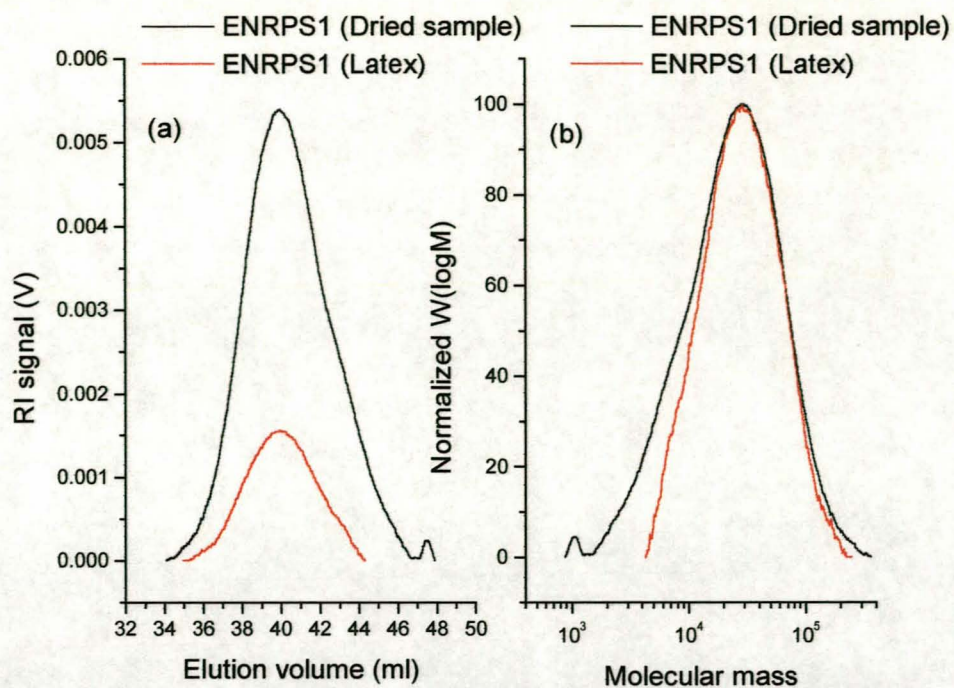
Figure 6.8: (a) Comparison of the RI signal of the dried sample and the latex sample and (b) comparison of the normalized RI signal for the dried and latex samples.

	Elution volume (ml)		Peak distribution (D)	
	UV	RI	UV	RI
ENRPS1 (dried)	39.75	39.92	2.282	2.349
ENRPS1 (latex)	39.75	39.94	1.538	1.959
ENRPS2 (dried)	40.88	40.60	3.475	3.040
ENRPS2 (latex)	41.00	40.80	4.656	3.421

Table 6.7: Comparison of elution volumes and peak distributions for the dried and latex samples of styrene-grafted ENR50.

6.4.2.2 Evaluation of the chemical changes of ENR50 as a result of the polymerization reaction needed for grafting

The rubber (ENR50) was subjected to the polymerization conditions to see if a change in structure occurred. Conditions used were as discussed earlier, in Section 6.4.1.4.

Both the ENR50 and polymerized ENR50 were subjected to SEC analysis. SEC results can be seen in Figure 6.9.
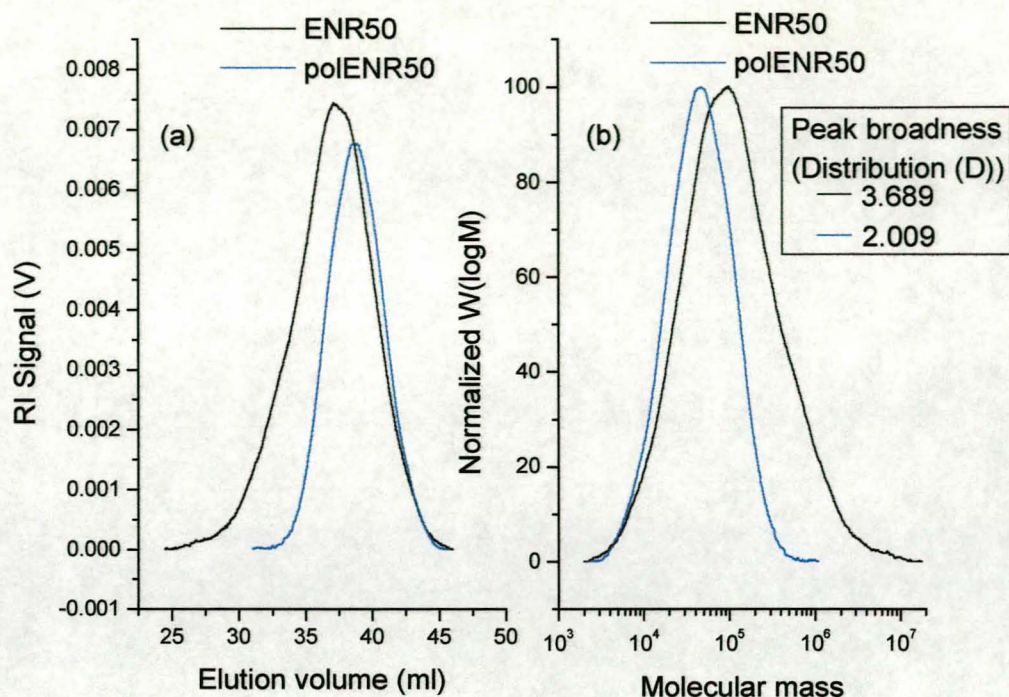

Figure 6.9: (a) RI and (b) normalized RI results of SEC analysis of ENR50 and polENR50.

SEC results of the polymerized ENR50 showed that the elution peak shifted from 37.25ml (for ENR50) to 38.88ml (for polymerized ENR50). As there was a shift to a higher elution volume, a lower molecular mass formed during the polymerization reaction. Furthermore, the molecular mass distribution narrowed substantially for the polymerized ENR50. It can therefore be said that a certain degree of breakdown of the rubber occurred during the polymerization reaction. This result, and that of FTIR analysis, therefore gives conclusive evidence that the rubber did undergo some structural changes during the polymerization reactions.

6.4.2.3 Interpretation of normalized ultra-violet (UV) vs. normalized refractive index (RI) signals of the grafted samples

A UV signal is a function of the amount of chromophores (in this case styrene) present in a sample.

In SEC the UV signal is therefore an indication of the concentration of the styrene in the sample as a function of the molecular mass distribution in the samples. The RI signal, on the other hand, is an indication of the concentration of the molecules with a particular molar mass.

The time difference between the signals taken at the UV and RI detectors is automatically measured and subtracted by the SEC software. The signals are therefore supposed to overlap when looked at in the normalized view. However, not all the samples showed overlapping of the UV and RI signals, but some of the UV peaks shifted to either the right or left of the RI peaks, as shown in Figure 6.10.
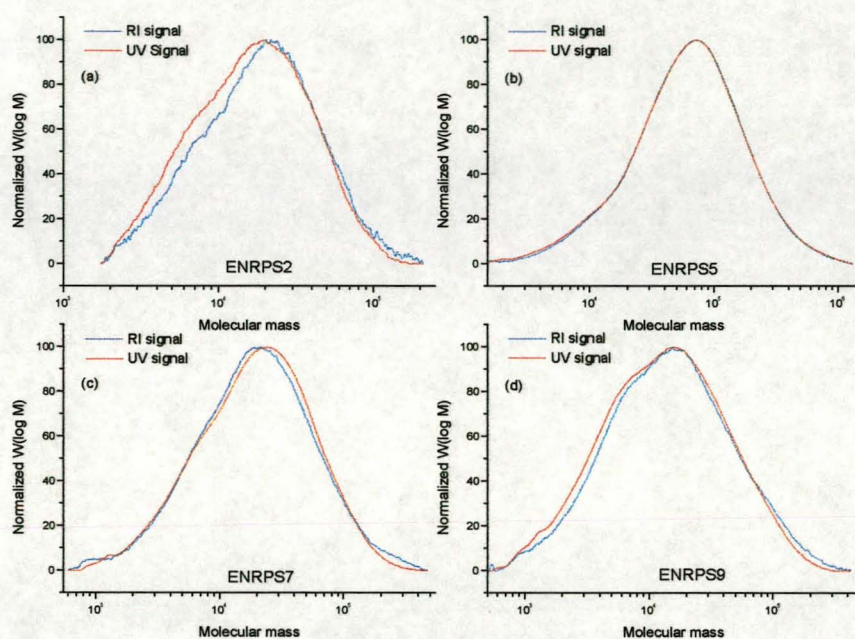

Figure 6.10: Analysis of the styrene content as a function of the molecular mass distribution of the grafted sample, by SEC

If the UV peaks shift to the right of the RI peak (Figure 6.10(c)), it is an indication that there is more styrene present in the higher molecular mass molecules than in the lower molecular mass molecules. When it shifts to the left (Figure 6.10(a)), then the lower molar mass molecules have more styrene. In ENRPS5 (Figure 6.10 (b)), complete overlapping of peaks occurred showing that the styrene is well represented over the whole molecular mass distribution of the sample. ENRPS9 (Figure 6.10(d)) also shows a slight shift to the right, indicating more styrene in the higher MM part. Similar results were obtained for the other grafted samples. These results can be seen in Appendix 13.

6.4.2.4 Analysis of the RI signal of ENR50 vs. the RI signal of the grafted samples

The RI signal of the samples compared to the RI signal of the ENR50 showed that all the samples, except one (ENRPS3), have a higher elution volume than ENR50. Results can be seen in Figures 6.11-6.16.
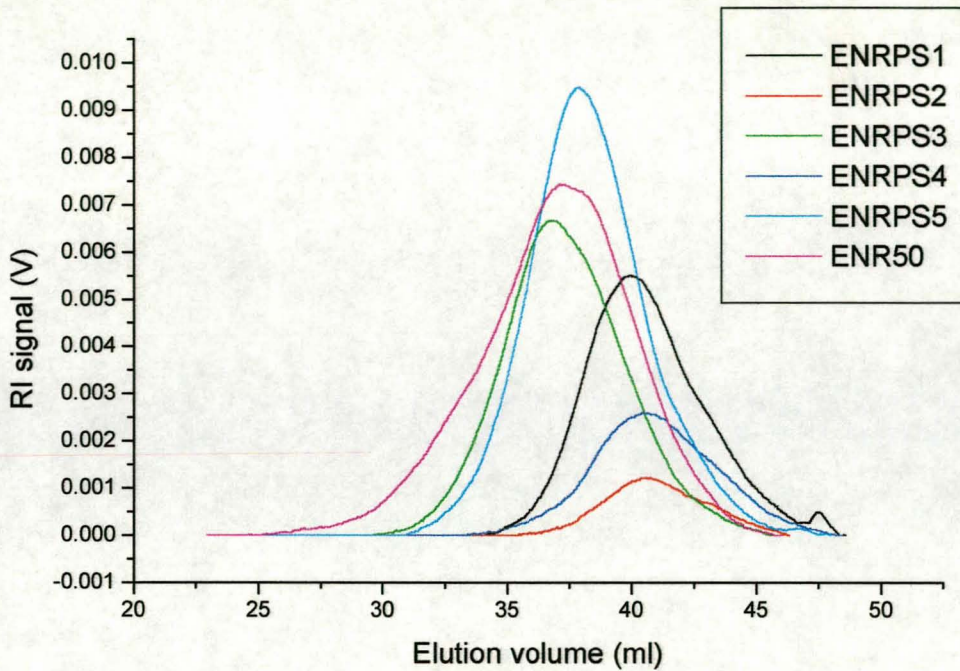

Figure 6.11: Comparison of RI signal of ENR50 with RI signals of grafted samples 1-5.
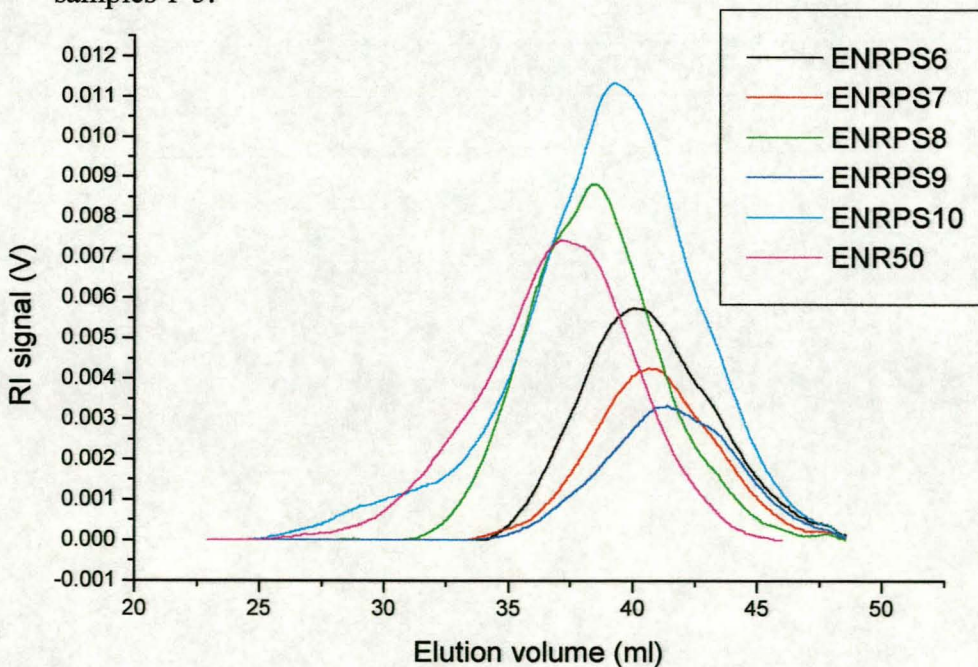

Figure 6.12: Comparison of RI signal of ENR50 with RI signals of grafted samples 6-10.
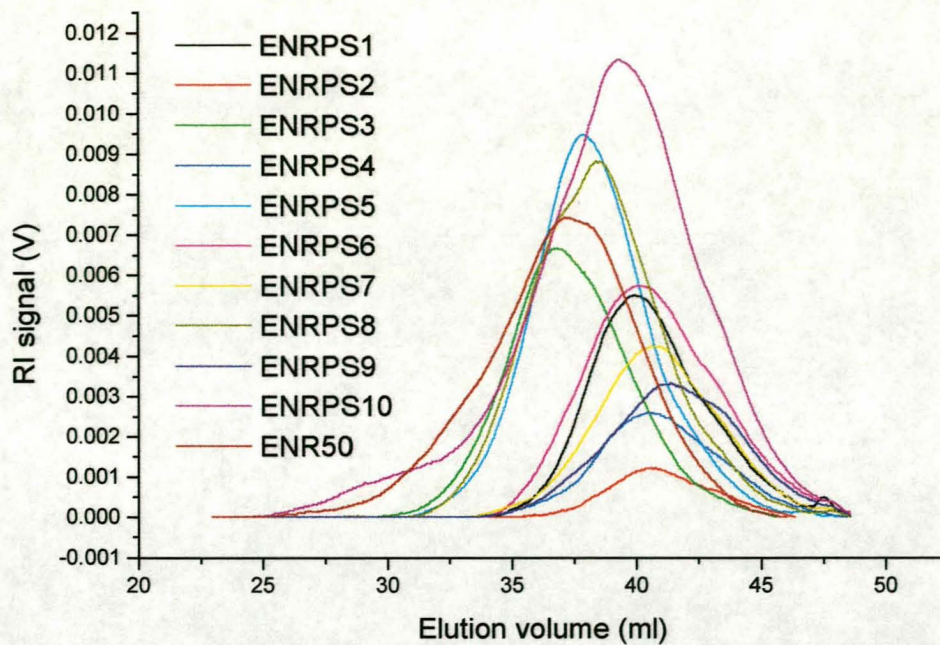
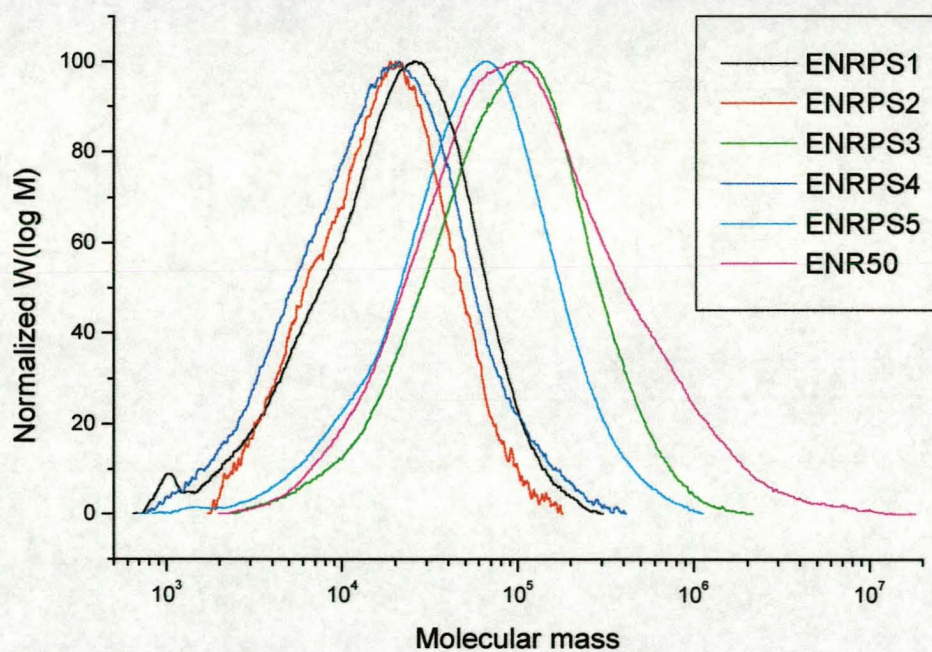Figure 6.13: Comparison of RI signal of ENR50 with RI signals of all the grafted samples.

Figure 6.14: Comparison of normalized RI signal of ENR50 with normalized RI signals of grafted samples 1-5.

A higher elution volume points to lower molecular mass. This can be accepted in the light of the polymerized ENR50 that shows breaking up of the rubber to a lower molecular mass.
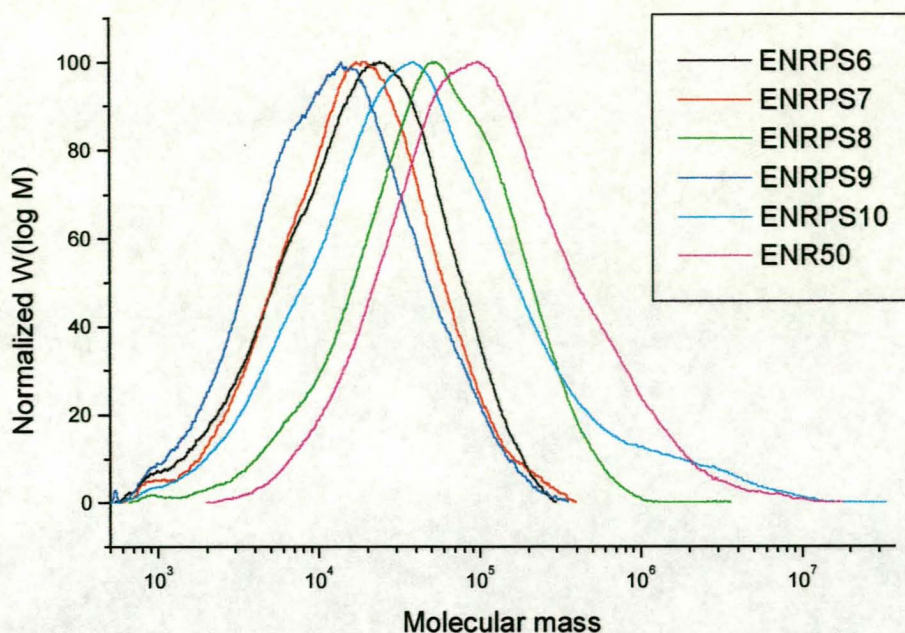
Figure 6.15: Comparison of normalized RI signal of ENR50 with normalized RI signals of grafted samples 6-10.
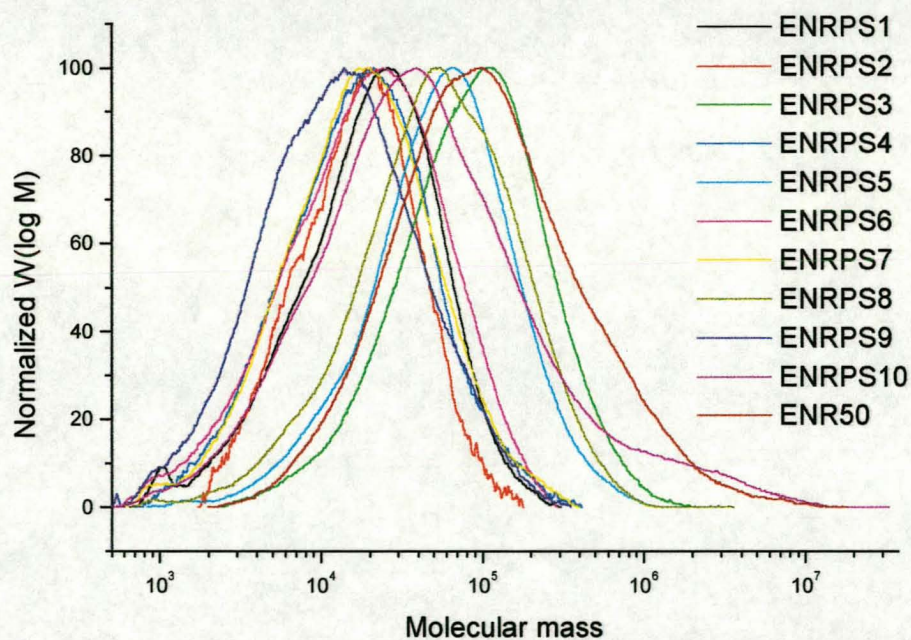

Figure 6.16: Comparison of normalized RI signal of ENR50 with normalized RI signals of all the grafted samples.

ENRPS3 shifted to a lower elution volume i.e. there was an increase in molecular mass. This is due to the fact that in this sample the highest amount of monomer and the lowest volume of initiator were used.

ENRPS8, which is supposed to correlate with ENRPS3, shows a higher elution volume. This is probably due to the fact that a newer latex was used in the polymerization reaction. To explain why some of the peaks shifted to a higher elution volume, the normalized UV graphs can be used (Figures 6.17-6.19). Refer also to Figure 6.2 of this chapter for better understanding of the following discussion.
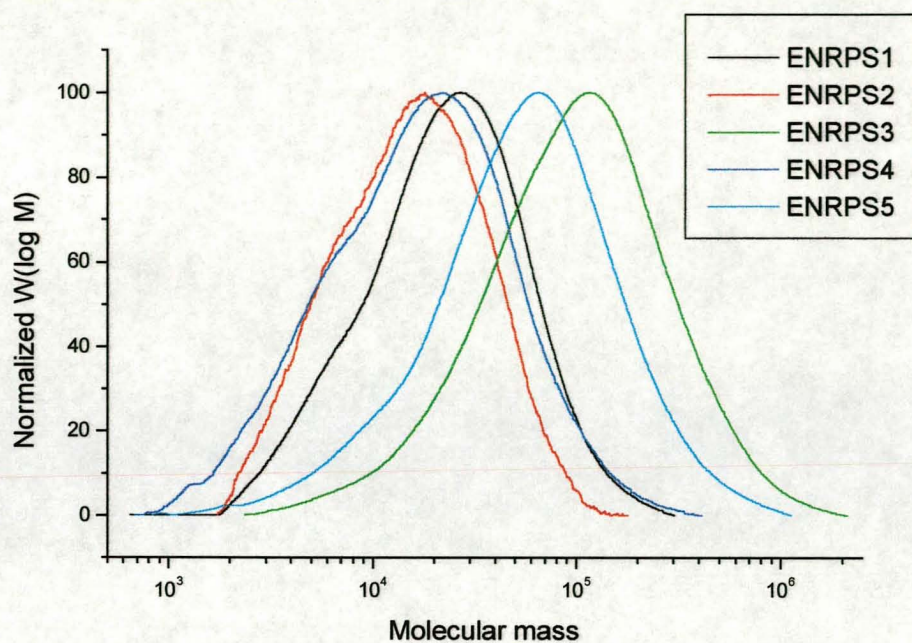

Figure 6.17: Comparison of the normalized UV signals of samples 1-5.
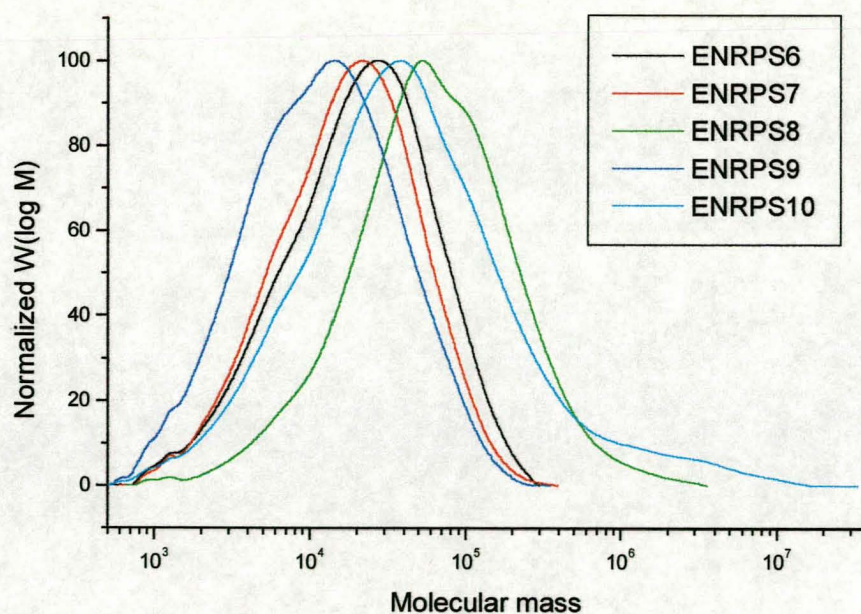

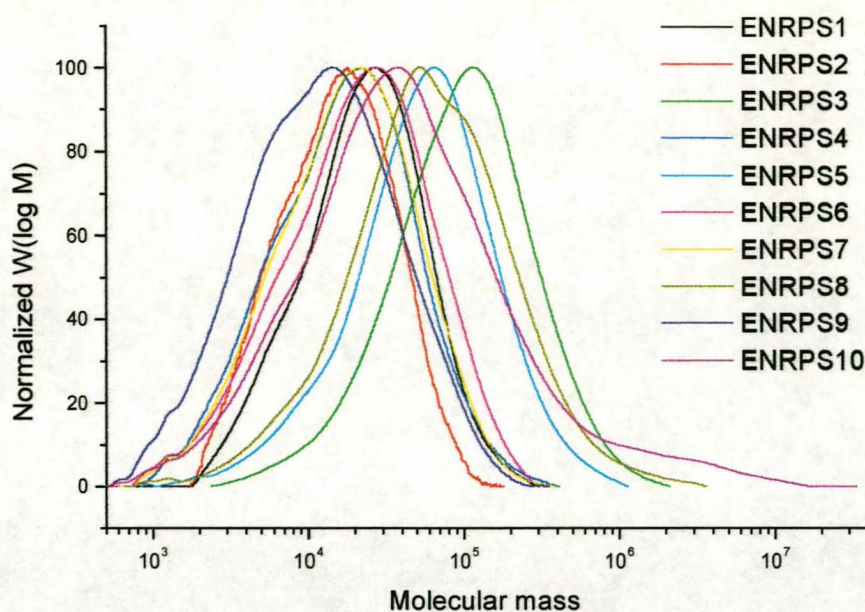Figure 6.18: Comparison of the normalized UV signals of samples 6-10.

Figure 6.19: Comparison of the normalized UV signals of all the samples.

From the normalized UV graphs it is clear that ENRPS3 has the highest molecular mass. ENRPS5 has a lower molecular mass because, in this case, the most monomer and most initiator were used. The reason why ENRPS5 has shifted to a lower molecular mass is because in the presence of a lot of initiator, short chains will form during polymerization. ENRPS3 has a higher molecular mass because less initiator was used, if compared to the ENRPS5, and therefore longer chains formed. ENRPS8 and ENRPS10 follow the same trend as ENRPS3 and ENRPS5 except that ENRPS8 and ENRPS10 have shifted a bit more to the right (higher elution volume and therefore lower molecular mass) and do not exactly coincide with ENRPS3 and ENRPS5. This is due to the fact that in ENRPS3 and ENRPS5 an older ENR50 latex was used in the polymerization reaction and it can be assumed that further crosslinking occurred through ageing in the older ENR50 latex, therefore producing the slightly higher molecular mass.

After ENRPS3, 5, 8 and 10, ENRPS1 and 6 follow, which can be expected because intermediate amounts of initiator and monomer were used. The lowest molecular mass sample produced was sample 9. Here, the highest concentration of the initiator and lowest amount of monomer were used. Again, due to the presence of a high amount of initiator, short chains formed. This compares very well with the fact that ENRPS9 exhibits better solubility, as has been seen in FTIR analysis and will be seen in gradient HPLC analysis.

ENRPS4, which correlates with ENRPS9, is slightly shifted to the right and again this is due to the ENR50 latex used. ENRPS2 and 7 are just above ENRPS9 because in these cases the lowest amounts of monomer and initiator were used.

6.4.2.5 Explanation of the UV chromatograms as obtained through SEC analysis

The UV spectra follow the total concentration of styrene used in the different polymerizations very well (Figures 6.20-6.22).
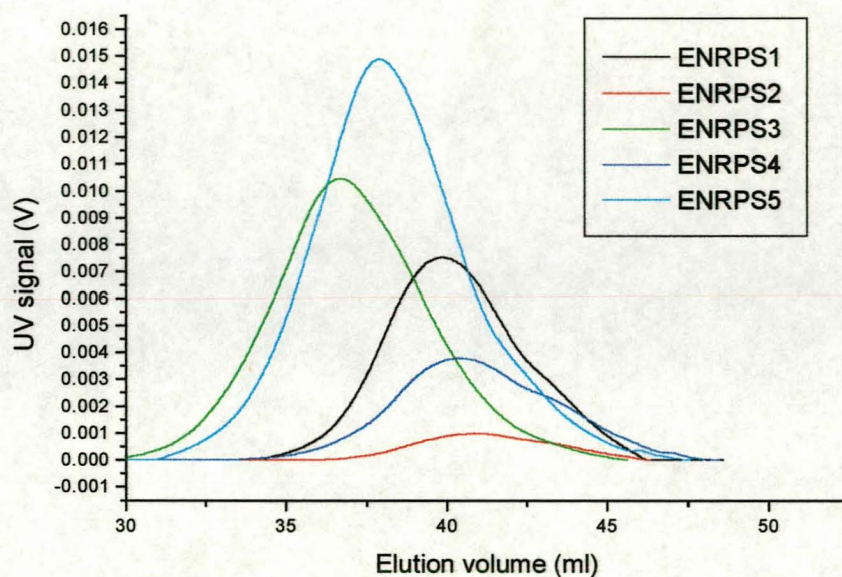

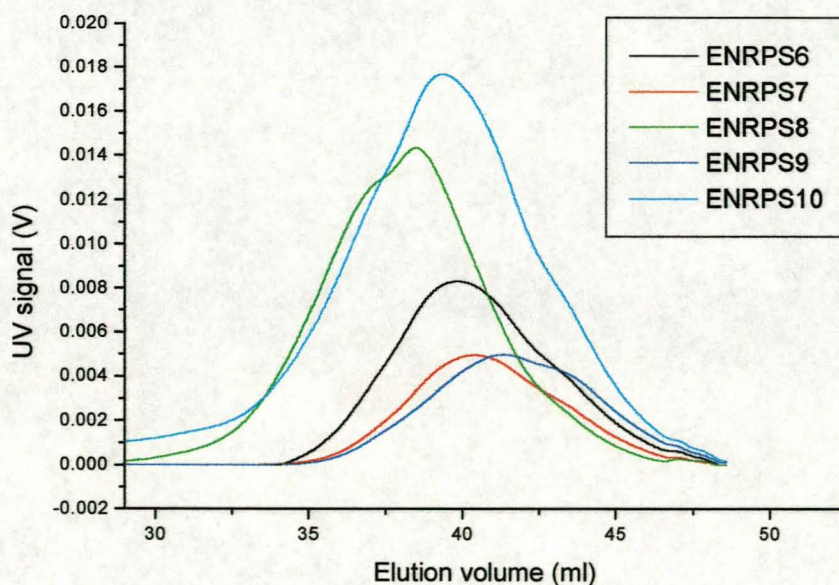Figure 6.20: Comparison of the UV signals of samples 1-5.

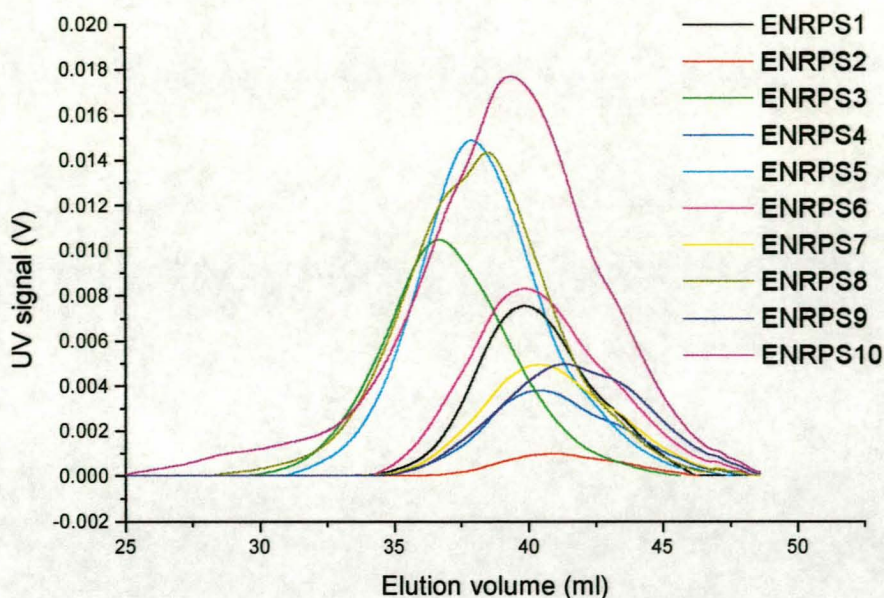Figure 6.21: Comparison of the UV signals of samples 6-10.

Figure 6.22: Comparison of the UV signals of all the samples.

It can be seen that ENRPS5 has the highest UV signal because the most monomer and most initiator were used. ENRPS3 follows because the most monomer but least initiator were used. Next is ENRPS1 because intermediate values were used, followed by ENRPS4 (most initiator and fewest monomer) and lastly ENRPS2 (fewest monomer and initiator). For ENRPS6-10, the same results, as for ENRPS1-5, were found.

6.4.3 GPC-FTIR analysis (LC-transform)

GPC-FTIR analysis was performed to evaluate the styrene distribution throughout the sample. Separation according to molecular mass was the first step in this analysis technique. Fractions of the sample exiting the GPC were automatically deposited on a germanium disk as dry, solvent-free spots which was then inserted in a FTIR spectrometer for further analysis. The fractions collected were therefore a complete representation of the molecular mass distribution of the sample in question and on doing FTIR analysis, the styrene content as a function of the molecular mass distribution could be mapped. The data collected was not an exact representation of an ordinary GPC analysis but is referred to as a Gram Schmidt representation of the separation. This can be defined as a graphical representation of series data that shows how the relative infrared response changed over the duration of the experiment.

In other words, the Gram Schmidt representation is the total infrared absorption as a function of time where the time axis of the trace can be correlated to molecular mass of the sample (high molecular mass eluting early and low molecular mass later). By using computer software, it is possible to look at the infrared signal at any point on the Gram Schmidt representation. This allows the opportunity to evaluate the ratio between the styrene (698 cm^{-1}) and styrene/ENR50 (1452 cm^{-1}) peaks at different time values, thereby making it possible to represent the relative styrene content as a function of the molecular mass distribution. Figure 6.23 shows the Gram-Schmidt representation of ENRPS1, Figure 6.24 the FTIR spectra at the different time intervals, Figure 6.25 the blown-up styrene and styrene and ENR50 regions for better visualization of the time dependence of the FTIR signal and Figure 6.26 a representation of the relative styrene content as a function of time.
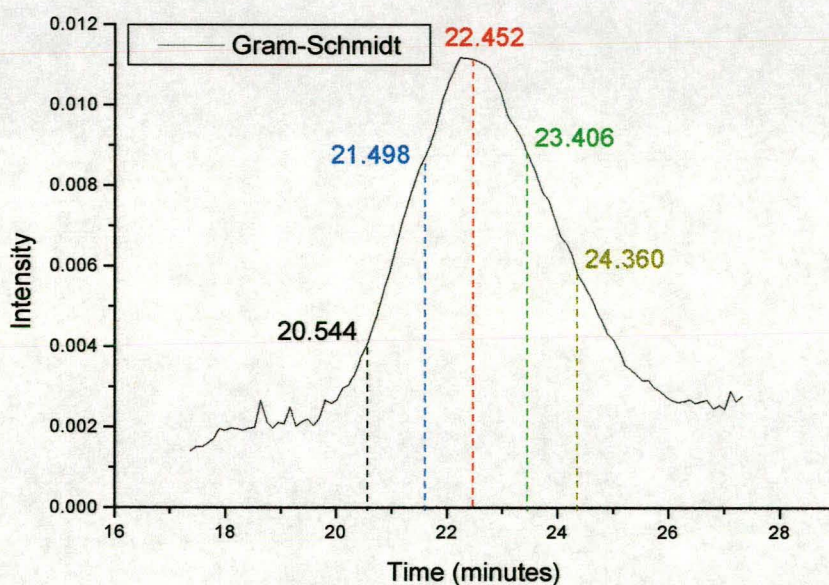
Figure 6.23: Gram-Schmidt representation of ENRPS1.

From the results (Figure 6.26) it is clear that there is more styrene present in the higher molecular mass region and that the relative styrene content decreases as the molecular mass decreases. The slight increase at 25 minutes is due to styrene monomer present in the sample. Results obtained for ENRPS1 correlate very well with GPC results (normalized RI signal vs. normalized UV signal) (Appendix 13). See also Appendices 20-29 for contour plots of all the grafted samples. From these plots the MMDs of the functional groups, i.e. the styrene and rubber, can be followed.
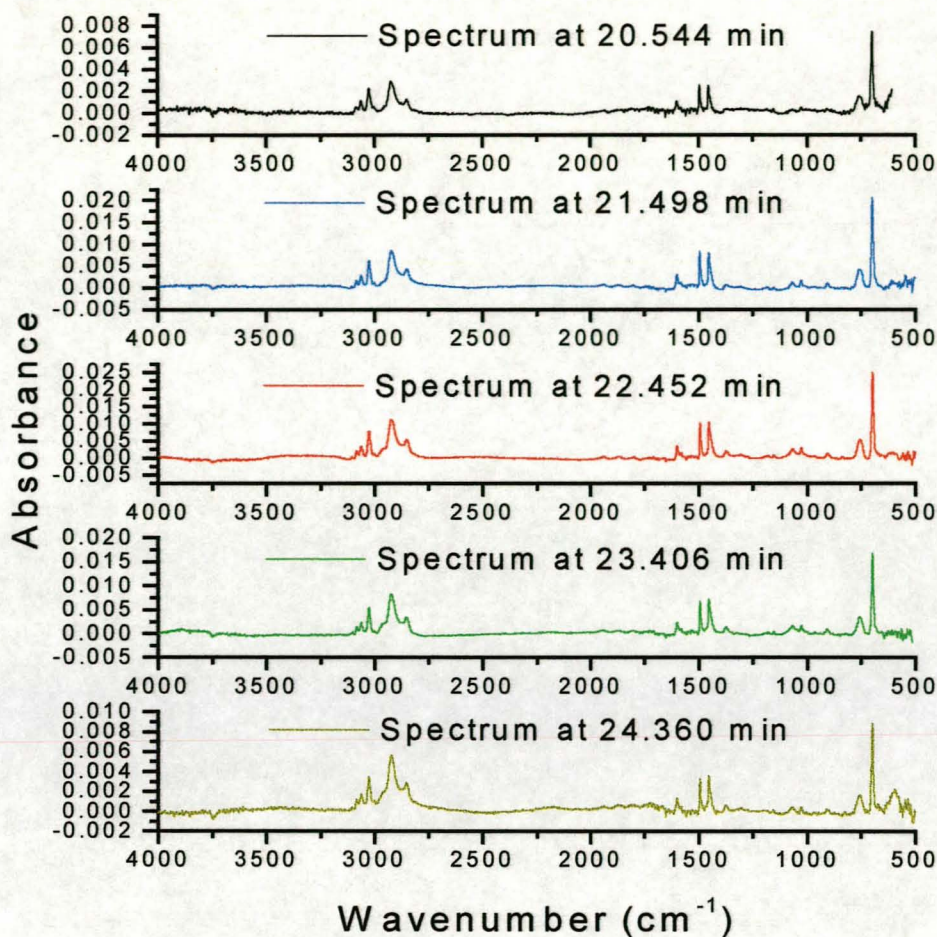
Figure 6.24: FTIR spectra of ENRPS1 at different time intervals (as indicated on the Gram-Schmidt graph).
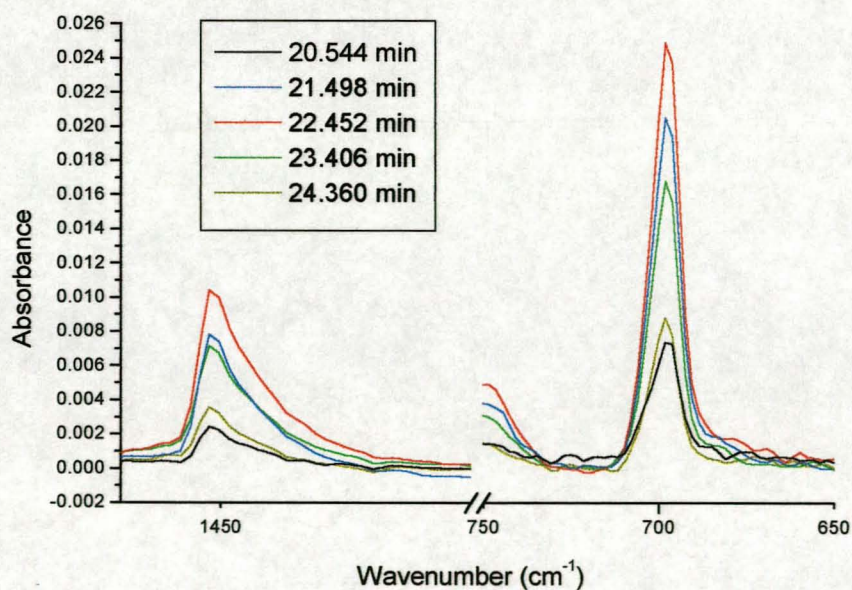
Figure 6.25: Blown-up region of the styrene peak (698 cm^{-1}) and the styrene and rubber peak (1452 cm^{-1}) to show the change in peak size as a function of time.
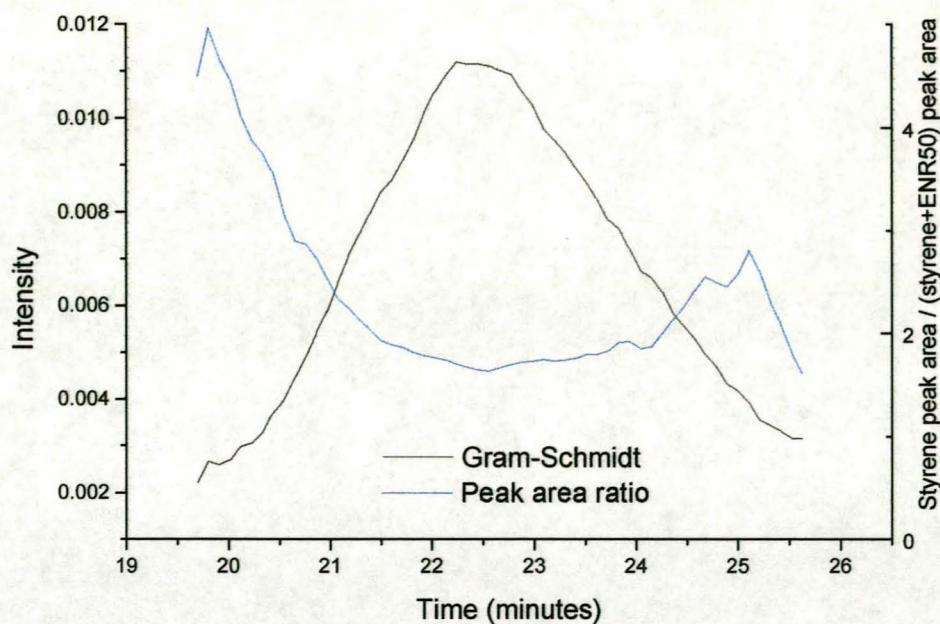
Figure 6.26: Representation of the relative styrene content in ENRPS1 as a function of time.

Similar results for the other samples were also obtained and can be seen in Figure 6.27. Figure 6.27 is the representation of the styrene peak area ratio vs. the retention time and valuable conclusions about the incorporation of the styrene as a function of the molecular mass can be made.
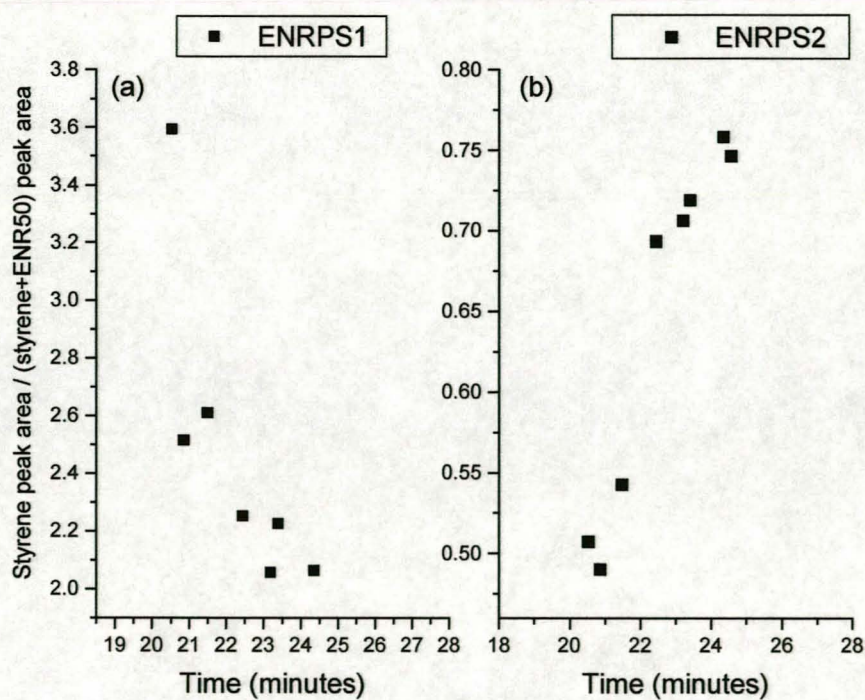
Figure 6.27(a,b): Styrene peak ratios of ENRPS1 and 2 as a function of the retention times.
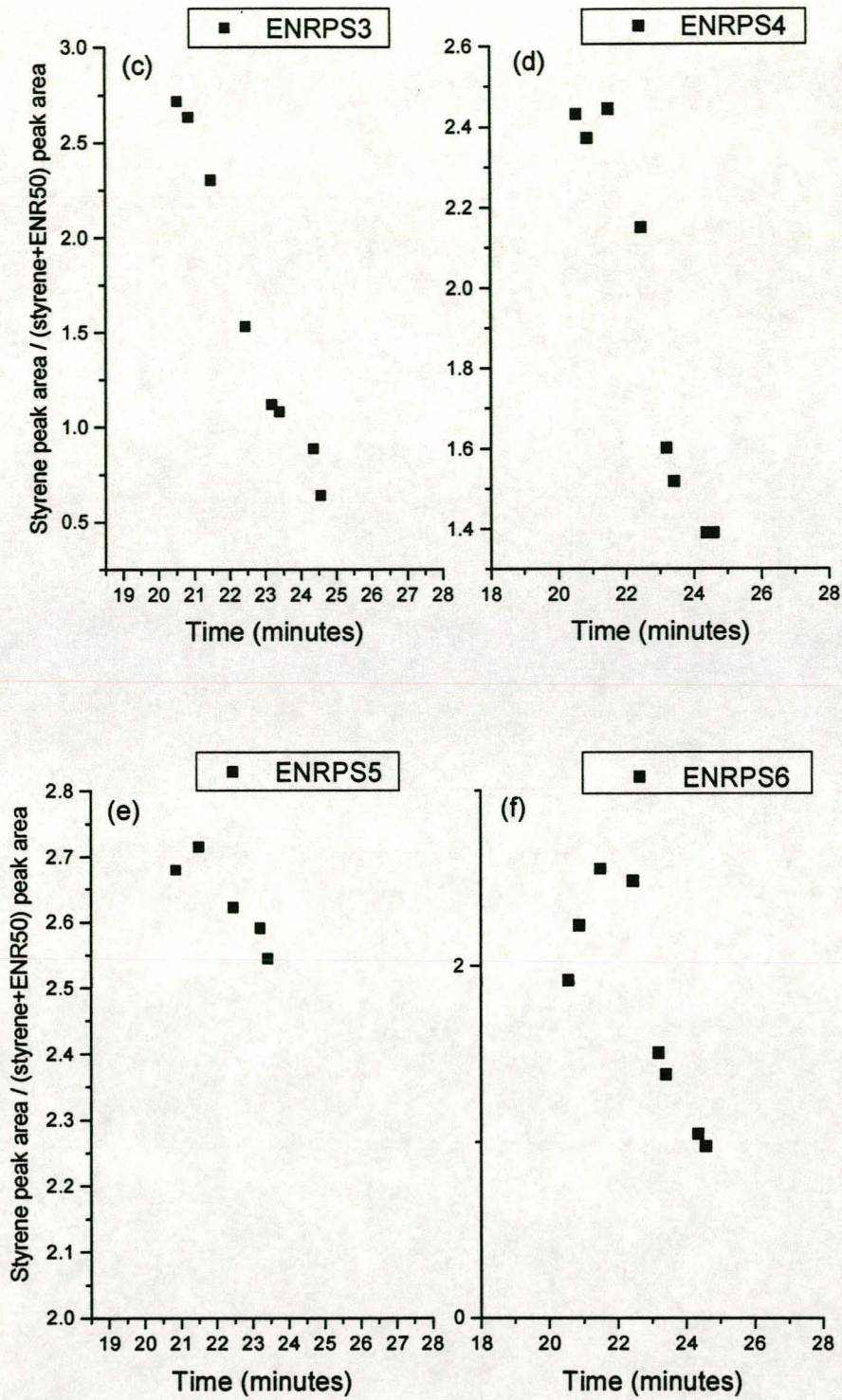
Figure 6.27(c-f): Styrene peak ratios of ENRPS3-6 as a function of the retention times.
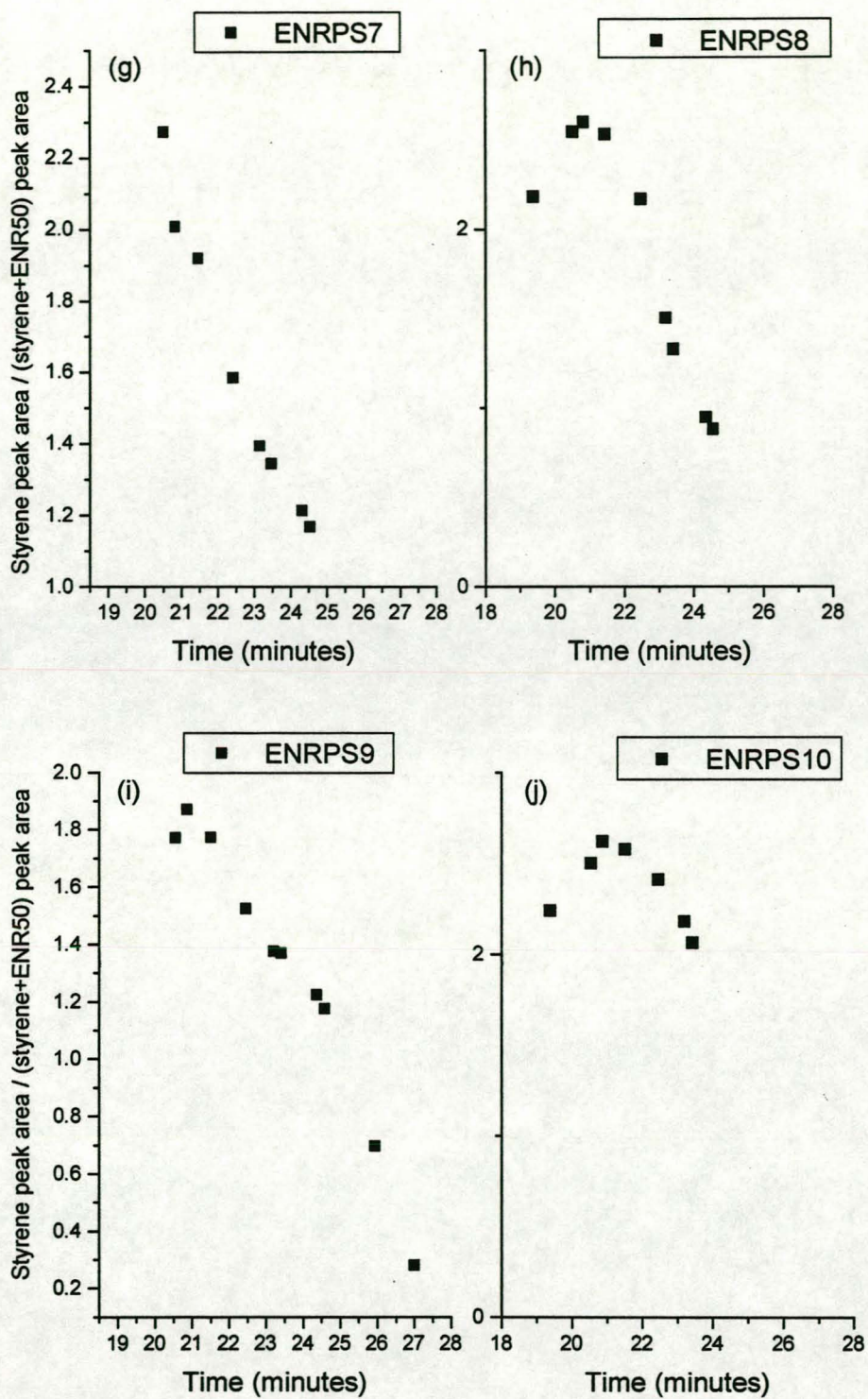
Figure 6.27(g-j): Styrene peak ratios of ENRPS7-10 as a function of the retention times.

The styrene peak ratio for ENRPS2 can be seen in Figure 6.27(b). Here there is more styrene present in the lower molecular mass part (higher retention time) of the sample. This can be compared with the normalized RI vs. normalized UV signal as obtained from GPC analysis in Figure 6.10(a) which shows the same result. ENRPS3 and ENRPS4 show a clear decrease in styrene content with a decrease in molecular mass. ENRPS5, however, shows that the styrene content stays very much the same through the distribution. Although it looks as if the styrene content decreases dramatically the ratio only changes from 2.71 to 2.54 and, if compared with the other samples, this represents a very even distribution of styrene throughout the molecular mass distribution. This is confirmed by the normalized RI vs. normalized UV signal in Figure 6.10(b). ENRPS7 and 9 (Figure 6.27(g,i)) again show that the styrene content is higher for the higher molecular mass material. ENRPS6 and 8 (Figure 6.27(f,h)) show a very interesting trend in which the styrene content first increases and then decreases, with a decrease in molecular mass. This also correlates exactly with normalized RI vs. normalized UV signal graphs (Appendix 13). ENRPS10 (Figure 6.27 (j)) is similar to ENRPS 5 and shows an even incorporation of styrene through the molecular mass distribution of the sample. A comparison with the normalized RI vs. normalized UV signal graph for ENRPS10 (Appendix 13) revealed the same result.

6.5 Conclusions

Questioning the necessity of carrying out preliminary experimental analyses might have arisen in the beginning of this chapter. Therefore, the concluding remarks will focus on justifying these experiments, by briefly explaining the need for them, and summarizing the goals achieved by using these techniques.

By performing FTIR on the different sample phases of styrene-grafted ENR50 i.e. dried phase, soluble phase and gel phase, it was possible to evaluate the presence and incorporation of styrene in these different phases. FTIR of the dried samples was used to correlate the styrene content in the final product with the starting monomer concentrations.

In other words, it was possible to see if all the styrene monomer that was consumed during the grafting reaction was indeed present in the product sample, either as the grafted polystyrene, ungrafted polystyrene or styrene monomer. Evaluations of the soluble and the gel phases of the samples were of utmost importance, to facilitate gradient HPLC analysis explanations. This analysis work also gave some insight into the solubility of the samples as a function of the amount of monomer and initiator used. Furthermore, analysis of the ENR50 and polymerized ENR50 showed that certain chemical changes occurred during the grafting reaction. This was confirmed by other scientists studying ENR [6,7].

GPC analysis yielded the molecular mass distribution of all the samples. Through the usage of a multi-detector system (RI and UV), the styrene incorporation as a function of the molecular mass distribution could be verified. Reproducibility between the soluble part of the dried sample and the soluble part of the latex was also analyzed and confirmed. GPC revealed a change in the molecular mass and molecular mass distribution indicating that there was a change in the chemical structure of the ENR50 which occurred as a result of the grafting reaction. Results of GPC also revealed that there was a change in molecular mass as a function of the concentration of the precursors, as used in the various grafting reactions. The change in molecular mass provided insight into the different chain length formations during grafting reactions and it was possible to trace this back to the amount of initiator and monomer used. UV graphs also provided a way to verify the amount of styrene used during the grafting reaction and this correlated very well with results of similar FTIR analyses.

GPC-FTIR was also performed to verify the styrene ratio as a function of the molecular mass distribution. Results showed similar trends to those of GPC analysis. By looking at the FTIR spectra through the molecular mass distribution, it was possible to see exactly how the sample changed through the entire molecular mass distribution.

Although all of the above experiments give insight into the molecular mass distribution and styrene incorporation, the results are necessary for the explanation of gradient HPLC analyses and the trends associated with gradient HPLC. It is therefore an absolute necessity to perform such experiments, especially in the light of the limited solubility of the grafted material under investigation.

6.6 References

1   H. Pasch, B. Trathnigg; HPLC of Polymers; Springer-Verlag, Berlin Heidelberg; 1998

2   G. Glöckner; Gradient HPLC of Copolymers and Chromatographic Cross-Fractionation; Springer-Verlag, Berlin Heidelberg; 1991

3   J.N. Willis, J.L. Dwyer, M.X. Liu; *Improvements in Size Exclusion Chromatography – FTIR Technology*; International GPC Symposium; 1996, 70-77

4   R.J. Papez; *Interactive use of GPC, LC-Transform and FTIR-Microscopy in the Analytical Laboratory*; International GPC Symposium; 1996, 78-86

5   S.M. Graef; MSc Thesis; Institute of Polymer Science, University of Stellenbosch; 1999

6   N.V. Bac, M. Mihailov, L. Terlemezyan; *Study of Polymer Analogues of Natural Rubber Obtained from Epoxidation in Latex and Subsequent Hydrobromination by Infrared Spectroscopy*; Journal of Polymeric Materials; 7, 1990, 55-62

7   N.V. Bac, Chu Chien Huu; *Synthesis and Application of Epoxidized Natural Rubber*; Pure and Applied Chemistry; A33(12), 1996, 1949-1955

Chapter 7

Gradient HPLC of Styrene-Grafted Epoxidized Natural Rubber (ENR50): Method Development, Results and Discussions

7.1 Introduction

Although gel permeation chromatography (GPC) is used extensively by the scientific community as a powerful analytical tool, certain complications regarding the samples analyzed, have rendered this technique a less important standard analytical procedure [1]. In the case of polymer mixtures, a serious problem is caused by overlapping hydrodynamic distributions leading to co-elution of the macromolecules. As many products have a very broad molecular mass distribution, peak overlapping can occur, thereby yielding unsatisfactory results. The usefulness of GPC must, however, not be misinterpreted. GPC is not to be disregarded but, in the analysis of heterogeneous polymers, analysis by gradient HPLC can give much better interpretations of the chemical composition distribution (CCD) of copolymers and polymer blends [2]. GPC analysis is still a necessity, as molecular mass and molecular mass distribution analyses remain important and the results can be used to clarify and explain trends in gradient HPLC analysis, as was discussed in Chapter 6, Section 6.4.2.

Gradient HPLC functions on the principal of precipitation and redissolution in a gradient solvent system i.e. going from a weak solvent to a strong solvent. In other words, a dissolved polymer is injected into a column filled with a non-solvent (NS) and consequently precipitates [3].

The precipitated polymer will adsorb to the stationary phase and will stay adsorbed until the solvent strength is sufficient for redissolution to take place (elution is observed only when the solvent reaches sufficient strength to displace the adsorptive interactions of the retained copolymer) [4]. The dissolved polymer will now be able to migrate through the column and undergo exclusion interactions. The above is represented in Figure 7.1.

From Figure 7.1 it follows that, on injection, the polymer will precipitate and it will therefore be in the adsorption region (high %NS). In this region the highest molecular mass polymers will have the highest retention time (RT) due to the fact that they are less soluble than the lower molecular mass polymers [5,6]. As the solvent strength increases, the polymer will enter the exclusion region where interaction with the column is governed by size exclusion effects (high %NS).
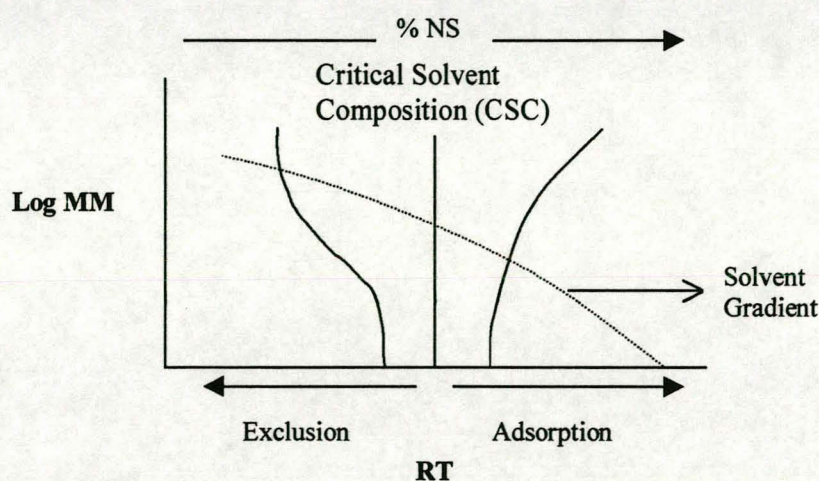
Figure 7.1: Plot of log MM versus the retention time (RT) in gradient HPLC [5].

Here the highest molecular mass polymers will have a decreased retention time due to the fact that they cannot enter the pores of the stationary phase as in the case of the lower molecular mass polymers.

Above is a typical scenario for gradient HPLC separation, in particular separation in reversed-phase (RP) chromatography. Reversed-phase chromatography has become the most popular mode of chromatography. In reversed-phase chromatography the stationary phase is non-polar and the mobile phase is polar.

In contrast to RP chromatography, the second mode of separation is normal phase (NP) chromatography. Normal phase chromatography is the classical form of chromatography in which polar stationary phases and non-polar mobile phases are used. Here the solute is retained by the interaction of its polar functional groups with the polar groups on the surface of the stationary phase [7]. Figures 7.3 and 7.4 (on page 127) are schematic representations of reversed- and normal phase chromatography to explain the difference between the two modes.

By using gradient HPLC it is therefore possible to obtain separations which are dependant on either the solubility (RP) or the polarity (NP) of the constituting parts of the sample. It is therefore possible to separate the polymer according to:

1. molecular mass,
2. chemical composition distribution,
3. functional type distribution (FTD) [8].

The difference in solubility or polarity between the building blocks of a copolymer and the copolymer itself therefore creates the opportunity to analyze the chemical composition distribution of copolymers. This is possible due to the fact that copolymers usually consist of ungrafted polymer A and B and grafted polymer AB, where A and B are the two precursor homopolymers [9] (Figure 7.2).
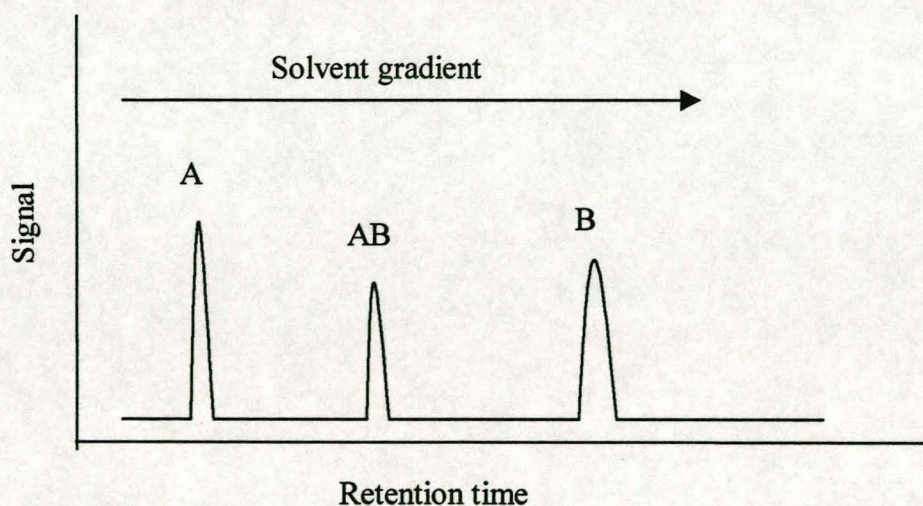

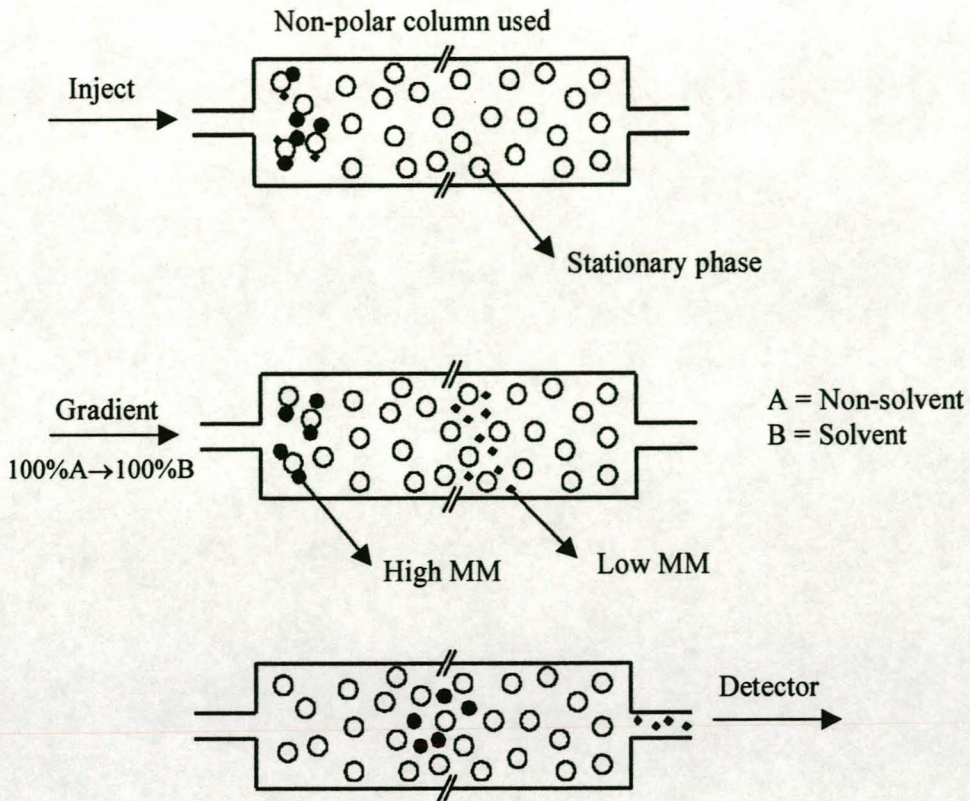Figure 7.2: Separation of copolymer AB and precursors A and B by gradient HPLC.

Figure 7.3: Schematic representation of reversed-phase chromatography.
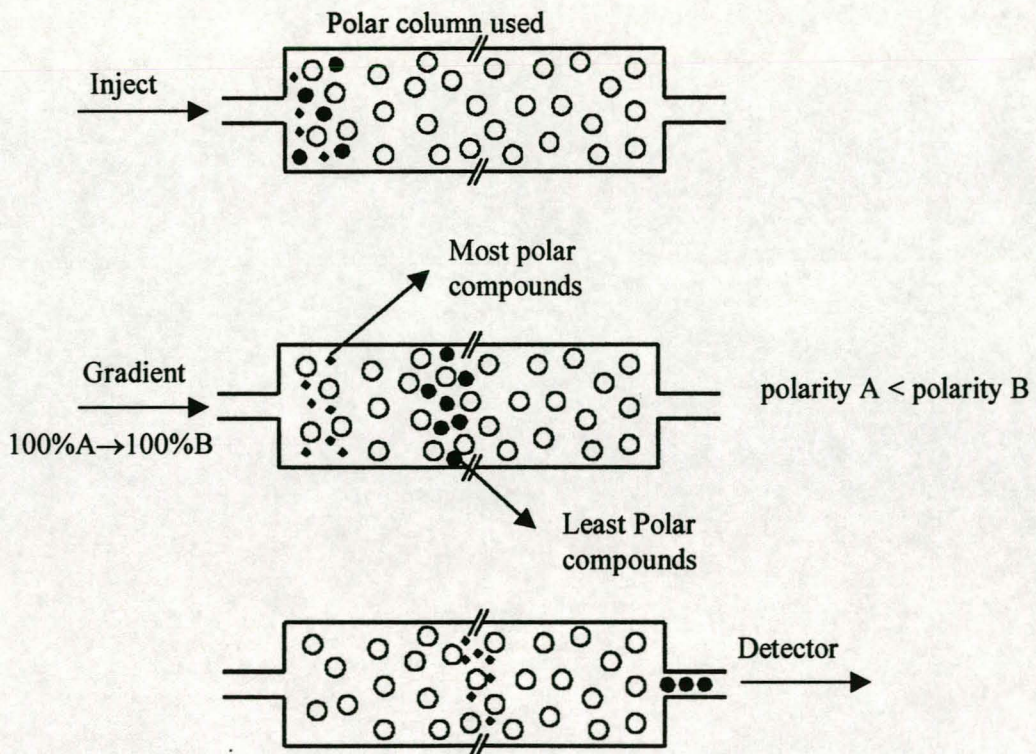
Figure 7.4: Schematic representation of normal phase chromatography.

Both RP and NP was utilized in gradient HPLC analysis of the styrene-grafted ENR50. Although analysis work was started on RP and later changed to NP, the reasons for doing so will be pointed out during the remainder of this chapter.

7.2 Experimental

7.2.1 Chromatography equipment, columns and solvents used

Two gradient HPLC systems were used in the analysis of the styrene-grafted ENR50 samples and standards (polystyrene and polyisoprene). The first and older one of the two was the Waters 616 which consisted of the following equipment:

- Waters 616 pump
- Waters 600S controller
- Waters 712 WISP (Waters Intelligent Sample Processor)
- Waters 490 programmable multiwavelength detector
- ACS 750/14 (Applied Chromatography Systems Ltd.) ELSD (Evaporative Light Scattering Detector)
- Separations Spark-Holland Mistral column oven
- Waters automated switching valve
- Millenium^{32} software

The newer gradient HPLC system was the Waters Alliance and consisted of the following:

- Waters 2690 Separations Module (Alliance)
- Waters 486 tunable absorbance detector
- Polymer Laboratories PL-EMD960 ELSD
- Waters SAT/IN module
- Millenium^{32} software

In both systems the UV detector was set at 254 nm, the column oven temperature was 35°C and the flow rate of the solvent was 0.5ml/min. The ELSD was, in both cases, operated at 70°C. The PL-EMD960 ELSD operated with a N_2 carrier gas flow rate of 4.9 l/min.

The following solvents were used in gradient HPLC analysis:

- Tetrahydrofuran (THF) HPLC-S (Biosolve Ltd.)
- Acetonitrile (ACN) HPLC-S (Biosolve Ltd.)
- N-Heptane (Biosolve Ltd.)
- Dichloromethane (DCM) HPLC (stabilized with amylene) (Biosolve Ltd.)
- Water (purified with a Milli-Q system from Millipore Corporation)

All the solvents were sparged with helium at a flow rate of 10 ml/min.

The columns used are tabulated in Table 7.1. Due to the fact that experiments were performed on both of the HPLC systems and with different solvent and column combinations, the gradient HPLC system used for the particular experiment, injection volume of the samples, solvent gradient, gradient steepness (time) and column used will be noted prior to the discussion of each experiment.

Columns	Particle size (μm)	Pore size (Å)	Dimensions (mm)	Column serial number
μ Bondapak CN (RP)	10	125	3.9 × 150	WAT 086688
Zorbax Sil	---	---	4.6 × 150	883952-701
Symmetry C_{18}	5	100	3.9 × 150	WAT 046980
Pre-columns				
Nova-Pak CN HP	4	---	3.9 × 20	WAT 046840
Nova-Pak Silica	4	---	3.9 × 20	WAT046845
Nova-Pak C_{18}	4	---	3.9 × 20	WAT 044380

Table 7.1: Columns and pre-columns used in gradient HPLC experiments.

7.2.2 Experimental setup

The experimental setup is shown in Figure 7.5.

The gradient pump, autosampler, valve switch, controller, UV and ELSD detectors are all connected to the computer.

Settings e.g. solvent flow rate, injection volume, gradient profile can be set by either using the computer or the controller which is situated on the chromatograph itself. Solvents are sparged with helium to remove any air, which might otherwise lead to bad analysis results.
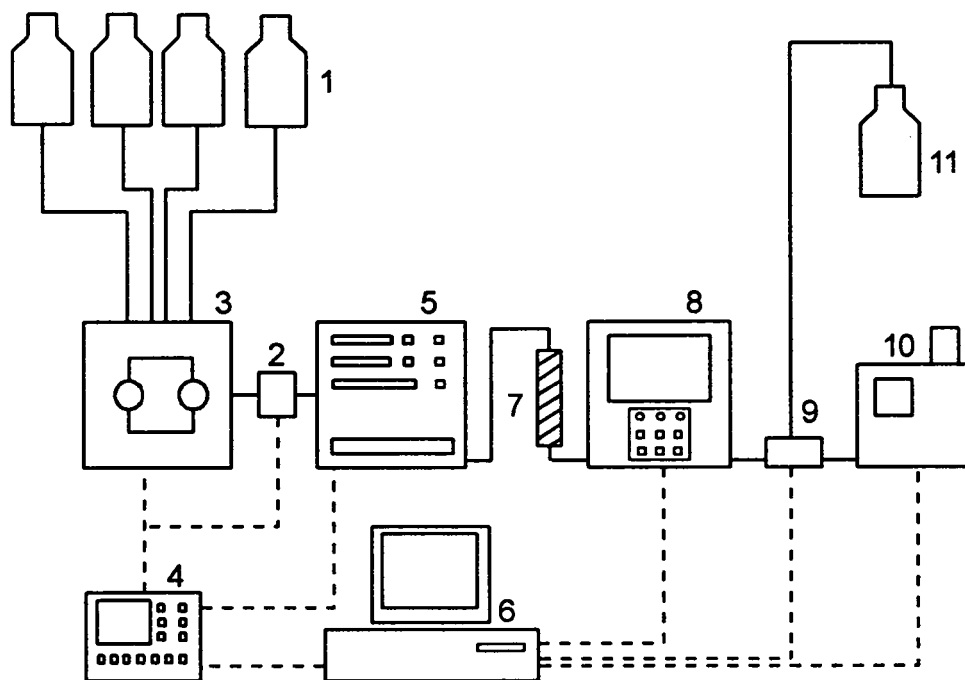
Figure 7.5: Schematic representation of a gradient HPLC experimental setup. Components are: (1) solvents, (2) mixing chamber, (3) gradient pump, (4) controller, (5) injector, (6) computer, (7) column, (8) UV detector, (9) switch valve, (10) ELSD detector, (11) solvent waste.

An online degasser is also situated inside the Waters 2690 or as a separate module in the case of the Waters 616 system for degassing solvents. Solvents are pumped with the gradient pump through the autosampler where the samples are injected. The solvent stream continues from here through the column, which is situated inside a column oven, and enters the UV detector. A switch valve can either direct the solvent stream to a waste bottle or to the ELSD detector as it exits the UV detector. Data collection is done automatically by the Millenium[32] software as soon as a gradient run starts, thereby providing suitable chromatograms for data analysis. Gradient profiles must be entered into the computer before the start of the actual gradient run. This will enable the computer to adjust the solvent mixture at a certain time in order to obtain the right solvent gradient.

An example of such a gradient profile can be seen below in Table 7.2.

$$50\%/50\% \text{ } H_2O/ACN \xrightarrow{4\%/min} 100\% \text{ } ACN \xrightarrow{4\%/min} 100\% \text{ } THF$$

Time (min)	Flow (ml/min)	% THF	% ACN	% H₂O
	0.5	0	50	50
12.5	0.5	0	100	0
37.5	0.5	100	0	0
40	0.5	100	0	0
45	0.5	0	50	50

Table 7.2: Example of a gradient profile setup in gradient HPLC.

The gradient starts at 50%/50% H_2O/ACN and has to go to 100 % ACN at a 4% solvent increase per minute. For a gradient steepness of 4%/min, 12.5 minutes must be allowed for the gradient change to occur. After this, the gradient has to go from 100% ACN to 100% THF. For the same gradient steepness, 25 minutes must be allowed, bringing the total time to 37.5 minutes.

After this the column is kept at 100% THF for 2.5 minutes to ensure that all the sample is flushed out of the column. During the following 5 minutes, the gradient is changed back to the starting conditions and is kept there for 15 minutes, bringing the total gradient run time to 60 minutes. The time needed for the solvent system (0.5 ml/min) to fill two column lengths is used to calculate the 15 minutes at which the column is kept at its starting conditions. This ensures that the column is sufficiently conditioned before the next injection is done. Other gradient profiles will be explained in the context of the experiments they are used in.

7.2.3 Sample preparation

Standards (PS and PiP) were prepared for gradient HPLC analysis by weighing off ±2 mg of each standard and dissolving it in 2 ml of THF (see Appendix 1) to obtain a 1% solution.

Styrene-grafted ENR50 and ENR50 were prepared by adding MeOH to the latex until the styrene-grafted rubber precipitated.

The precipitated rubber was left overnight in a fume-hood for the residual MeOH to vaporize. The precipitated rubber was then placed in a vacuum oven and dried at room temperature. Appendices 14, 15 and 16 show the concentrations of the PS, PiP and ENRPS samples (grafted samples) solubilized in DCM. Appendix 17 shows the concentrations of the ENR50 and milled ENR50 samples solubilized in THF.

7.3 Reversed-Phase Chromatography

7.3.1 Cloudpoint measurements performed chromatographically and the relevant theoretical observations made through these analyses

Results of chromatographic cloudpoint measurement have already been shown in Chapter 5. In this section it will, however, be shown how these results were obtained and the theoretical implications. Analyses where performed on the Waters 2690 separations module. The UV detector was set at 254 nm and the injection volume varied between 2 and 10μl (specific volumes given in Figures 7.6 to 7.9). Two different gradient profiles were used:

A   50%/50% H$_2$O/ACN $\xrightarrow{\text{4\%/min}}$ 100% ACN $\xrightarrow{\text{4\%/min}}$ 100% THF

B   50%/50% H$_2$O/ACN $\xrightarrow{\text{4\%/min}}$ 100% THF

The Symmetry C$_{18}$ column (Table 7.1) was used in the cloudpoint measurements. PS and PiP standards were injected for each gradient profile. Results can be seen in Figures 7.6-7.9. In Figure 7.6 it can be seen how cloudpoints were evaluated chromatographically. Another important phenomenon that is clearly visible is the fact that the retention times of the higher molecular mass standards seem to decrease. This is not only visible for the PS standards, but can also be seen in the evaluation of the PiP standards. Information in Figures 7.1 and 7.10 will be used to explain this.

At a low solvent concentration i.e. at the beginning of the solvent gradient, the polymer will, thermodynamically, be in the adsorption region (Figure 7.1).
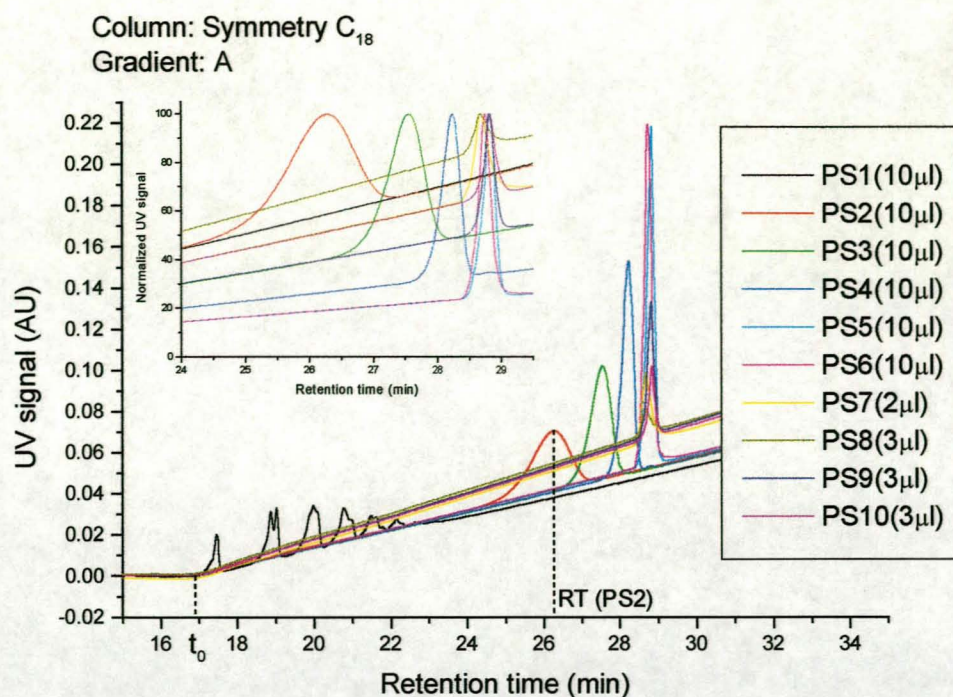
Figure 7.6: Cloudpoint measurements performed on PS standards for gradient A. [1]
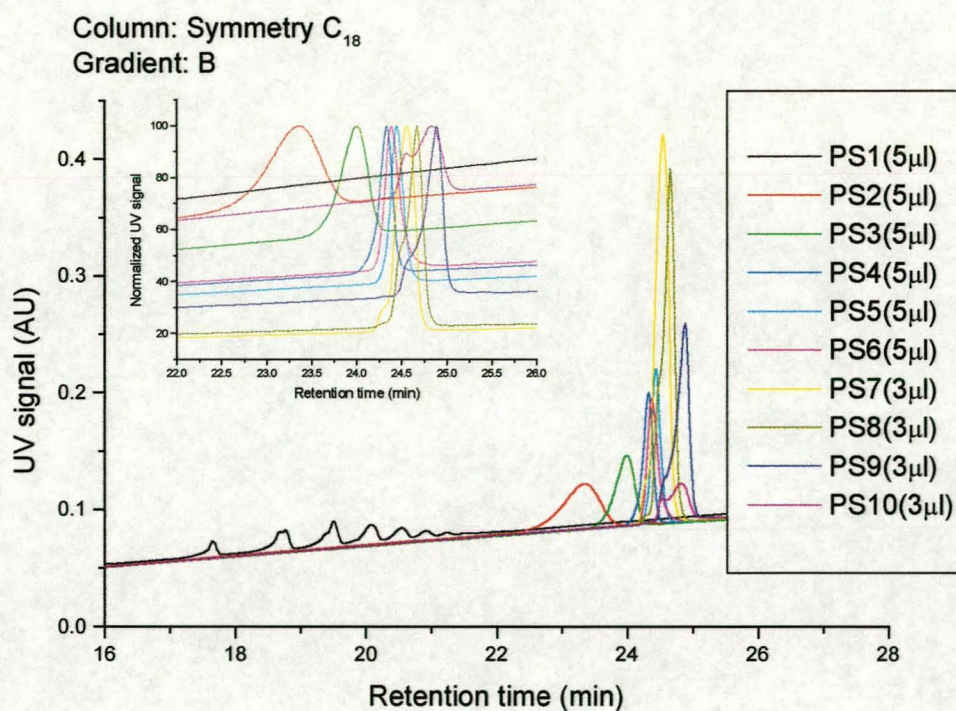
Figure 7.7: Cloudpoint measurements performed on PS standards for gradient B.

---

[1] The measurement of the retention time (RT) and the dead time (t_0) can be seen above for PS2. The inlay shows the normalized UV signal to emphasize the decrease in RT for higher molecular mass samples.

Column: Symmetry C$_{18}$
Gradient: A
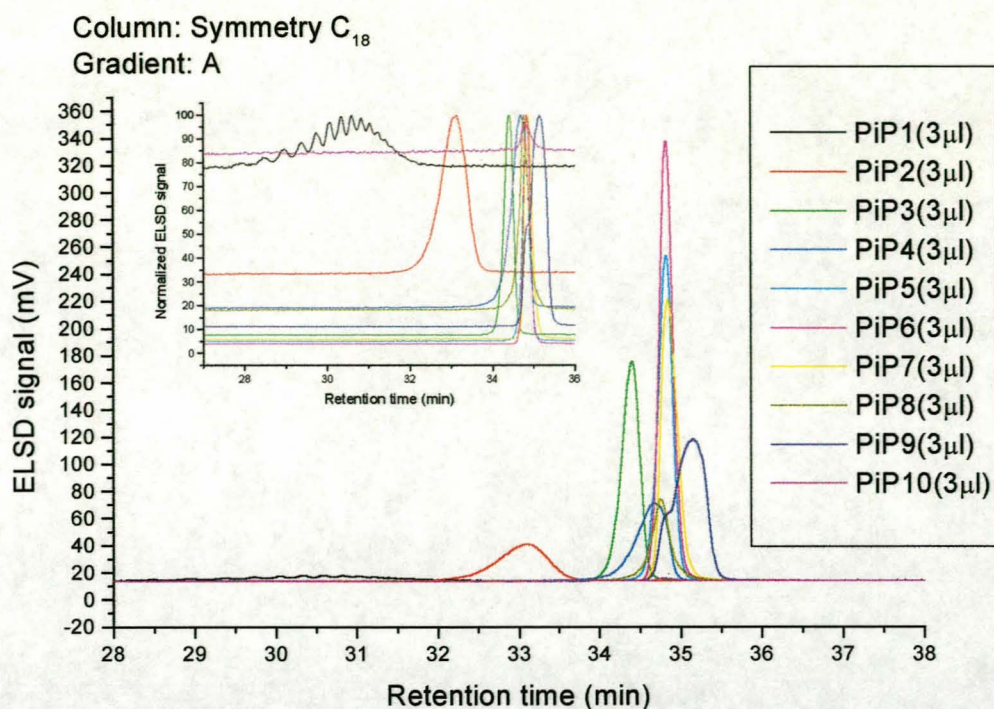
Figure 7.8: Cloudpoint measurements performed on PiP standards for gradient A. [2]

Column: Symmetry C$_{18}$
Gradient: B
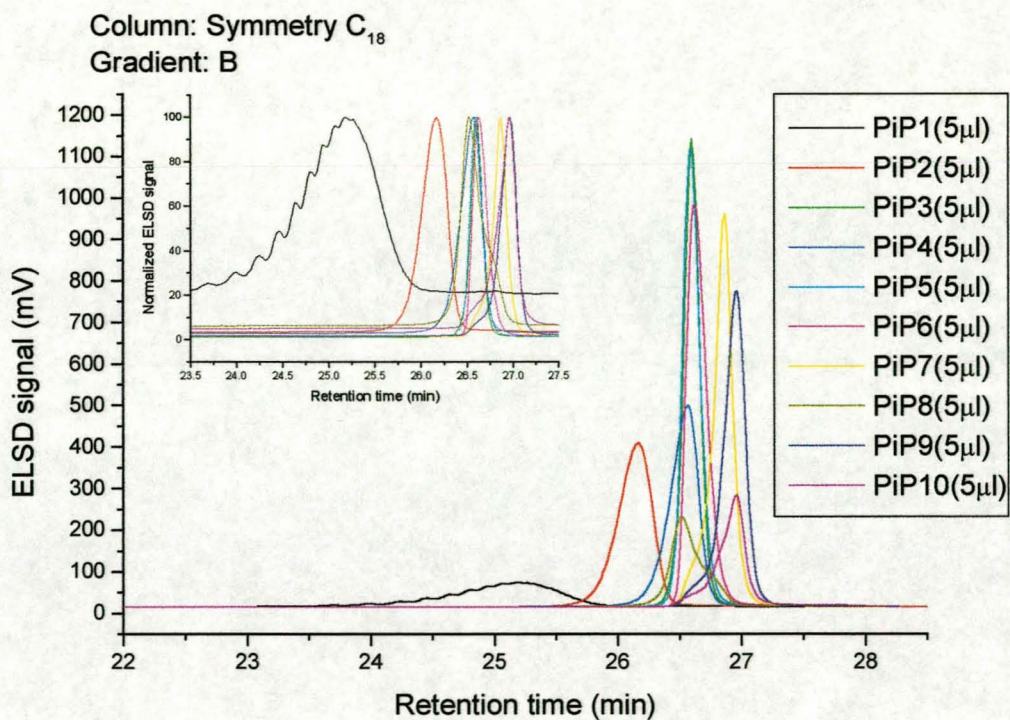

Figure 7.9: Cloudpoint measurements performed on PiP standards for gradient B.

---

[2] Note that the ELSD detector was used due to the fact that PiP does not absorb UV radiation. Similar trends for the high MM standards can be observed in the inlay.

The low molecular mass polymers which dissolve in this region will therefore adsorb to the column and the packing material and the retention time (RT) will increase. When the gradient reaches a high solvent content, the high molecular mass polymers will dissolve. These polymers are in the exclusion solvent region (Figure 7.1). These polymers are too large for the 100 Å pores and will therefore not enter the pores of the packing material and so will move faster than the solvent. RT will therefore decrease. At a certain point in time, the higher molecular mass polymers can move with, or just in front of, the solvent front that dissolved it. This will cause reprecipitation of the polymer in the column and cloudiness will appear as the solvent front loses solubility due to the mixing of poorer solvent from the pores of the packing material; Figure 7.10 is a graphical representation of this.

Glöckner [10] also explained this phenomenon by comparing the velocity of the high molecular mass polymer in the interstitial volume and the linear velocity of the eluent. According to him the linear velocity of the polymer in the interstitial volume (exclusion region) can be expressed as follow:

$$U_p = \frac{L}{V_I/F_{rate}} \tag{7.1}$$

where L is the length of the column, V_I the interstitial volume and F_{rate} the flow rate. In contrast to this, the eluent has access to the pore volume (V_P) of the packing material as well as the interstitial volume (V_I) and the total volume accessible by the eluent can therefore be expressed as V_{mob} where $V_{mob} = V_I + V_P$. The linear velocity of the eluent can therefore be expressed as

$$U_E = \frac{L}{V_{mob}/F_{rate}} = \frac{L}{(V_I + V_P)/F_{rate}} \tag{7.2}$$

but $V_{mob} > V_I$.

This implies that the velocity of the eluent is smaller than the velocity of the polymer.

The polymer bypasses the pores and thus always overtakes the eluent having sufficient elution strength. The polymer is retained again until a more powerful eluent reaches its position.
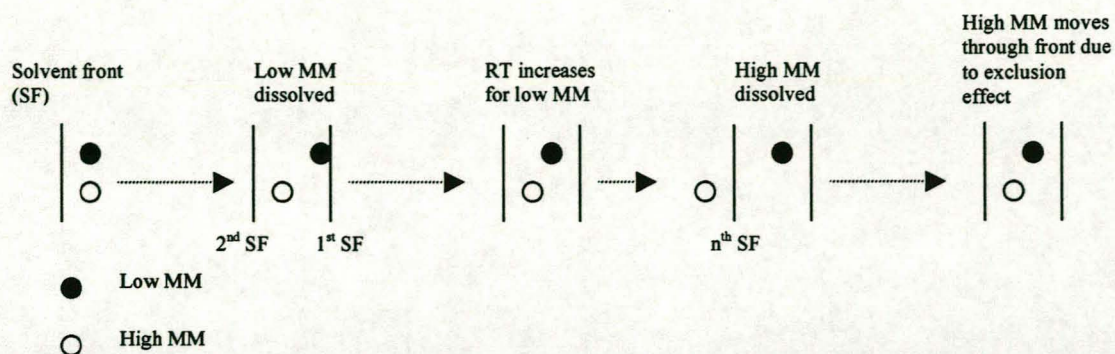
Figure 7.10: Adsorption, size exclusion competition between high and low molecular mass solutes and the consequent influence on retention time in gradient HPLC.

For an infinitely long column, all the peaks resulting from the different molecular masses of the same polymer will therefore elute at the same retention time (Figure 7.11).
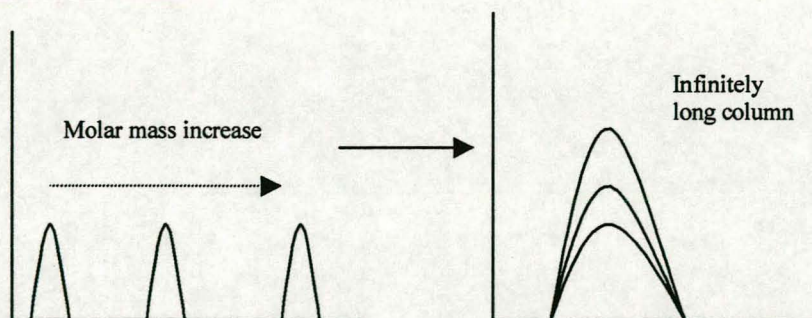
Figure 7.11: Co-elution of molecular masses from an infinitely long column.

To give further evidence for the above statements, it was proven that the higher molecular mass polymers did reprecipitate. This was done by using the UV detector for both PS and PiP standards at 400 nm. At this wavelength, no UV radiation absorption can be detected unless the particles scatter it, thus scattering shows that precipitation occurred in polystyrene standards PS9 and PS10 at 7 and 20 million molar mass respectively. Results can be seen in Figures 7.12 and 7.13.
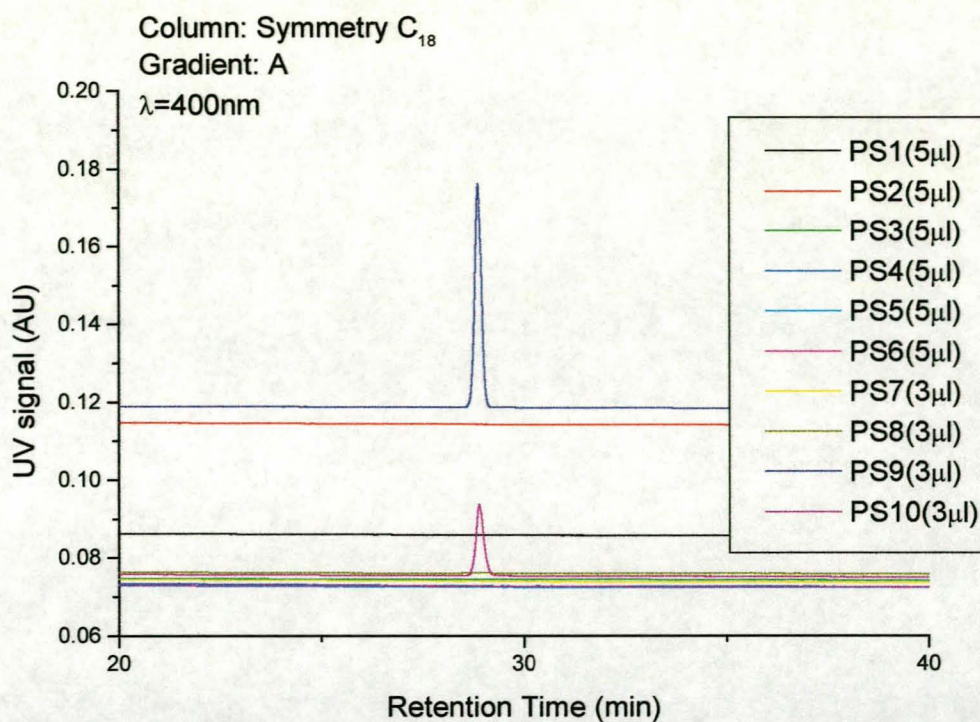
Figure 7.12: Confirmation of reprecipitation of high MM PS standards through UV analysis at 400 nm.
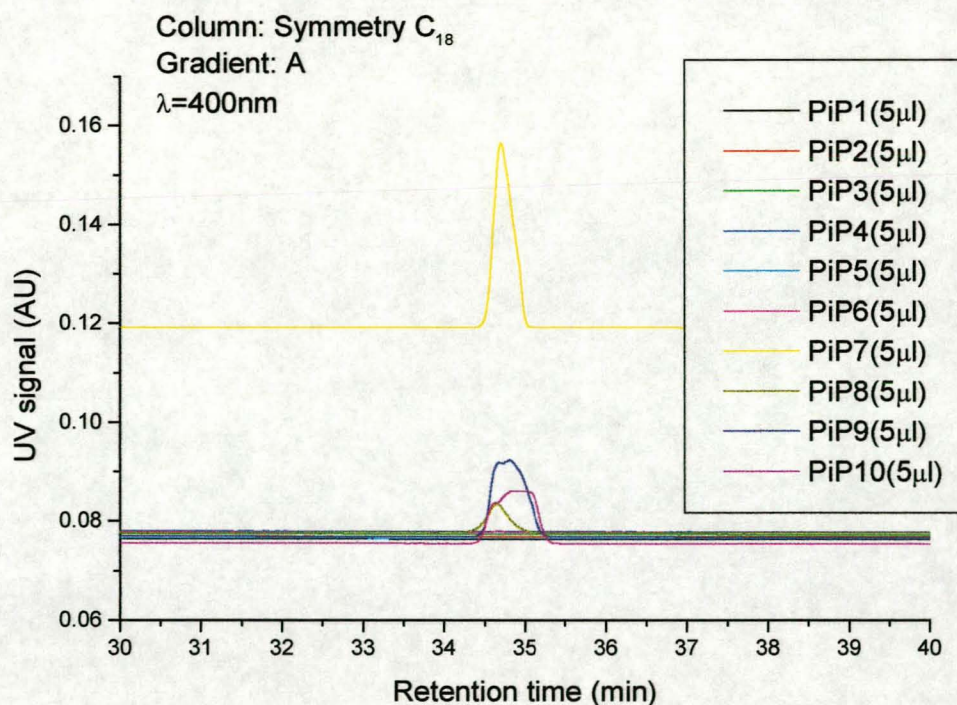
Figure 7.13: Confirmation of reprecipitation of high MM PiP standards through UV analysis at 400 nm.

Similar results were also obtained for the PS and PiP standards for gradient B (Appendices 18, 19).

The above explanation gives sufficient evidence for the shape of the cloudpoint curves (Chapter 5, Figure 5.6) as well as peak swapping that can occur in gradient HPLC analysis. It is therefore clear that for the higher molecular masses the gradient curve will shift to the left (in comparison with the titration curve) due to the decrease in RT. The opposite holds true for the lower molecular masses (RT increase).

Not only does cloudpoint measurements give important answers concerning the separation process, but it also explains certain theoretical facts that cannot otherwise be explained. This, in conjunction with work done in Chapter 5, emphasizes the importance of cloudpoint evaluations.

7.3.2 Evaluation of the separation between ENR50, milled ENR50 samples and PS standards

Although polyisoprene (PiP) was used in cloudpoint evaluations due to the fact that its chemical structure was the closest to that of ENR50, the retention time of the ENR50 had to be compared to the retention time of the PS standards to see if optimum separation was possible. The ENR50 was also milled on a twin-mill roll for 2, 4, 6, 8, 10, 12, 14 and 16 minutes. The gradient HPLC results of these samples were compared to the analysis results of the unmilled ENR50 sample. This was done to see whether milling had any significant effect on the ENR50 and if milled grafted samples could be used in gradient experiments as well. Comparison of the gradient HPLC results for ENR50 and milled ENR50 samples can be seen in Figure 7.14. All analyses were done on the Waters 2690 Separations Module (Alliance).
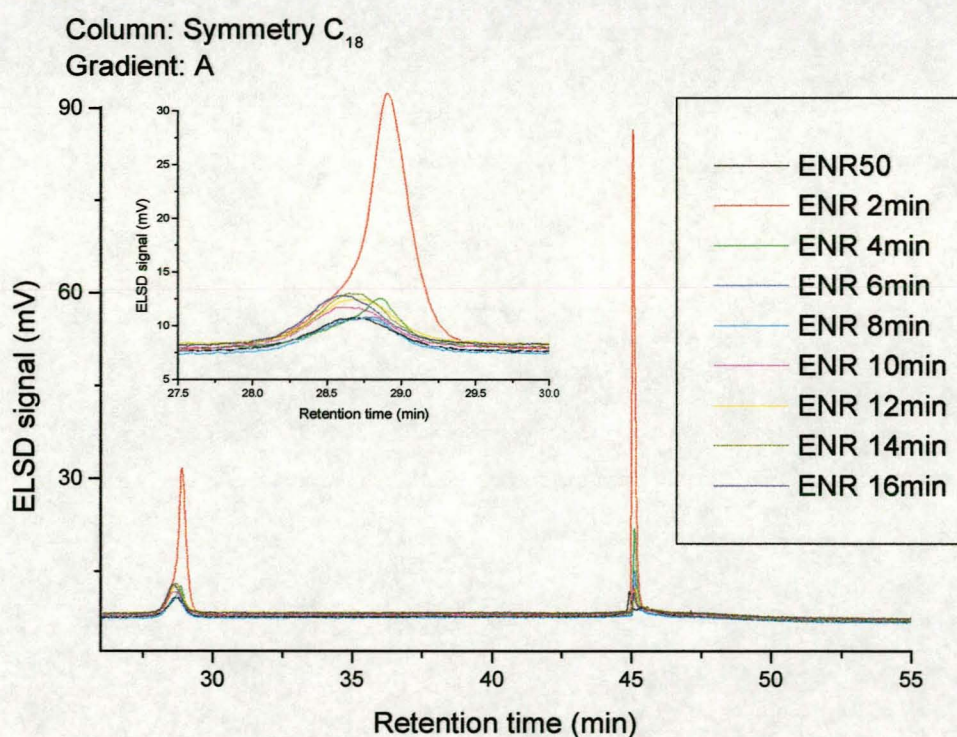
Figure 7.14: Comparison of gradient HPLC results of ENR50 with that of milled ENR50 samples. (Sample volumes 5µl throughout.)

From Figure 7.14 it follows that the peaks at ±28.5 min were caused by the ENR50 and milled ENR50 samples. The peaks at 45 min are caused by microgels.

The peak for the ENR50 was small due to the limited solubility of the sample. The 2-minute milled sample, however, showed a very big peak (compared to that of the unmilled sample). This peak was the result of light scattered by high molecular mass ENR50 polymer chains which were now in solution due to chain scission caused by the milling process. In the other milled samples, the peak heights were dramatically reduced. This was due to the fact that crosslinking recurred, reducing solubility again. The peaks also shifted slightly to the left thereby implying that a lower molecular mass remained uncrosslinked. By comparison of the experimental results of the ENR50 and milled samples, it is possible to say that the soluble portion of both milled and unmilled samples can be used in gradient HPLC analysis.

The next step was to evaluate the separation between the ENR50 and the styrene standards. Results of this can be seen in Figure 7.15.
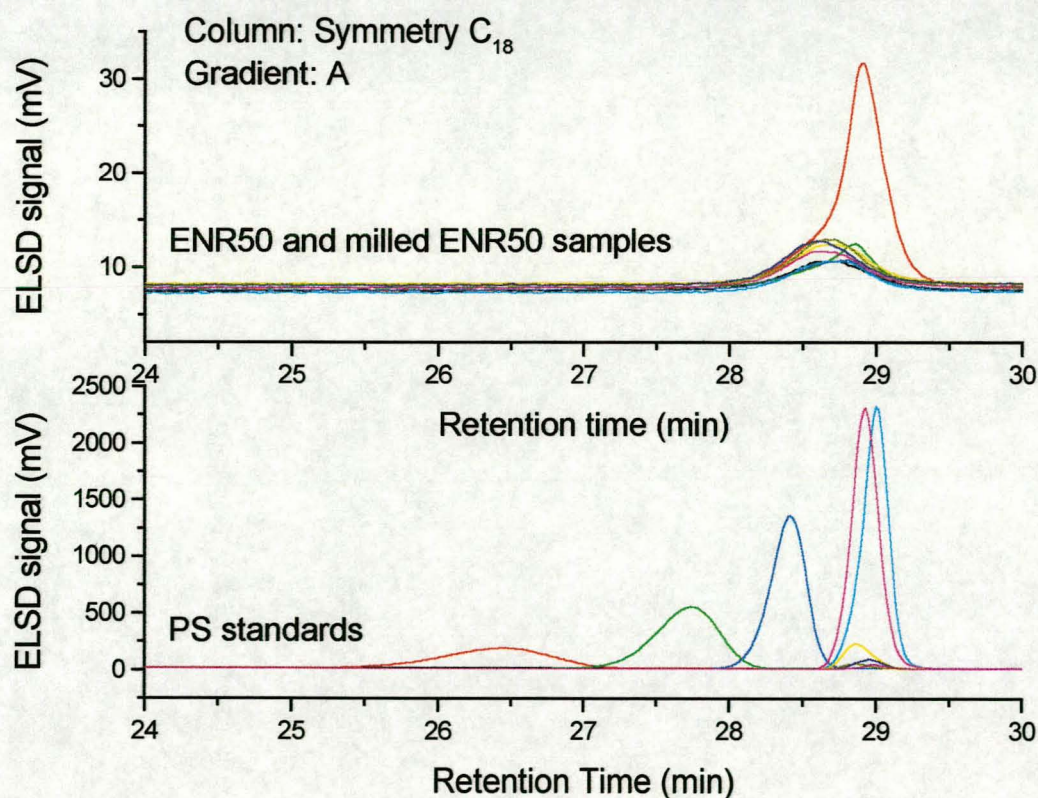
Figure 7.15: Comparison of the retention times of ENR50, milled ENR50 samples and PS standards for gradient A. (Injection volume of rubber samples: 5µl. Injection volume of PS standards: refer to Figure 7.12.)

From Figure 7.15 it is clear that no separation between the PS standards and ENR50 was achieved. Although cloudpoint evaluations of PiP and PS standards showed that gradient B was not sufficient for separation, it was also evaluated in the light of the above result (Figure 7.16).
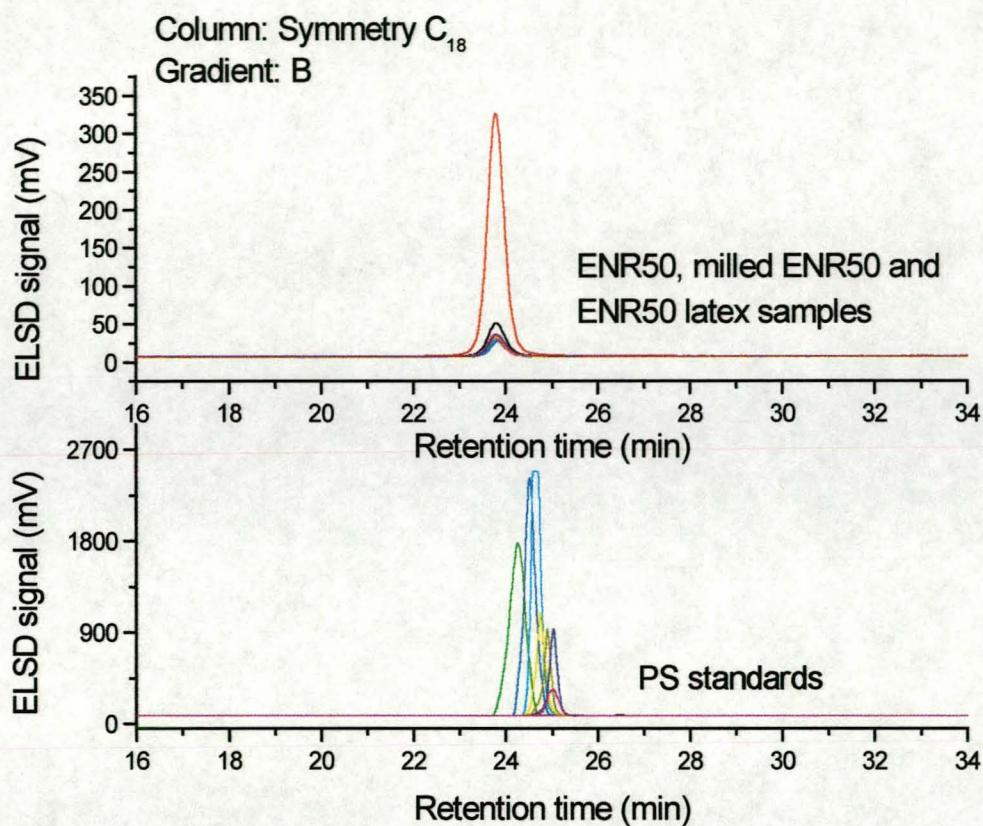
Figure 7.16: Comparison of the retention times of ENR50, milled ENR50 samples and PS standards for gradient B. (Injection volumes were as in Figure 7.15.)

According to Figure 7.16, gradient B cannot be used to separate the ENR50 and PS standards sufficiently. The epoxide group of the ENR50 was a possible reason for the inconsistency in the above results and the results obtained through cloudpoint evaluations. The above results meant therefore that other gradient and column systems had to be used to obtain suitable separation. Hence, the next step was to evaluate a heptane/THF gradient in conjunction with silica, CN and Symmetry C_{18} columns.

7.3.3 Evaluation of the separation between ENR50 and PS standards by using a heptane/THF gradient and silica, CN and Symmetry C_{18} columns

Due to the fact that gradients A and B proved to be insufficient for separation, other gradient and column systems had to be evaluated. To try and obtain better separation, it was thought to be a good idea to use a more polar column (silica) (Table 7.1) and a weaker solvent (heptane). The aim of using the weak solvent and a more polar column was to obtain better adsorption, hence better separation. Analysis was done on the Waters 616. The heptane/THF gradient (C) was as follows:

C   100% Heptane $\xrightarrow{\text{4\%/min}}$ 100% THF

The total run time for the experiment was 50 minutes. Detectors used were the Waters 490 (λ=254nm) and ACS ELSD (70°C). PS standards and ENR50 (2 minutes milled) were injected and the results can be seen in Figure 7.17.
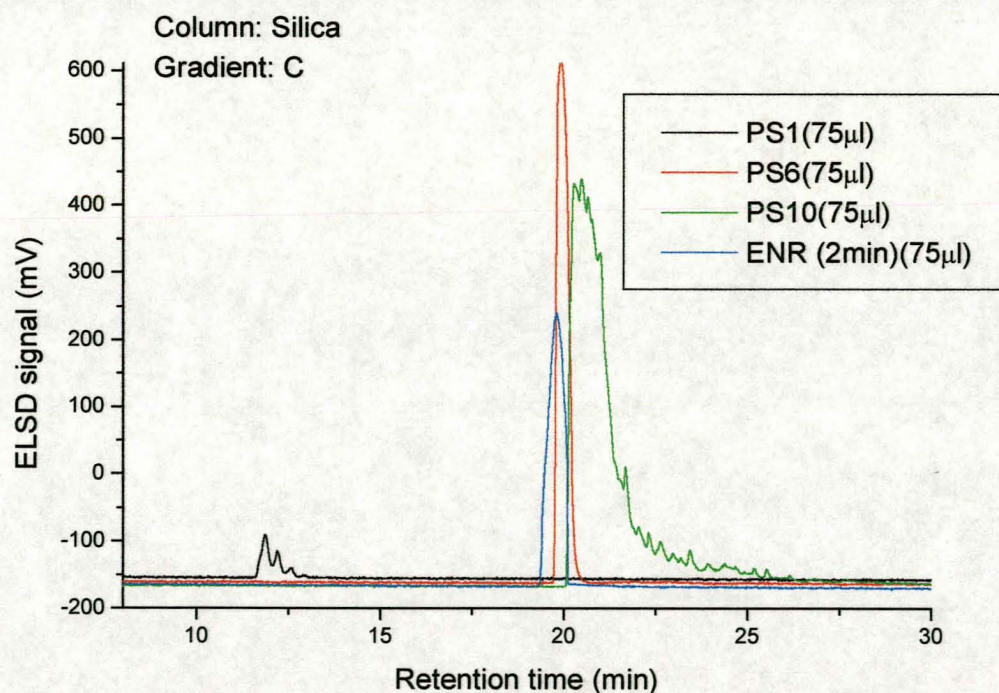
Figure 7.17: Gradient HPLC analysis of milled ENR50 and PS standards on a silica column.

Figure 7.17 shows that the ENR50 elutes in the same region as the PS standards, indicating that separation is not possible here.

Further optimization was therefore necessary and this was done by using a Symmetry C_{18} column and a CN column (Table 7.1). The Waters 616 was used and gradient C was applied in both cases. All other settings were the same as used with the silica column. Unfortunately, similar results to those obtained with the silica column, were obtained (Figures 7.18, 7.19).
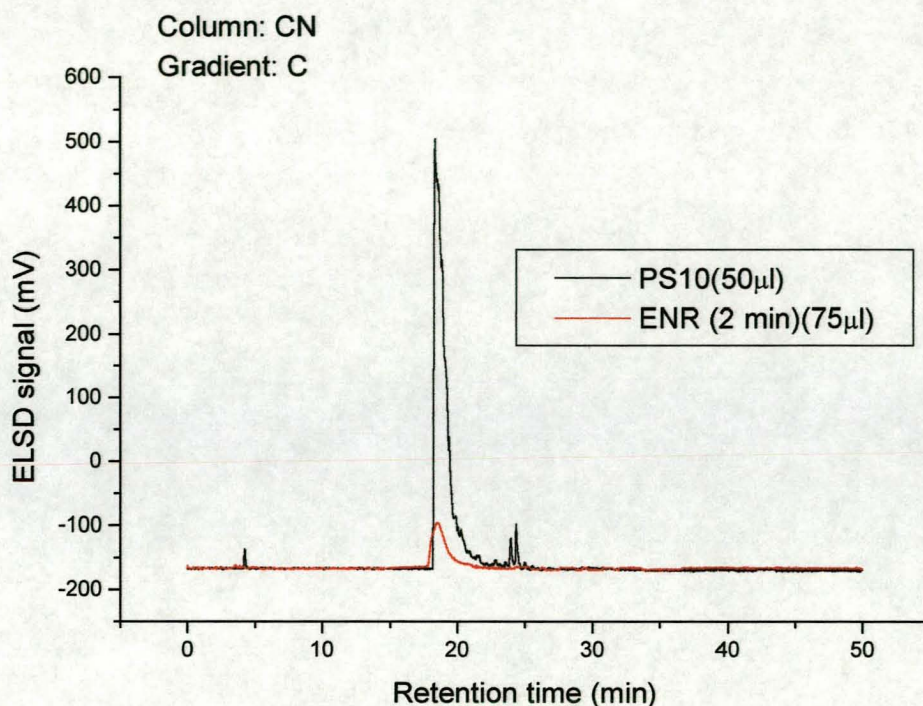
Figure 7.18: Gradient HPLC analysis of milled ENR50 and PS standards on a CN column.

Gradients A, B and C used in conjunction with the silica, CN and Symmetry C_{18} columns proved to be inadequate to provide the necessary separation between the PS standards and the ENR50. This was again an indication of the importance of doing preliminary cloudpoint evaluations on the precursors that were used in the grafting reactions. However, the above analyses were not a total lost.

In all the above cases RP chromatography had been used, in other words, separation was based on solubility and adsorption. Now the opposite, namely NP chromatography, was to be used. NP chromatography is based on polarity and due to the lack of polarity of the PS and high polarity of the epoxide group of the ENR50, there was reason to believe that NP may cause adequate separation.
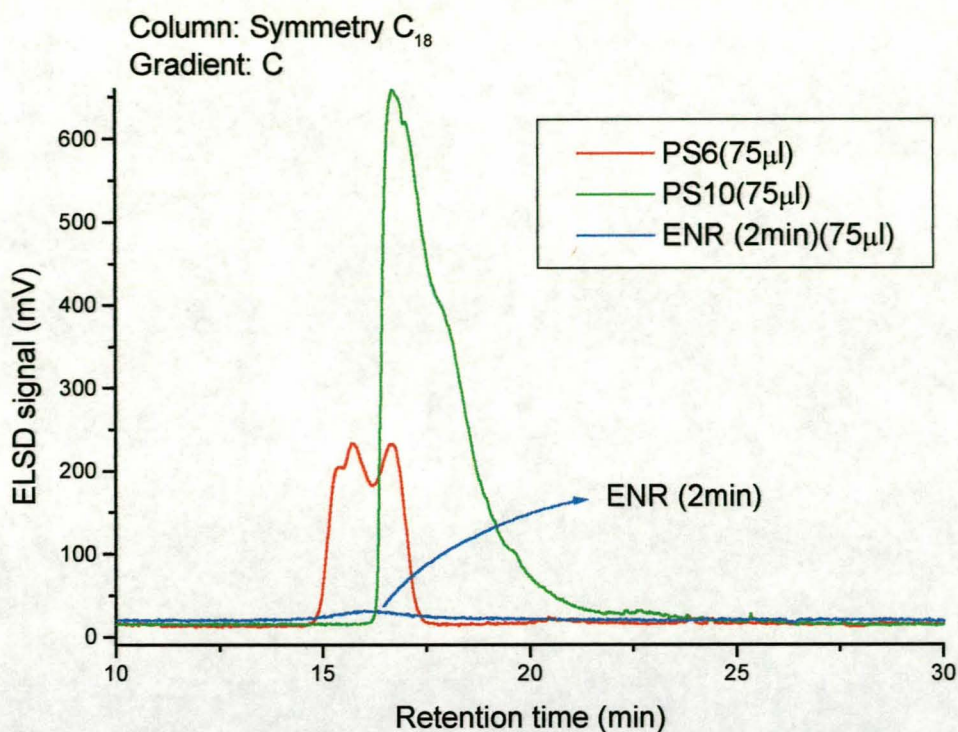
Figure 7.19: Gradient HPLC analysis of milled ENR50 and PS standards on a Symmetry C_{18} column.

7.4 Normal Phase Chromatography

7.4.1 Evaluation of the separation between ENR50 and PS standards on a CN and silica column

Normal phase gradient HPLC requires the use of a polar column together with a gradient whose polarity increases during the gradient run [11]. Sample retention will therefore increase with increasing sample polarity. In the light of the above, CN and silica where chosen as the polar columns and the gradient went from dichloromethane (DCM) (polarity = 3.1) to tetrahydrofuran (THF) (polarity = 4.0). The criteria for a NP system were therefore met. In addition, the epoxide group of the ENR50 would also provide a high polarity site in comparison with the low polarity of the PS. In theory, separation between the two chemical precursors is therefore inevitable, the only difficulty being to fine-tune the gradient system for optimum separation.

The gradient systems used are listed below.

D   100% DCM $\xrightarrow{0.2\%/min}$ 10% THF $\xrightarrow{4\%/min}$ 100% THF

E   100% DCM $\xrightarrow{0.1\%/min}$ 10% THF $\xrightarrow{4\%/min}$ 100% THF

F   100% DCM $\xrightarrow{10\%/min}$ 100% THF

The total running time for gradients D, E and F were 95, 145 and 35 minutes. The Waters 616 was again used for chromatographic evaluations and settings were similar to those used for previous discussions (Section 7.3.3). The DCM had to be degassed prior to use to avoid unnecessary bubble formation during gradient runs.

In the first two experiments, the samples were dissolved in THF and gradients D and E were used. The results, as obtained with the UV and ELSD detectors for gradient D, can be seen in Figures 7.20 and 7.21.

Figure 7.20: Gradient HPLC analysis of ENR50 and PS standards using gradient D and a UV detector. [3]

---

[3] Note the peaks at 3.43 minutes. This is due to an inherent property (stabilizer or contaminant) of the THF which was used as both solvent and polar eluent.
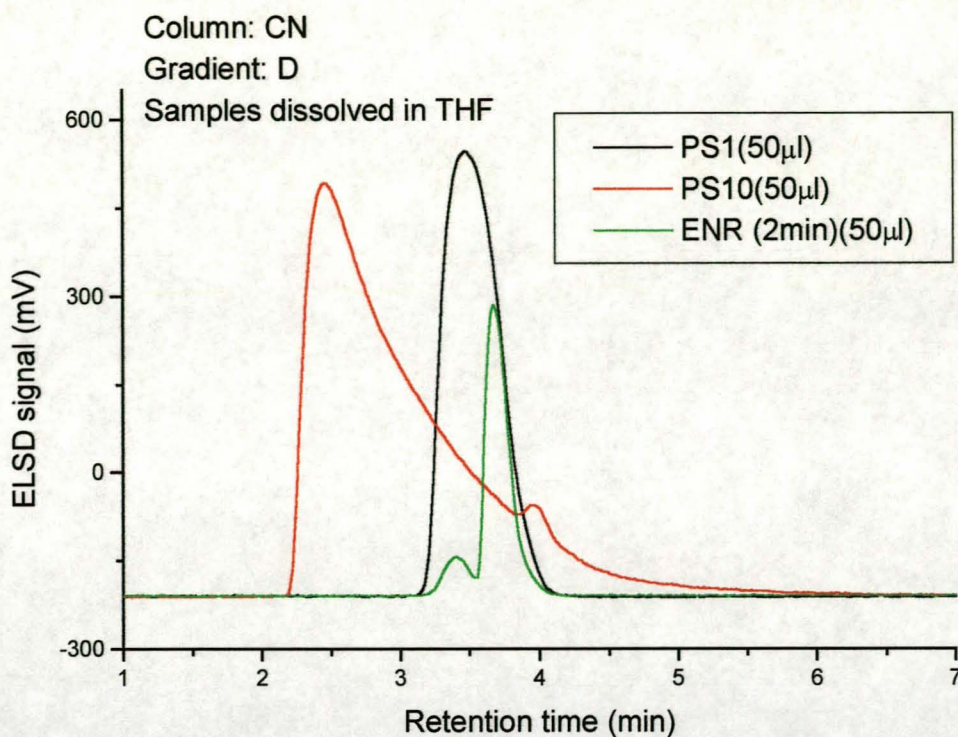
Figure 7.21: Gradient HPLC evaluation of ENR50 and PS standards using gradient D and an ELSD detector.

The graphs show the effect of the polar column very well in the sense that the higher molecular mass PS elutes first, followed by the lowest molecular mass PS and then the ENR50. Thus, although separation was not obtained, the NP system showed promising results. An even slower gradient was therefore applied to see if it was not possible to "pull" the groups apart. In Figures 7.22 and 7.23 the effects of gradient E can be seen.

From the graphs it follows that the decrease in gradient rate for the first 10% THF is not necessary due to the fact that there is no change in retention times in comparison with gradient D results. A reason for the lack of separation might be the use of the THF as solvent for the ENR50 and PS standards. The fact that the THF is a more polar solvent than the DCM can cause fewer interactions between the column and the compounds. This is due to the fact that the stronger solvent is already interacting with the column on injection, rather than the compound. If the compounds were dissolved in a less polar solvent (e.g. DCM) the compounds would interact with the column and not the solvent used for solubilizing it, thereby causing the compounds to elute later from the column.

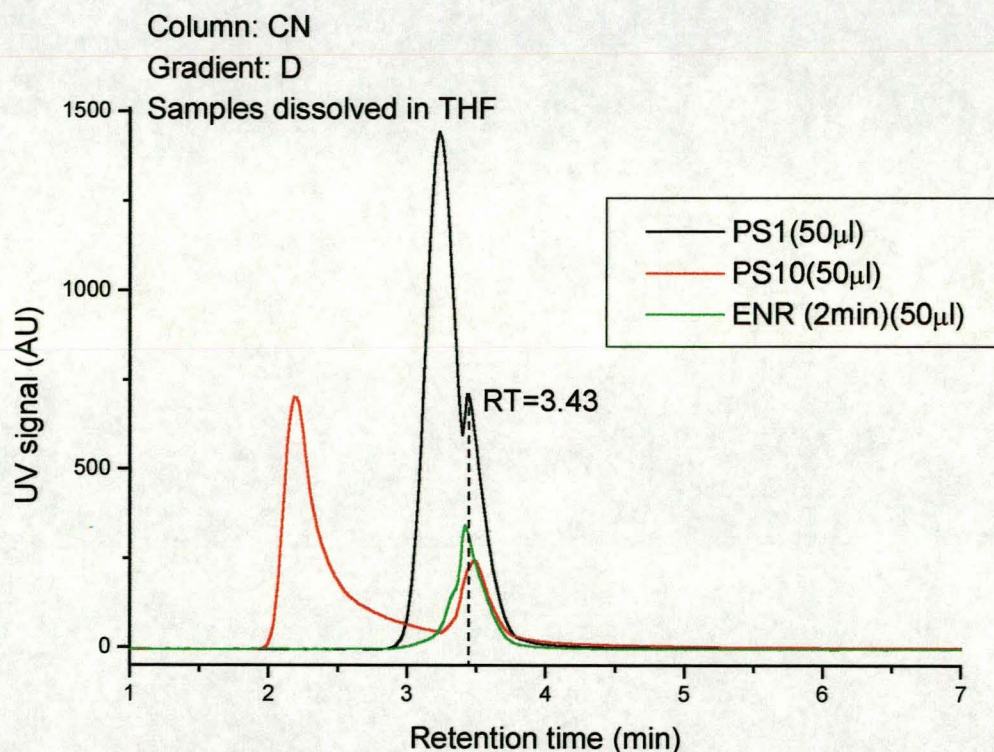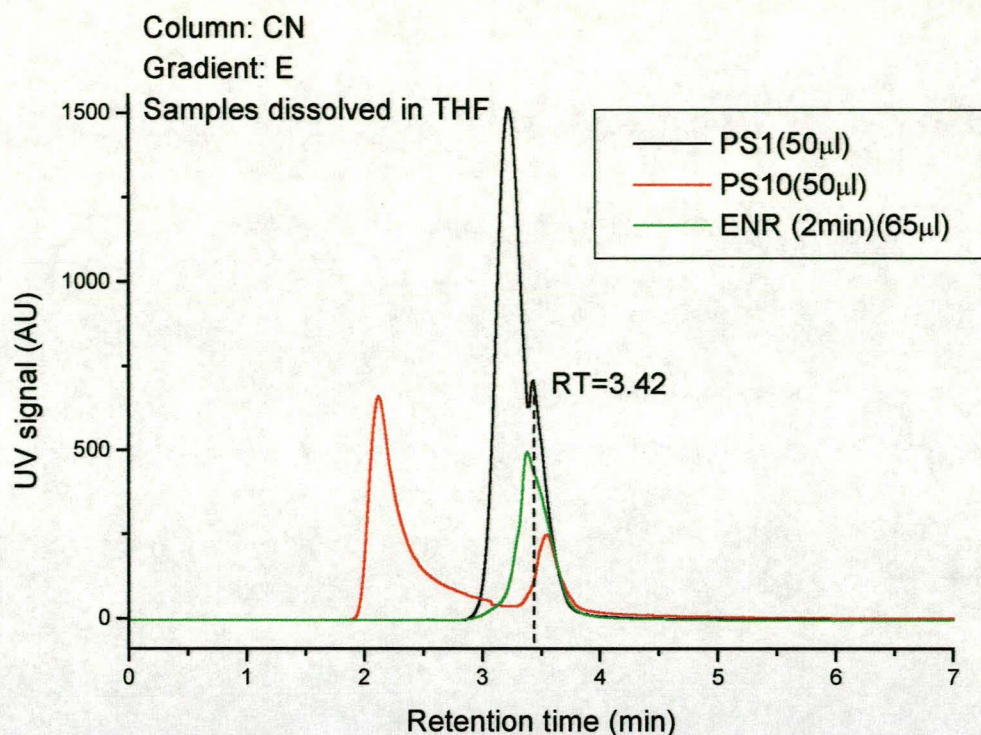Figure 7.22: Gradient HPLC evaluation of ENR50 and PS standards using gradient E and a UV detector. [4]
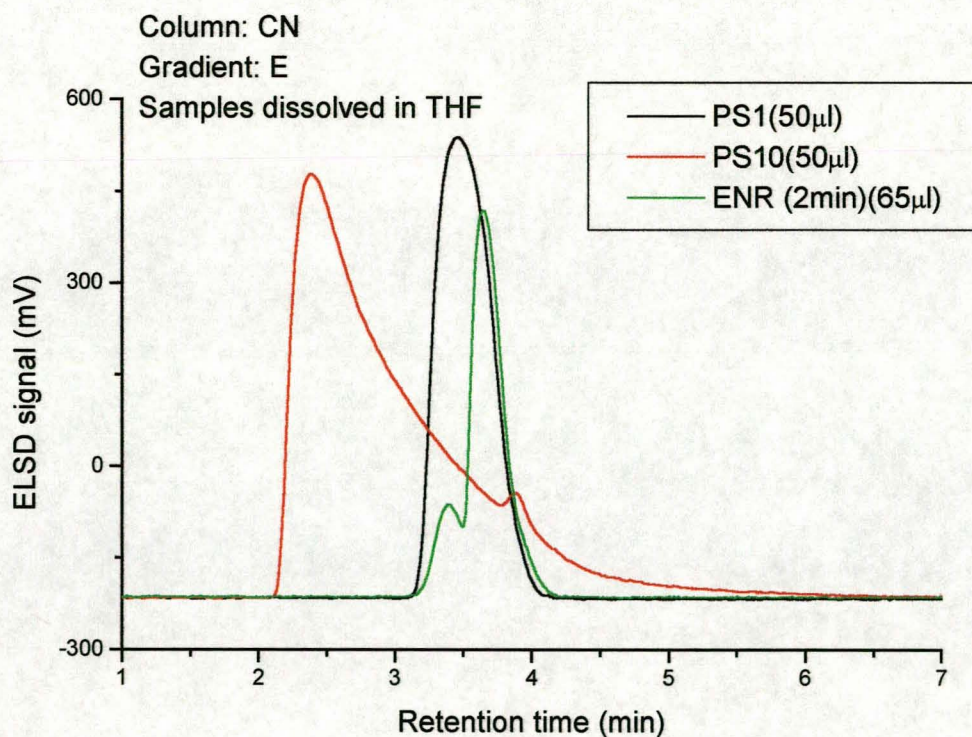
Figure 7.23: Gradient HPLC analysis of ENR50 and PS standards using gradient E and an ELSD detector.

---

[4] Again note the peaks at 3.42 minutes that are inherent of the THF used.

Apart from the lack in separation, the increase in the ENR50 peak height due to the higher volume injected looked promising. All experiments from this point forward were done on samples dissolved in DCM. Gradient E was therefore re-evaluated with the DCM-solubilized samples to see if any improvement occurred. Results can be seen in Figure 7.24.
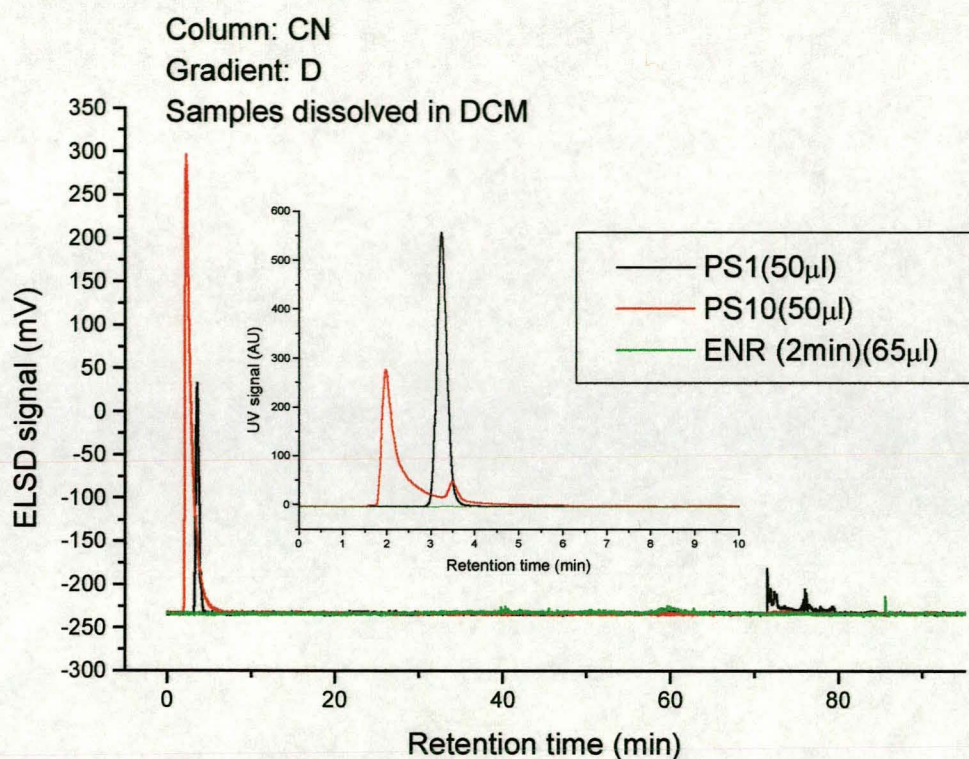
Figure 7.24: Gradient HPLC analysis of ENR50 and PS standards using UV and ELSD detectors and gradient D.

In Figure 7.24, no signal for the ENR50 was visible although the PS peaks were very prominent. This was an indication that the volume of ENR50 injected was not sufficient. This was therefore investigated and results presented in Figure 7.25. Here, the injection volume was increased from 85 to 150 μl and the effect can easily be seen. What was also very noteworthy, was the fact that the ENR50 peak showed a lot of spreading. This was ascribed to the very slow gradient rate that was applied and the rate was therefore adapted to allow for better ENR50 peak resolution. By applying gradient F, separation was finally evident, as can be seen in Figure 7.26.
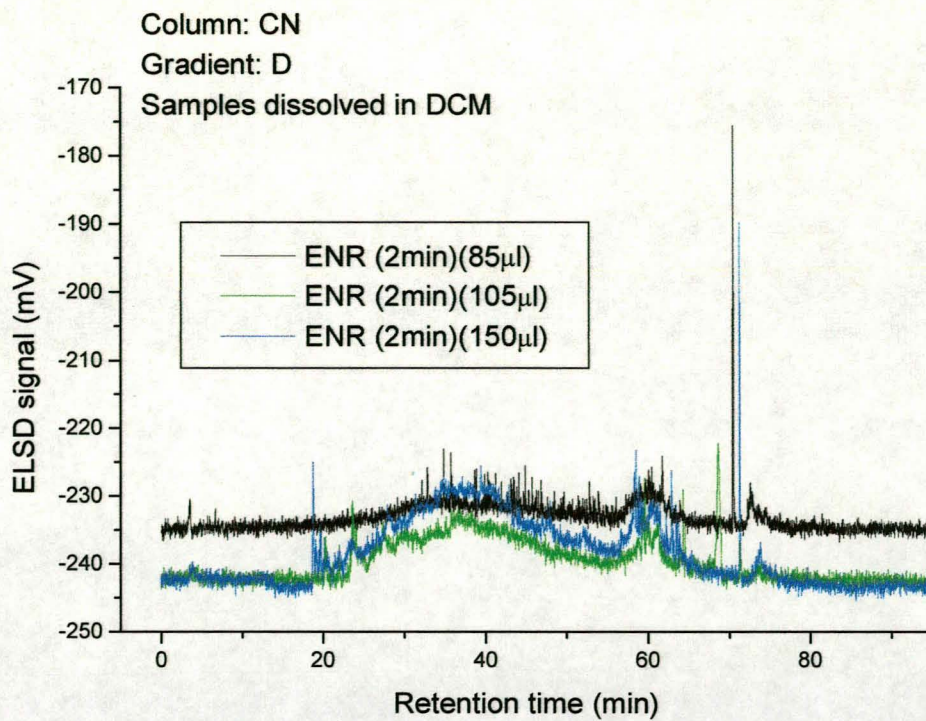
Figure 7.25: Evaluation of different injection volumes of ENR50.
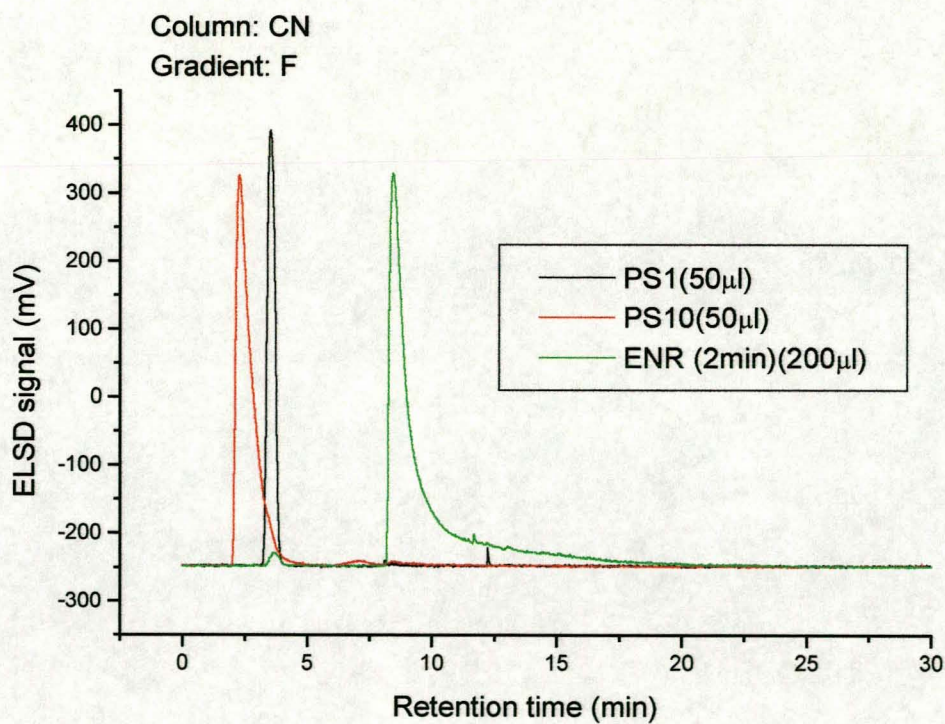
Figure 7.26: Separation between ENR50 and PS standards as obtained on a CN column and by using gradient F. (An ELSD detector was used for detection.)
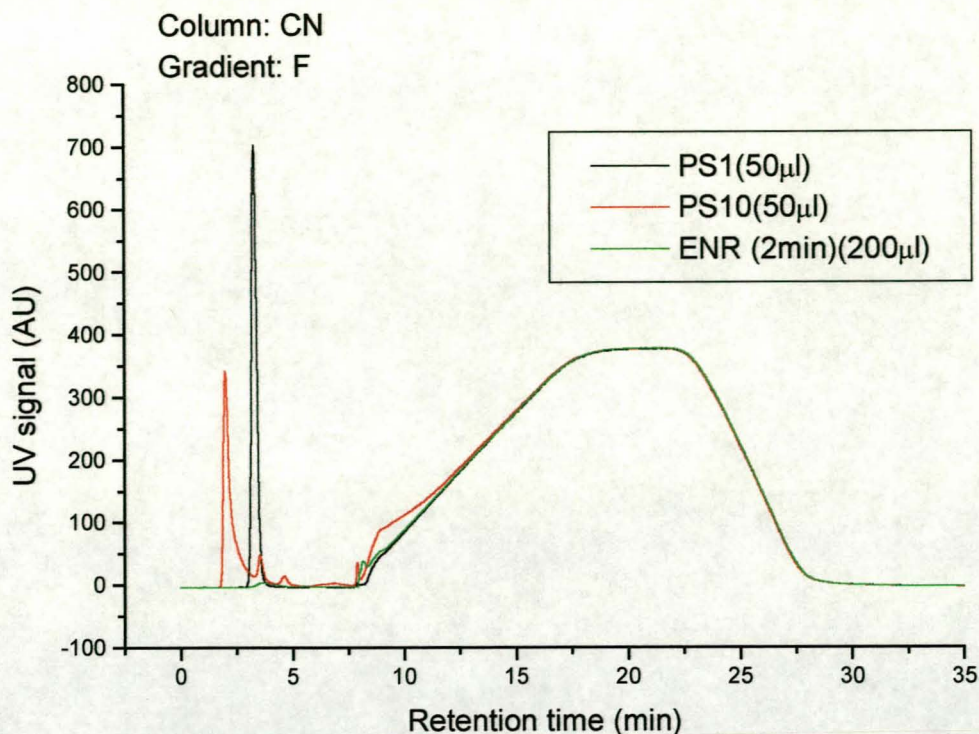
Figure 7.27: UV signal of separation between PS standards.

Figure 7.26 shows separation between the PS standards and the ENR50. Figure 7.27, showing the UV signal, is proof that the first two signals are produced by the PS standards. No signal for the ENR50 is visible with the UV detector. This is correct as ENR50 does not have a UV chromophore.

Evaluations were also performed on a silica column as this column is more retentive than the CN. It was therefore believed that better separation would be possible. The only drawback of the silica column is the very low hydrophobicity (one of its major characteristics). Samples had therefore to be completely water-free. This is always a problem with the rubbery nature of the samples as water can be trapped inside the rubber network. Despite this, analyses were still done and results shown in Figure 7.28 and 7.29. What is very strange from these results is that the PS standards also show peaks at 10.73min with the ELSD detector; that is exactly where the ENR50 elutes. A reason might be that as soon as the gradient starts, the water-containing groups of the PS standards that are strongly retained by the polar column are replaced by the THF molecules which will now interact with the column. This will therefore cause the peaks at 10.73min.
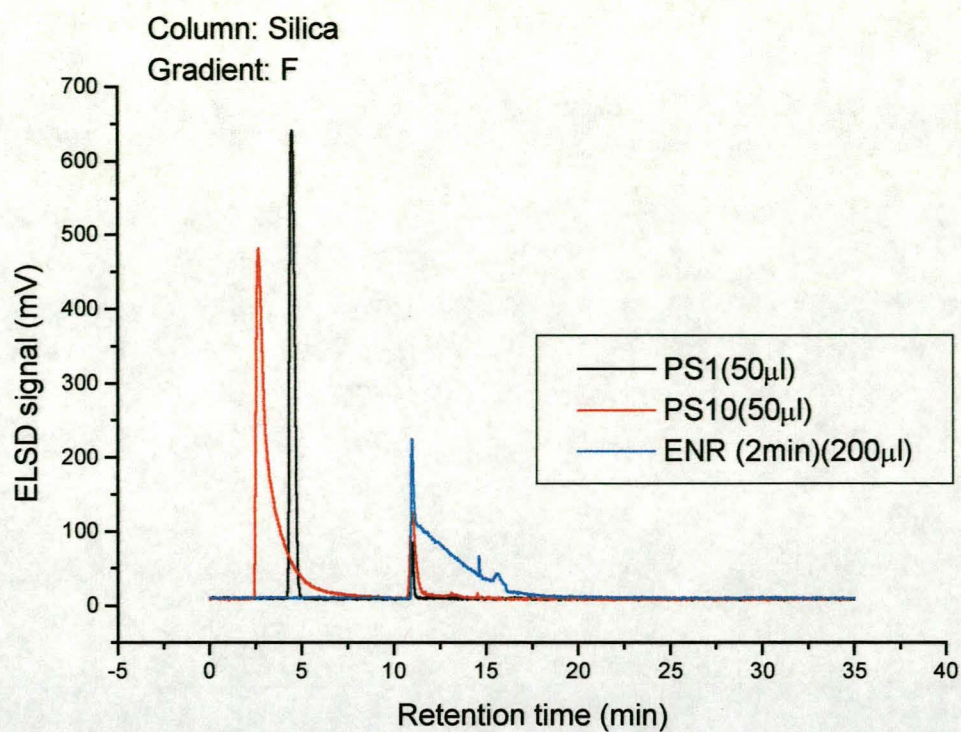
Figure 7.28: Gradient HPLC evaluation of ENR50 and PS standards using an ELSD detector and silica column.
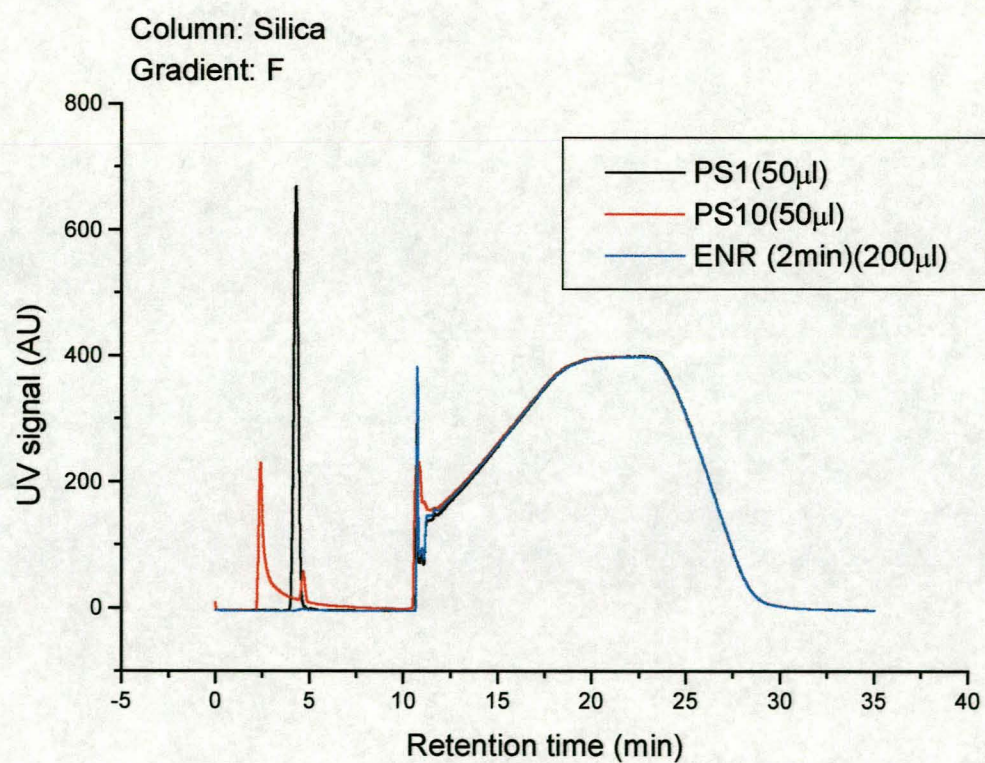
Figure 7.29: Gradient HPLC evaluation of ENR50 and PS standards using a UV detector and silica column.

This might also be the reason for the tailing of the high molecular mass PS standard peak in Figure 7.27. Although separation was therefore also possible on a silica column, the fact that water played such a big role made this a less favored method for analysis. Results of separation of the grafted samples will, however, also be shown for the silica column.

7.4.2 Evaluation of the grafted samples by using the Waters 2690 Separations Module

Although separation was obtained by using the Waters 616 chromatographic system, the final analyses of the grafted samples were performed on the Waters 2690 Separations Module (Alliance). This was done because of the better baseline stability, lower noise and better resolution obtainable from the Alliance. Results can be seen in Figures 7.30-7.33. Figure 7.30 shows the ELSD signals of the PS standards and ENR50. These were compared with the ELSD signals obtained from the grafted samples (Figure 7.31). By doing this it was possible to see whether or not free PS, grafted product or free ENR50 formed during the initial graft reaction. Figure 7.30 also shows excellent separation between the PS standards and the ENR50. The ENR50 peak shows tailing, which is caused by microgels in the injected solution. There is no styrene monomer peak visible, as the monomer is vaporized during drying or on entering the heated chamber of the ELSD detector.

As was mentioned above, Figure 7.31 shows the ELSD signals obtained from the grafted samples. The graph shows very prominent free PS peaks. This means that a lot of the styrene monomer that was used in the graft reaction polymerized to form PS homopolymer instead of grafting with the ENR50. Much of the homopolymer will be extracted from the gel by the solvent. At 6 minutes, the rubber peaks can also be seen followed by humps from 7 to 11 minutes. These humps are caused by the microgels, in the solution, that was injected into the column. At 4.67 minutes, the grafted peaks can be seen, but unfortunately they are very small. The reason for this is the limited solubility of the partially crosslinked ENR50, even when grafted. Since grafting was performed in latex form, it was not possible to perform the 2 minute milling to reduce molecular mass and increase solubility. Therefore a partially crosslinked rubber (result of epoxidation) was used for grafting.

Figure 7.30: Gradient chromatograph of PS standards, ENR50 and styrene monomer obtained with an ELSD detector and a CN column.

Figure 7.31: Chromatograph of styrene-grafted ENR50 obtained with an ELSD detector and a CN column.

Figure 7.32: Gradient chromatograph of PS standards, ENR50 and styrene monomer obtained with a UV detector and a CN column.
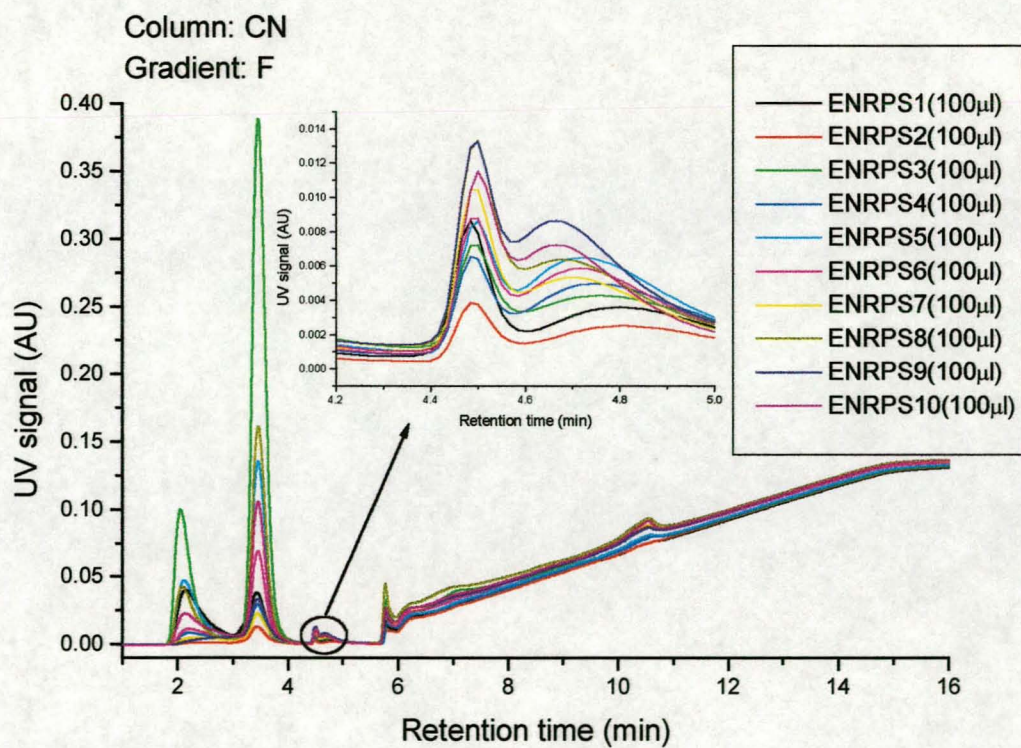
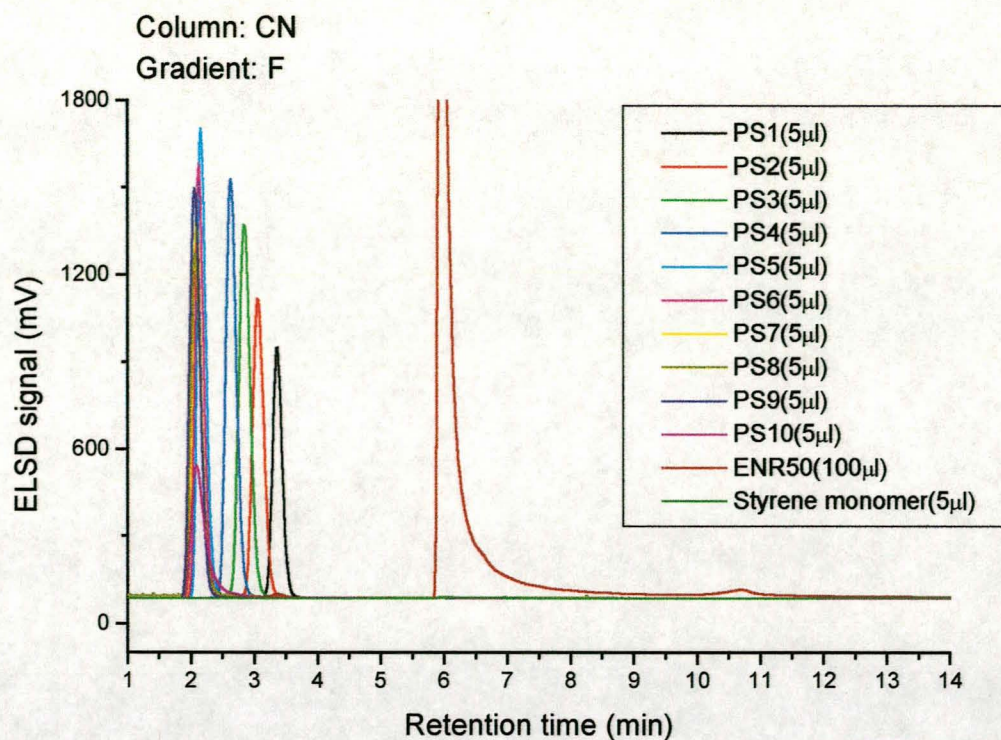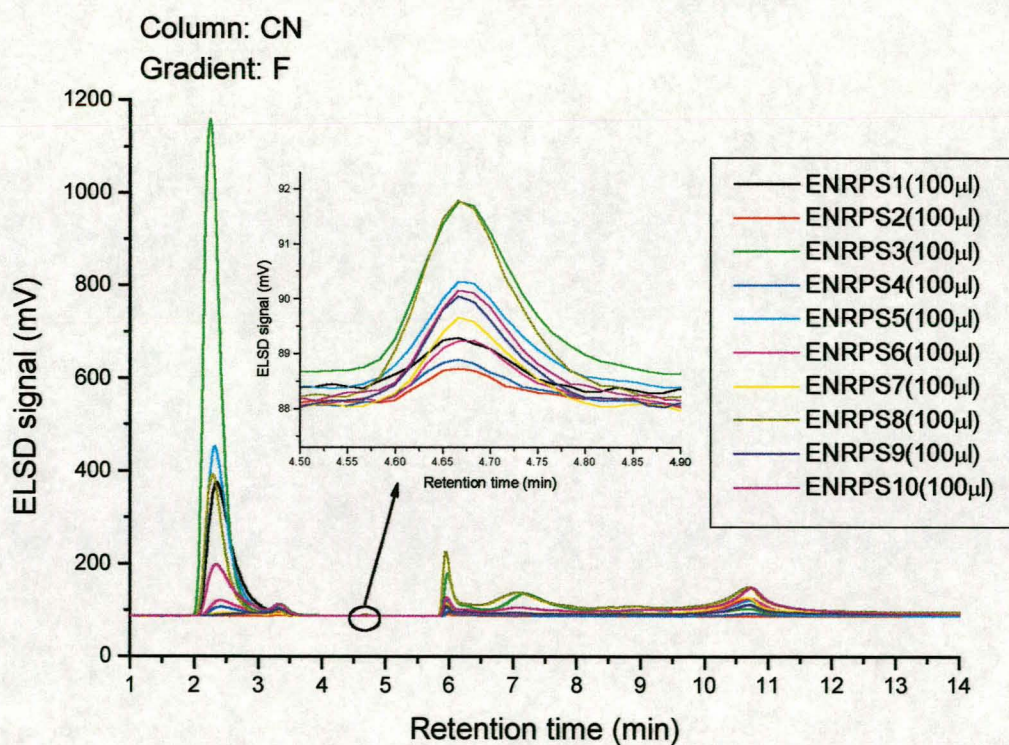Figure 7.33: Chromatograph of styrene-grafted ENR50 obtained with a UV detector and a CN column.

This does not interfere with this research endeavor to determine if grafting takes place by HPLC techniques.

The ELSD signals caused by the free PS dwarf the ELSD signals from the grafted samples and this made it very difficult to see the graft peaks. The retention times of the free PS peaks coincide with the retention time of the high molecular mass PS standards, thus pointing to and confirming the formation of long PS chains. The inlay graph of Figure 7.31 shows the grafted peaks. The intensity of the grafted peaks can be traced to the starting conditions of the graft reactions. Samples 3 and 8 show the biggest ELSD peaks. This is because the most monomer and least initiator were used, leading to the formation of long PS chains grafted onto the ENR50. Although this led to the formation of big molecules and therefore decreased solubility, the size of the molecules caused scattering of light and consequently a big ELSD signal. These peaks are closely followed by samples 5 and 10. In this case, the same amounts of monomer as in samples 3 and 8 were used, except that the initiator concentration was higher. This lead to the formation of shorter chains, therefore smaller particles and consequently smaller ELSD signals. Following these peaks are samples 9 and 7 and 1 and 6. This was a bit of a surprise as samples 1 and 6 used more monomer than 9 and 7 and should therefore have formed bigger molecules. The reason for this is that less initiator was used than for sample 9. Therefore, although samples 1 and 6 had higher molecular masses, a smaller molecule formed due to the intermediate amount of monomer and initiator used, leading to a lot of smaller branches. Sample 9 had the highest solubility (refer to FTIR analysis, Section 6.4.1.3) and therefore more molecules were in solution. This also contributed to more scattered light and hence a bigger signal. Sample 7 used less initiator but the same amount of monomer as sample 9. This resulted in longer grafts and therefore less solubility, hence a smaller signal than 9. Samples 2 and 4 showed the smallest signals. This was probably due to the fact that an older ENR50 latex was used for these graft reactions, leading to a still lower solubility. Despite this, the lowest amount of monomer (same as for samples 7 and 9) was used, leading to the formation of small particles. The fact that solubility played a role led to fewer small particles in solution, hence a small ELSD signal.

Figure 7.32 shows the UV signals of the PS standards and styrene monomer. No ENR50 peak is visible under UV detection. The UV signals can be used just as the ELSD signals were used to identify the free PS and grafted samples.

Figure 7.32 represents the UV signals of the grafted samples. The small ELSD peaks for the grafted samples are confirmed here due to the fact that bigger grafted UV peaks can be seen. This is therefore a sure confirmation of grafting.

The UV graphs show evidence of huge, free PS peaks. This is another indication that grafting took place on a very small scale. These big ungrafted peaks also dwarf the graft peaks, making it difficult, but much easier in comparison to ELSD, to evaluate them.

Sample 9 and 8 showed the biggest grafted peaks. This correlates with FTIR analyses of samples 8 and 9 which showed a higher amount of styrene content relative to the rubber content in the gel analysis. If assumed that the gel part also contained grafted sample, this correlates with the gradient analysis. For the FTIR analysis the samples were solubilized for 24 hours and then analyzed. For gradient work, the samples were kept in solution for a considerable time, thus allowing more solubility from the gel. Samples 8 and 10 also show larger graft peaks because of the large amount of monomer used. Here solubility is not as effective due to the longer grafted chains. After these samples, samples 7 and 6 follow. What is interesting is that the samples showing a higher styrene content were all prepared from the newer latex. A question that might arise is: why does sample 9 show a big UV peak, but a smaller ELSD peak than sample 3? The reason is solubility. Although the solubility of sample 3 is much lower, due to the presence of bigger particles, it only takes a few of these big particles to scatter a lot of light, hence creating a big ELSD peak. Therefore, although the peaks do not follow the same order in ELSD and UV, the two detectors do not measure the same quantity and would therefore differ.

The graft peaks that follow sample 6, are 1, 5, 3, 4 and 2. This is also understandable as grafting was done on the older latex, leading to inferior solubility.

In all the above cases it is not actually correct to try and accurately correlate the graft peaks with the starting conditions as not all the monomer is situated in the grafted products. Much of the styrene is situated in the free PS and most of the rest is situated in the microgels.

Analysis of the grafted material on the silica column did not reveal any grafted peaks at all. This might be due to the fact that the silica column is extremely water sensitive and that all the graft peaks elute at the same time as the ENR50. Gradient results are shown in Figures 7.34-7.37.
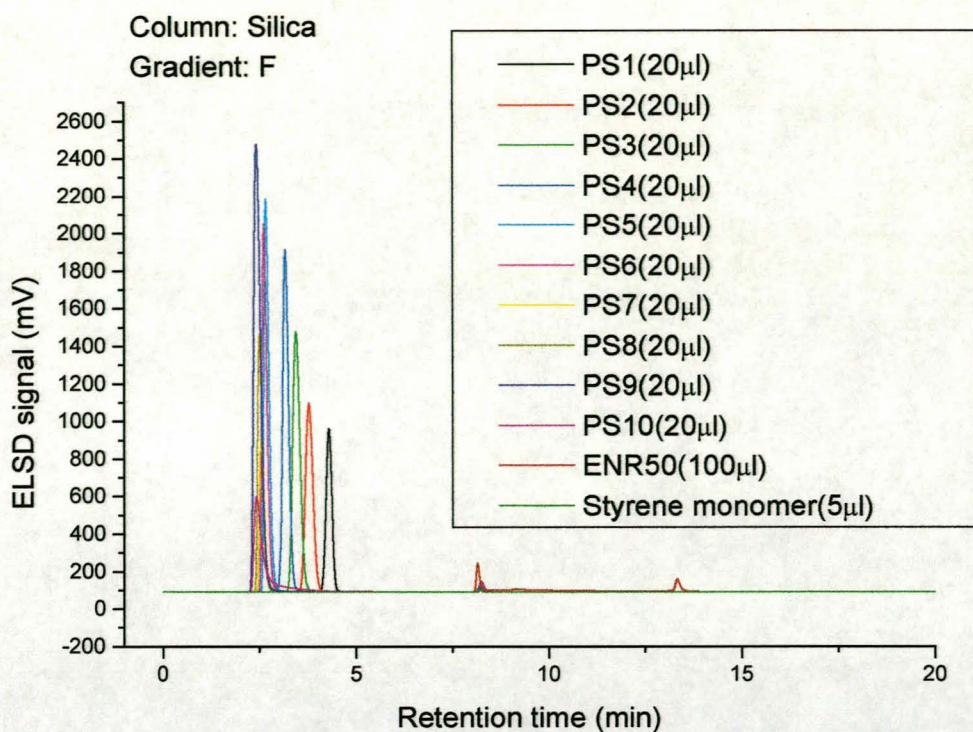
Figure 7.34: Gradient chromatograph of PS standards, ENR50 and styrene monomer obtained with an ELSD detector and a silica column.
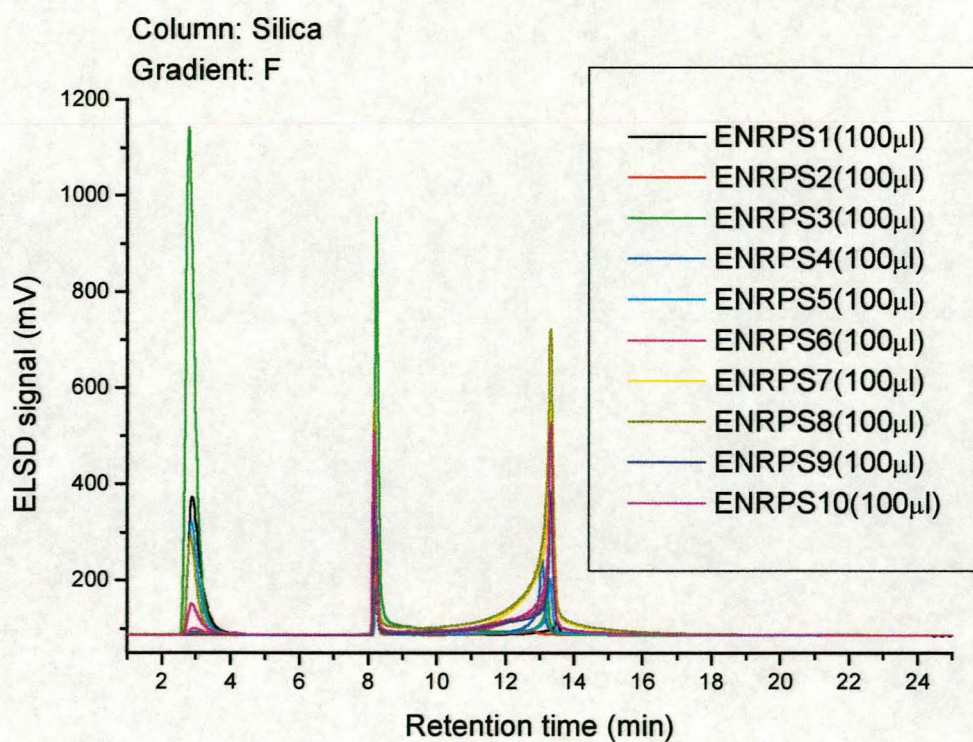
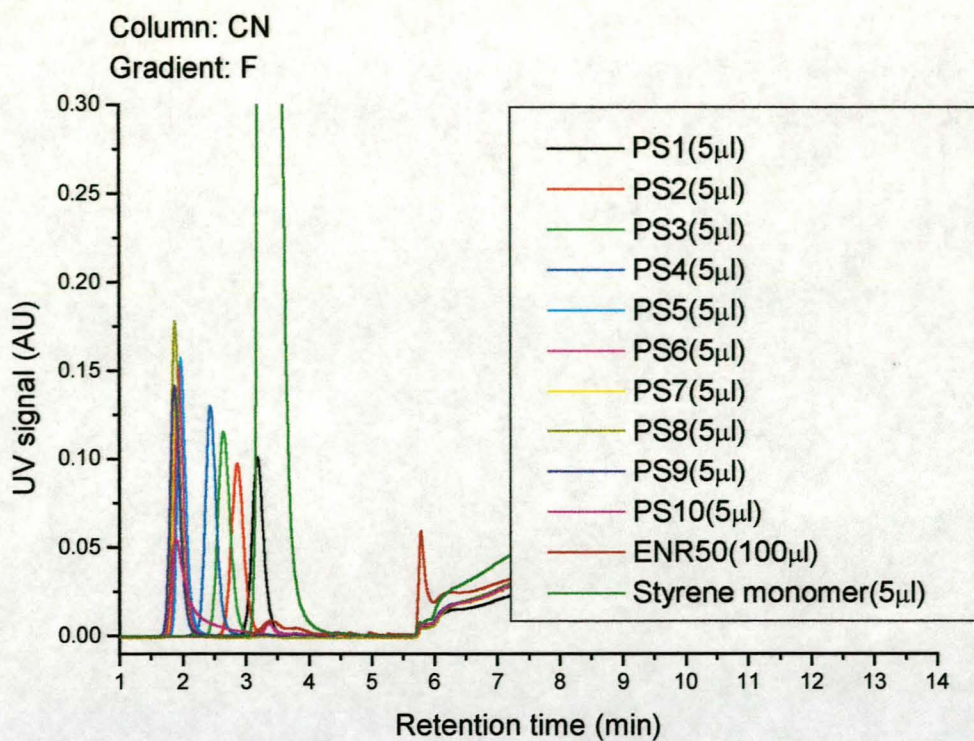Figure 7.35: Chromatograph of styrene-grafted ENR50 obtained with an ELSD detector and a silica column.
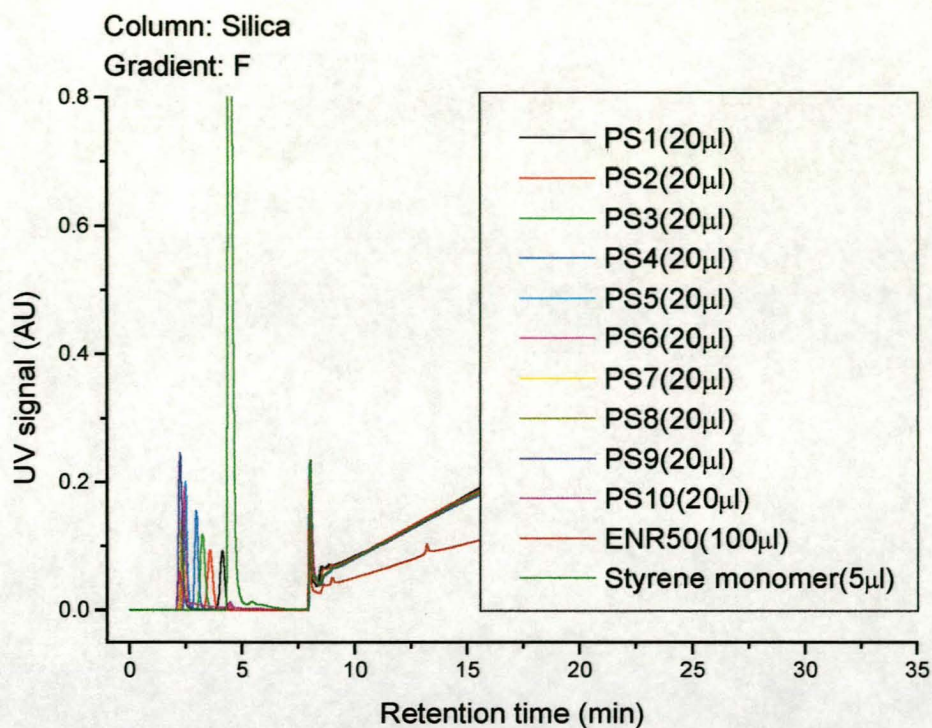
Figure7.36: Gradient chromatograph of PS standards, ENR50 and styrene monomer obtained with a UV detector and a silica column.
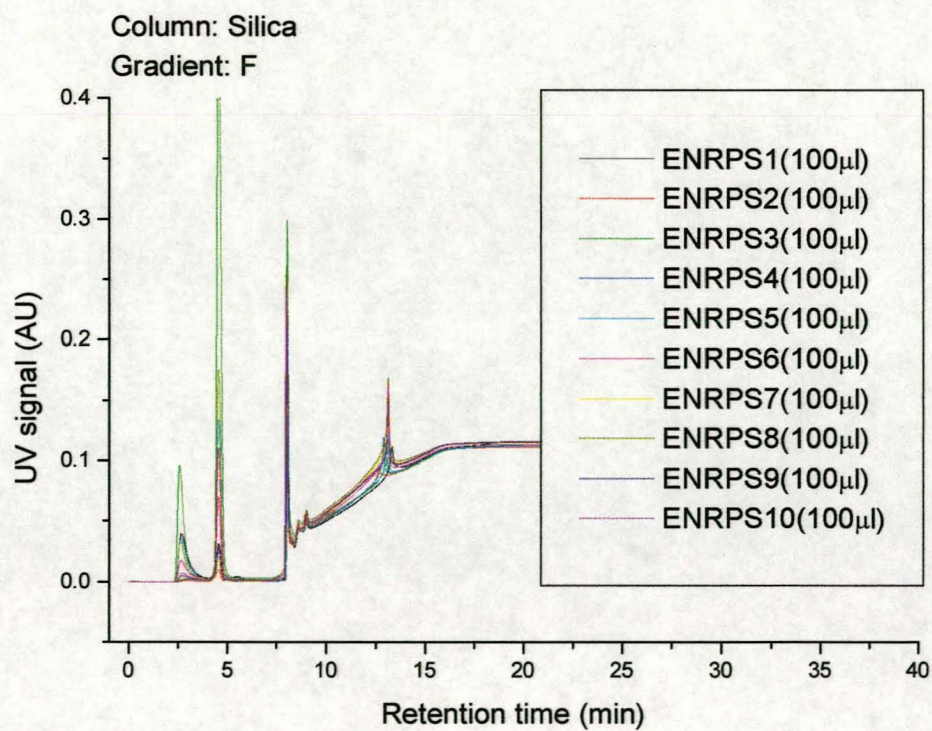
Figure 7.37: Chromatograph of styrene-grafted ENR50 obtained with a UV detector and a silica column.

Although the UV graphs showed signs of free PS, no grafted peaks could be seen. It looked as if the grafted peaks just eluted at 8 minutes, in other words they had the same retention time as the ENR50. The silica column was therefore not suitable for analysis of the grafted samples and therefore no further investigation was done with it.

7.5 Conclusions

Despite quite a few drawbacks during the gradient HPLC analyses of the grafted samples, the technique proved itself in the end. Although this is not an easy, straightforward technique and optimization is inevitable throughout sample evaluation, it is still an enormous necessity for any analytical laboratory. When used in conjunction with GPC and LC-transform, samples can be analyzed quite thoroughly. As was shown throughout this chapter, method development is very important. Although cloudpoint evaluation can point the analyst in the right direction and give certain indications of how samples are going to behave, the actual sample behavior in a certain gradient system and column still needs to be exploited further, until the optimum conditions are found. Only then will it be able to separate according to chemical composition distribution. This technique is also not only used as a qualitative analytical tool but, if solubility is not a factor, it can also be used as a quantitative tool. That is, by first injecting standards with known concentrations and measuring the signal intensities, the signal intensities of the ungrafted precursors can be measured and the amount of grafted precursors calculated.

Gradient HPLC is therefore a very valuable technique with a vast amount of analytical options and applications.

7.6 References

1   W.J. Staal, P. Cools, A.M. van Herk, A.L. German; *Monitoring of Originated Polymer in Pure Monomer with Gradient Polymer Elution Chromatography (GPEC)*®; Journal of Liquid Chromatography; 17(14&15), 1994, 3191-3199

2   S. Mori; *Determination of Chemical Composition and Molecular Weight Distribution of High-Conversion Styrene-Methyl Methacrylate Copolymers by Liquid Adsorption and Size Exclusion Chromatography*; Analytical Chemistry; **60**, 1999, 1125-1128

3   P.J.C.H. Cools, F. Maesen, B. Klumperman, A.M. van Herk, A.L. German; *Determination of the Chemical Composition Distribution of Copolymers of Styrene and Butadiene by Gradient Polymer Elution Chromatography*; Journal of Chromatography A; **736**, 1996, 125-130

4   T.C. Schunk; *Composition Distribution Separation of Methyl Methacrylate-Methacrylic Acid Copolymers by Normal –Phase Gradient Elution High-Performance Liquid Chromatography*; Journal of Chromatography A; **661**, 1994, 215-226

5   P.J.C.H. Cools, A.M. van Herk, A.L. German, W. Staal; *Critical Retention behavior of Homopolymers*; Journal of Liquid Chromatography; 17(14&15), 1994, 3133-3143

6   H.J.A. Philipsen, B. Klumperman, A.L German; *Characterization of Low-Molar-Mass Polymers by Gradient Polymer Elution Chromatography I. Practical Parameters and Applications of the Analysis of Polyester Resins under Reversed Phase Conditions*; Journal of Chromatography A; **746**, 1996, 211-224

7   G. Glöckner; Control of Adsorption and Solubility in Gradient High Performance Liquid Chromatography I. Principles of Sudden Transition Gradients and Elution Characteristics of Copolymers from Styrene and Methacrylates; Chromatographia; **37**(1/2), July 1993, 7-12

8   B. Klumperman, P. Cools, H. Philipsen, W. Staal; A Qualitative Study to the Influence of Molar Mass on Retention in Gradient Polymer Elution Chromatography (GPEC); Macromolecular Symposia; **110**, 1996, 1-13

9   H. Pasch, B. Trathnigg; HPLC of Polymers; Springer-Verlag, Berlin Heidelberg; 1998

10   G. Glöckner; Gradient HPLC of Copolymers and Chromatographic Cross-Fractionation; Springer-Verlag, Berlin Heidelberg; 1991

11   P. Jandera; Optimization of Gradient Elution in Normal-Phase High-Performance Liquid Chromatography; Journal of Chromatography A; **797**, 1998, 11-22

Chapter **8**

Summary and Conclusions

8.1 Summary

Although the synthesis and analysis of styrene-grafted ENR50 by means of gradient HPLC techniques were the main objectives of this research, gradient HPLC analysis was not the only analytical technique that was to be performed on the grafted samples. From the first synthesis reaction it was evident that other evaluations had to be performed to ease gradient analysis. Without the additional information gathered from these evaluations, certain concepts such as the variation between the peak intensities of the grafted samples would not have been understood and explanations of the gradient HPLC results would have been inadequate. It was therefore of utmost importance to structure experiments in order to create a solid base to work from. This base included both the use of very important analytical tools, namely, GPC, FTIR and LC-transform, and the solubility determinations of the chemical precursors as well as the grafted material. The latter played a very significant role throughout the thesis.

Although the whole idea of gradient HPLC analysis seems very simple, a theoretical knowledge is very important. A thorough study was therefore made of the theory of HPLC, which included not only a comparison to isocratic HPLC, but also a comparison between reversed-phase (RP) and normal phase (NP) gradient HPLC. This facilitated a much better understanding of the gradient process, enabling the process to be optimized. The theory was also used to perform cloudpoint evaluations chromatographically through the calculation of retention times.

Upon synthesizing the grafted samples it was found that the reaction conditions and surfactants had to be carefully selected to obtain a stable latex system.

Although certain reaction products were stable, others were not, due to the different monomer and initiator concentrations used. After evaluating different ways of polymerization, it was found that feeding the monomer and initiator into the ENR50-filled reactor was the best way to perform this task. By doing it this way, the rubber was kept under constant stirring which prevented it from coagulation. Certain surfactants were also evaluated during the reactions and sodium lauryl sulfate (SLS) was found to be most suitable over the entire monomer/initiator concentration range.

Solubilizing the ENR50 proved to be troublesome from the start. This prompted the urgency to calculate solubility parameter values for the ENR50. Solvents are also very important for gradient HPLC and it is always necessary to choose solvents for polymers, hence the theory of solubility parameters was also studied and the necessary parameters calculated. Although complete solubility of the samples could not be achieved due to crosslinking, the most suitable solvents could now be found by applying solvent parameter principles. Not only was it possible to find solvents, but also non-solvents, which were used for cloudpoint evaluations.

Cloudpoint evaluations were performed on the ENR50, PS and PiP to determine their regions of solubility and insolubility. This was done by both chromatographic and titrimetric methods. By doing this it was possible to predict where the sample would precipitate; hence it created the opportunity to choose solvents which allowed the best separation in gradient HPLC analysis. Cloudpoints were not only evaluated to ease the development of the gradient method, but were also done to obtain a better understanding of the gradient theory. By comparing chromatographic and titrimetric results it was possible to see the influence of molecular mass on retention time as a sample moved through the column. Without these evaluations it would not have been possible to explain certain gradient phenomena. This confirmed the importance of cloudpoint evaluations.

Other solubility experiments included the study of the solubility of ENR50 after being exposed to certain chemical and physical treatments. From these experiments it was found that milling the sample led to the best solubility of the ENR50. Unfortunately, milling of the grafted samples, even for 15 minutes, was not successful due to the poor green strength of the samples on the mill.

Because of the problem of solubility and also some other problems, involving reproducibility and a slight change in the structure of the ENR50, the execution of certain preliminary experimental analyses, which included GPC, FTIR and LC-transform, were necessary. From GPC results molecular masses and molecular mass distributions of the grafted samples were obtained and these results were used to correlate with starting monomer/initiator concentrations. Through the dual detector method it was also possible to evaluate the styrene content as a function of the molecular mass distribution. Furthermore, reproducibility (ENR50 latex vs. precipitated ENR50) and structural changes of the ENR50 (due to the reaction conditions) were assessed and confirmed.

FTIR analyses of the samples were done on the completely dried sample, soluble part of the sample as well as the gel part of the sample. By comparing the styrene peak ($698 cm^{-1}$) with the styrene and rubber peak ($1452 cm^{-1}$) in the FTIR spectra, the styrene ratio was determined. For the dried sample, this ratio was used to correlate with the starting monomer/initiator concentrations. Analyses of the soluble and gel parts were used to confirm, or explain, certain trends in gradient analysis.

LC-transform is a relatively new technique that is used to check the incorporation of a certain precursor as a function of the molecular mass distribution. By analyzing the Gram-Schmidt distribution, which is the total FTIR absorption as a function of time, the FTIR spectra of the samples were followed as a function of the molecular mass distribution. Similar to what was done with FTIR analyses, the styrene ratio was calculated and presented as a function of the MMD. This created the opportunity to compare the results with those of GPC analyses and they correlated very well.

Although all the preliminary experiments seemed to be unnecessary initially, they proved to be very valuable and much needed supplement to gradient HPLC. As was mentioned before, cloudpoints were performed chromatographically on PS and PiP. PiP was chosen as it was the standard with the closest resemblance to the chemical structure of ENR50. Unfortunately, the ENR50 did not perform similarly to the PiP standards and further method development of gradient HPLC was needed. During this task, different columns, gradients and gradient steepnesses were evaluated. After starting with RP chromatography, it was later found to be insufficient for separation.

NP chromatography provided the necessary separation and this was mainly due to the big polarity difference between the styrene and ENR50 (polarity provided by the epoxide group). After analysis of the grafted samples, it was found that limited grafting had taken place during the graft reactions.

Although gradient HPLC analysis confirmed that limited grafting had taken place, the main goal of the research work was still achieved. Through method development and gradient and column optimization, it was possible to obtain the chemical composition distribution of the grafted samples. This made it possible to say that grafting did take place although not at very satisfactory levels. Nonetheless, the knowledge obtained through method development and optimization, made the use of this technique an enormous success. Not only did it provide meaningful results, it also provided very much needed HPLC knowledge on the separation of copolymers under gradient conditions. A flow diagram of all the results achieved and possible future work can be seen in Figure 8.1.

For future work, two techniques (chain scissioning and ozonolysis) will be mentioned which could be used to obtain better results.

By exposing the grafted rubber to ozonolysis i.e. subjecting it to ozone or osmium tetroxide, the grafted chains can be isolated by breaking the polymer backbone. This would lead to increased solubility of the grafted samples and better results. The second technique is chain scission parallel with epoxidation or just before epoxidation, possibly even after. In this instance the ENR50 can first be treated with initiator before epoxidation or conversely the grafted rubber can have $NaNO_2$ added to it and chain scission allowed to take place. This will also produce better soluble polymers; hence better results.
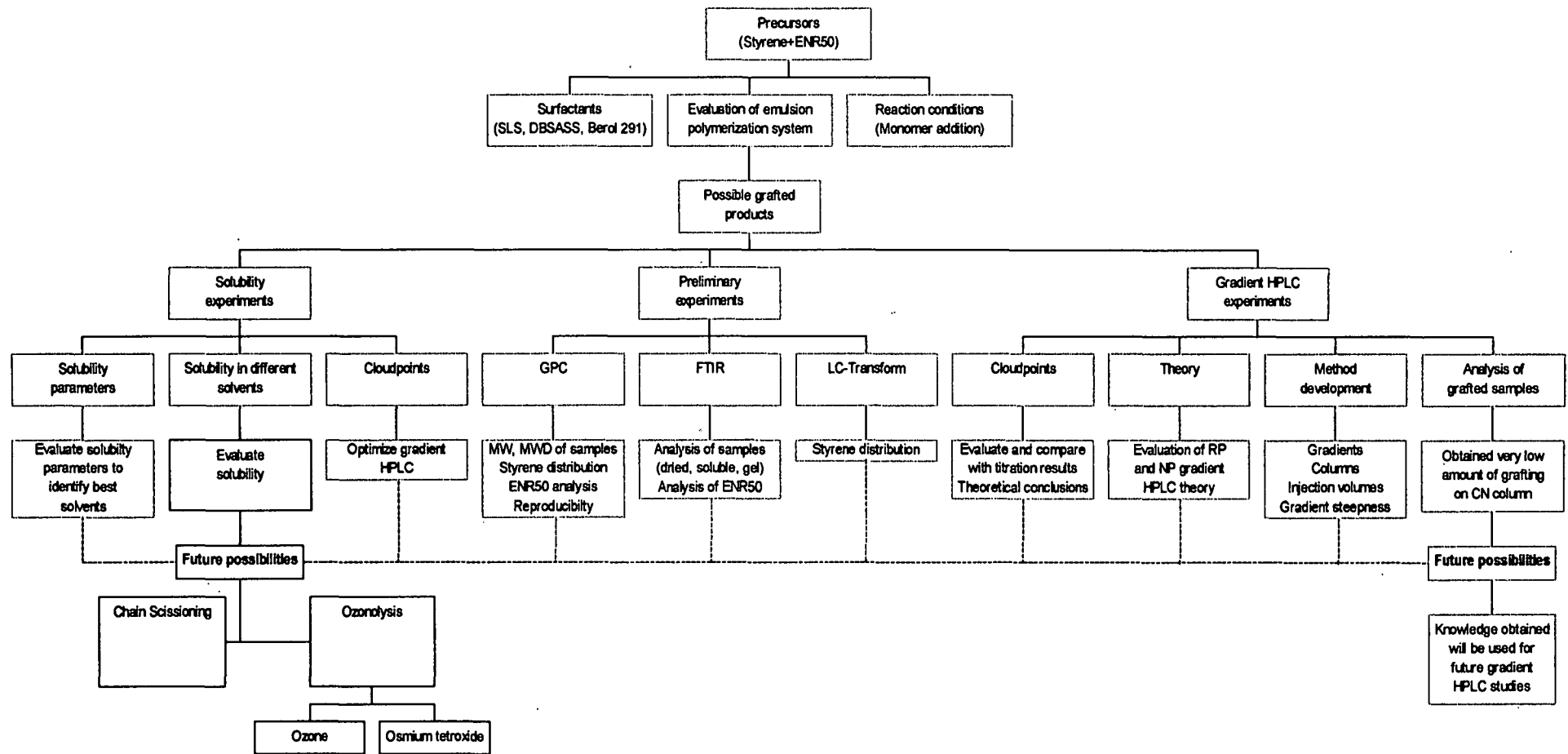
Figure 8.1: Flow diagram of achievements of this research and ideas for future research.

8.2 Conclusions

The conclusions of this research endeavor are as follows:

1. A stable latex system was possible by keeping the ENR50 under constant stirring, thereby preventing coagulation. SLS proved to be the best surfactant for the particular latex system.

2. By performing solubility parameter calculations, suitable solvents (THF and DCM) and suitable non-solvents (MeOH, EtOH etc.) were found for the styrene, ENR50 and styrene-grafted ENR50.

3. Solubility of the ENR50 increased dramatically when subjected to milling on a twin-mill roll. Unfortunately the grafted samples could not be milled.

4. Cloudpoints were evaluated to provide necessary answers for theoretical purposes and to develop the gradient HPLC method. Cloudpoints were obtained titrimetrically and chromatographically. By doing this, the molecular mass dependence of the retention time was studied.

5. The theory of gradient (NP and RP) and isocratic HPLC was studied and the knowledge obtained was used to adapt and to optimize the gradient HPLC method.

6. Preliminary analyses of the styrene-grafted ENR50 included GPC, FTIR and LC-transform. These analyses provided answers to the molecular masses, molecular mass distributions and the incorporation of a certain precursor as a function of the molecular mass of the styrene-grafted ENR50 samples. Not only did these analyses provide answers to the structural changes of the ENR50 due to the reaction conditions, but gradient HPLC results could also be better explained in the light of the preliminary experimental results.

7. Development of the gradient HPLC method was done by using different columns, gradients and gradient steepnesses. Although analysis was started on a RP gradient system, NP chromatography proved to be better in providing the necessary separation between the precursors and grafted material.

8. Optimization of the gradient method was done by changing the injection volumes of the grafted material and gradient steepness of the applied gradient (as obtained by the method development above).

The study was concluded when grafting was confirmed by gradient HPLC.

To conclude this chapter, the author would like to stress the importance of gradient HPLC analysis. The enormous number of copolymers created and the more than often careless and uninformative way in which they are analyzed, have created an analytical gap. Through gradient HPLC this gap no longer needs to exist, due to the competent way in which chemical composition distributions can now be analyzed. Very important information is therefore obtainable which helps the polymer scientist to enhance physical and chemical properties of products. It is therefore needless to say that this technique is a very important tool and a must for every analytical polymer laboratory.

Appendices

Date solubilized: 13/07/1998

	Polystyrene (PS)				cis-Polyisoprene (PiP)		
	M_p	M_w/M_n	Mass weighed (mg)		M_p	M_w/M_n	Mass weighed (mg)
PS1	500	1.14	2.05	PiP1	1350	1.07	2.07
PS2	2450	1.05	1.99	PiP2	3190	1.06	2.03
PS3	5050	1.05	2.02	PiP3	8000	1.03	1.95
PS4	9200	1.03	1.96	PiP4	27000	1.02	1.97
PS5	66000	1.03	1.97	PiP5	62800	1.02	2.08
PS6	156000	1.03	2.01	PiP6	115000	1.02	2.04
PS7	570000	1.05	1.98	PiP7	295000	1.04	2.03
PS8	1075000	1.05	2.07	PiP8	550000	1.03	2.04
PS9	7100000	1.11	2.08	PiP9	1200000	1.03	1.91
PS10	20000000	1.30	2.07	PiP10	3300000	1.04	2.05

Appendix 1: PS and PiP standards solubilized in THF.

All standards, except PS1, were obtained from Polymer Laboratories. PS1 was obtained from TSK Standards (Tosoh Corporation). The THF used was HPLC grade and was obtained from Biosolve Ltd.

Polystyrene
Non-solvent: H_2O
Solvent: THF

Molar Mass	Mass weighed (mg)	NS in ml	% NS	% S	log MM
500	9.93	2.132	51.60	48.40	2.70
2450	9.98	0.995	33.22	66.78	3.39
5050	10.04	0.696	25.82	74.18	3.70
9200	10.07	0.535	21.10	78.90	3.96
66000	9.98	0.329	14.13	85.87	4.82
156000	9.92	0.292	12.74	87.26	5.19
570000	9.98	0.246	10.95	89.05	5.76
1075000	9.95	0.259	11.47	88.53	6.03
7100000	9.97	0.243	10.83	89.17	6.85
20000000	10.09	0.235	10.51	89.49	7.30

Appendix 2: Titrametric cloudpoint measurements of PS standards in a THF/H_2O S/NS system.

Polystyrene
Non-solvent: ACN
Solvent: THF

Molar Mass	Mass weighed (mg)	NS in ml	% NS	% S	log MM
500	9.93	0	0.00	100.00	2.70
2450	9.98	0	0.00	100.00	3.39
5050	10.04	0	0.00	100.00	3.70
9200	10.07	9.178	82.11	17.89	3.96
66000	9.98	3.182	61.40	38.60	4.82
156000	9.92	2.72	57.63	42.37	5.19
570000	9.98	2.392	54.46	45.54	5.76
1075000	9.95	2.291	53.39	46.61	6.03
7100000	9.97	2.061	50.75	49.25	6.85
20000000	10.09	2.268	53.14	46.86	7.30

Appendix 3: Titrametric cloudpoint measurements of PS standards in a THF/ACN S/NS system.

Polystyrene
Non-solvent: H_2O/ACN
Solvent: THF

Molar Mass	Mass weighed (mg)	NS in ml	% NS	% S	log MM
2450	9.98	1.768	46.92	53.08	3.39
5050	10.04	1.187	37.25	62.75	3.70
9200	10.07	0.902	31.08	68.92	3.96
66000	9.98	0.559	21.84	78.16	4.82
156000	9.92	0.499	19.97	80.03	5.19
570000	9.98	0.46	18.70	81.30	5.76
1075000	9.95	0.442	18.10	81.90	6.03
7100000	9.97	0.434	17.83	82.17	6.85
20000000	10.09	0.435	17.86	82.14	7.30

Appendix 4: Titrametric cloudpoint measurements of PS standards in a THF/(H_2O/ACN) S/NS system.

Polystyrene
Non-solvent: Heptane
Solvent: THF

Molar Mass	Mass weighed (mg)	NS in ml	% NS	% S	log MM
500	9.93	0	0.00	100.00	2.70
2450	9.98	0	0.00	100.00	3.39
5050	10.04	0	0.00	100.00	3.70
9200	10.07	0	0.00	100.00	3.96
66000	9.98	4.988	71.38	28.62	4.82
156000	9.92	4.019	66.77	33.23	5.19
570000	9.98	3.403	62.98	37.02	5.76
1075000	9.95	3.228	61.74	38.26	6.03
7100000	9.97	3.045	60.36	39.64	6.85
20000000	10.09	3.047	60.37	39.63	7.30

Appendix 5: Titrametric cloudpoint measurements of PS standards in a THF/heptane S/NS system.

Polyisprene (cis) (PiP)
Non-solvent: H_2O
Solvent: THF

Molar Mass	Mass weighed (mg)	NS in ml	% NS	% S	log MM
1350	10.01	0.950	32.20	67.80	3.13
3190	10.01	0.541	21.29	78.71	3.50
8000	9.91	0.297	12.93	87.07	3.90
27000	10.11	0.208	9.42	90.58	4.43
62800	9.91	0.173	7.96	92.04	4.80
115000	10.01	0.163	7.54	92.46	5.06
295000	10.00	0.140	6.54	93.46	5.47
550000	10.06	0.168	7.75	92.25	5.74
1200000	9.99	0.137	6.41	93.59	6.08
3300000	9.99	0.140	6.54	93.46	6.52

Appendix 6: Titrametric cloudpoint measurements of PiP standards in a THF/H_2O S/NS system.

Polyisprene (cis) (PiP)
Non-solvent: ACN
Solvent: THF

Molar Mass	Mass weighed (mg)	NS in ml	% NS	% S	log MM
1350	10.01	0.000	0.00	100.00	3.13
3190	10.01	3.249	61.90	38.10	3.50
8000	9.91	1.602	44.48	55.52	3.90
27000	10.11	1.070	34.85	65.15	4.43
62800	9.91	0.900	31.03	68.97	4.80
115000	10.01	0.839	29.55	70.45	5.06
295000	10.00	0.770	27.80	72.20	5.47
550000	10.06	0.845	29.70	70.30	5.74
1200000	9.99	0.738	26.95	73.05	6.08
3300000	9.99	0.731	26.77	73.23	6.52

Appendix 7: Titrametric cloudpoint measurements of PiP standards in a THF/ACN S/NS system.

Polyisprene (cis) (PiP)
Non-solvent: H_2O/ACN
Solvent: THF

Molar Mass	Mass weighed (mg)	NS in ml	% NS	% S	log MM
1350	10.01	1.418	41.49	58.51	3.13
3190	10.01	0.790	28.32	71.68	3.50
8000	9.91	0.478	19.29	80.71	3.90
27000	10.11	0.340	14.53	85.47	4.43
62800	9.91	0.289	12.63	87.37	4.80
115000	10.01	0.260	11.50	88.50	5.06
295000	10.00	0.248	11.03	88.97	5.47
550000	10.06	0.284	12.43	87.57	5.74
1200000	9.99	0.241	10.75	89.25	6.08
3300000	9.99	0.240	10.71	89.29	6.52

Appendix 8: Titrametric cloudpoint measurements of PiP standards in a THF/(H_2O/ACN) S/NS system.

PS
Gradient : 50/50 H_2O/ACN ———▶ 100 % ACN ———▶100 % THF

RT (min)	t_0 (min)	MM	RT - t_0 (min)	$\Delta\phi_s$ (%)	%S	log MM
19.987	16.89	500	3.097	4	12.388	2.69897
26.277	16.89	2450	9.387	4	37.548	3.389166
27.551	16.89	5050	10.661	4	42.644	3.703291
28.23	16.89	9200	11.34	4	45.36	3.963788
28.825	16.89	66000	11.935	4	47.74	4.819544
28.741	16.89	156000	11.851	4	47.404	5.193125
28.676	16.89	570000	11.786	4	47.144	5.755875
28.673	16.89	1075000	11.783	4	47.132	6.031408
28.81	16.89	7100000	11.92	4	47.68	6.851258
28.824	16.89	20000000	11.934	4	47.736	7.30103

Appendix 9: Chromatographic cloudpoint measurements of PS standards in gradient A.

PS
Gradient : 50/50 H$_2$O/ACN ———▶ 100 % THF

RT (min)	t$_0$ (min)	MM	RT - t$_0$ (min)	Δφ$_s$ (%)	%S	log MM
19.509	4.39	500	15.119	4	60.476	2.69897
23.356	4.39	2450	18.966	4	75.864	3.389166
23.996	4.39	5050	19.606	4	78.424	3.703291
24.329	4.39	9200	19.939	4	79.756	3.963788
24.441	4.39	66000	20.051	4	80.204	4.819544
24.381	4.39	156000	19.991	4	79.964	5.193125
24.551	4.39	570000	20.161	4	80.644	5.755875
24.664	4.39	1075000	20.274	4	81.096	6.031408
24.881	4.39	7100000	20.491	4	81.964	6.851258
24.827	4.39	20000000	20.437	4	81.748	7.30103

Appendix 10: Chromatographic cloudpoint measurements of PS standards in gradient B.

PiP
Gradient : 100 % ACN ———▶ 100 % THF

| RT (min)	t$_0$ (min)	MM	RT - t$_0$ (min)	Δφ$_s$ (%)	%S	log MM
30.334	16.89	1350	13.444	4	53.776	3.130334
33.114	16.89	3190	16.224	4	64.896	3.503791
34.402	16.89	8000	17.512	4	70.048	3.90309
34.681	16.89	27000	17.791	4	71.164	4.431364
34.826	16.89	62800	17.936	4	71.744	4.79796
34.825	16.89	115000	17.935	4	71.74	5.060698
34.844	16.89	295000	17.954	4	71.816	5.469822
35.15	16.89	1200000	18.26	4	73.04	6.079181
34.704	16.89	3300000	17.814	4	71.256	6.518514

Appendix 11: Chromatographic cloudpoint measurements of PiP standards in gradient A.

PiP

Gradient : 50/50 ACN/H$_2$O ⟶ 100 % THF

RT (min)	t$_0$ (min)	MM	RT - t$_0$ (min)	$\Delta\phi_s$ (%)	%S	log MM
25.186	4.39	1350	20.796	4	83.184	3.130334
26.165	4.39	3190	21.775	4	87.1	3.503791
26.601	4.39	8000	22.211	4	88.844	3.90309
26.564	4.39	·27000	22.174	4	88.696	4.431364
26.591	4.39	62800	22.201	· 4	88.804	4.79796
26.625	4.39	115000	22.235	4	88.94	5.060698
26.863	4.39	295000	22.473	4	89.892	5.469822
26.961	4.39	1200000	22.571	4	90.284	6.079181
26.958	4.39	3300000	22.568	4	90.272	6.518514

Appendix 12: Chromatographic cloudpoint measurements of PiP standards in gradient B.
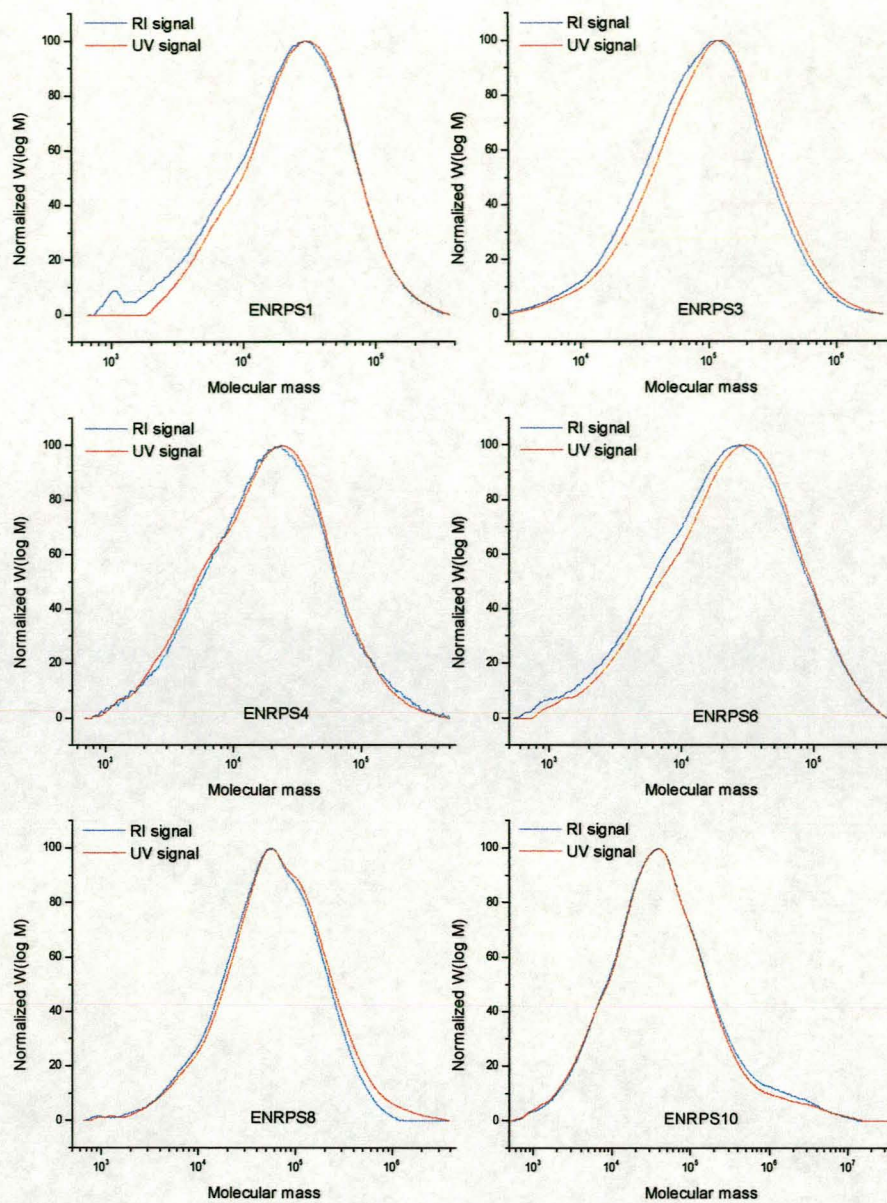
Appendix 13: Analysis of the styrene content as a function of the molecular mass distribution of the grafted sample.

Date solubilized: 02/09/1998

All standards dissolved in 10 ml DCM.

Polymer (Standards)	Supplier	M_p	M_w/M_n	Mass weighed (mg)	Concentration (mg/ml)
PS1	TSK	500	1.14	10.00	1.000
PS2	PL	2450	1.05	9.97	0.997
PS3	PL	5050	1.05	10.00	1.000
PS4	PL	9200	1.03	10.11	1.011
PS5	PL	66000	1.03	9.96	0.996
PS6	PL	156000	1.03	10.03	1.003
PS7	PL	570000	1.05	10.00	1.000
PS8	PL	1075000	1.05	10.01	1.001
PS9	PL	7000000	1.11	10.36	1.036
PS10	PL	20000000	1.3	9.97	0.997
PiP1	PL	1350	1.07	9.94	0.994
PiP2	PL	3190	1.06	10.14	1.014
PiP3	PL	8000	1.03	9.92	0.992
PiP4	PL	27000	1.02	10.31	1.031
PiP5	PL	62800	1.02	9.87	0.987
PiP6	PL	115000	1.02	9.81	0.981
PiP7	PL	295000	1.04	10.26	1.026
PiP8	PL	1200000	1.03	10.39	1.039
PiP9	PL	3300000	1.04	7.14	0.714

Appendix 14: Concentrations for PS and PiP standards solubilized in DCM.

All standards were dissolved in dichloromethane (DCM) (HPLC grade obtained from Biosolve Ltd.). Standards were obtained from Polymer Laboratories (PL) and TSK Standards (TSK). Solutions were filtered before use through a 589 Black Ribbon (ashless) paper filter (Ref. no. 300 008).

Date solubilized: 02/09/1998

Sample	Solvent	Mass weighed (mg)	Concentration (mg/ml)
ENR50	DCM	9.97	0.997
ENRPS1	DCM	9.88	0.988
ENRPS2	DCM	10.07	1.007
ENRPS3	DCM	10.28	1.028
ENRPS4	DCM	10.27	1.027
ENRPS5	DCM	9.92	0.992
ENRPS6	DCM	10.08	1.008
ENRPS7	DCM	10.24	1.024
ENRPS8	DCM	10.37	1.037
ENRPS9	DCM	9.93	0.993
ENRPS10	DCM	9.99	0.999

Appendix 15: Concentrations for grafted samples and ENR50 solubilized in DCM.

Date solubilized: 02/09/98

Sample	Solvent	Mass weighed (mg)	Volume solvent used (ml)	Concentration (mg/ml)
ENRPS1	DCM	10.01	10	1.001
ENRPS2	DCM	9.99	10	0.999
ENRPS3	DCM	9.94	10	0.994
ENRPS4	DCM	9.80	10	0.980
ENRPS5	DCM	10.05	10	1.005
ENRPS6	DCM	10.01	10	1.001
ENRPS7	DCM	19.85	20	0.993
ENRPS8	DCM	20.21	20	1.011
ENRPS9	DCM	20.76	20	1.038
ENRPS10	DCM	20.09	20	1.005

Appendix 16: Concentrations for grafted samples solubilized in DCM.

Date solubilized: 05/08/98

Speed of mill set at 20 rev/min; nip set at 2 mm.

Sample	Remarks	Solvent used	Volume solvent (ml)	Mass weighed (mg)	Concentration (mg/ml)
ENR50	unmilled	THF	10	9.98	0.998
ENR50	2 min milled	THF	10	9.93	0.993
ENR50	4 min milled	THF	10	10.07	1.007
ENR50	6 min milled	THF	10	9.92	0.992
ENR50	8 min milled	THF	10	10.07	1.007
ENR50	10 min milled	THF	10	9.75	0.975
ENR50	12 min milled	THF	10	9.78	0.978
ENR50	14 min milled	THF	10	10.04	1.004
ENR50	16 min milled	THF	10	10.02	1.002

Appendix 17: Sample concentrations for milled and unmilled ENR50.
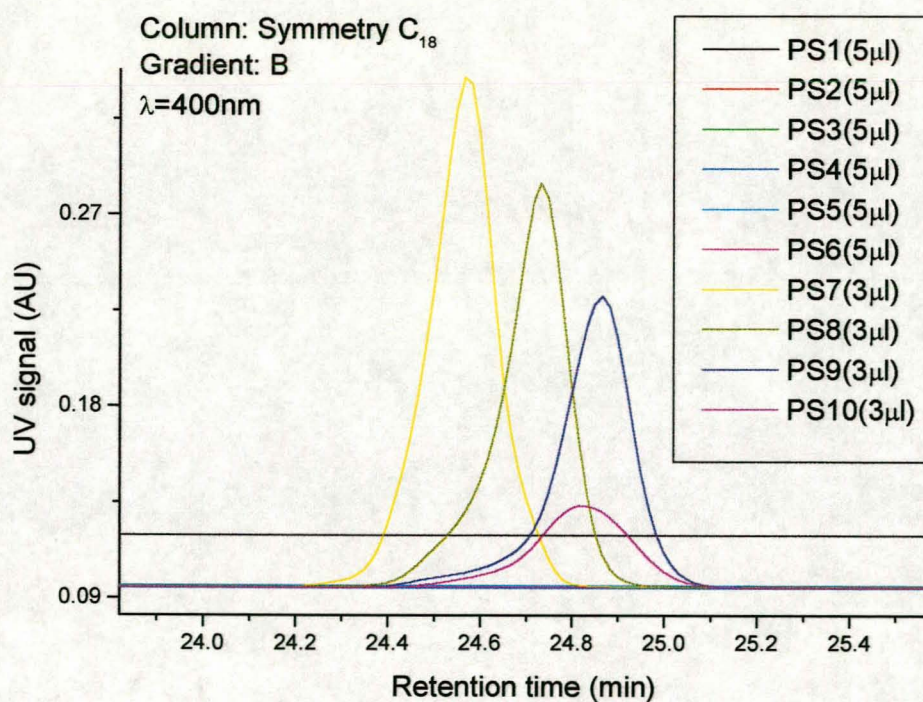
Appendix 18: Confirmation of reprecipitation for high MM PS standards through UV analysis at 400 nm.
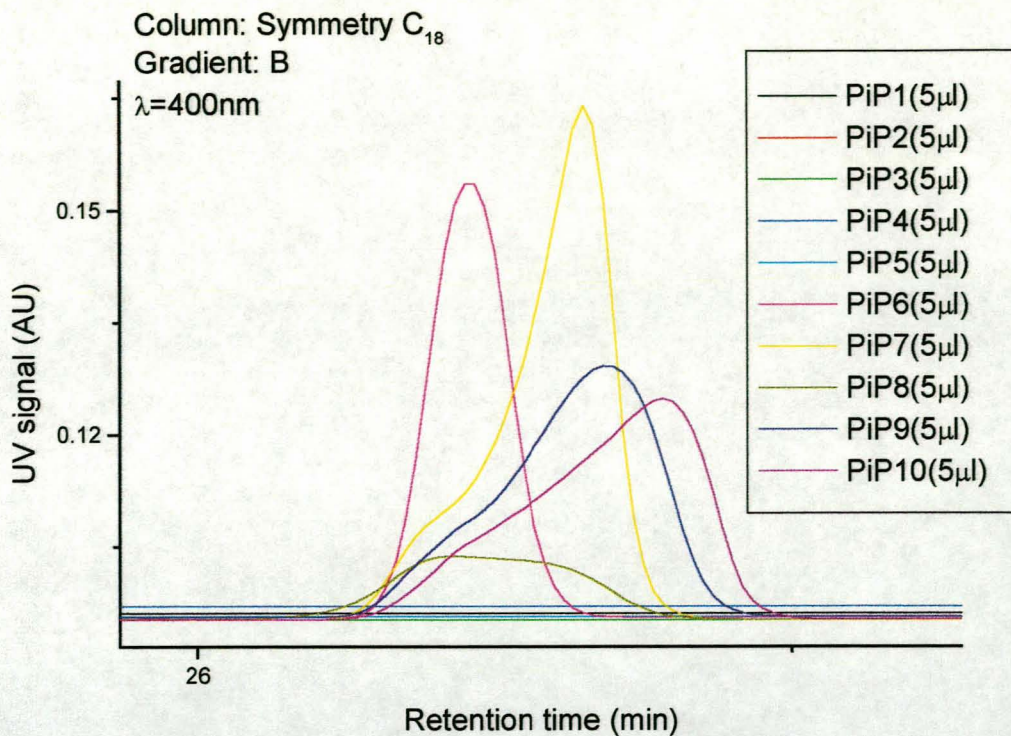
Appendix 19: Confirmation of reprecipitation for high MM PiP standards through UV analysis at 400 nm.
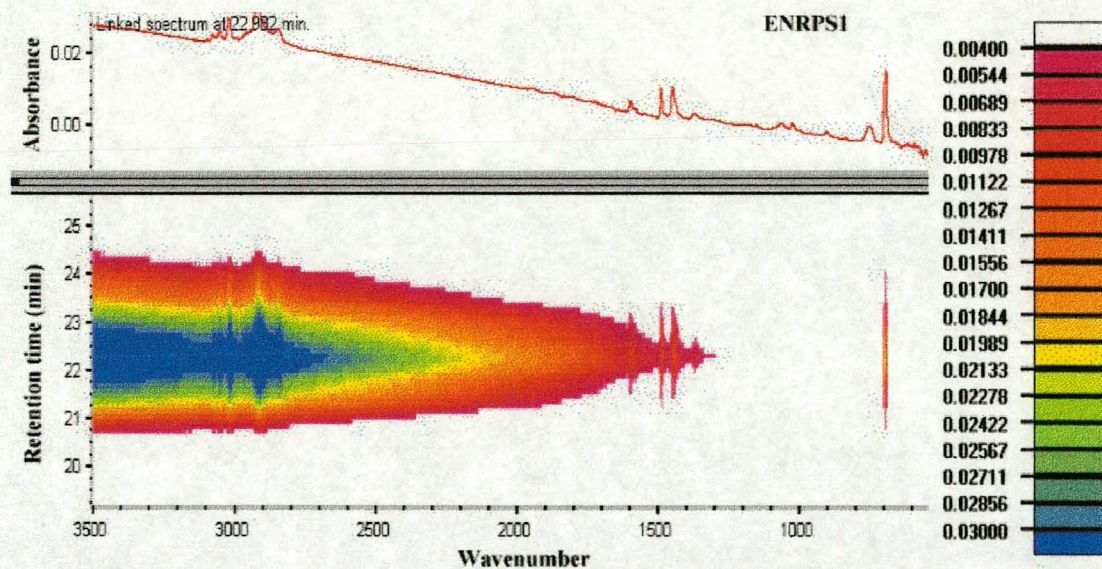
Appendix 20: Contour plot of ENRPS1. The scale on the right-hand side represents the intensity of the FTIR absorption. The FTIR spectrum at the top (taken at 22.982 min) was enclosed to show the baseline rise which unfortunately could not be corrected with the FTIR software. Due to this baseline rise, the contour plot also shows an increase in baseline as can be seen by the increase in area from 1500 to 3500 cm^{-1}. Note the MMD of the styrene peak at 698 cm^{-1}.
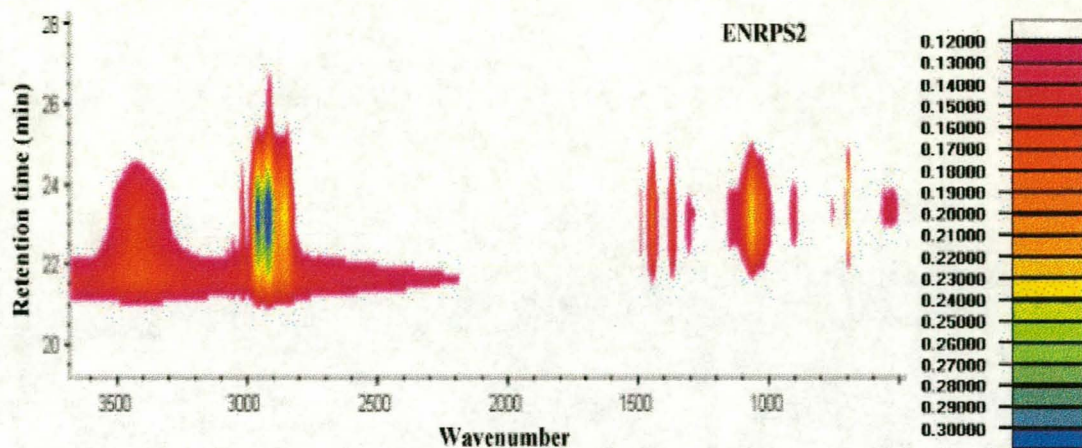
Appendix 21: Contour plot of ENRPS2.
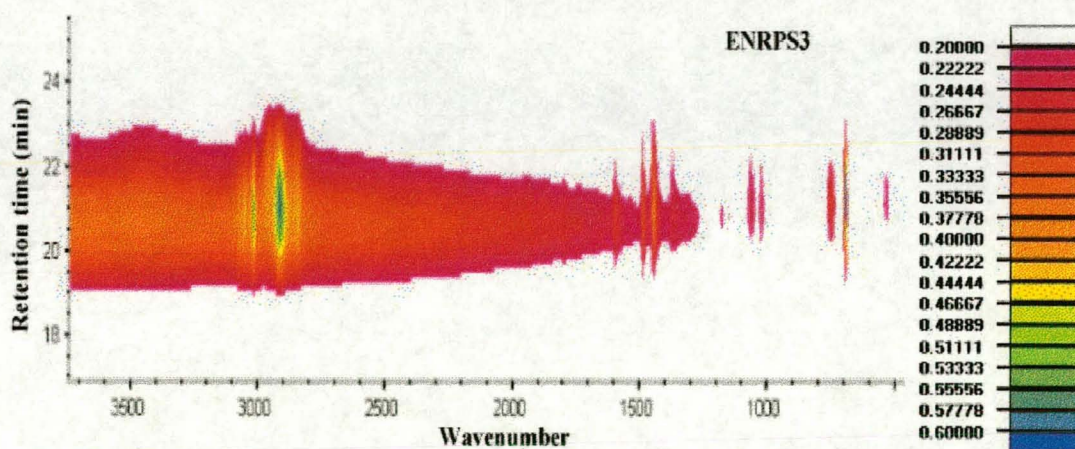
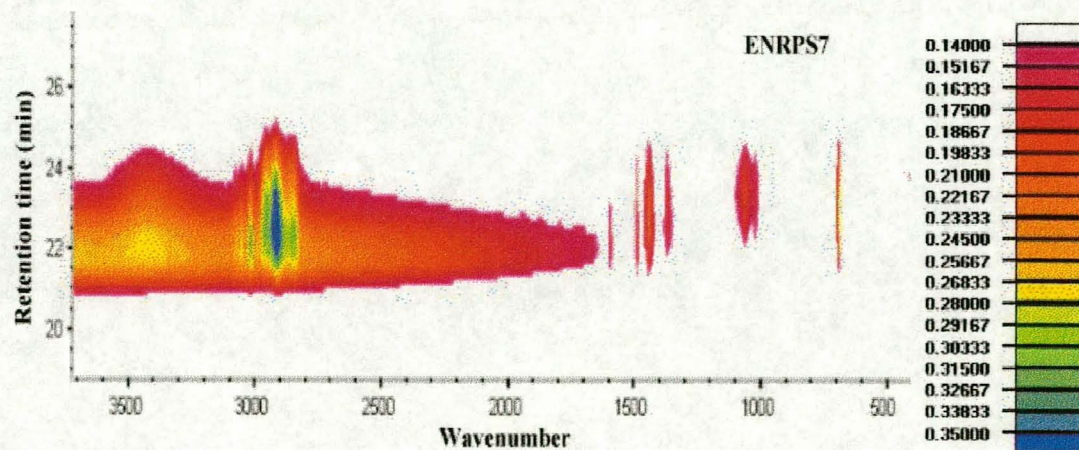Appendix 22: Contour plot of ENRPS3.
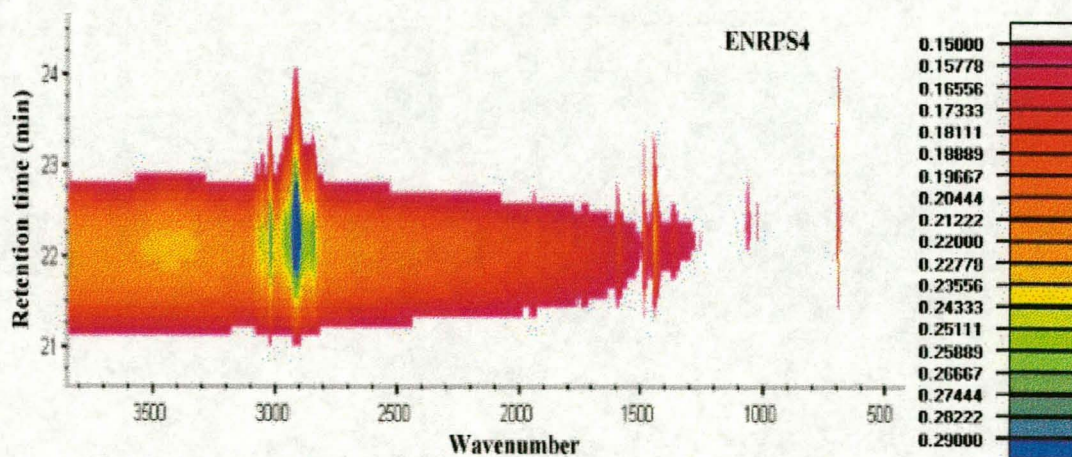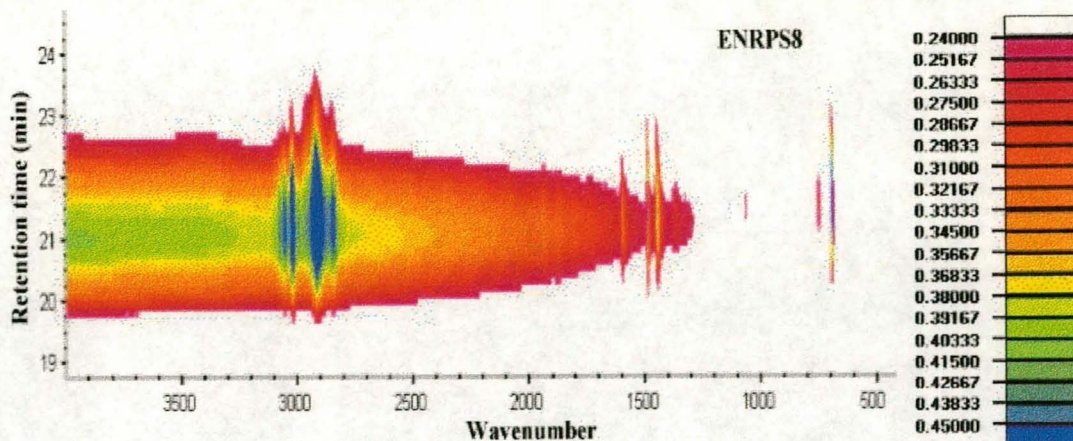

Appendix 23: Contour plot of ENRPS4.
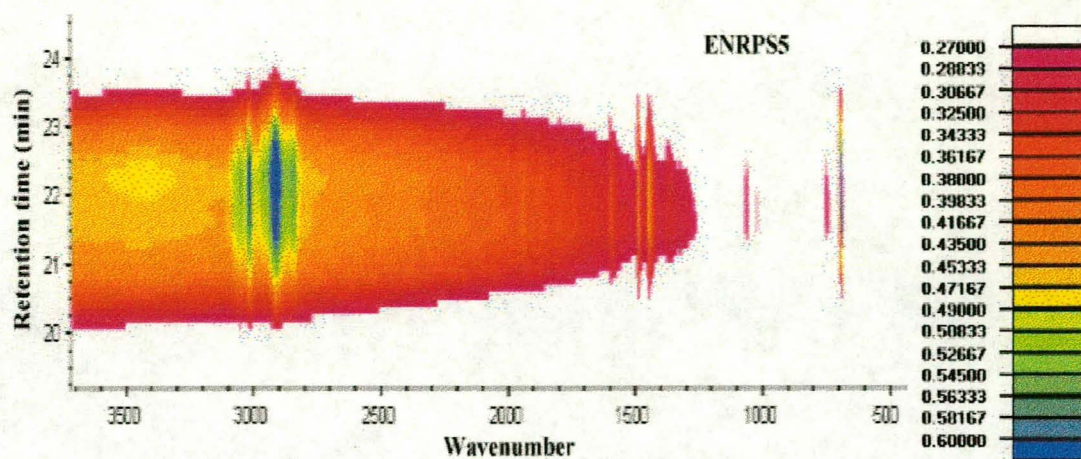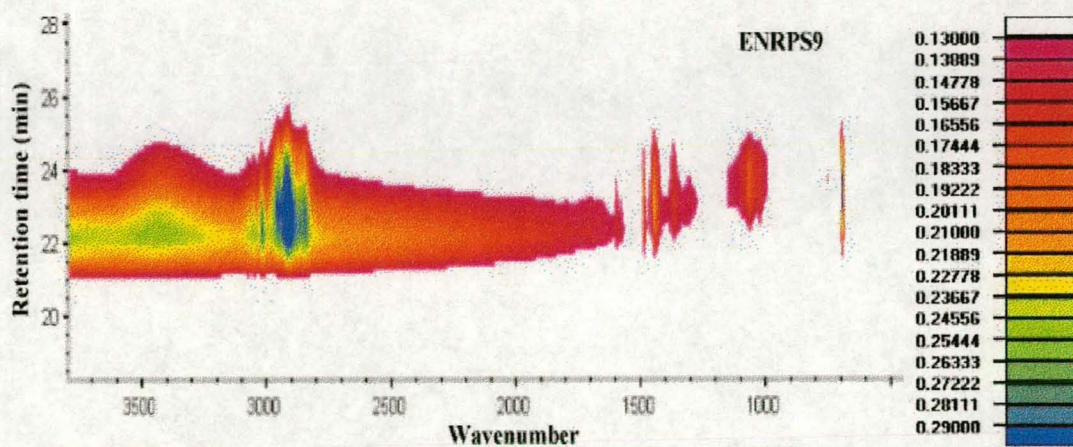
Appendix 24: Contour plot of ENRPS5.
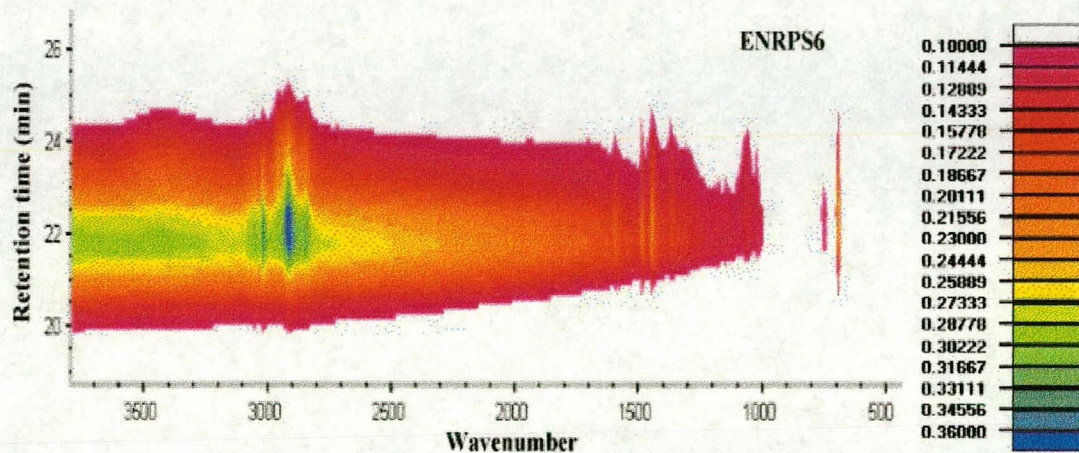
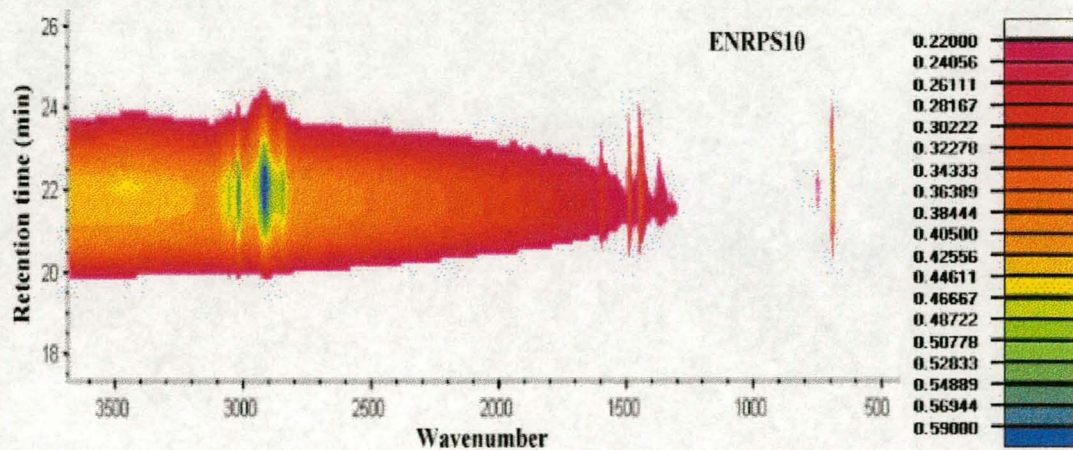Appendix 25: Contour plot of ENRPS6.

Appendix 26: Contour plot of ENRPS7.

Appendix 27: Contour plot of ENPS8.

Appendix 28: Contour plot of ENRPS9.

Appendix 29: Contour plot of ENRPS10.